Architecture de l'Holotranslocon SecYEG-DF-YajC-YidC

Mathieu Botte

UNIVERSITÉ DE GRENOBLE

EMBL

THESIS / THÈSE

To obtain the title of / Pour obtenir le grade de

DOCTEUR DE L'UNIVERSITÉ DE GRENOBLE

Discipline / Spécialité : **Structural Biology and Nanobiology**

Arrêté ministériel : 7 août 2006

Presented by / Présentée par

Mathieu Botte

Thesis supervisor / Thèse dirigée par : **Dr. Christiane Schaffitzel**

Thesis prepared at / Thèse prepare au sein du
European Molecular Biology Laboratory (EMBL), Grenoble Outstation
In / Dans l'**École Doctorale de Chimie et Sciences du Vivant**

Architecture of the SecYEG-DF-YajC-YidC Holotranslocon

Architecture de l'holotranslocon SecYEG-DF-YajC-YidC

Public defense on / Thèse soutenue publiquement le **13.12.2013**,

Jury members / Devant le jury compose de :

Dr. Christiane Schaffitzel Thesis supervisor/Directrice de thèse
Team leader, EMBL-Grenoble, France.

Prof. Julia Fritz-Steuber Reviewer/Rapporteur
Professor, University of Hohenheim, Germany.

Dr. Patrick Schultz Reviewer/Rapporteur
Group leader, IGBMC, Illkirch, France.

Prof. Uwe Schlattner Examiner/Examinateur
Professor, Joseph Fourier University, Grenoble, France.

Prof. Ian Collinson Examiner/Examinateur
Professor, University of Bristol, United Kingdom.

Dr. Jean-Michel Jault Examiner/Examinateur
Group leader, IBS, Grenoble, France.

Université Joseph Fourier / Université Pierre Mendès France /
Université Stendhal / Université de Savoie / Grenoble INP

Acknowledgements

First of all, I would like to thank my supervisor, Dr. Christiane Schaffitzel for giving me the great opportunity to work on this fascinating and challenging project and for her guidance throughout these four years.

I am also thankful to the members of my thesis advisory committee, Prof. Eva Pebay-Peyroula, Prof. Matthias Wilmanns and Dr. Imre Berger for their helpful suggestions and advices during my annual reports.

I would also like to thank my thesis jury members, Prof. Julia Fritz-Steuber, Prof. Ian Collinson, Dr. Jean-Michel Jault, Prof. Uwe Schlattner and Dr. Patrick Schultz for taking the time to examine this PhD work.

Now, I would like to acknowledge all the people which have been involved in this project and more especially Gabor Papai and Patrick Schultz (IGBMC Illkirch, France), James Riches and Wim Hagen (EMBL-Heidelberg, Germany) for their help and sharing their knowledge in term of electron microscopy and image processing for successful cryo-electron microscopy studies. I would also like to thank Ian Collinson (University of Bristol, United Kingdom) and Imre Berger (EMBL-Grenoble, France) for discussions, advices and fruitful collaborations, Julien Marcoux (Carol Robinson laboratory, University of Oxford, United Kingdom), Yohann Coute (CEA Grenoble, France), Sophie Feurstein and Christine Ebel (IBS Grenoble, France) for their contributions to this project.

I would like to give special thanks to all the past and present members of the Berger and Schaffitzel laboratories and more especially to Aurélien Deniaud, Karine Huard, Kèvin Knoops, Manikandan Karuppasamy and Jelger Lycklama à Nijeholt for the greatly appreciated help and discussions form which I benefited during these four years.

I personally think that the EMBL was a great place to work and it gave me the opportunity to meet a lot of people and especially the EMBL Predocs 2009, Carmen Aguilar, Kasia Tarnawska, Tilman Plass, Daniel Mende, Sander Timmer, Veli Vural Uslu and many others with whom I share a lot of scientific discussion and a great “European friendship”.

Now I would like to say few words in French for my family and friends.

En premier lieu, je tiens à faire part de mon immense gratitude à ma mère ainsi qu’à ma sœur pour leur soutien et la compréhension dont elles ont fait preuve tout au long de mes études. Un grand merci à ma mère pour m’avoir toujours encouragé et soutenu dans mes études et à ma sœur pour le renfort qu’elle a été dans les moments difficiles.

Enfin, je voudrais adresser un énorme remerciement à ma deuxième famille, Boris, Mathieu, Xavier, Pierre-Loup, Julien, Laura, Stéphane, Élodie, Olivier, Charlotte, Grégory, Guillaume et Benjamin. Tout simplement merci d'avoir été là, pendant les bon moments comme les difficiles et de m'avoir encouragé et supporté durant toutes ces années.

Abstract

Targeting of proteins to their proper location in the cell is crucial to the cell. The targeting information is provided in form of a signal sequence by the polypeptide itself. In *Escherichia coli*, membrane proteins are targeted co-translationally via the signal recognition particle (SRP) to the membrane whereas secretory proteins follow the post-translational translocation pathway characterized by the proteins SecB and SecA involved in the targeting process. Both pathways converge at the protein-conducting channel SecYEG. Interestingly, SecYEG has the possibility to recruit accessory domains SecDF-YajC and YidC, forming the holotranslocon (HTL) complex. Current research on protein translocation mostly focuses on the structure and function of the conserved bacterial heterotrimeric protein conducting channel SecYEG. Not much is known about the structure and function of the additional components of the translocation machinery SecD, SecF and YidC which are essential for *E. coli*. This is largely due to the lack of a purified, recombinant SecYEG-DF-YidC holotranslocon (HTL) complex. Accordingly, a thorough biophysical and structural analysis of this large, seven-membered transmembrane complex is still pending.

Using a new recombineering-based vector system for expression of multi-protein complexes in *E. coli*, we successfully over-produced the SecYEG-DF-YajC-YidC holotranslocon and its subcomplex consisting of SecDF-YajC-YidC (DFYY). We also succeeded in detergent-solubilising and purifying these complexes. The purified holotranslocon was used to biochemically characterize the complex and to determine the structure of the holotranslocon. First of all, the HTL seems to be more competent for co-translational membrane proteins insertion compared to SecYEG alone. Regarding the post-translational translocation of a β-barrel outer-membrane protein, driven by SecA and ATP, the proton-motive force dependence of this process is increased. Furthermore, the presence of the accessory domains seems to enhance the binding of the ribosome to the translocon. By using cells depleted of SecDF and YajC, we identified possible HTL-substrates which have to be confirmed and further analyzed yet by *in vitro* translocation experiments.

Subsequently, we solved by cryo-electron microscopy (EM) and single particle analysis the structure of the holotranslocon. By comparing the EM reconstructions of the HTL complex with the subcomplex of the accessory domains SecDF-YajC-YidC, we were able to localize the core complex SecYEG. The HTL cryo-EM structure could be refined to a resolution of 10.5 Å. This structure allows the placement of the available high–resolution crystal structure of SecYEG, SecDF, and YidC to generate a quasi-atomic model of the holotranslocon.

In order to confirm our quasi-atomic model, we made use of different crosslinking- and mass spectroscopy-based approaches (CLMS) to characterize the protein-protein interactions within the holotranslocon complex. These CLMS data sets are large and suffer from a high rate of ‘false positives’, possibly caused by inter-complex crosslinks. Thus, they need to be carefully evaluated and interesting fits should be confirmed by an independent method. In the future, structural studies of the ribosome-HTL complex by cryo-EM together with reconstitution of the HTL into nanodiscs will be undertaken to reveal the conformation of the actively translocating HTL in a more physiological environment. Additional biochemical studies on the molecular mechanism of co- and post-translocation by HTL and its substrate spectrum are addressing the question about the physiological role of the holotranslocon in the cell.

Résumé en français

L'adressage des protéines vers leur correct emplacement est crucial pour la cellule. L'information d'adressage est fournie sous la forme d'une séquence signale par le polypeptide lui-même. Chez *Escherichia coli*, les protéines membranaires sont adressées vers la membrane de façon co-traductionnelle via la particule de reconnaissance du signal (SRP) tandis que les protéines sécrétées suivent la voie de translocation post-traductionnelle caractérisée par les protéines SecB et SecA qui sont impliquées dans le processus d'adressage. Ces deux voies convergent au niveau du canal de translocation des protéines SecYEG. Chose intéressante, SecYEG a la possibilité de recruter les domaines accessoires SecDF-YajC et YidC et ainsi former le complexe holotranslocon (HTL). La recherche actuelle sur la translocation des protéines se concentre principalement sur la structure et fonction du canal de translocation des protéines hétérotrimérique bactérien SecYEG qui est conservé. Peu de choses sont connues concernant la structure et la fonction des composants additionnels SecD, SecF et YidC formant la machinerie de translocation et qui sont essentiels pour *E. coli*. Ceci est dû principalement à l'absence d'un complexe holotranslocon SecYEG-DF-YidC (HTL) recombinant purifié. En conséquence, une analyse biophysique et structurale minutieuse de ce large complexe transmembranaire composé de sept sous-unités est toujours en suspens.

En utilisant un nouveau système d'expression pour des complexes multi-protéiques basé sur la recombinaison de vecteur chez *E. coli*, nous avons avec succès surproduit l'holotranslocon SecYEG-DF-YajC-YidC et son sous-complexe composé de SecDF-YajC-YidC (DFYY). Nous avons également réussi à solubiliser avec l'aide de détergents et à purifier ces complexes. L'holotranslocon purifié a ensuite été utilisé afin de caractériser de façon biochimique le complexe et de déterminer la structure de l'holotranslocon. Premièrement, le complexe HTL semble être plus compétent pour l'insertion co-traductionnelle des protéines membranaires comparé à SecYEG isolé. Concernant la translocation post-traductionnelle d'une protéine de la membrane externe à tonneau β, dépendante de la présence de SecA et d'ATP, l'influence de la force proton motrice sur ce processus est augmentée. De plus, la présence du domaine accessoire semble améliorer l'attachement du ribosome au translocon. En utilisant des cellules déplétées de SecDF et YajC, nous avons identifié des substrats possibles de HTL qui doivent maintenant être confirmés et analysés manière plus approfondie par des expériences de translocation *in vitro*.

Par la suite, nous avons résolu la structure de l'holotranslocon par cryo-microscopie électronique (ME) et analyse des particules isolées. En comparant les reconstructions de ME

du complexe HTL avec le sous-complexe de domaine accessoire SecDF-YajC-YidC, nous avons été capable de localisé le complexe principal SecYEG. La structure de HTL par cryo-ME a pu être affinée jusqu'à une résolution de 10.5 Å. Cette structure permet le placement des structures à haute résolution disponibles de SecYEG, SecDF et YidC afin de générer un modèle quasi-atomique de l'holotranslocon.

Dans le but de confirmer notre modèle quasi-atomique, nous avons fait usage de différentes approches basées sur la réticulation et la spectrométrie de masse (CLMS) afin de caractériser les interactions protéine-protéine au sein du complexe holotranslocon. Les jeu de données ainsi obtenus sont volumineux et souffrent d'un taux élevé de « faux positifs », probablement dû à des réactions de réticulation inter-complexe. C'est pourquoi ils nécessitent une évaluation minutieuse et les résultats intéressants devraient être confirmés par une méthode indépendante. Dans le futur, des études structurales du complexe ribosome-HTL par cryo-ME ainsi qu'une reconstitution de HTL dans des nanodisques vont être menées pour révéler la conformation de HTL en cours de translocation dans un environnement plus physiologique. Des études biochimiques complémentaires sur le mécanisme de co- et post-translocation par HTL et son spectre substrats abordent la question du rôle physiologique de l'holotranslocon dans la cellule.

Table Of Contents

List of figures

List of abbreviations

1-9

2xYT: Bacterial growth media
70S: Prokaryotic ribosome

A

Å: Angstrom (1 Å = 0.1 nm)
ABC: ATP-binding cassette
ADP: Adenosine-5'-diphosphate
Arg: Arginine
Asn: Asparagine
Asp: Aspartic acid
ATP: Adenosine-5'-triphosphate

B

BS3: Bis[sulfosuccinimidyl] suberate

C

CaM: Calmodulin (calcium-modulated protein)
CBP: Calmodulin binding protein
CL: Crosslink
CLMS: Crosslinking coupled to mass spectrometry
Cryo-EM: Cryo-electron microscopy
CTL: Control

D

DDM: n-Dodecyl-β-D-maltoside
DFYY: SecD-SecF-YajC-YidC
DNA: Deoxyribonucleic acid
DTT: Dithiothreitol

E

EDC: 1-Ethyl-3-[3dimethylaminopropyl] carbodiimide hydchloride
EGTA: Ethyleneglycol-bis(β-aminoethyl)-N,N,N′,N′-tetraacetic acid
EM: Electron microscopy
EMDB: Electron microscopy data bank

F

FRET: Fluorescence resonance energy transfer
FT: Flow through

G

GDP: Guanosine diphosphate
Gln: Glutamine
GTP: Guanosine triphosphate

H

H^+: Proton
HSD: Helical scaffold domain
HSW: High salt wash
HTL: Holotranslocon
HWD: Helical wing domain

I

IEX: Ion exchange chromatography
IgG: Immunoglobulin G
IMAC: Immobilized metal ion affinity chromatography
IP: Immunoprecipitation

IPTG: Isopropyl-β-D-thiogalactopyranoside

K

kDa: Kilodalton
KO: Knock-out
kV: Kilovolts

L

LB: Lysogeny broth
LC-MS/MS: Liquid chromatography coupled to tandem mass spectrometry

M

M: Protein marker; Molar
MES: 2-(N-morpholino)ethanesulfonic acid
MS: Mass spectrometry
MSP: Membrane scaffold protein

N

NBD: Nucleotide binding domain
Ni-NTA: Nickel-nitrilotriacetic acid
Nm: Nanometer
nM: Nanomolar
NS: Negative stain

O

OD: Optical density

P

PDB: Protein database
PEG: Polyethylene glycol
Phe: Phenylalanine
pI: Isoelectric point
PMF: Proton motive force
PPXD: Preprotein crosslinking domain
preMBP: Precursor of the maltose-binding protein
proOmpA: Precursor of the outer membrane protein A

R

RNA: Ribonucleic acid
RNC: Ribosome-nascent-chain
Rpm: Revolutions per minute
rRNA: Ribosomal RNA

S

SDA: Succinimidyl-diazirine
SDS-PAGE: Sodium dodecyl sulfate polyacrylamide gel electrophoresis
SEC: Size exclusion chromatography
SF6: Sulfur hexafluoride
SRP: Signal recognition particle

T

TEM: Transmission electron microscopy
TF: Trigger factor
TM: Transmembrane
tRNA: Transfer RNA
Tyr: Tyrosine

U

UV: Ultraviolet

W

WT: Wildtype

Chapter 1 : Introduction – part 1

Résumé en français / French summary

L'adressage des protéines vers leur correct lieu de fonction à l'intérieur de la cellule, dans la membrane ou dans l'espace extracellulaire est crucial pour la cellule. L'information d'adressage est fournie sous forme de séquence signal par la protéine elle-même. Chez *E. coli*, ce sont principalement des protéines membranaires qui sont adressées de manière co-traductionnelle via la particule de reconnaissance du signal (SRP) vers la membrane. SRP et son récepteur sont tous deux des GTPases qui transfèrent le complexe ribosome-chaîne naissante au canal de translocation des protéines. Par la suite, le polypeptide naissant est transloqué dans ou au travers de la membrane. Jusqu'à présent, une quantité de données biochimiques ainsi qu'un certain nombre de structures de complexes importants le long de cette voie de translocation sont disponibles ce qui jette un éclairage sur le mécanisme moléculaire du processus d'adressage et de translocation.

Publication 1

Escherichia coli co-translational targeting and translocation

Authors:
Ottilie von Loeffelholz, Matthieu Botte, Christiane Schaffitzel

ENCYCLOPEDIA OF LIFE SCIENCES (ELS), John Wiley & Sons, Ltd: Chichester, DOI: 10.1002/9780470015902.a0023170.

Escherichia coli Cotranslational Targeting and Translocation

Ottilie von Loeffelholz, *European Molecular Biology Laboratory, Grenoble Outstation, Grenoble, France*

Matthieu Botte, *European Molecular Biology Laboratory, Grenoble Outstation, Grenoble, France*

Christiane Schaffitzel, *European Molecular Biology Laboratory, Grenoble Outstation, Grenoble, France*

Advanced article

Article Contents

Online posting date: 17th January 2011

Targeting of proteins to their proper location inside the cell, in the membrane or in the extracellular space is crucial to the cell. The targeting information is provided in form of a signal sequence by the protein itself. In *Escherichia coli*, mostly membrane proteins are targeted cotranslationally via the signal recognition particle (SRP) to the membrane. The SRP and its receptor are both guanosine triphosphatases (GTPases) which handover the ribosome-nascent chain complex to the protein-conducting channel. Subsequently, the nascent polypeptide is translocated into or across the membrane. To date, a host of biochemical data and a number of structures of important complexes along the pathway are available which shed light on the molecular mechanism of the targeting and translocation process.

Introduction

About one-third of the genome of organisms encodes membrane proteins. Membrane proteins are involved in most essential processes of the cell and are at the core of many diseases and their treatment. In all kingdoms of life, membrane proteins are inserted cotranslationally in the lipid bilayer via the signal recognition particle (SRP) pathway (Walter and Johnson, 1994; Rapoport, 2007). The cotranslational insertion is essential as membrane proteins contain at least one transmembrane segment consisting of approximately 20 hydrophobic amino acids which would aggregate in the cytosol. **See also**: Membrane Proteins; Protein Translocation across Membranes

The biogenesis of membrane proteins is a multistep process which is well coordinated in time and space involving targeting, translocation, folding and assembly of complexes. During cotranslational targeting, the SRP recognises and tightly binds hydrophobic signal sequences of the nascent polypeptide emerging from the ribosomal tunnel (**Figure 1**). The interaction of the SRP with its receptor (FtsY in bacteria) at the membrane allows the ribosome-nascent chain complex (RNC) to be delivered to the translocation machinery (Shan and Walter, 2005). In bacteria, mostly membrane proteins are directed to the SRP-dependent pathway. In contrast, secreted proteins favour the posttranslational route which, in bacteria, requires the chaperone SecB and the motor ATPase SecA (**Figure 1**). The posttranslational reaction differs widely between bacteria and eukaryotes, whereas the cotranslational process is universally conserved. **See also**: Ribosome Structure and Shape

Both modes of translocation (co- and posttranslational) converge at the Sec complex in the membrane (**Figure 1**). The Sec translocon allows the passage of hydrophilic sequences across and the integration of hydrophobic segments into the lipid bilayer. The energy for translocation is provided by the binding partner, that is, by the translating ribosome or by the ATPase SecA. During cotranslational translocation, the nascent polypeptide is transferred directly from the ribosomal tunnel into the protein-conducting channel. The protein-conducting channel is a heterotrimeric complex consisting of SecY, SecE and SecG (SecYEG) in bacteria (Rapoport, 2007). Additional factors associate with the conserved protein-conducting channel to form the holo-translocon complex. These factors, YidC, SecD, SecF and YajC, contribute to membrane protein insertion, folding and assembly and posttranslational translocation (Xie and Dalbey, 2008). **See also**: Bacterial

ELS subject area: Structural Biology

How to cite:
von Loeffelholz, Ottilie; Botte, Matthieu; and Schaffitzel, Christiane (January 2011) *Escherichia coli* Cotranslational Targeting and Translocation. In: Encyclopedia of Life Sciences (ELS). John Wiley & Sons, Ltd: Chichester.
DOI: 10.1002/9780470015902.a0023170

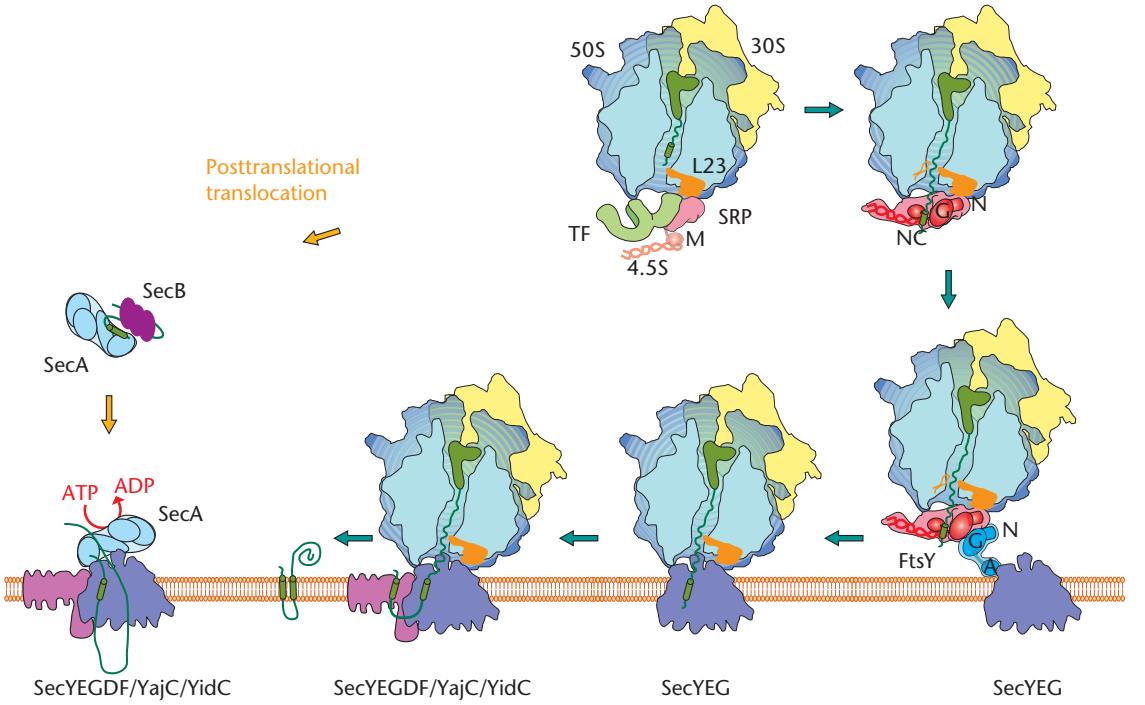

Figure 1 Protein export and membrane protein insertion. Exported proteins are targeted posttranslationally via the SecB chaperone and the SecA ATPase to the translocation machinery in the membrane (left). SecA provides the energy for translocation across the membrane. The signal recognition particle (SRP) and its receptor (FtsY) target nascent membrane proteins cotranslationally to the SecYEG protein-conducting channel (right). Additional proteins (SecD, SecF, YajC and YidC) can associate with SecYEG and assist in the translocation across or into the membrane.

Cytoplasmic Membrane; Cotranslational Translocation of Proteins into Microsomes: Methods; Protein Translocation across Membranes; Signal Peptides

Signal Sequences

To date, it is still poorly understood how the SRP ensures faithful delivery of the correct RNCs to the translocation machinery in the membrane. Signal sequences that are recognised by the SRP lack a consensus motif and are highly divergent in length, shape and amino acid composition like other topogenic sequences responsible for protein localisation. Consequently, the SRP needs to be highly adaptable to bind diverse signal sequences. The primary feature of signal sequences bound by the SRP is a hydrophobic core. However, the difference between signal sequences that are targeted via the SRP and signal sequences that lead to posttranslational translocation is relatively small. Secreted proteins contain usually shorter *N*-terminal signal sequences consisting of 7–12 hydrophobic amino acids that are later cleaved off and degraded. **See also**: Protein Translocation across Membranes; Signal Peptides

In the cytosol, the molecular chaperone Trigger Factor also plays a role in the sorting process: Trigger Factor and the SRP compete for nascent chain binding at the exit of the ribosomal tunnel (Eisner *et al.*, 2006). Less hydrophobic sequences are bound by Trigger Factor and targeted via SecA/B to the membrane (**Figure 1**). Overexpression of Trigger Factor leads to slower export of secreted proteins (Lee and Bernstein, 2001). Importantly, the folding of translocated proteins can be affected by the mode of translocation: cotranslationally exported proteins fold in a more vectorial manner than posttranslationally translocated proteins because translation is about 10-fold slower than translocation (Kadokura and Beckwith, 2009). **See also**: Chaperones, Chaperonin and Heat-Shock Proteins; Protein Folding and Chaperones; Protein Folding *In Vivo*; Ribosomal Proteins: Role in Ribosomal Functions; Ribosome Structure and Shape

In many inner membrane proteins, the first transmembrane helix (TM) is extremely hydrophobic (Lee and Bernstein, 2001). It serves as the signal sequence which decides not only the targeting but also the topology of the membrane protein in the lipid bilayer. Depending on the orientation of the first TM, the *N*-terminal region of the membrane protein remains in the cytosol or is translocated across the membrane. Accordingly, the orientation of subsequent TMs is predetermined by the orientation of the signal sequence. In general, the insertion of the signal sequence into the membrane follows the 'positive-inside rule': the positively charged end of the hydrophobic signal sequence remains in the cytoplasm. Several mutations in SecY have been reported to affect the orientation of the signal sequence indicating that the Sec translocon is

responsible for integration of signal sequences according to the 'positive-inside rule' (Junne *et al*., 2007).

Signal Recognition Particle

In the cytosol, the SRP binds to the ribosome and screens the emerging nascent chain for the presence of a signal sequence. Upon signal sequence recognition, the SRP binds the ribosome with high affinity (1 nM or less). The *Escherichia coli* SRP represents a minimal functional version: it is a RNA–protein complex consisting of one 4.5S RNA and one 48 kDa protein (Ffh, the homologue of the eukaryotic SRP54 protein) (Poritz *et al*., 1990; Romisch *et al*., 1989). Both components are conserved in all kingdoms of life and essential for viability. The 4.5S RNA is 114 nucleotides long and forms a stable hairpin with bulges. The Ffh protein consists of three domains: the N, G and M domain (**Figure 2**). The *N*-terminal four-helix bundle (N domain) is responsible for ribosome binding via ribosomal protein L23 which is located at the exit of the ribosomal tunnel (Gu *et al*., 2003). The N domain tightly packs against the central GTPase G domain forming a structural and functional unit (NG domain). The G domain is homologous to the classical *Ras* GTPase fold. The Ffh GTPase contains an additional 'Insertion Box Domain' (IBD) which is unique to the SRP-type GTPases and critical for activating GTP hydrolysis upon formation of the SRP–FtsY complex. The methionine-rich M domain is flexibly linked to the NG domain. It contains the binding site for the SRP RNA and for the signal sequence (**Figure 2**; Doudna and Batey, 2004; Keenan *et al*., 2001). **See also**: Ribosomal Proteins: Role in Ribosomal Functions

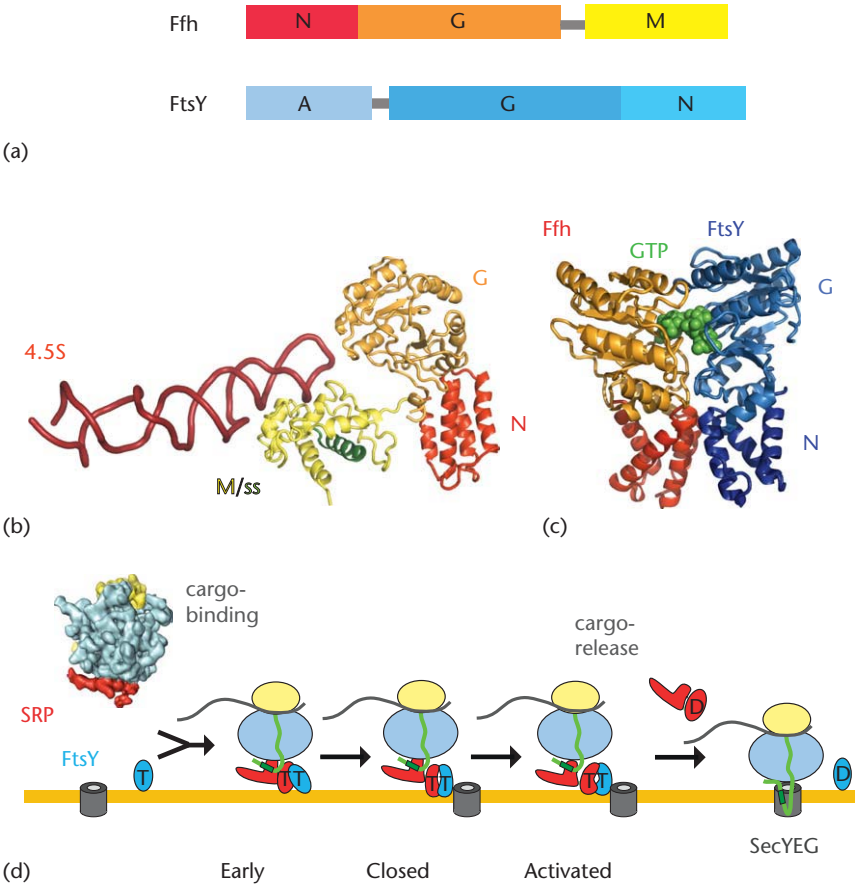

Figure 2 Cotranslational targeting. (a) Scheme of the domain architecture of *E. coli* Ffh (the SRP protein) and FtsY (SRP receptor). (b) Atomic model of the *E. coli* SRP in the extended conformation which is observed when the SRP binds the translating ribosome (2J28.pdb) (Halic *et al*., 2006). The Ffh N domain is depicted in red, the GTPase domain in orange, the M domain in yellow, the signal sequence in green and the 4.5S RNA in dark red. (c) Co-crystal structure of the NG domains of Ffh and FtsY from *Thermus aquaticus* (1OKK.pdb) (Egea *et al*., 2004; Focia *et al*., 2004). The two GTPase domains form a composite active site. The two GTP analogues are shown as green spheres. The FtsY NG domain is depicted in blue. (d) Model of the SRP and FtsY conformational states during cotranslational targeting (adapted from Zhang *et al*., 2009). First, the ribosome nascent chain complex (cargo) is recognised and tightly bound by the SRP. The cryo-EM structure of the RNC-SRP (filtered to 15 Å resolution, Halic *et al*., 2006) is depicted with the same colour coding as the cartoon drawings of the other complexes. Subsequently, the SRP and FtsY form a GTP-independent *early* intermediate. In the presence of GTP, the *early* intermediate rearranges into the *closed* conformation. Rearrangements in the catalytic loops of the GTPase domains activate GTP hydrolysis (*activated* state). This leads to cargo-release, that is, handover of the RNC to the SecYEG translocon and dissociation of the SRP–FtsY complex.

The most important contact between the Ffh N domain and ribosomal protein L23 is also formed with non-translating ribosomes and ribosomes displaying a nascent chain which is scanned by the SRP (Gu *et al*., 2003; Schaffitzel *et al*., 2006). Further ribosomal contacts are only formed upon recognition of the signal sequence. Then, the SRP binds close to the exit of the ribosomal tunnel and adopts an elongated structure (Halic *et al*., 2006; Schaffitzel *et al*., 2006; **Figure 2**). The four ribosomal contacts observed in cryo-electron microscopy structures (cryo-EM) explain the high affinity of the SRP to the RNC. In the RNC–SRP complex, the signal sequence is tightly bound at the interface between the M domain and the ribosome. **See also**: Single Particle EM

The eukaryotic SRP is much larger than the *E. coli* SRP consisting of 7S RNA and six proteins (Nagai *et al*., 2003). Importantly, the eukaryotic SRP contains an Alu domain which is absent in *E. coli*. The Alu domain arrests translation and thus ensures that the RNC stays in a translocation-competent state. The cryo-EM structure of the eukaryotic RNC–SRP complex reveals the mechanism of the translation arrest: the Alu domain blocks access of the aminoacyl-tRNAs to the active site (Halic *et al*., 2004). Efficient eukaryotic targeting is incompatible with normal cellular translation rates due to rate-limiting concentrations of the SRP receptor (Lakkaraju *et al*., 2008); therefore, the translation arrest is essential. In contrast, the *E. coli* SRP is too small to arrest translation by a related mechanism and most likely, translation continues during cotranslational targeting. **See also**: Cotranslational Translocation of Proteins into Microsomes: Methods; Protein Translocation across Membranes; Signal Peptides

SRP Receptor FtsY

The bacterial SRP receptor consists of a single protein FtsY (Luirink *et al*., 2005). FtsY exists as a membrane-associated form and as a cytoplasmic form. The membrane-associated form is suggested to be the active SRP receptor that can interact with the phospholipids and the translocon. Ffh and FtsY contain homologous NG domains (**Figure 2a**) (Keenan *et al*., 2001). The crystal structure of the complex of the NG domains of the *Thermus aquaticus* SRP and FtsY revealed a heterodimer with a quasi-two-fold symmetry (**Figure 2c**; Egea *et al*., 2004; Focia *et al*., 2004). In the structure, the NG domains of Ffh and FtsY form a composite active site with two bound nucleotides (non-hydrolysable GTP analogues) suggesting a mechanism for the reciprocal GTPase activation upon complex formation. This mechanism is markedly different from the Ras-like GTPases which need external factors for activation and nucleotide exchange to switch between the active and inactive states. In addition to the NG domain, the *E. coli* FtsY contains an acidic, *N*-terminal A domain that is unique to bacteria and poorly conserved. The A domain is involved in the association of FtsY with anionic phospholipids and interaction with the SecYEG translocon (Weiche *et al*., 2008). However, FtsY lacking the A domain is functional *in vivo*.

During cotranslational targeting, recognition of the RNC by the SRP (cargo-binding), complex formation with FtsY and delivery to the translocon (cargo-release) needs to be tightly regulated to avoid mistargeting. Several discrete conformational states of the SRP and FtsY have been characterised along the SRP–FtsY binding and activation cycle leading to the following model (Zhang *et al*., 2009; **Figure 2d**): In the presence of a RNC with a signal sequence, the SRP and FtsY quickly bind one another adopting an '*early*' conformation which forms independently of GTP. The *early* state is stabilised by the ribosome and most likely also serves as a checkpoint to reject incorrect cargos (e.g. RNCs with a weak signal sequence). In the presence of translocon, the switch from the *early* to the *closed* conformation of the SRP–FtsY complex is triggered in a step requiring GTP. The *activated* state forms by a subsequent rearrangement of multiple catalytic residues in the active site of both NG domains. This leads to handover of the RNC to the translocon, then activates GTP hydrolysis and finally drives disassembly of the SRP–FtsY complex (**Figure 2d**). The crystal structure of the Ffh–FtsY NG domains represents the NG domains in the *closed*/*activated* state (**Figure 2c**).

A recent cryo-EM structure of the nucleotide-independent *early* conformation of the RNC–SRP–FtsY complex reveals a critical role of the 4.5S RNA in stabilising the complex (Estrozi *et al*., 2010). The SRP is prepositioned by the cargo (RNC) to bind the FtsY NG domain. The complex is stabilised by a direct interaction between the FtsY GTPase domain and the SRP RNA. A clear switch from the cargo-binding mode with four ribosomal connections in the RNC–SRP complex to the cargo-release mode with one remaining ribosomal contact in the RNC–SRP–FtsY complex can be observed in the respective cryo-EM structures (Schaffitzel *et al*., 2006; Estrozi *et al*., 2010).

The bacterial SRP and FtsY can replace their eukaryotic homologues to carry out efficient targeting of mammalian substrates into ER microsomal membranes (Powers and Walter, 1997) indicating that the targeting process is highly conserved.

SecYEG Translocon

The translocase is a membrane protein complex consisting of the conserved, hetero-trimeric Sec protein-conducting channel (Rapoport, 2007). The crystal structure of the archaeal SecYEβ complex provided important insight into how protein translocation is achieved (**Figure 3a** and **b**; Van den Berg *et al*., 2004). The SecY subunit with 10 transmembrane helices forms the pore of the channel (**Figure 3a**). SecY has internal symmetry: helices 1–5 form one half of the channel and helices 6–10 the other half. The loop between helices 5 and 6 and one helix of SecE serve as hinge in the back of the molecule. Thus, the SecY complex

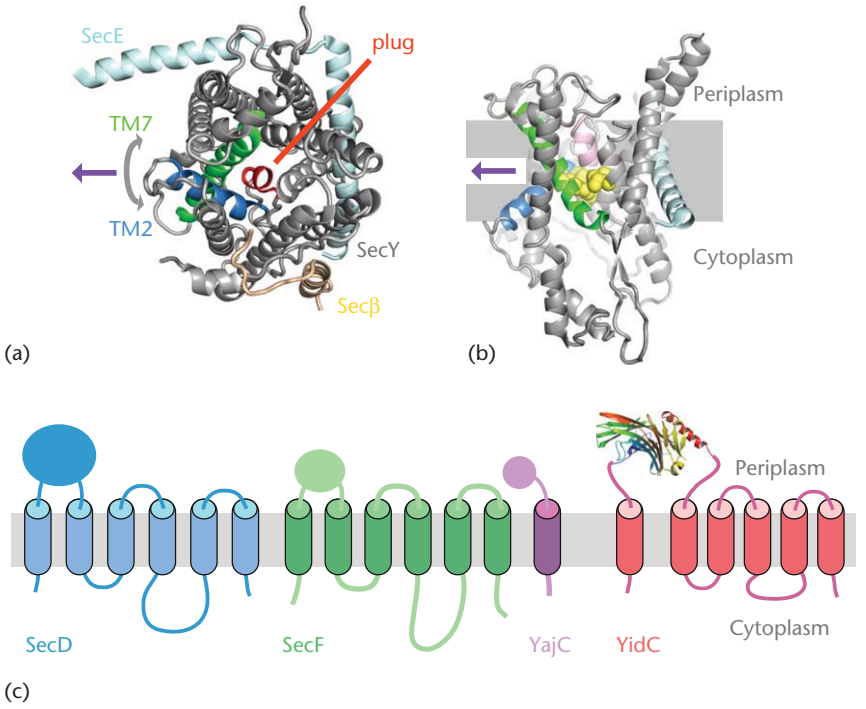

Figure 3 The translocation machinery. The crystal structure of the archaeal SecYEβ (top, 1RHZ.pdb) (Van den Berg *et al.*, 2004) shown from the cytoplasm (a) and as a side view (cut in the middle of the protein-conducting channel) (b). SecY is depicted in grey; TM2 and TM7 of SecY that line the lateral gate are highlighted in blue and green, respectively. The inactive translocation pore is sealed by a small helix on the periplasmic site (the plug, depicted in red). The ring of hydrophobic amino acids that seals the translocation pore is highlighted in yellow. (c) Topology of the additional translocation factors SecD, SecF, YajC and YidC. The periplasmic domain of *E. coli* YidC (3BLC.pdb) (Oliver and Paetzel, 2008) is the only high-resolution structural information of these proteins currently available.

has the form of a clam-shell that can open laterally at the front. The interior of the channel is mostly hydrophilic, but has a constriction in the middle which consists of a ring of hydrophobic amino acids (**Figure 3b**; Rapoport, 2007). This ring is suggested to prevent the passage of ions across the membrane. On the periplasmic side, the inactive channel is sealed by a small alpha helix, the plug (**Figure 3a**). Biochemical experiments indicate that the plug is displaced by the nascent polypeptide in the active state (Tam *et al.*, 2005).

The cotranslational translocation process starts with binding of the cytosolic loops of SecY to the ribosome. This seems to induce conformational changes leading to transient displacement of the translocon plug. Second, the signal sequence intercalates into the walls of the SecY channel (the lateral gate) such that the signal sequence contacts phospholipids and the protein channel. This leads to opening of the channel and insertion of the nascent polypeptide as a loop into the channel. The polypeptide crosses the membrane as an unfolded polypeptide or as an α helix. The speed of translocation is determined by the rate of translation, which is approximately 10 times slower than translocation (Kadokura and Beckwith, 2009).

During the synthesis of membrane proteins, all helices have to move from the interior of the SecY channel into the lipid bilayer. The lateral gate is formed by SecY transmembrane helices at the front of the two SecY halves (**Figure 3a** and **b**). The lateral gate is suggested to open and close during translocation and thus to expose hydrophobic helices to the lipid bilayer. It seems that such protein–lipid interactions of the hydrophobic helices are critical during membrane protein insertion allowing the partitioning of TMs into the membrane (Hessa *et al.*, 2007; Rapoport, 2007). In general, TMs seem to mirror the physical properties of the lipid bilayer and the statistical distribution of a given amino acid in the membrane correlates well with its hydrophobicity (Hessa *et al.*, 2007).

Positive charges and folded *N*-terminal domains are retained in the cytosol. In this case, the nascent polypeptide is inserted as a loop as it is the case for secreted proteins. Alternatively, the TM can flip across the channel such that the *N*-terminus is located in the periplasm. The translocation of a large periplasmic loop or domain of a membrane protein requires SecA ATPase (Neumann-Haefelin *et al.*, 2000). The following TM after a periplasmic loop then acts as a stop-transfer sequence. Cytosolic loops can probably move through the gap between the ribosome and the translocation channel which has been visualised in cryo-EM structures of the RNC–SecYEG complex (Menetret *et al.*, 2007; Mitra *et al.*, 2005). **See also**: Ribosome Structure and Shape

In bacteria, most exported proteins are translocated posttranslationally. After completion of protein synthesis,

the preproteins with a cleavable, moderately hydrophobic signal sequence remain unfolded with the help of the chaperone SecB (**Figure 1**). The energy for translocation is provided by the ATPase SecA (Rapoport, 2007) which associates with SecYEG. The substrate is translocated by a pushing mechanism, where SecA binds first the signal peptide and triggers the translocon channel to open (Simon and Blobel, 1992). In an ATP driven cycle, SecA pushes the polypeptide chain into the channel, releases the chain and then grabs a new part of the polypeptide (Economou *et al*., 1995). However, the clear discrimination between co- and posttranslational translocation is questionable since SecA was crosslinked to nascent polypeptide chains (Eisner *et al*., 2006) and is required for the insertion of membrane proteins with a large periplasmic loop (Neumann-Haefelin *et al*., 2000). In fact, it is more likely that protein secretion and membrane protein folding share similar translocation mechanisms. **See also**: Cotranslational Translocation of Proteins into Microsomes: Methods; Protein Translocation across Membranes

The crystal structure of the Sec translocon and biochemical experiments indicate that translocation is mediated via a single SecYEG that forms the channel (Rapoport, 2007). However, in the membrane the Sec complex has a tendency to oligomerise (Breyton *et al*., 2002; Snapp *et al*., 2004). In *E. coli* SecYEG dimers appear to be the preeminent version, in both post- and cotranslational reactions (Osborne and Rapoport, 2007; Mitra *et al*., 2005). In such an oligomer, only one copy could be active at any given time in the SecYEG oligomer. Similarly, the mitochondrial transporters Tom40 and Tim22 which are responsible for protein translocation across the outer and inner mitochondrial membrane, respectively, exist as oligomers and only one pore is active (Rehling *et al*., 2003).

SecYEG-independent Translocation by YidC

The energy-transducing membranes of bacteria, mitochondria and chloroplasts have a high demand for the insertion and assembly of respiratory complexes and ATP synthases. The ATPase and respiratory chain complexes depend on the function of YidC which in *E. coli* is essential for vitality (Samuelson *et al*., 2000). YidC works in conjunction with the SecYEG translocon in the holo-translocon complex (below) and as a Sec-independent insertase. YidC and its mitochondrial and chloroplast homologues Oxa1 and Alb3 are responsible for the integration of an important subset of inner membrane proteins (Luirink *et al*., 2005; Kiefer and Kuhn, 2007; Xie and Dalbey, 2008). Well-characterised substrates of YidC include the F_0c subunit of the essential F_1F_0-ATPase, CyoA (subunit II of the cytochrome 0 oxidase) and the mechanosensitive channel MscL. These YidC substrates have in common that they are rather small and often consist of two TMs connected via a short hairpin. Biochemical data indicate that the YidC substrates are targeted via the SRP pathway to the YidC insertase and inserted cotranslationally into the membrane. Cryo-EM of YidC in the membrane and of YidC in complex with a translating ribosome suggests that YidC functions as a dimer and forms a second protein-conducting channel in the membrane (Kohler *et al*., 2009). To date, only the nonessential periplasmic domain of YidC has been solved at high resolution (**Figure 3c**) (Oliver and Paetzel, 2008). The conserved core of the *C*-terminal five TMs remains unknown. The *N*-terminal extension consisting of an additional TM and the large periplasmic domain of YidC are likely to play a role in the function of YidC in the Sec-dependent translocation pathway. In fact, a mutation in the periplasmic loop of YidC has been described to impair only the Sec-dependent function of YidC (Xie and Dalbey, 2008). **See also**: ATPases: Ion-motive; Bacterial Cytoplasmic Membrane

Interestingly, it has been reported that YidC depletion had no effect on the membrane insertion of the mechanosensitive channel MscL, but the formation of the pentameric MscL complex was almost completely abolished indicating a novel role for YidC in the assembly of membrane proteins (Pop *et al*., 2009). In the membrane, YidC is much more abundant than SecYEG. Therefore, it is likely that it exists both as a complex with SecYEG-SecDFYajC and in an unbound form (Nouwen and Driessen, 2002).

Holo-translocon Complex

The SecYEG translocon can associate with further membrane proteins to form the holo-translocon complex consisting of at least seven members (Arkowitz and Wickner, 1994; Luirink *et al*., 2005). The additional constituents of the holo-translocon YidC, YajC, SecD and SecF also contribute to the secretion and insertion reaction by a yet unknown mechanism.

In the Sec-dependent pathway, YidC has been suggested to be involved in membrane protein folding, assembly and quality control (Beck *et al*., 2001; Nagamori *et al*., 2004; van Bloois *et al*., 2008). Biochemical experiments suggest that some nascent membrane proteins first interact with the SecY channel and are later transferred to YidC to prevent aggregation. In fact, several consecutive TMs could all be crosslinked to YidC after leaving the SecY channel (Beck *et al*., 2001). Therefore, YidC has been suggested to act as a membrane chaperone mediating the formation of helix bundles before their release into the lipid bilayer. Furthermore, YidC interacts with the FtsH/HflK/C complex suggesting a direct link between membrane protein integration, folding and quality control (van Bloois *et al*., 2008). FtsH is an ATP-dependent protease that dislocates membrane proteins from the lipid bilayer to the cytoplasm where they are degraded. **See also**: Protease Complexes

The interaction of YidC with the SecYEG translocon is thought to be mediated via the accessory complex SecDFYajC (Nouwen and Driessen, 2002). YajC, SecD, SecF and YidC form a complex that appears to be associated

with SecYEG at least transiently (Luirink *et al*., 2005). There is no evidence that SecDF and YajC contribute to the protein-conducting channel or interact with the translocated polypeptide. Deletion of SecD and SecF results in a severely defective phenotype (Pogliano and Beckwith, 1994). In contrast, YajC is not needed for functionality in *E. coli*. SecDF–YajC have been implicated in the regulation of an activated or inserted state of SecA, and are required for a high capacity of protein translocation through SecYEG (Duong and Wickner, 1997). SecD and SecF seem to enforce the posttranslational translocation reaction by coupling it to the proton-motive force (PMF) (Arkowitz and Wickner, 1994). Both SecD and SecF are highly conserved in bacteria and archaea, and each protein contains six transmembrane helices and a large periplasmic domain (**Figure 3c**). Structurally, SecDF have been suggested to be related to the resistance-nodulation-division (RND) efflux super-family that includes the multidrug transporter AcrB, another proton-driven membrane transporter. Other protein translocation systems in mitochondria and thylakoids have also been shown to require the PMF. However, in contrast to the primary energy (ATP/GTP)-coupled translocation reaction, the PMF-driven activity has until now not been reconstituted from purified components and therefore the mechanism remains unknown. **See also**: Bacterial Cytoplasmic Membrane

Membrane Protein Folding

The simplest model for membrane protein folding is exclusively cotranslational (Skach, 2009; Xie and Dalbey, 2008). It requires that all TMs are recognised as signal anchor or as stop-transfer sequences. The former induce loop insertion and translocation across the membrane. The stop-transfer sequence replaces the TM in the lateral gate, terminates translocation and directs the following polypeptide into the cytosol until a new signal anchor sequence reinitiates translocation. Thus, to integrate a polytopic membrane protein the translocation must be highly dynamic to be able to change the direction of the peptide movement in a rapid succession. However, biochemical data indicate that the folding of polytopic membrane proteins does not occur exclusively cotranslational. Instead, less hydrophobic helices can be integrated in a subsequent step, in a process called topological maturation (Skach, 2009). It is likely that the nonmature membrane proteins remain associated with the holo-translocon complex and that the holo-translocon assists in the maturation by reducing the energy barrier for membrane insertion and by providing a folding interface.

In summary, while the process of cotranslational targeting and insertion is comparatively well understood, the determinants for membrane protein folding, quality control and assembly are still enigmatic. Future *in vitro* and *in vivo* biochemical as well as structural work has to reveal the underlying principles of this vital biological process.

References

Arkowitz RA and Wickner W (1994) SecD and SecF are required for the proton electrochemical gradient stimulation of preprotein translocation. *EMBO Journal* **13**(4): 954–963.

Beck K, Eisner G, Trescher D *et al*. (2001) YidC, an assembly site for polytopic *Escherichia coli* membrane proteins located in immediate proximity to the SecYE translocon and lipids. *EMBO Reports* **2**(8): 709–714.

van Bloois E, Dekker HL, Froderberg L *et al*. (2008) Detection of cross-links between FtsH, YidC, HflK/C suggests a linked role for these proteins in quality control upon insertion of bacterial inner membrane proteins. *FEBS Letters* **582**(10): 1419–1424.

Breyton C, Haase W, Rapoport TA, Kühlbrandt W and Collinson I (2002) Three-dimensional structure of the bacterial protein-translocation complex SecYEG. *Nature* **418**(6898): 662–665.

Doudna JA and Batey RT (2004) Structural insights into the signal recognition particle. *Annual Review of Biochemistry* **73**: 539–557.

Duong F and Wickner W (1997) The SecDFyajC domain of preprotein translocase controls preprotein movement by regulating SecA membrane cycling. *EMBO Journal* **16**(16): 4871–4879.

Economou A, Pogliano JA, Beckwith J, Oliver DB and Wickner W (1995) SecA membrane cycling at SecYEG is driven by distinct ATP binding and hydrolysis events and is regulated by SecD and SecF. *Cell* **83**(7): 1171–1181.

Egea PF, Shan SO, Napetschnig J *et al*. (2004) Substrate twinning activates the signal recognition particle and its receptor. *Nature* **427**(6971): 215–221.

Eisner G, Moser M, Schäfer U, Beck K and Müller M (2006) Alternate recruitment of signal recognition particle and trigger factor to the signal sequence of a growing nascent polypeptide. *Journal of Biological Chemistry* **281**(11): 7172–7179.

Estrozi LF, Boehringer D, Shan S, Ban N and Schaffitzel C (2010) Cryo-EM Structure of the *E. coli* translating ribosome in complex with SRP and its receptor. *Nature Structural and Molecular Biology*. http://dx.doi.org/10.1038/nsmb.1952.

Focia PJ, Shepotinovskaya IV, Seidler JA and Freymann DM (2004) Heterodimeric GTPase core of the SRP targeting complex. *Science* **303**(5656): 373–377.

Gu SQ, Peske F, Wieden HJ, Rodnina MV and Wintermeyer W (2003) The signal recognition particle binds to protein L23 at the peptide exit of the *Escherichia coli* ribosome. *RNA* **9**(5): 566–573.

Halic M, Becker T, Pool MR *et al*. (2004) Structure of the signal recognition particle interacting with the elongation-arrested ribosome. *Nature* **427**(6977): 808–814.

Halic M, Blau M, Becker T *et al*. (2006) Following the signal sequence from ribosomal tunnel exit to signal recognition particle. *Nature* **444**(7118): 507–511.

Hessa T, Meindl-Beinker NM, Bernsel A *et al*. (2007) Molecular code for transmembrane-helix recognition by the Sec61 translocon. *Nature* **450**(7172): 1026–1030.

Junne T, Schwede T, Goder V and Spiess M (2007) Mutations in the Sec61p channel affecting signal sequence recognition and membrane protein topology. *Journal of Biological Chemistry* **282**(45): 33201–33209.

Kadokura H and Beckwith J (2009) Detecting folding intermediates of a protein as it passes through the bacterial translocation channel. *Cell* **138**(6): 1164–1173.

Keenan RJ, Freymann DM, Stroud RM and Walter P (2001) The signal recognition particle. *Annual Review of Biochemistry* **70**: 755–775.

Kiefer D and Kuhn A (2007) YidC as an essential and multifunctional component in membrane protein assembly. *International Review of Cytology* **259**: 113–138.

Kohler R, Boehringer D, Greber B *et al*. (2009) YidC and Oxa1 form dimeric insertion pores on the translating ribosome. *Molecular Cell* **34**(3): 344–353.

Lakkaraju AK, Mary C, Scherrer A, Johnson AE and Strub K (2008) SRP keeps polypeptides translocation-competent by slowing translation to match limiting ER-targeting sites. *Cell* **133**(3): 440–451.

Lee HC and Bernstein HD (2001) The targeting pathway of *Escherichia coli* presecretory and integral membrane proteins is specified by the hydrophobicity of the targeting signal. *Proceedings of the National Academy of Sciences of the USA* **98**(6): 3471–3476.

Luirink J, von Heijne G, Houben E and de Gier JW (2005) Biogenesis of inner membrane proteins in *Escherichia coli*. *Annual Review of Microbiology* **59**: 329–355.

Menetret JF, Schaletzky J, Clemons WM Jr *et al*. (2007) Ribosome binding of a single copy of the SecY complex: implications for protein translocation. *Molecular Cell* **28**(6): 1083–1092.

Mitra K, Schaffitzel C, Shaikh T *et al*. (2005) Structure of the *E. coli* protein-conducting channel bound to a translating ribosome. *Nature* **438**(7066): 318–324.

Nagai K, Oubridge C, Kuglstatter A *et al*. (2003) Structure, function and evolution of the signal recognition particle. *EMBO Journal* **22**(14): 3479–3485.

Nagamori S, Smirnova IN and Kaback HR (2004) Role of YidC in folding of polytopic membrane proteins. *Journal of Cell Biology* **165**(1): 53–62.

Neumann-Haefelin C, Schäfer U, Müller M and Koch HG (2000) SRP-dependent co-translational targeting and SecA-dependent translocation analyzed as individual steps in the export of a bacterial protein. *EMBO Journal* **19**(23): 6419–6426.

Nouwen N and Driessen AJ (2002) SecDFyajC forms a heterotetrameric complex with YidC. *Molecular Microbiology* **44**(5): 1397–1405.

Oliver DC and Paetzel M (2008) Crystal structure of the major periplasmic domain of the bacterial membrane protein assembly facilitator YidC. *Journal of Biological Chemistry* **283**(8): 5208–5216.

Osborne AR and Rapoport TA (2007) Protein translocation is mediated by oligomers of the SecY complex with one SecY copy forming the channel. *Cell* **129**(1): 97–110.

Pogliano JA and Beckwith J (1994) SecD and SecF facilitate protein export in *Escherichia coli*. *EMBO Journal* **13**(3): 554–561.

Pop OI, Soprova Z, Koningstein G *et al*. (2009) YidC is required for the assembly of the MscL homopentameric pore. *FEBS Journal* **276**(17): 4891–4899.

Poritz MA, Bernstein HD, Strub K *et al*. (1990) An *E. coli* ribonucleoprotein containing 4.5S RNA resembles mammalian signal recognition particle. *Science* **250**(4984): 1111–1117.

Powers T and Walter P (1997) Co-translational protein targeting catalyzed by the *Escherichia coli* signal recognition particle and its receptor. *EMBO Journal* **16**(16): 4880–4886.

Rapoport TA (2007) Protein translocation across the eukaryotic endoplasmic reticulum and bacterial plasma membranes. *Nature* **450**(7170): 663–669.

Rehling P, Model K, Brandner K *et al*. (2003) Protein insertion into the mitochondrial inner membrane by a twin-pore translocase. *Science* **299**(5613): 1747–1751.

Romisch K, Webb J, Herz J *et al*. (1989) Homology of 54 K protein of signal-recognition particle, docking protein and two *E. coli* proteins with putative GTP-binding domains. *Nature* **340**(6233): 478–482.

Samuelson JC, Chen M, Jiang F *et al*. (2000) YidC mediates membrane protein insertion in bacteria. *Nature* **406**(6796): 637–641.

Schaffitzel C, Oswald M, Berger I *et al*. (2006) Structure of the *E. coli* signal recognition particle bound to a translating ribosome. *Nature* **444**(7118): 503–506.

Shan SO and Walter P (2005) Co-translational protein targeting by the signal recognition particle. *FEBS Letters* **579**(4): 921–926.

Simon SM and Blobel G (1992) Signal peptides open protein-conducting channels in *E. coli*. *Cell* **69**(4): 677–684.

Skach WR (2009) Cellular mechanisms of membrane protein folding. *Nature Structural and Molecular Biology* **16**(6): 606–612.

Snapp EL, Reinhart GA, Bogert BA, Lippincott-Schwartz J and Hegde RS (2004) The organization of engaged and quiescent translocons in the endoplasmic reticulum of mammalian cells. *Journal of Cell Biology* **164**(7): 997–1007.

Tam PC, Maillard AP, Chan KK and Duong F (2005) Investigating the SecY plug movement at the SecYEG translocation channel. *EMBO Journal* **24**(19): 3380–3388.

Van den Berg B, Clemons WM Jr, Collinson I *et al*. (2004) X-ray structure of a protein-conducting channel. *Nature* **427**(6969): 36–44.

Walter P and Johnson AE (1994) Signal sequence recognition and protein targeting to the endoplasmic reticulum membrane. *Annual Review of Cell Biology* **10**: 87–119.

Weiche B, Burk J, Angelini S *et al*. (2008) A cleavable *N*-terminal membrane anchor is involved in membrane binding of the *Escherichia coli* SRP receptor. *Journal of Molecular Biology* **377**(3): 761–773.

Xie K and Dalbey RE (2008) Inserting proteins into the bacterial cytoplasmic membrane using the Sec and YidC translocases. *Nature Reviews. Microbioloby* **6**(3): 234–244.

Zhang X, Schaffitzel C, Ban N and Shan SO (2009) Multiple conformational switches in a GTPase complex control co-translational protein targeting. *Proceedings of the National Academy of Sciences of the USA* **106**(6): 1754–1759.

Further Reading

Cross BC, Sinning I, Luirink J and High S (2009) Delivering proteins for export from the cytosol. *Nature Reviews Molecular Cell Biology* **10**(4): 255–264.

Facey SJ and Kuhn A (2010) Biogenesis of bacterial inner-membrane proteins. *Cellular and Molecular Life Sciences* **67**: 2343–2362.

Gasper R, Meyer S, Gotthardt K, Sirajuddin M and Wittinghofer A (2009) It takes two to tango: regulation of G proteins by dimerization. *Nature Reviews Molecular Cell Biology* **10**(6): 423–429.

Rapoport TA (2008) Protein transport across the endoplasmic reticulum membrane. *FEBS Journal* **275**(18): 4471–4478.

Chapter 1 : Introduction – part 2

Résumé en français / French summary

Les voies d'adressage des protéines membranaires et des protéines sécrétées convergent à la membrane au niveau du translocon SecYEG. Les protéines membranaires utilisent principalement la voie d'adressage et de translocation co-traductionnelle afin de rallier leur bonne localisation. Au contraire, les protéines sécrétées sont principalement adressées via SecA and SecB, i.e. la voie d'adressage post-traductionnelle. Ces deux voies se différencient par les acteurs protéiques impliqués et par les protéines « moteur » fournissant l'énergie requise pour le processus de translocation. La voie de sécrétion est initiée après la terminaison de la traduction. Les preprotéines ont besoin d'être gardées sous une forme dépliée par la protéine chaperonne SecB afin d'être compétente pour la translocation. Le transfert de la preprotéine depuis SecB vers SecA induit l'attachement du complexe SecA-preprotéine au canal de translocation des protéines SecYEG. Cette interaction est cruciale étant donné que SecA est une ATPase qui fournit l'énergie pour le processus de translocation. Pour la voie de translocation co-traductionnelle, le ribosome lui-même s'amarre à SecYEG et utilise l'énergie de la traduction afin de diriger le processus d'insertion des protéines membranaires. Les deux voies peuvent recruter des domaines accessoires composés de SecD, SecF, YajC et YidC au niveau du translocon principal SecYEG, formant ainsi le complexe holotranslocon (HTL). Il a été proposé que SecDF puisse accélérer le processus de translocation avec l'aide de la force proton motrice, tandis que YidC est requis par certaines protéines membranaires pour l'insertion et le repliement correct du domaine transmembranaire de ces protéines. Beaucoup d'informations structurales sont disponibles sur les différentes sous-unités de HTL, mais l'architecture moléculaire et l'interaction des sous-unités au sein de l'holotranslocon est énigmatique. C'est pourquoi, un aperçu structural de l'architecture du complexe HTL approfondira grandement notre compréhension du processus de translocation.

In this part of the introduction, we will describe in more detail the post-translational translocation pathway. Moreover, every subunit of the SecYEG-SecDFYajC-YidC holotranslocon will be analyzed in more detail in terms of structure and function to shed light on their possible role in the holotranslocon complex.

1-1. The post-translational translocation pathway

In bacteria, two main targeting routes exist that converge at the SecYEG translocon (Valent et al., 1998): the co- and the post-translational pathway (Chapter 1 - part 1). The main difference which characterizes these two pathways is the destination of the preprotein. The co-translational translocation is mostly used for insertion of membrane proteins into the lipid bilayer (Ulbrandt et al., 1997). The post-translational pathway is mainly used to translocate secretory proteins across the membrane (H. G. Koch et al., 1999). The two targeting pathways use different cytosolic components to drive the translocation process. In *E. coli*, the post-translational translocation pathway is energized by the motor protein SecA, whereas the cytosolic chaperone SecB keeps the preprotein in a translocation-competent state (Hartl et al., 1990).

1-1-1. SecB, the cytosolic chaperone

SecB is a cytosolic protein of 17 kDa, which forms a homotetramer [Fig. 1-1].

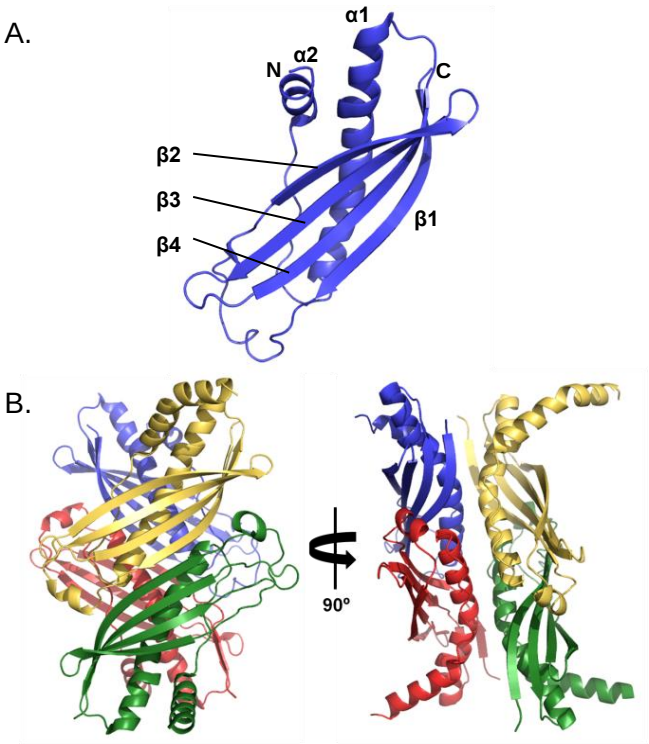

Figure 1-1. **Structure of SecB from *Haemophilus influenzae* at 2.5 Å resolution.** **A.** Structure of a monomer of SecB. The N- and C-terminus are labeled respectively N and C. **B.** Structure of a SecB tetramer. Each molecule in the tetramer is colored differently. (PDB code: 1FX3; (Xu et al., 2000)).

The monomer of SecB folds into two antiparallel α-helices and a β-sheet formed by four strands [Fig. 1-1.A]. The interface of a homodimer is mainly mediated by the interaction between the β-strand 1 and the α-helix 1. To stabilize the tetramer, polar interactions between the 4 helices $\alpha 1$ form the tetramerisation interface of the SecB multimer [Fig. 1-1.B].

SecB has two functions: it binds preproteins in the cytosol and keeps them in a partly unfolded, translocation-competent state. Second, it hands over the preprotein to SecA for subsequent translocation (Hartl et al., 1990). Based on the crystal structure, a peptide binding site has been suggested [Fig. 1-2] (Xu et al., 2000).

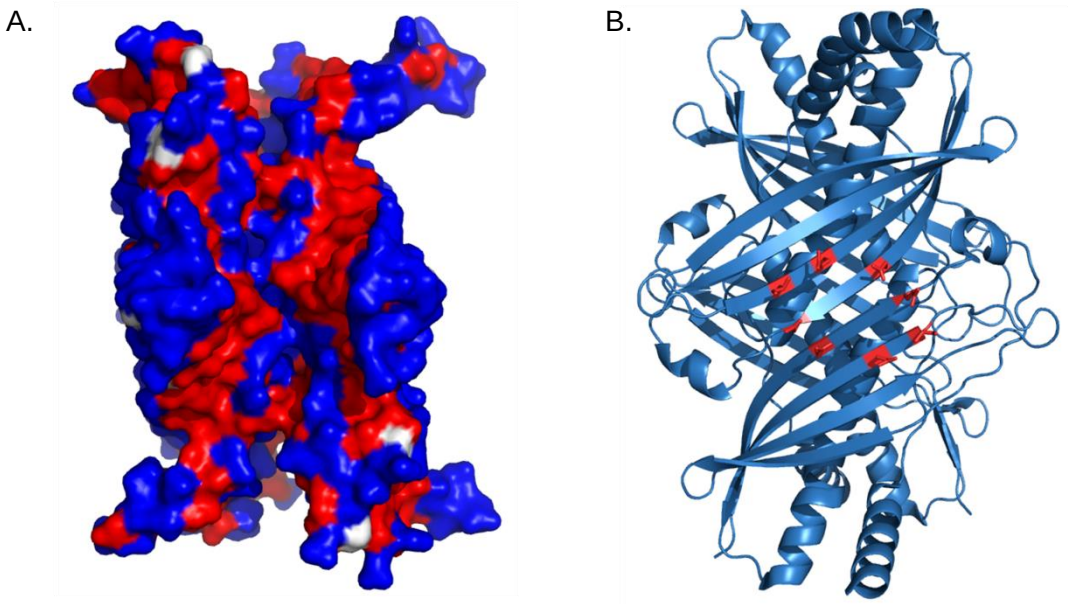

Figure 1-2. **Functional sites of the SecB tetramer from *Haemophilus influenzae*. A.** Peptide binding site. Neutral residues are colored in white; noncharged polar and charged residues are colored in blue and hydrophobic residues are colored in red. **B.** Residues in the SecB tetramer involved in binding to SecA are colored in red (PDB code: 1FX3; (Xu et al., 2000)).

A groove formed by the helix $\alpha 2$ and the strand $\beta 2$ of one SecB shows the expected properties of a peptide binding site [Fig. 1-2.A]. This groove is at the surface of the tetramer and accessible for binding of an unfolded polypeptide. The hydrophobic nature of the groove allows the chaperone to stabilize the unfolded preprotein by hydrophobic interactions. (Randall & Hardy, 2000; Randall et al., 1998). The groove of one subunit fuses with the groove of the neighboring subunit to form a 70 Å long binding site. A tetramer contains two binding sites, one on each sides of the oligomer. In addition to the chaperone function of SecB, it has been suggested that SecB could also be involved in the targeting process of the preprotein to the SecYEG channel (Hartl et al., 1990). Through a high affinity binding of SecB to the C-terminus of SecA, the preprotein could be transferred to the SecYEG-SecA translocation complex (Fekkes et al., 1998; Kimsey et al., 1995). Upon mutagenesis studies,

several research groups highlighted the residues which are involved in binding to SecA [Fig. 1-2.B] (Fekkes et al., 1997; Woodbury et al., 2000).

1-1-2. SecA, the motor protein

The motor protein SecA can be located either in the cytosol or as a membrane-bound protein (Cabelli et al., 1991) via binding to negatively charged phospholipids (Lill et al., 1990). SecA is an ATPase of the RecA family with a molecular weight of 100 kDa [Fig. 1-3].

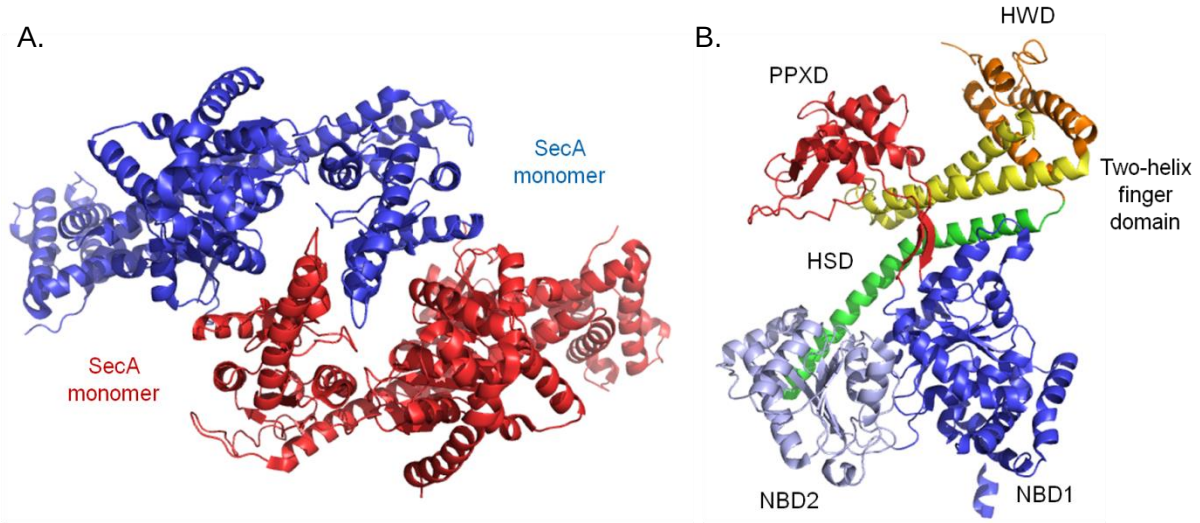

Figure 1-3. **Structure of SecA. A.** Crystal structure of a SecA dimer from *Escherichia coli* solved at 2 Å. The two monomers are represented in red and blue (PDB code: 2FSF, Papanikolau, Y. et al., *J Mol Biol* 366 (2007)). **B.** Crystal structure of a SecA monomer from *Bacillus subtilis* at 2.9 Å. The NBD1 domain is colored in dark blue, the NBD2 domain in light blue, the PPXD domain in red, the HSD domain in green, the HWD domain in orange and the two-helix finger motif in yellow. (PDB code: 1TF2, (Osborne et al., 2004)).

The crystal structure of SecA was solved in different functional states: with ADP, ATP or nucleotide analogues (Hunt et al., 2002; Osborne et al., 2004; Papanikolau et al., 2007), with a peptide (Zimmer & Rapoport, 2009) and in complex with SecYEG (Zimmer et al., 2008). Dimeric forms of SecA have been proposed, one is shown in figure 1-3.A. To date, no function could be assigned to dimeric SecA; structural and biochemical data indicate that the functional form is the SecA monomer (Osborne & Rapoport, 2007; Zimmer et al., 2008). A monomer of SecA is composed of 6 distinct domains, the nucleotide binding domains 1 and 2 (NBD1 and NBD2), the preprotein crosslinking domain (PPXD), the helical scaffold domain (HSD), the helical wing domain (HWD) and the C-terminal linker (CTL) [Fig. 1-3.B] (Papanikolau et al., 2007). The NBD domains contain the Walker A and B motifs and their interface forms the binding site for the ATP molecule. ATP hydrolysis takes place at the

same NBD1 / NBD2 domain interface. Preprotein binding is mediated by the PPXD and the NBD2 domains, which form a substrate binding clamp, together with the HSD domain (Cooper et al., 2008; Zimmer & Rapoport, 2009). The hydrophobic properties of the surface of the clamp confirm this hypothesis. As mentioned earlier, the CTL is important for SecB binding and for membrane localization. Notably, all the domains of SecA are shown to interact with the SecYEG complex except for the HWD domain (Das & Oliver, 2011; Mori & Ito, 2006; Zimmer et al., 2008).

As pointed out previously, SecA has been crystallized in different states. In the major part of the crystals, SecA was found to be a homodimer organized in an antiparallel manner. The question whether the dimer is the functional state of SecA is still unresolved even though the crystal structure of the SecA in complex with the SecYE translocon shows only one monomer of SecA [Fig. 1-4] (Zimmer et al., 2008).

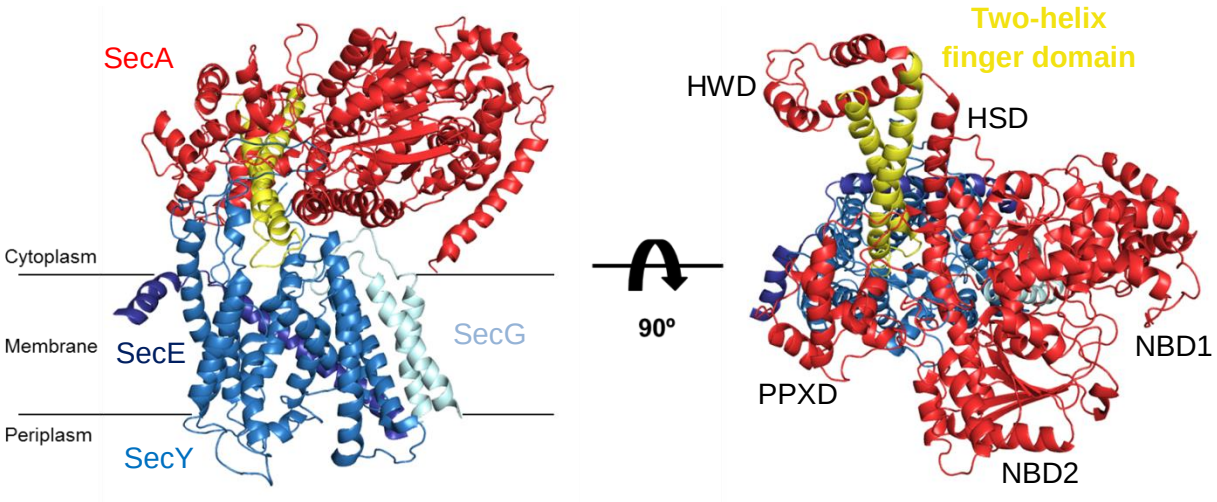

Figure 1-4. **Structure of the SecA-SecYEG complex from *Thermotoga maritima* at 4.5 Å.** View of the SecA-SecYEG complex from the plane of the membrane (**left**) and from the cytoplasmic side (**right**). The SecY is represented in light blue, SecE in dark blue, SecG in cyan and SecA in red. The two-helix finger domain of SecA is represented in yellow (PDB code: 3DIN; (Zimmer et al., 2008)).

This crystal structure reveals the binding interface of the SecA/SecY complex. The main interaction between SecA and SecYEG consists of the PPXD domain of SecA interacting with the cytoplasmic loops C4, C5 and C6 of SecY. Another contact is mediated by the HSD domain of SecA with the C-terminal tail of SecY. Interestingly, the binding surfaces for SecB and SecYEG are located on opposite sides of SecA. The crystal structures of SecA provided detailed mechanistic insight into its function during post-translational translocation.

1-1-3. The protein-conducting channel SecYEG

As mentioned in chapter 1 – part 1, the first detailed structure of the SecYEG complex was obtained by a crystal structure from an archeal homologue, *Methanococcus jannaschii*, which was solved at 3.2 Å resolution [Fig. 1-5] (Van den Berg et al., 2004).

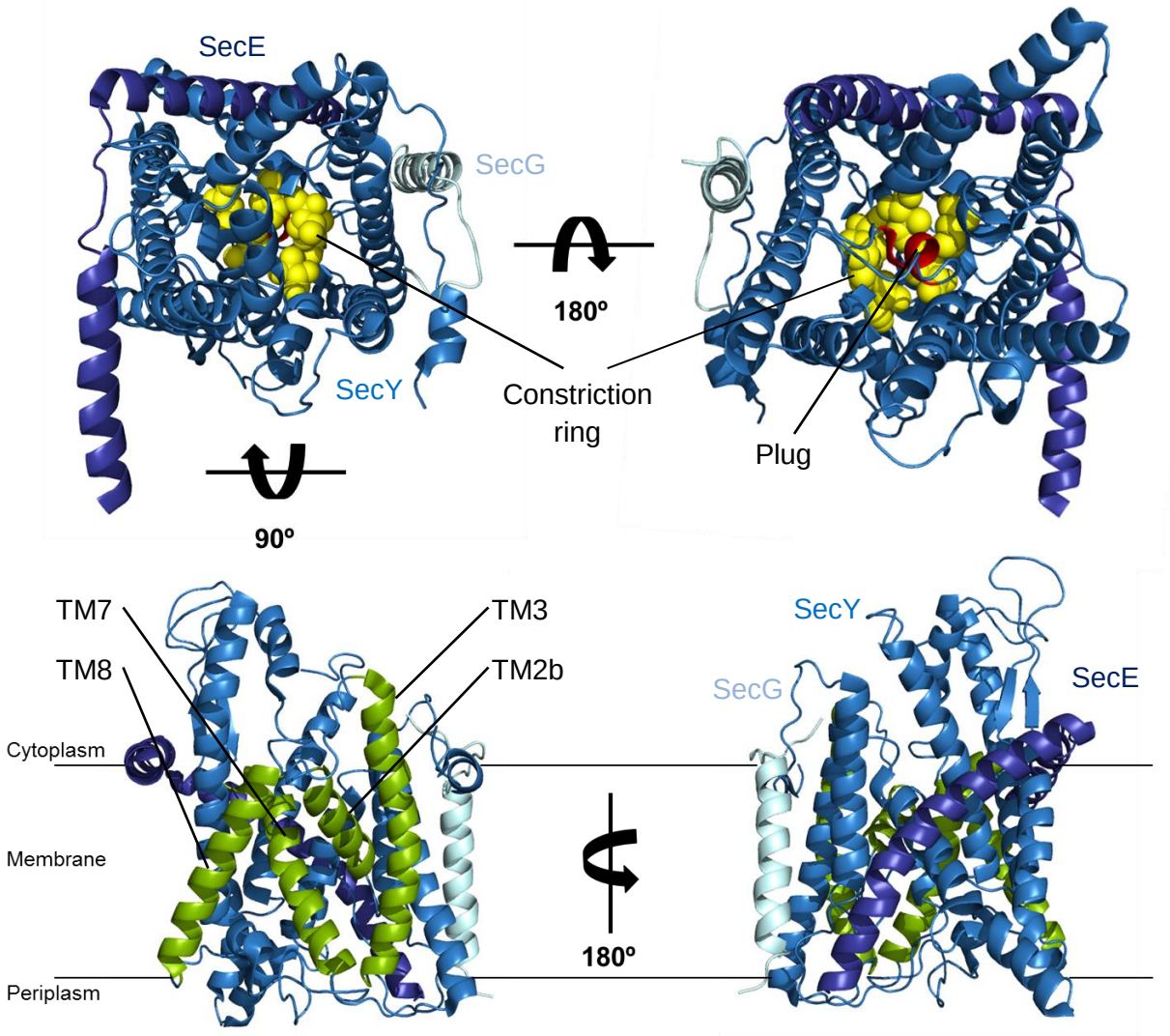

Figure 1-5. **Structure of the SecYEβ complex from *Methanococcus jannaschii* at 3.2 Å.** Cytoplasmic view (**top-left**), periplasmic view (**top-right**), front view (**bottom-left**) and back view (**bottom-right**). SecY is represented in blue, SecE in dark blue and the β subunit in cyan. Residues involved in the constriction ring are represented in yellow. The plug domain is represented in red. The transmembrane helices involved in the lateral gate are represented in green. The membrane bilayer is represented by the black lines. (PDB code: 1RHZ; (Van den Berg et al., 2004)).

In *E. coli*, SecYEG is composed of 15 transmembrane helices. The core protein SecY consists of 10 helices which are organized pseudo-symmetrically with transmembrane helices 1-5 on one side and transmembrane helices 6-10 on the other. As a channel, SecY needs to be sealed when translocation is not occurring to avoid leakage of ions and water.

By looking at the crystal structure from the membrane plane, SecYEG has an hourglass shape [Fig. 1-5]. The channel is closed in the middle by a constriction ring formed by hydrophobic residues. These residues are well conserved and their side chains are protruding into the center of the channel thus sealing it. Additionally, SecY contains a plug which blocks the periplasmic side of the channel [Fig. 1-5]. This plug domain is a short α-helix which is a part of the transmembrane domain 2a of SecY. Crosslinking of the plug domain to SecE which results in a translocon complex incapable of blocking the periplasmic side of the funnel, has been shown to be toxic for the cell (Harris & Silhavy, 1999). Based on electrophysiology experiments plug deletion also shows a leakage of ions (Saparov et al., 2007). Cysteine crosslinking experiments on the plug domain show movement of the plug domain away from the center of the channel during translocation of a polypeptide (Tam et al., 2005).

SecY is organized as a clamshell-like structure [Fig. 1-5]. This allows the complex to open laterally to the lipid bilayer in order to allow the insertion of a transmembrane segment. This was confirmed by crosslinking the signal sequence to lipids (Martoglio et al., 1995). The lateral gate is formed by the transmembrane segments 2b, 3, 7 and 8 [Fig. 1-5]. The segments 2 and 7 have been shown by crosslinking studies to interact with the signal sequence (Plath et al., 1998). Because 2 of the residues which form the constriction ring belong to transmembrane segments of the lateral gate, opening of the lateral gate is accompanied with widening of the channel. More recently, a structure was determined by electron crystallography of SecYEG which actually shows a signal sequence in the lateral gate (Hizlan et al., 2012). Molecular dynamics simulation suggests an additional role for the plug domain (Zhang & Miller, 2010). Zhang et al. suggested that the plug domain would stay close to its closed-state position and serve as a sensor to determine the hydrophobicity of the preprotein. Therefore, if a preprotein is highly hydrophobic the plug would remain close to guide the preprotein to the lateral gate for insertion into the lipid bilayer.

To stabilize the structure, SecE is thought to support the clamshell structure at the “back” of the channel formed by SecY (the “front” referring to the lateral gate) [Fig. 1-5]. The amount of transmembrane helices displayed by SecE varies from one to three transmembrane helices in different organisms, with a conserved domain corresponding to the linker region between the C-terminal transmembrane helix and the amphipathic helix which serves as a hinge (Murphy & Beckwith, 1994). Even though SecE is highly variable in size, the conserved domain of SecE is essential for the viability of the cell. It was shown by depleting SecE or by overexpressing SecY that SecY alone is unstable and degraded by the protease FtsH (Kihara et al., 1995).

SecG is not essential for the function of the translocon and its depletion is not lethal for the cell even though it inhibits the translocation efficiency. Reconstitution studies showed that the minimal complex required for translocation was composed of SecY and SecE (Brundage et al., 1990). In addition, crystal structures of the protein conducting channel often contain only SecY and SecE (Tsukazaki et al., 2008; Zimmer et al., 2008). However, SecG has been shown to speed up the translocation, especially at low temperature or when the proton motive force was disrupted (Hanada et al., 1993; Nishiyama et al., 1994; Nishiyama et al., 1993). Moreover, several studies suggest that the topological inversion of SecG (Nishiyama et al., 1996) would improve translocation by stimulating SecA (Matsumoto et al., 1998; Nagamori et al., 2002; Sugai et al., 2007). However crosslinking of SecG to SecY resulted in the same translational activity compared to a wild-type SecYEG translocon (van der Sluis, van der Vries, et al., 2006). Therefore the exact role of SecG in translocation remains unclear.

1-1-4. Mechanism of the post-translational translocation

After binding of a preprotein to SecB, the preprotein/SecB complex binds SecA and transfers the preprotein to SecA [Chapter 1 – part 1, figure 1].

Crystal structures of this intermediate complex are not available, but it was suggested that two subunits of one SecB tetramer could bind to one molecule of SecA (Xu et al., 2000). Subsequently, binding of ATP to the SecA/SecB complex destabilizes the complex and leads to release of SecB (Fekkes et al., 1997). Subsequently, the SecA/preprotein complex binds to SecYEG. During that step, the signal sequence of the bound preprotein adopts an α-helical shape (Chou & Gierasch, 2005) which is thought to bind to the substrate binding clamp of SecA [Fig. 1-6] (Zimmer et al., 2008). In subsequent events, the signal sequence of the preprotein is placed in proximity of the SecYEG pore. The crystal structure of SecA/SecYEG which corresponds to the state where the preprotein is bound to the clamp of SecA shows that the PPXD and the NBD2 domains place the preprotein right above the pore of SecYEG [Fig. 1-4] (Zimmer et al., 2008). After ATP hydrolysis, the signal sequence is likely transferred to SecYEG and inserted into the lateral gate of SecYEG (du Plessis et al., 2009; Egea & Stroud, 2010; Zimmer et al., 2008). This interaction causes an opening of the channel by displacement of the plug domain and an increase of the pore-ring diameter of SecY (Tam et al., 2005). The open state is stabilized by insertion of the following polypeptide segment into the pore (Zhang & Miller, 2010).

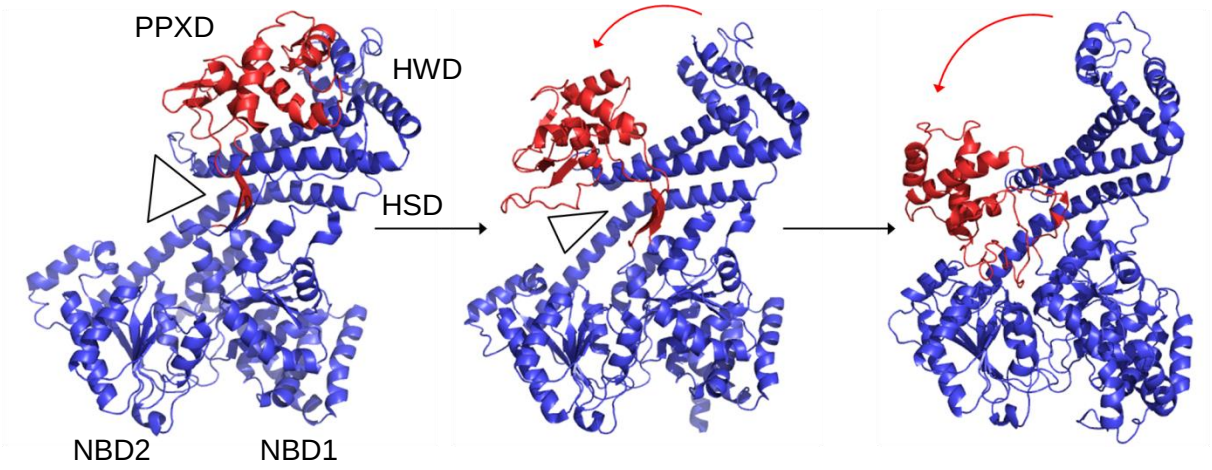

Figure 1-6. **The clamp movement of SecA during translocation of a preprotein.** Different crystal structures of SecA reflect the conformational states of the clamp of SecA, open (**left**) (PDB code: 1M74 Hunt et al., 2002), partially closed (**middle**) (PDB code: 1TF2, Osborne et al., 2004) and closed (**right**) (PDB code: 3DIN, Zimmer et al., 2008). SecA is represented in blue except for the PPXD domain which is represented in red. The black triangles represent the opening of the clamp. The red arrows show the movement of the PPXD domain during the closure of the clamp (adapted and modified from (Park & Rapoport, 2012)).

The following ATP hydrolysis cycle has been shown to allow the passage of approximately 30 to 40 amino acids through the channel (Schiebel et al., 1991). Several models are currently debated regarding the active translocation of the polypeptide through the pore. In the first model, the so-called “power-stroke model” (Erlandson et al., 2008), preprotein translocation is mediated by ATP binding to the NBD domains of SecA, followed by opening of the clamp [Fig. 1-6] and conformational change of the two-helix finger of the HSD domain of SecA which will push it into the channel. In agreement with this model, it has been shown that the tip of the two-helix finger was indeed binding to the preprotein (Erlandson et al., 2008). This is further supported by the crystal structure of the SecA/SecYEG complex, where the two-helix finger is inserted into the cytoplasmic funnel of the channel and the tip is directly located above the translocation pore [Fig. 1-4]. After ATP hydrolysis, the two-helix finger would reset its position, and the clamp would capture the polypeptide again and prepare for the next cycle of ATP hydrolysis. More recently, crosslinking of the SecA two-helix finger to SecY by a disulfide bond indicated that the movement of the SecA two-helix finger is not crucial for the preprotein translocation (Whitehouse et al., 2012).

The second model is the “Brownian ratchet model” (Tomkiewicz et al., 2007). According to this model, the role of the SecA ATPase activity is to avoid any backward movements of the preprotein which is translocated by Brownian motion through SecY. SecA traps the preprotein within the “clamp” and allows the movement only in one direction.

However, this model cannot explain the step-wise translocation mechanism observed previously (Schiebel et al., 1991).

1-2. YidC acts as a Sec-independent translocase and as a molecular chaperone in complex with SecYEG

As mentioned in chapter 1 – part 1, YidC can work in two contexts, either in a Sec-independent or in a Sec-dependent pathway. YidC is composed of six transmembrane helices and a large periplasmic loop (called P1 domain) connecting the transmembrane helix 1 and the transmembrane helix 2. Interestingly, even though the P1 domain represents more than 50% percent of the protein and is conserved in gram negative bacteria, the function of this large periplasmic domain remained enigmatic. It has been shown that if 90% of this domain is deleted, the membrane insertion of proteins and the cell growth are not affected in *E. coli* (Jiang et al., 2003; Xie et al., 2006). Therefore, the insertase activity of YidC seems to be located in the transmembrane helices 2 to 6 including ~20 amino acids from the C-terminal part of the P1 domain. In fact, this part of YidC is conserved in mitochondria and chloroplasts (A. Kuhn et al., 2003). More recently, it has been shown by disulfide crosslinking that YidC transmembrane helices 2, 3 and 5 are responsible for the substrate binding in the context of membrane insertion (Klenner & Kuhn, 2012).

YidC can interact with a lot of partners. Firstly, YidC is able to dimerize (Lotz et al., 2008) but whether the dimer or the monomer is the active form is still under debate. Second, co-purification studies showed that YidC is forming a complex with SecDF-YajC (Nouwen & Driessen, 2002). Deletion constructs indicate that this interaction is mediated by SecF and that the residues 215−265 of the periplasmic loop of YidC are crucial for binding to SecF (Xie et al., 2006). It has been suggested that this interaction between YidC and SecDF-YajC is required to associate YidC with SecYEG (Chen et al., 2005; Nouwen & Driessen, 2002; Xie et al., 2006). More recently, Sachelaru et al. showed that YidC was not only interacting with SecDF but also directly contacts the core translocon SecYEG (Sachelaru et al., 2013). Crosslinking experiments indicate that YidC interacts with several residues located in the lateral gate of SecY. Furthermore, these contacts were not dependent on the presence of SecDF-YajC, even though they were weaker in the absence of SecDF-YajC (Sachelaru et al., 2013). Moreover, the SecYEG-YidC contacts seem to become dynamic upon binding of 70S or ribosome-nascent-chain complex. Additional crosslinking experiments showed direct interactions of YidC with substrates when associated with SecYEG (Urbanus et al., 2001). The crosslinks showed that YidC was interacting with transmembrane segments of translocated proteins at the exit from the lateral gate of SecY. This finding suggests that YidC plays a role in the release of the preprotein from the lateral gate to the lipidic environment

and could play a role as chaperone by ensuring the correct topology and the correct assembly of multi-spanning membrane protein (Beck et al., 2001; Wagner et al., 2008). Furthermore, based on crosslinking and co-purification results which showed that YidC was interacting with FtsH, it has been suggested that YidC could also be implicated in the quality control of membrane protein (van Bloois et al., 2008). Taken together, these results indicate that YidC despite its relatively small size (63 kDa) is a very dynamic membrane protein that can act alone or in complex with numerous factors exerting different functions.

Oxa1 in mitochondria, which is homologous of YidC can form a complex with the ribosome via its C-terminal domain (Jia et al., 2003). By single particle cryo-EM, Kohler et al. were able to determine the structure of YidC bound to a ribosome nascent chain complex (RNC) [Fig. 1-7] (Kohler et al., 2009).

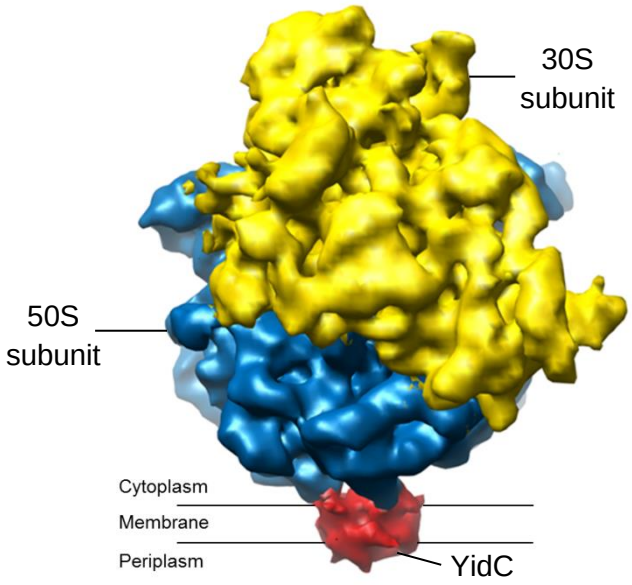

Figure 1-7. **Structure of YidC bound to a translating ribosome from *Escherichia coli* at 14.4 Å resolution.** The large subunit of the ribosome is represented in blue, the small subunit in yellow and the dimer of YidC in red. The membrane bilayer is represented by the black lines. (image taken and adapted from the EMDB website; EMDB code: EMD-1615; (Kohler et al., 2009)).

Thus, YidC can associate with the ribosome to act as a translocase in a co-translational manner (Kohler et al., 2009; Sachelaru et al., 2013).

1-2-1. Structure of the YidC periplasmic domain

The only high resolution information available for YidC is the crystal structure of the periplasmic domain P1 of YidC [Fig. 1-8] (D. C. Oliver & Paetzel, 2008; Ravaud et al., 2008). The periplasmic loop is organized in a *beta*-sandwich motif constituted of 2 *beta*-sheets (18 *beta*-strands in total) and of 3 *alpha*-helices. Many conserved residues are involved in the interaction between *alpha*-helix 3 and *beta*-sheet 2 suggesting that this interaction may have a functional or structural role (D. C. Oliver & Paetzel, 2008).

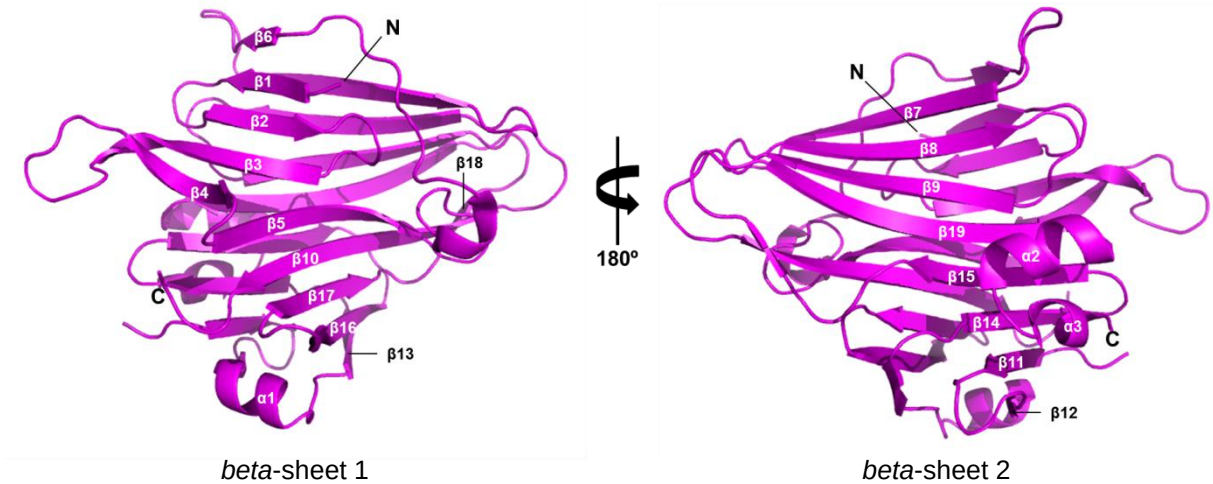

beta-sheet 1 *beta*-sheet 2

Figure 1-8. **Structure of the periplasmic domain of YidC from *Escherichia coli* solved at 1.8 Å.** *alpha*-helices and the *beta*-strands forming the *beta*-sheet 1 (**left**) and the *beta*-sheet 2 (**right**) are labeled. The N- and C-terminus are labeled respectively N and C. (PDB code: 3BS6; (Ravaud et al., 2008)).

In addition, the structure allows the localization of the important areas identified in biochemical analysis. The C-terminal part of the P1 domain which was characterized by Xie et al. as important for cell viability and insertase activity corresponds to the *alpha*-helix 3 (Ravaud et al., 2008; Xie et al., 2006). *beta*-strand 11-15 and *alpha*-helix 1 are the residues likely to be responsible for the binding to SecF [Fig. 1-9] (Xie et al., 2006).

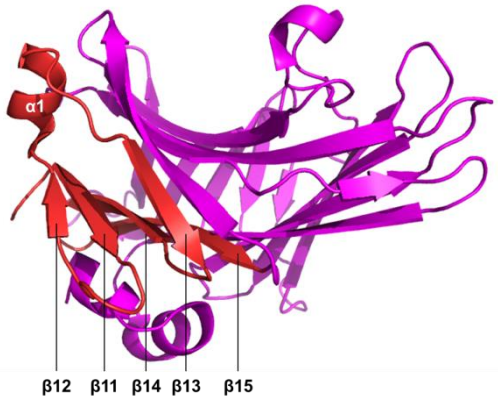

Figure 1-9. **Map of the SecF interaction with the periplasmic domain of YidC.** Residues which are involved in the binding of SecF are represented in red and the *beta*-strands and the *alpha*-helix are labeled (PDB code: 3BS6; (Ravaud et al., 2008)).

This surface is composed of a negatively charged patch next to a positively charged patch, indicating that the interaction between SecF and YidC may be electrostatic. However, this could not be observed by NMR titration or isothermal titration calorimetry experiments suggesting that this interaction might be transient and might have a low affinity binding (Ravaud et al., 2008; Xie et al., 2006).

The presence of a PEG molecule bound to an elongated cleft in the YidC periplasmic domain suggests a possible binding pocket for an elongated peptide or acyl chain in P1 [Fig.

1-10] (Ravaud et al., 2008). This cleft is formed by 22 residues on the surface of *beta*-sheet 1. The cleft is predominantly hydrophobic and formed by conserved residues located in the center of the binding cleft. This finding implicates that the P1 domain of YidC could interact directly with the periplasmic parts of the translocated substrates.

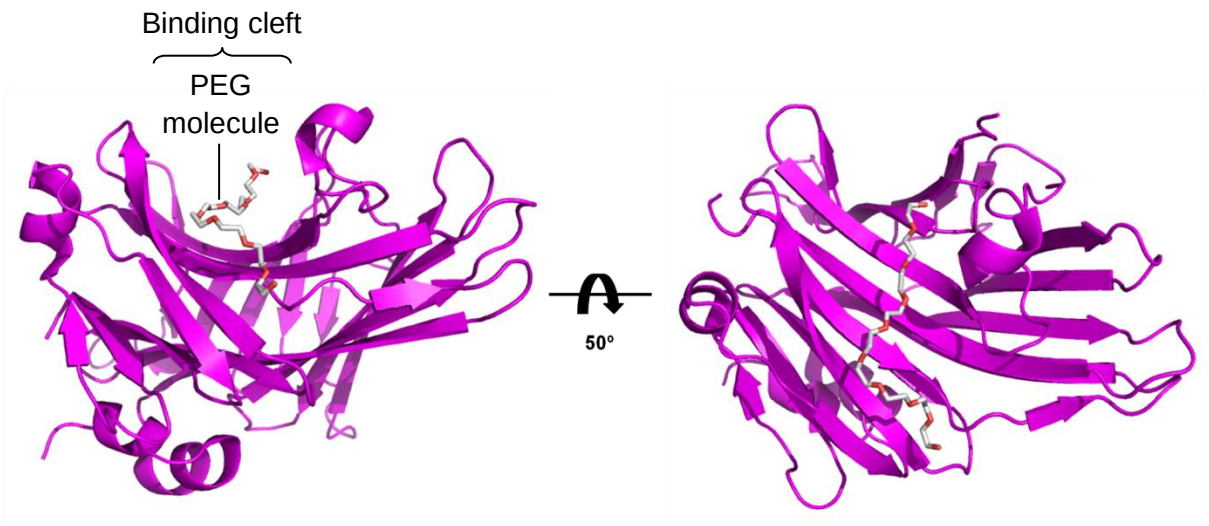

Figure 1-10. **Binding cleft of the periplasmic domain of YidC.** The PEG molecule is shown in a stick representation. (PDB code: 3BS6; (Ravaud et al., 2008)).

One region of the P1 domain (residues 323-346) is suggested to link the periplasmic loop to the membrane and has been shown to be crucial for cell viability and the insertase function (Jiang et al., 2003; Xie et al., 2006). Furthermore, bioinformatics analyses gave more information about the residues 330-346: the alpha-helix 3 seems to be composed of 9 additional residues (residues 323-338) and seems to have a hydrophobic C-terminus which will allow interaction with the membrane. In addition, the following amino acids (residues 340-355) are predicted to be an amphipathic helix which could interact or insert into the membrane. The orientation of the P1 domain and how it is exactly connected to the membrane part is still enigmatic.

1-3. The accessory domain SecDFYajC

1-3-1. Structure/function of SecDF

The structural and biochemical characterization of SecDF provided detailed insight in the function of this accessory membrane complex. The crystal structure of *Thermus thermophilus* SecDF was solved at 3.3 Å resolution and structure based mutations were used to understand the role of SecDF in the translocation event [Fig. 1-11] (Tsukazaki et al., 2011).

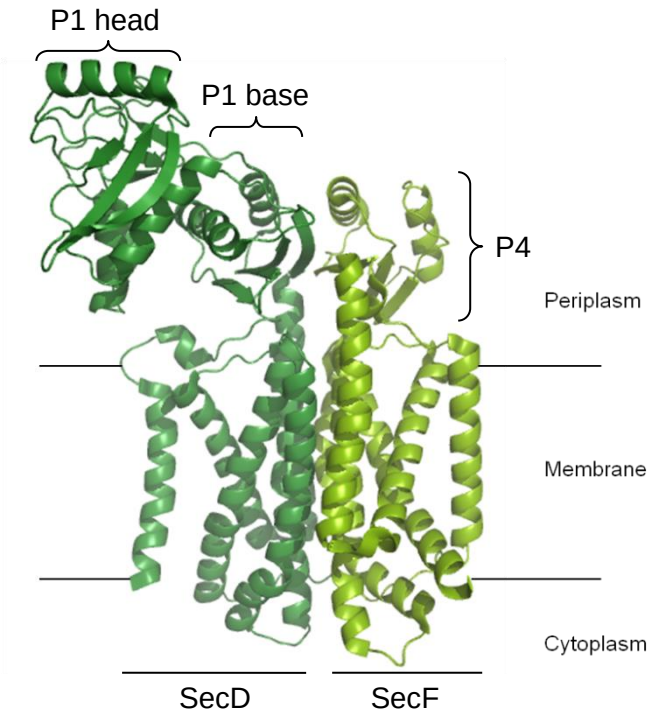

Figure 1-11. **Structure of SecDF from *Thermus thermophilus* at 3.3 Å.** The part corresponding to SecD is represented in dark green and the part corresponding to SecF domain in light green. The membrane bilayer is represented by the black lines. (PDB code: 3AQP; (Tsukazaki et al., 2011)).

Contrary to *E. coli* where SecD and SecF are composed as a heterodimer containing 6 transmembrane segments each, *T. thermophilus* SecDF is composed of a single chain containing 12 transmembrane helices. The interface between SecD and SecF is formed by the transmembrane helices 4 and 10. The complex contains two large periplasmic domains called P1 (SecD periplasmic domain) and P4 (SecF periplasmic domain). Previous experiments indicated that that the SecDF complex accelerates translocation by SecYEG by using the proton motive force (PMF) (Arkowitz & Wickner, 1994; Duong & Wickner, 1997a). Furthermore, it was suggested that SecDF could play a role in the late stage of the translocation when the preprotein interacts with the periplasmic domains of SecD and SecF (Matsuyama et al., 1993; Nouwen et al., 2005; Schiebel et al., 1991). The structure of the isolated P1 domain indicated that the SecD periplasmic domain was composed of a base and a head subdomain (Tsukazaki et al., 2011). The P1 base has a similar structure to the SecF P4 domain. Superposition of the P1 domain alone and the SecDF structure indicated that this P1 domain can rotate 120 degrees around the hinge region between the head and base and thus adopt at least two different conformations called F and I [Fig. 1-12]. These conformations were confirmed by crosslinking experiments and complementation analyses indicated that the two forms were present *in vivo*. Thus, this conformational change is likely to be crucial for the function of SecDF (Tsukazaki et al., 2011).

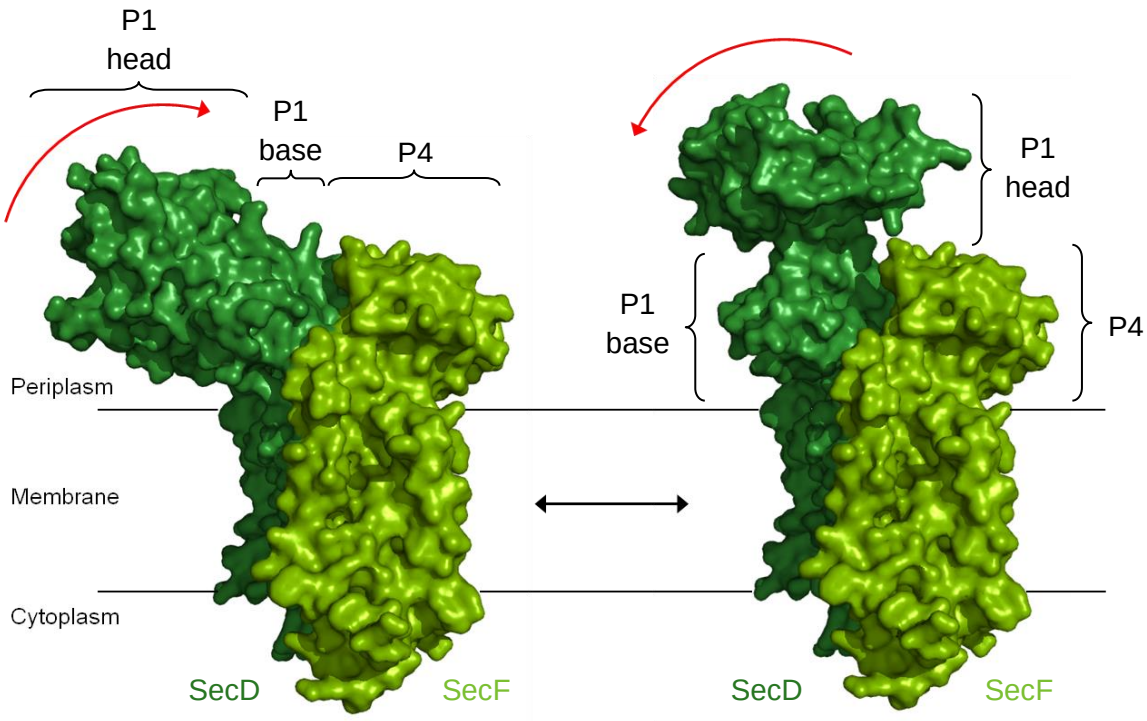

Figure 1-12. **Conformational change of the P1 head domain of SecDF.** Movement between the F form (**left**) and I form of SecDF (**right**) are represented by the red arrows. The SecD domain is represented in dark green and SecF domain in light green. The membrane bilayer is represented by the black lines. (PDB code: 3AQP and 3AQO; (Tsukazaki et al., 2011)).

Furthermore, Tsukazaki et al. analyzed the role of SecDF in the translocation process. They confirmed that in *in vitro* translocation experiments, SecDF is required as well as the proton motive force for ATP-independent translocation (Schiebel et al., 1991; Tsukazaki et al., 2011). SecDF belong to the resistance nodulation and cell division superfamily (RND). In fact in the crystal structure, the transmembrane domains of SecD and SecF are assembled pseudo-symmetrically like in AcrB (Tsukazaki et al., 2011). Mutation of conserved SecDF residues which are important for function of AcrB resulted in SecDF variants which were inactive in patch clamp experiments (Tsukazaki et al., 2011). These residues are located at the interface of SecD and SecF and are thought to be involved in the proton transport through the membrane.

Previously it was suggested that the periplasmic domain P1 of SecD could bind an unfolded protein like the preprotein which would come out of the translocon (Matsuyama et al., 1993; Tsukazaki et al., 2011). In patch clamp experiments, a mutant which lacked the head domain of P1 was inactive in proton transport (Tsukazaki et al., 2011). This finding is supported by Matsuyama et al. who showed that pretreating spheroplasts with anti-SecD IgG was blocking the secretion of proOmpA and preMBP (Matsuyama et al., 1993). Furthermore, based on time course experiments they showed that SecD was involved in late stage of the

release of the preprotein. Taken together, these results suggest that SecD is involved in the release of the preprotein as soon as it crosses the SecYEG channel and that the proton motive force may be the energy source for the conformational change occurring in the head domain of P1.

These findings allowed to suggest a possible model of the translocation process by the SecYEG-SecDF complex in the presence of a proton motive force [Fig. 1-13] (Tsukazaki et al., 2011). In that model, after binding of SecA or the RNC on the holotranslocon, the translocation of the protein will start with the binding of the signal (anchor) sequence to the lateral gate inducing its opening and the enlargement of the central pore of the channel. The translocation of the protein in the channel will continue until the nascent chain/preprotein interacts with the periplasmic domain of SecD preventing any backward movement. In a second step, by using the proton motive force as energy, SecD will undergo a conformational change [Fig. 1-12] where its periplasmic domain will pull the substrate. If a second hydrophobic sequence is detected as a possible transmembrane domain, the initial signal sequence could be transferred to YidC and the next transmembrane segment could stabilize the opening of the gate. After that, SecD could return to its F form and wait for another round of interaction with the translocation substrate.

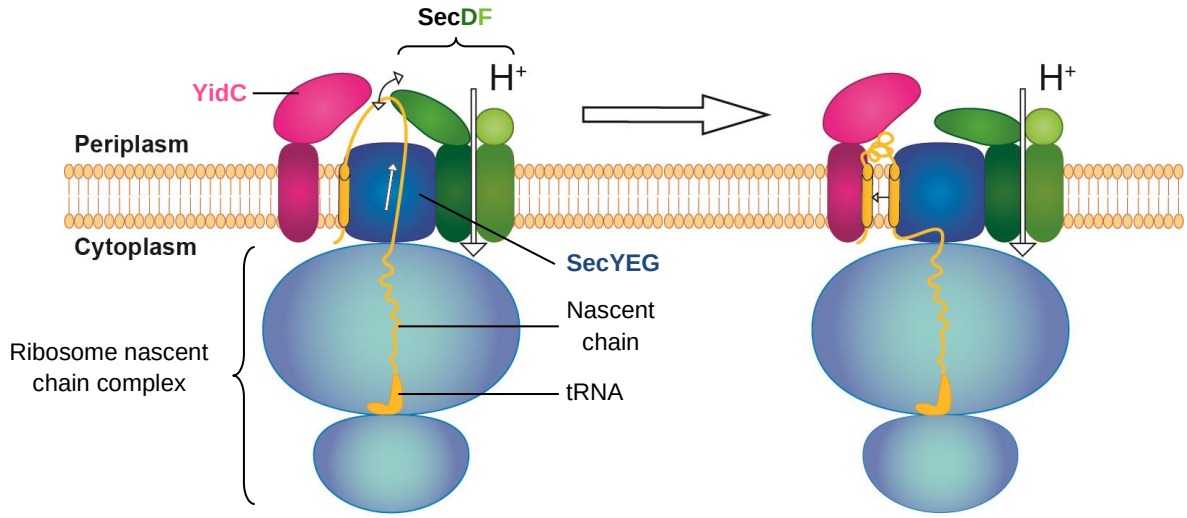

Figure 1-13. **Proposed model of the role of SecDF and the PMF in the translocation process.** The ribosome is colored in light blue, the P-site tRNA and the nascent polypeptide chain in yellow, YidC in magenta, SecYEG in blue, SecD in dark green, SecF in light green, lipids in orange. The movement of proton is represented by the white arrow. (adapted and modified from (Tsukazaki et al., 2011)).

1-3-2. YajC, a single helix membrane-spanning protein

SecDF can form a complex with YajC (Duong & Wickner, 1997a; Nouwen & Driessen, 2002). YajC is a small membrane protein of 110 amino acids. YajC is not needed for the function of the holotranslocon (Duong & Wickner, 1997a) and the exact role of YajC is not known. A structure of a part of YajC (residues 19 to 55) has been solved in complex with AcrB, a homolog of SecDF [Fig. 1-14] (Törnroth-Horsefield et al., 2007).

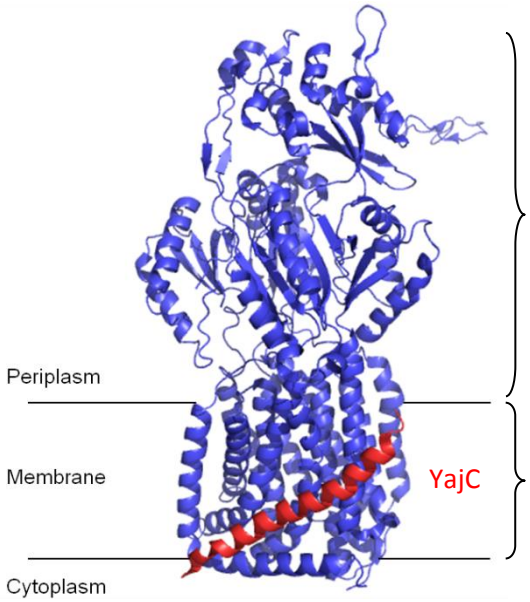

Figure 1-14. **Structure of YajC in complex with a monomer of AcrB from *Escherichia coli* solved at 3.5 Å resolution.** YajC is represented in red and the monomer of AcrB is represented in blue. The membrane bilayer is represented by the black lines. (PDB code: 2RDD; (Törnroth-Horsefield et al., 2007)).

In the AcrB-bound context, YajC forms a long tilted helix in the membrane plane and interacts with the transmembrane domain of AcrB at the interface with the lipids. As AcrB is a homolog of SecDF, it is suggested that YajC will bind in the same manner to SecDF.

Recently, based on this structure, Fang and Wei undertook to characterize YajC in more details (Fang & Wei, 2011). Using secondary structure prediction tools and circular dichroism spectroscopy, they determined that YajC contained 2 α-helices on the N-terminus and 5 short β-strands on the C-terminus. Regarding the N-terminal and C-terminal part of YajC, the crystal structure showed additional disjoint densities which could fit these domains (Törnroth-Horsefield et al., 2007). In order to check the topology of YajC in the membrane, the authors performed a biotin labeling and a topology assay to localize precisely the N- and C-terminus of YajC. They found that the C-terminus of YajC was localized in the cytoplasm and that the N-terminus was embedded in the membrane. Tryptic digestion, circular dichroism spectroscopy and gel filtration analysis suggests that the C-terminal part of YajC forms a soluble and compact domain, which forms a homotetramer. It has been shown that YajC is expressed in the cell at a higher level than SecDF, with ~200 copies of YajC

compared to ~30 copies of SecDF (K. J. Pogliano & J. Beckwith, 1994). Most likely, YajC exists in different forms in the cell, in complex with AcrB, in complex with SecDF, in complex with unknown partners or forming homo-oligomers (Fang & Wei, 2011; Törnroth-Horsefield et al., 2007).

1-4. Co-translational translocation components

During co-translational translocation, the most important partner of SecYEG is the ribosome. The ribosome will initiate the opening of the channel and supply the energy required for the translocation. Several cryo-EM structures are available providing insights into the binding and function of the RNC-SecYEG complex [Fig. 1-15] (Frauenfeld et al., 2011; Ménétret et al., 2007; Mitra et al., 2005). The most recent structure was obtained after reconstitution of the SecYEG complex into nanodiscs which mimics the membrane environment (Bayburt et al., 2002). The use of a stalled intermediate of a translating ribosome allows analysis of an early state of co-translational translocation and its effect on the SecYEG conformation. In addition to the helices of the SecYEG complex, another helix was observed. After generation of an atomic model by flexible fitting of the crystal structures, this extra helix was fitted in the lateral gate of the SecYEG channel and thus could represent the signal anchor sequence. . In agreement with the previous studies using Sec translocon in a detergent solubilized state (Beckmann et al., 2001; Ménétret et al., 2007; Mitra et al., 2005), a gap of about 15-25 Å was visualized between the ribosome and the SecY channel. This gap has been suggested to allow the folding of cytoplasmic loops of membrane proteins. The main contacts between the ribosome and the SecYEG complex are formed by the cytoplasmic loops C6 and C8 of SecY with ribosomal RNA helices and with ribosomal protein L23. Furthermore, an additional contact between SecE and the ribosomal proteins L23 and L29 was reported (Frauenfeld et al., 2011).

In the cryo-EM structure with the SecYE nanodisc, the rRNA helix 59 seems to contact the lipids which are in proximity of the lateral gate (Frauenfeld et al., 2011). Molecular dynamics simulation confirmed these findings. Based on these results, Frauenfeld et al. suggest that the contact between the ribosome and the membrane in proximity to the lateral gate could facilitate the insertion of the transmembrane helices into the bilayer by destabilizing the membrane and therefore minimizing the energy required by the transmembrane domain to enter the lipid bilayer. This implicates that the ribosome does not only act only as the motor of the translocation but is also a catalyst of the membrane insertion event.

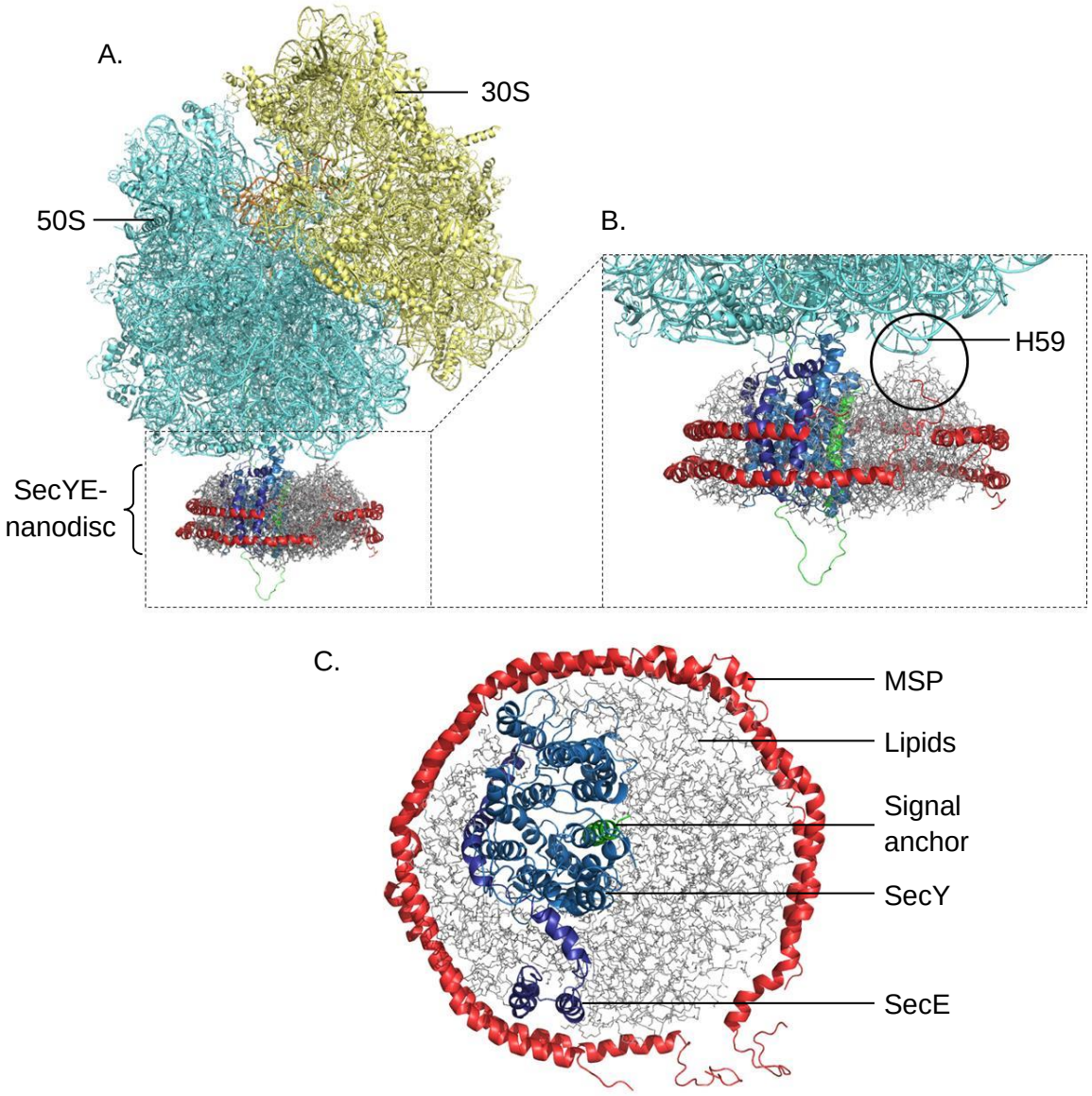

Figure 1-15. **Ribosome-SecYE complex in a nanodisc. A.** Atomic model of the ribosome-SecYE complex in a nanodisc based on cryo-EM reconstruction. **B.** Zoom into the region of interaction between SecYE and the ribosome. The black circle highlights the interaction between the ribosome and the lipid bilayer. **C.** Organization of the SecYE and the signal anchor sequence within the nanodisc view from the cytoplasmic side. MSPs are represented in red, SecY in blue, SecE in dark blue, the ribosomal large subunit in light blue, the ribosomal small subunit in yellow, tRNA in orange, the nascent chain in green and the lipids in gray. (PDB code: 3J00, 3J01; (Frauenfeld et al., 2011)).

An additional SecYEG binding partner involved in co-translational targeting and translocation is the SRP receptor FtsY. This was shown by crosslinking and fluorescence resonance energy transfer (FRET) measurements (Angelini et al., 2005; P. Kuhn et al., 2011). After binding of the RNC-signal recognition particle (SRP) complex to FtsY, the subsequent interaction of FtsY with SecY is required to handover the RNC from the SRP to the translocon. Furthermore, Kuhn et al. provided evidence that the binding site used by FtsY,

the cytoplasmic loops C4 and C5 of SecY are also involved in the binding of other partners like SecA or RNCs. Based on the crystal structure [Fig. 1-5], these cytoplasmic loops are protruding in the cytosol (Cheng et al., 2005; P. Kuhn et al., 2011; Mori & Ito, 2006). Therefore, Kuhn et al. suggested that this shared binding site could serve as a sensor to determine the occupancy of a SecYEG complex.

1-5. Aim of this study

The structure and function of SecYEG complex and its partners have been studied extensively during the last decades. However, the exact interactions which would yield to a holotranslocon "supercomplex" composed of SecYEG, SecDFYajC and YidC remain unclear. This is mostly due to the fact that until recently the holotranslocon complex could not be purified in sufficient quality and quantity. Consequently, the role of such a complex and the role of the accessory proteins have not been studied to date. Here, we establish the purification of the SecYEG-SecDFYajC-YidC holotranslocon. We use the purified complex consisting of seven membrane proteins for biophysical analyses and single-particle cryo-electron microscopy (EM) to characterize the precise organization of this complex. This study aims to reveal the stoichiometry and molecular organization of the holotranslocon and to shed light on the functional interplay of its subunits.

Based on a previous study which showed that it is possible to overexpress and purify a SecYEG-SecDF-YidC complex (Bieniossek et al., 2009), we established a purification protocol yielding homogenous holotranslocon and SecDFYajC -YidC subcomplexes with the aim to study their structure by electron microscopy.

A high resolution cryo-EM structure would allow us to generate a quasi-atomic model of the holotranslocon complex by fitting the available crystal structure of the subunits into the EM density. Such a quasi-atomic model would reveal the molecular interactions of the different subunits of the holotranslocon which could be challenged subsequently by mutagenesis or crosslinking experiments.

Chapter 2 : Holotranslocon purification optimization

Résumé en français / French summary

Une étude pilote décrivant le système d'expression ACEMBL pour des complexes mutli-protéiques ainsi que la première purification de l'holotranslocon a montré que ce complexe peut être surexprimé, solubilisé à l'aide de détergent et purifié (Bieniossek et al., 2009). Cependant, les analyses suivantes par microscopie électronique à coloration négative ont mis en évidence un échantillon hautement hétérogène. De plus, la stœchiométrie des sous-unités variait entre les purifications. C'est pourquoi le protocole de purification a nécessité une optimisation afin d'obtenir un matériel de qualité suffisante afin de mener une étude de biologie structurale par cryo-microscopie électronique. Pour ce faire, nous avons testé plusieurs constructions exprimant l'holotranslocon, et avons obtenu un échantillon de qualité supérieure en co-exprimant YajC avec une étiquette CBP. Un complexe incluant les sept protéines membranaires a pu alors être purifié de manière homogène grâce au système de purification Ni-NTA et chromatographie d'affinité pour la calmodulin suivis par une étape de centrifugation sur gradient de glycérol combiné avec du glutaraldéhyde.

2-1. Holotranslocon expression

The holotranslocon is a membrane protein complex consisting of 7 membrane proteins, SecY, SecE, SecG, SecD, SecF, YajC and YidC. In order to be able to express such a large complex, with 34 transmembrane helices, we used the ACEMBL technology which was developed in collaboration with the Berger laboratory (Bieniossek et al., 2009). This approach allows recombinant production of challenging multiprotein complexes in bacteria in a rapid, flexible and automatable manner. Different plasmids were generated, one containing 6 genes (SecYEGDF-YidC), three containing 7 genes (SecYEGDF-YidC-YajC) and one encoding for SecDF-YajC-YidC [Fig. 2-1].

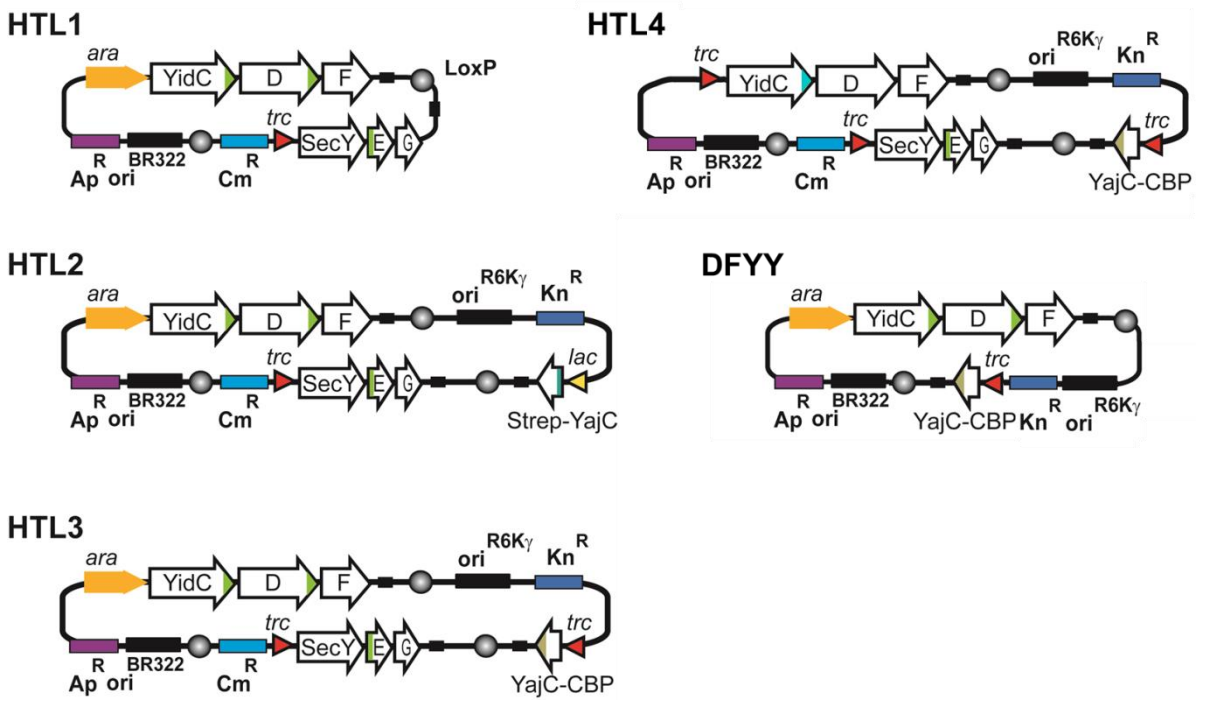

Figure 2-1. **Holo-translocon expression constructs based on the ACEMBL expression system.** HTL1 (**top-left**) consists of the pACE acceptor and the pDC donor vector combined by Cre-loxP fusion (LoxP, grey circles). A polycistron encoding for YidC, SecD (D), SecF (F) with an arabinose promoter (ara, yellow) has been subcloned into pACE. A second polycistron encoding for SecY, SecE (E) and SecG (G) with a trc promoter (trc, red) has been cloned into pDC. HTL2 (**middle-left**) is a fusion of the HTL1 construct with the donor vector pDK encoding Strep-tagged YajC with lactose promoter (lac, yellow). HTL3 (**bottom-left**) is a fusion of HTL1 with pDK encoding CBP-tagged YajC with trc promoter. HTL4 (**top-right**) is a HTL3 based construct with a Strep-tagged YidC and a tag-free SecD where all genes are under the control of a trc promoter. DFYY (**bottom-right**) is a fusion of the previous pACE and pDK vectors. The position of hexahistidine-tags in YidC, SecD and SecE is indicated in green. The position of the CBP-tag in YajC is indicated in grey. The transcription terminators are shown as black squares. Origins of replication (BR322 and R6Kγori) are indicated. Antibiotic resistance genes confer resistance to the following antibiotics: Ap, ampicillin; Cm, chloramphenicol and Kn, kanamycin.

The initial construct HTL1 was designed in order to express the main components of the holotranslocon which are known to be essential for *E. coli*. This plasmid did not encode the YajC protein which is not essential for *E. coli* viability (Duong & Wickner, 1997a). In order to generate a construct containing all the known subunits of holotranslocon, HTL2 was designed including YajC encoded by a donor vector. In that construct, a Strep-tagged YajC was under the control of a lactose promoter. This strategy was causing problems of stoichiometry because of the usage of three different promoters. In fact, expression of Strep-tagged YajC could never be detected by Western blotting (not shown). Therefore, the HTL3 construct was generated. This construct was showing good yields of expression for all seven proteins. The HTL4 strategy was developed in order to have a different tag on each subcomplex of the holotranslocon. Strep-tagged YidC, His-tagged SecYEG and CBP-tagged SecDF-YajC would allow isolating holotranslocon complexes only by three subsequent affinity purification steps. The initial test with the HTL4 construct showed however a rather weak expression compared to the previous constructs. This could be caused by the leakiness of the trc promoter. For this reason and because the work done so far with the HTL3 construct was progressing well concerning the expression tests and the purification trials, we decided to use the HTL3 construct and the DFYY construct [Fig. 2-1] for further experiments.

After choosing our construct, the first task was to optimize the expression of the holotranslocon complex and the DFYY subcomplex in order to obtain as much material as possible. We tested the expression of our constructs using two different strains which are commonly used for membrane protein expression, BL21Star (DE3) (Invitrogen) and C43 (DE3) (Miroux & Walker, 1996). These strains minimize potential toxicity associated with the over-expression of membrane proteins. The cells were grown in 2xYT medium. Expression of the holotranslocon (HTL) was induced by addition of 0.5mM IPTG and 0.2% L-arabinose. After 3 hours of induction, expression levels were analyzed by SDS-PAGE analysis [Fig.2-2].

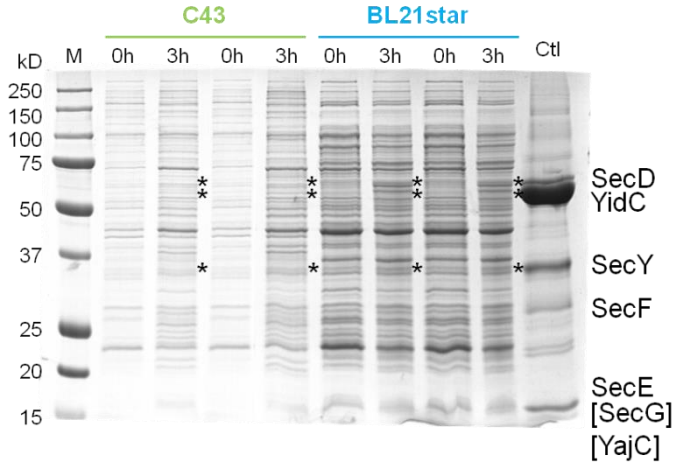

Figure 2-2. **Holo-translocon expression test.** Whole cells were analyzed on a coomassie-stained SDS-PAGE gel. Samples were taken before (0h) and after induction (3h). Four different cell cultures were analyzed, two for the culture using C43 cells and two for the culture using BL21 Star (DE3) cells. The same volume of cell culture was loaded for each condition. Purified HTL has been used as control (Ctl). The asterisks show the positions of the proteins of interest.

Using BL21 Star (DE3) as expression strain, we were able to express HTL3 and DFYY with good yields. The expression level was high enough to be able to localize the induced proteins of interest within the whole cells on a SDS-PAGE. Regarding the expression of the complexes in the C43 cells, the growing phase was slower compared to the expression using BL21 Star (DE3). Under the same growth conditions, reaching the optical density (OD) required for induction (OD_{600nm} = 0.6) was taking twice the time for C43 compared to BL21 Star (DE3) cells. Therefore, the BL21 Star (DE3) strain was chosen for the expression of the HTL3 and DFYY constructs in the subsequent experiments.

2-2. Holotranslocon affinity purification

With the confidence that the proteins of interest were expressed with good yields, we next optimized the purification scheme in order to obtain homogenous material for biochemical characterization and electron microscopy studies. After expression, membranes were prepared using a well-established protocol in our laboratory. The cells were disrupted in HSGM buffer (20mM Hepes-KOH pH8.00, 130mM NaCl, 5mM $Mg(OAc)_2$, 10% glycerol) at 18 kpsi using a microfluidizer followed by an ultracentrifugation step to isolate the membrane fraction. The membranes were then solubilized using 1.5% DDM (n-Dodecyl β-D-Maltopyranoside) for two hours. As mentioned previously, for the purification, different affinity tags were added, a histidine-tag on SecD, SecE and YidC and a CBP-tag on YajC [Fig. 2-1]. The initial purification scheme comprised a Ni^{2+}-NTA affinity chromatography step (immobilized metal ion affinity chromatography, IMAC) followed by a second affinity chromatography to “pull-down” the complexes containing the CBP–tagged YajC protein. The IMAC purification protocol included in an overnight wash at 4°C with HSGM buffer supplemented with 30mM imidazole and 0.1% DDM. After a second wash with a high salt buffer (20mM Hepes-KOH pH8.00, 130mM NaCl, 5mM $Mg(OAc)_2$, 30mM imidazole, 10% glycerol, 0.1% DDM) a final wash was performed with HSGM buffer supplemented with 100mM imidazole and 0.1% DDM. Proteins were eluted from the column with HSGM buffer supplemented with 300mM imidazole and 0.1% DDM. All seven membrane proteins are co-eluting from the column as indicated by SDS-PAGE [Fig. 2-3]. As shown on the Coomassie-stained SDS-PAGE [Fig. 2-3], a lot of proteins were lost during the various washing steps of the affinity purification. Therefore, we changed the imidazole concentration during the wash steps and shortened the wash steps (no overnight wash step). The optimized IMAC protocol consisted of an initial wash at 4°C with HSGM buffer supplemented with 10mM imidazole and 0.1% DDM until the UV_{280nm} signal reached the baseline. The second wash with a high salt buffer (20mM Hepes-KOH pH8.00, 130mM NaCl, 5mM $Mg(OAc)_2$, 10mM imidazole, 10% glycerol, 0.1% DDM) was followed by a final wash with HSGM buffer supplemented with

40mM imidazole and 0.1% DDM. Proteins were eluted from the column with HSGM buffer supplemented with 300mM imidazole and 0.1% DDM. Compared to the initial protocol, we lost less holotranslocon proteins during the wash steps [Fig. 2-4].

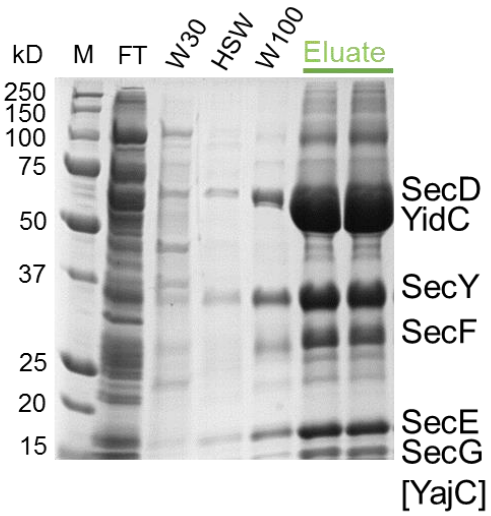

Figure 2-3. **Ni^{2+} affinity chromatography of the Holo-translocon.** SDS-PAGE showing the protein composition of the main purification steps. M, marker ; FT, flow through ; W30, 30mM imidazole wash ; HSW, high salt wash ; W100, 100mM imidazole wash.

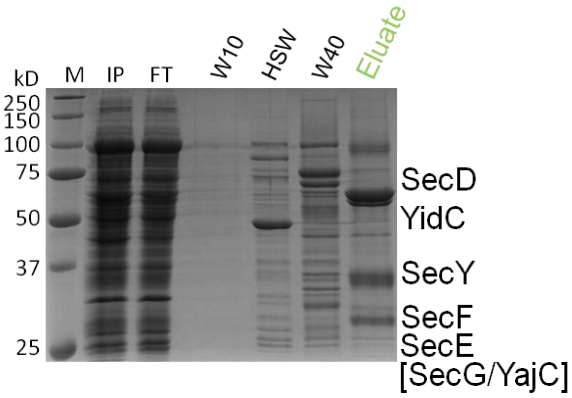

Figure 2-4. **Optimized Ni^{2+} affinity chromatography of the holo-translocon.** SDS-PAGE showing the protein composition of the main purification steps. M, marker ; IP, input ; FT, flow through ; W10, 10mM imidazole wash ; HSW, high salt wash ; W40, 40mM imidazole wash.

As a result of the optimized NiNTA purification protocol, the stoichiometry of the proteins in the eluate is more reproducible and is closer to the 1:1:1:1:1:1:1 expected for the HTL. For example, in figure 2-3, there is clearly a huge excess of YidC. This is considerably improved in figure 2-4.

Following this first affinity purification, we performed a calmodulin (CaM) affinity purification using the CBP-tag fused to YajC. This affinity purification system is based on the high affinity of the CaM for the CBP-tag in presence of calcium ions. Upon removal of the calcium ions from the environment by addition of the chelator EGTA, CaM undergoes a conformational change that results in the release and elution of the tagged protein. After elution from the first affinity column, the proteins were desalted using a HiTrap Desalting column (GE Healthcare) equilibrated with CBP binding buffer (50mM Hepes-KOH pH8.00, 130mM NaCl, 10% glycerol, 2mM $CaCl_2$, 0.03% DDM). Subsequently, the proteins were incubated overnight with calmodulin affinity resin (Stratagene) equilibrated with the CBP

binding buffer. The resin was washed with CBP washing buffer (50mM Hepes-KOH pH8.00, 130mM NaCl, 10% glycerol, 0.2mM $CaCl_2$, 0.03% DDM) prior to the elution with CBP elution buffer (50mM Hepes-KOH pH8.00, 400mM NaCl, 10% glycerol, 2mM EGTA, 0.03% DDM). Again, all the holotranslocon proteins are co-eluting as shown by SDS-PAGE and Western blot against the CBP-tag indicating that they indeed form a complex [Fig. 2-5].

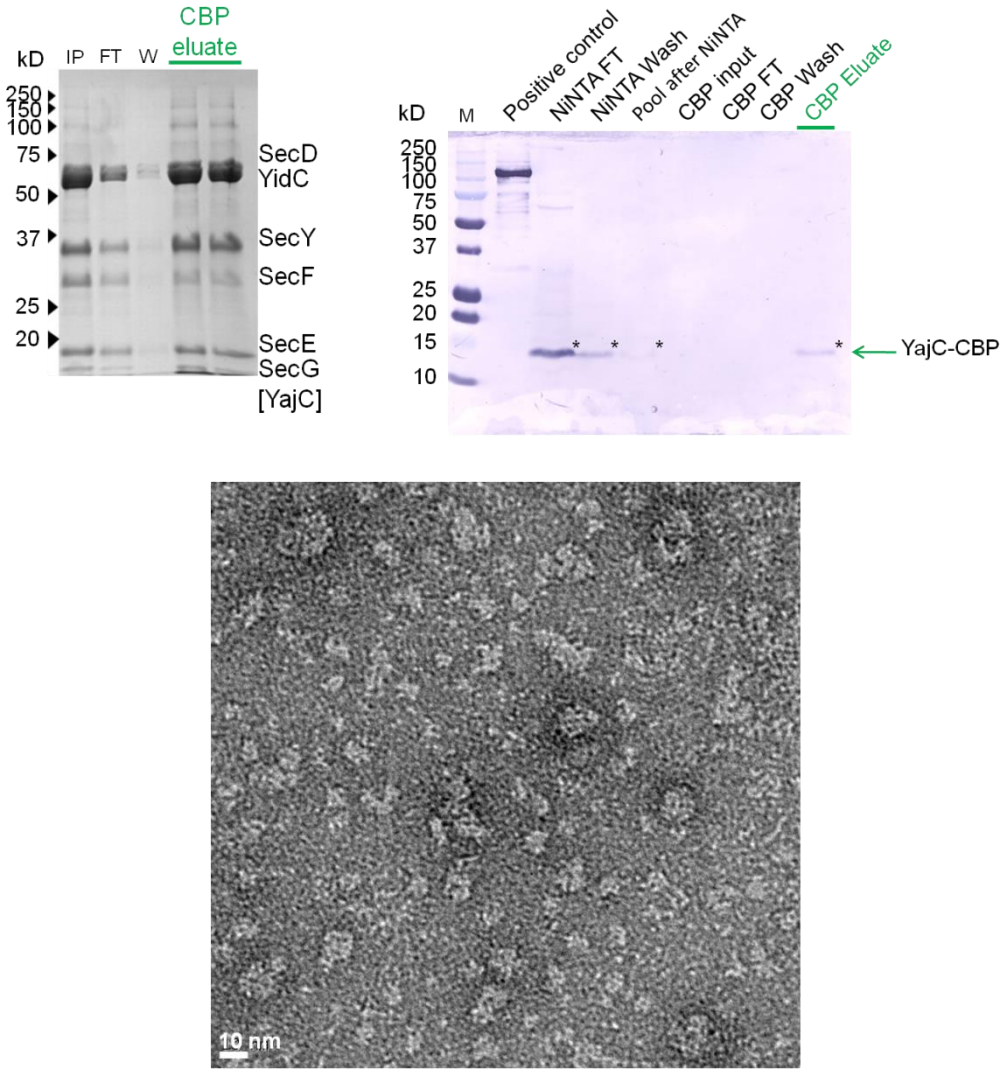

Figure 2-5. **Calmodulin affinity chromatography of the holo-translocon.** HTL3 purified on a NiNTA column was incubated with calmodulin resin. The purity was estimated by SDS-PAGE (**top-left**), western blot (**top-right**) and negative stain electron microscopy after coloration with 2% uranyl acetate (**bottom**). IP, input NiNTA purified HTL3; FT, flow through; W, wash. The asterisks indicate the position of the CBP-tagged YajC in the western blot. The micrograph clearly shows sample heterogeneity.

However, the expression and stoichiometry of this complex slightly differs in each of the purifications. As the CBP-tag is placed on YajC, the calmodulin affinity chromatography can “pull-down” at least two complexes, HTL and DFYY (possibly also SecDF-YajC). Moreover, the eluted proteins are very heterogenous in size as shown by negative stain electron

microscopy [Fig. 2-5]. Therefore, the sample was subjected to a size exclusion chromatography using a Superdex 200 equilibrated with HSGM buffer supplemented with 0.03% DDM in order to improve the homogeneity of the complex. The proteins were eluting continuously starting from the void volume to the dead volume of the column indicating aggregation and considerable heterogeneity of the sample.

With the affinity chromatography protocol described here, we could not solve the problem of heterogeneous holotranslocon sample. To further improve the isolation of a homogeneous holotranslocon complex, two strategies were pursued: First, additives were added to the current purification protocol in order to stabilize the complex (other detergents, lipids) and thus to increase the ratio of HTL in solution. The second approach included a further purification step to separate the different complexes in solution.

2-3. Effects of detergents and lipids

During membrane protein complex purification, a high concentration of detergent can perturb the interaction between the membrane protein complex and lead to heterogeneity of the sample. In chapter 3, we show that this is indeed the case for the holotranslocon. A DDM concentration higher than 0.05% is destabilizing the holotranslocon complex and generating SecYEG and DFYY complexes. Therefore, we always used a DDM concentration of 0.03% and avoided concentrating the sample as this would lead to higher detergent concentrations as well.

The addition of lipids during the purification steps can help stabilizing membrane complexes (Lund et al., 1989). The instability of a membrane protein complex can be caused by delipidation of the complex due to the detergent solubilization. The lipids have a role of stabilization of the transmembrane domains and if the detergent is removing these lipids, this can lead to dissociation or aggregation of the complex. Cardiolipin was shown to play a very important role in stabilizing the SecYEG-SecYEG complex (Gold et al., 2010). Accordingly, we added cardiolipin during the purification of holotranslocon in order to reintroduce this lipid which likely is bound at the interface between protein and detergent. The rationale was to see whether this increases the stability of the HTL complex. After IMAC, the lipid-depleted sample was incubated overnight at 4 °C with a 10-fold molar excess of cardiolipin followed by a CaM affinity chromatography. The resulting complexes were analyzed by SDS-PAGE and negative-stained electron microscopy. Unlike with SecYEG dimer complex (Gold et al., 2010), we were not able to detect any improvement of the homogeneity of the sample. Cardiolipin was not able to stabilize the holotranslocon complex in our hands. Therefore, we

decided to try the second approach consisting of addition of a purification step in order to further increase the homogeneity of the holotranslocon sample.

2-4. Ion exchange purification of the SecDF-YajC-YidC

In order to obtain more homogenous holotranslocon sample, we decided to first focus our optimization on the sub-complex composed of the four "regulatory" proteins (Nouwen & Driessen, 2002): SecD and SecF, YidC and YajC. These proteins were always present in different stoichiometry in the holotranslocon preparations. In addition, based on previous experiments (Nouwen & Driessen, 2002), this subcomplex was shown to be quite stable. However in contrast to SecYEG, the SecDF-YajC-YidC complex tends to aggregate during the purification described above. Therefore, we concluded that most of the problems during the purification of the holotranslocon complex arise from the SecDF-YajC-YidC subcomplex. Another source of the inhomogeneity is the instability of the holotranslocon complex – we address this issue in the next chapter (GraFix).

We first tried to purify DFYY by ion exchange chromatography (IEX). This approach makes use of the protein functional groups that can have both positive and negative charges and allows adsorption and reversible binding of charged sample molecules to oppositely charged groups attached to an insoluble matrix. By adjusting the buffer pH and/or the ionic concentration, various proteins can be separated. The pH value at which a protein carries no net charge is called the isoelectric point (pI). This value is protein specific. When exposed to a pH below its pI, the protein will carry a positive charge and will bind to a cation exchanger (negatively charged groups). The pI of a membrane protein complex is difficult to obtain and can deviate significantly from the theoretical pI of the subunits. When we calculated the theoretical pI of SecDF-YajC-YidC (DFYY), we realized that the complex is predicted to be uncharged at pH 8.0 and only weakly charged between pH 7.0 and 8.0 [Fig. 2-6]. In fact, this may explain the observed aggregation problems we had with the complex when applying the purification scheme described above. We therefore decided to use a pH value for IEX at which the complex of SecD, SecF, YidC and YajC predicted to be more soluble (pH<7.0; aggregation was observed at pH8). To purify DFYY, Ni^{2+}-NTA affinity chromatography followed by a cation exchange column, SP sepharose, was used. Elution was performed by a linear gradient from buffer A (20mM MES pH 6.00, 40mM NaCl, 10% glycerol, 0.03% DDM) to 50% of buffer B (20mM MES pH 6.00, 1.5M NaCl, 10% glycerol, 0.03% DDM).

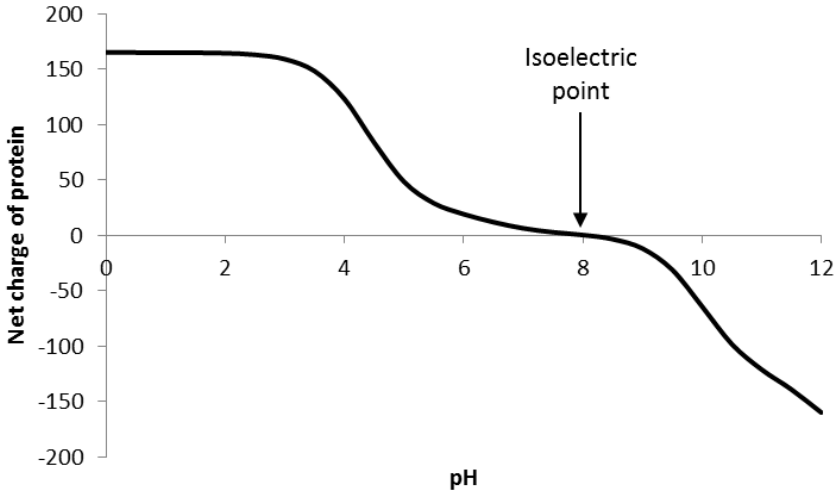

Figure 2-6. **Titration curve of the DFYY complex.** The titration curve for DFYY was obtained by submitting the sequences of the four individual subunits as the sequence of a single protein on the Protein Calculator of the Scripps Research Institute (www.scripps.edu/~cdputnam/protcalc.html).

Two different pools were eluted from the cation exchange column: pool 1 eluted at 600 mM NaCl; pool 2 eluted at 750 mM NaCl. The two pools were loaded separately onto a size exclusion column (SEC, superdex200 HiLoad 16/60) equilibrated with HSGM buffer supplemented with 0.03% DDM. The quality of SecDF-YajC-YidC sample was estimated by SDS-PAGE and by negative stain electron microscopy [Fig. 2-7]. Both pools of DFYY were eluting as a single peak from the gel filtration column with the same elution volume [Fig. 2-7]. The main difference was detected by the SDS-PAGE analysis of the eluted fractions. In pool 1, an excess of YidC was observed compared to SecD and SecF. In the second pool, the stoichiometry seemed to be equal for SecD, SecF and YidC. YajC could not be detected by Coomassie staining. However, negative stain electron microscopy indicated considerable inhomogeneity of both samples as evidenced by the detection of particles which were much larger than expected for a 180kDa complex (assuming that the DFYY complex consists of one copy of each protein) [Fig. 2-7].

Taken together, we concluded from our purification experiments that the holotranslocon complex is not very stable and is further destabilized during the different purification steps and/or during the grid preparation. Therefore, we decided to chemically stabilize the complex using a combined glycerol and crosslinking agent gradient centrifugation (GraFix).

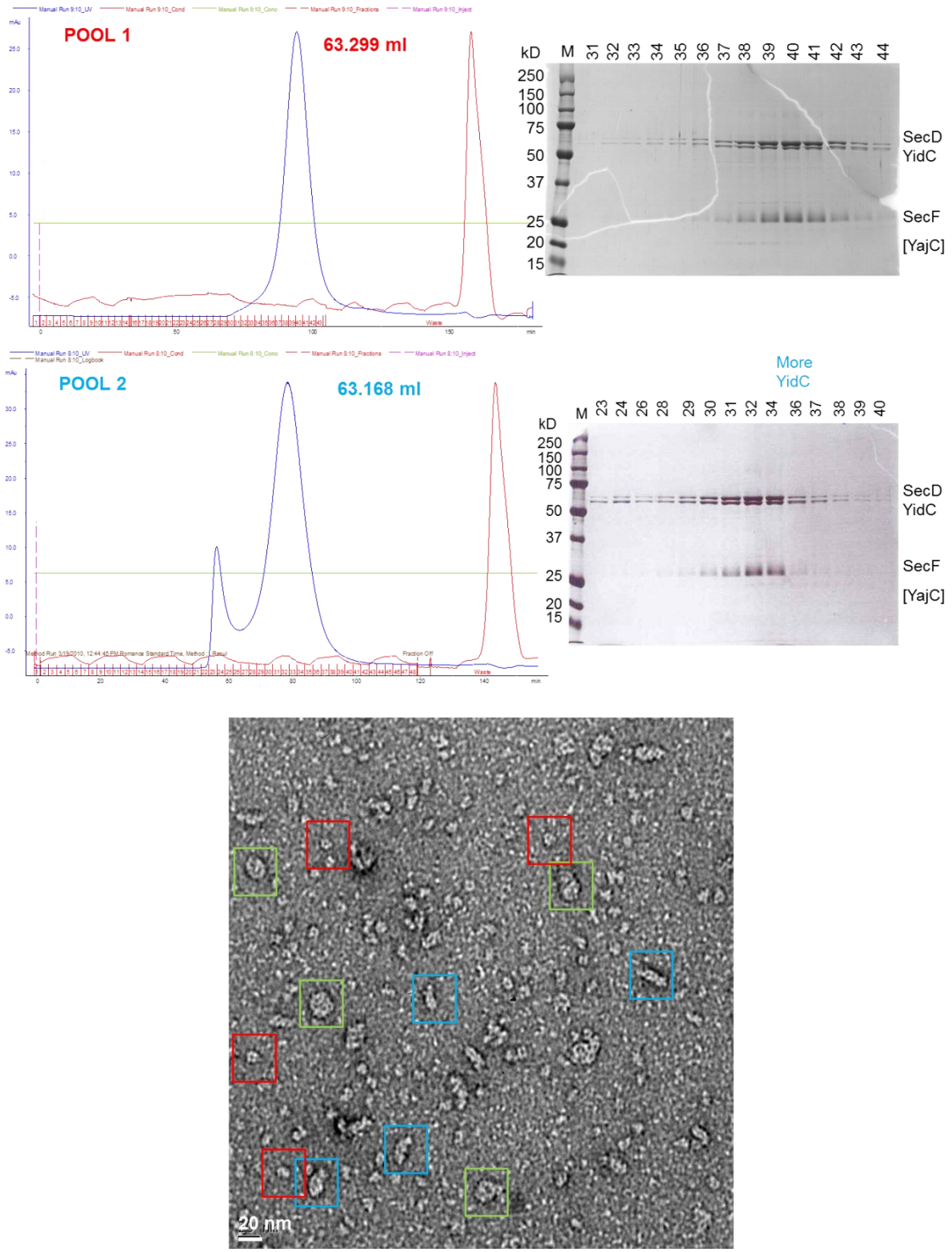

Figure 2-7. **Analysis of DFYY purified by anion exchange chromatography.** Chromatogram and SDS-PAGE of the first pool which eluted at lower salt concentration from the SP sepharose column (**top**) and of the second pool (**middle**) eluting at higher salt concentration from the IEX column. The elution volume is indicated in milliliter (ml). Negative stain analysis of the gel filtration peak fraction of the second pool (**bottom**). Proteins were stained with 2% uranyl acetate. Red squares represent particles of a size expected for a 180 kDa complex (assuming a 1:1:1 stoichiometry). Green and blue squares on the micrograph represent different sizes of bigger particles.

2-5. GraFix

We observed that the complexes were eluting as a single peak from the gel filtration column, but were extremely heterogeneous during electron microscopy studies. Therefore, we considered that the size exclusion chromatography (SEC) was too harsh for the integrity of our complex. SEC could induce dissociation of DFYY yielding to a mixture of subcomplexes on the electron microscopy grid. Alternatively, grid preparation which involves adsorption of the complex to a carbon film and staining with uranyl acetate at pH 4 could destroy the otherwise homogenous complexes. A widely used technique to increase the stability of a protein complex is chemical crosslinking (CL). This approach aims to stabilize protein-protein interactions by creating a covalent bond between two residues in close proximity. In addition to the crosslinking reaction, a separation step according to the size of the complexes is beneficial to separate the different crosslinked products (i.e. complexes which are crosslinked between the subunits from inter-complex crosslinking products which have a larger molecular weight).

The GraFix method (Kastner et al., 2008) allows to separate different complexes in solution and to stabilize them via a crosslinking reaction. This approach combines a fixation gradient (crosslinker gradient) to stabilize the complex with a density gradient centrifugation in order to separate the crosslinked complexes based on their size. In this combination, the crosslinking occurs at a relatively high dilution in the gradient. In fact, the crosslinking concentration is zero at the top of the tube where the sample is loaded in high concentration. Thus, the crosslinking occurs only during centrifugation when the complexes migrate into the glycerol gradient according to their size. The dilution and separation of the sample according to size and molecular weight largely avoids inter-complex crosslinking. After an ultracentrifugation step and fractionation of the gradient, the quality of the sample is assayed by negative stain electron microscopy [Fig. 2-8].

A 10 to 30% glycerol gradient was used containing a gradient from 0 to 0.15% glutaraldehyde as crosslinking agent. To obtain this gradient, two glycerol solutions were mixed using a gradient mixer (Biocomp). The upper buffer contained 20mM Hepes-KOH pH8.00, 130mM NaCl, 5mM $Mg(OAc)_2$, 10% glycerol, 0.03% DDM. The lower buffer was composed of 20mM Hepes-KOH pH8.00, 130mM NaCl, 5mM $Mg(OAc)_2$, 30% glycerol, 0.03% DDM and 0.15% glutaraldehyde.

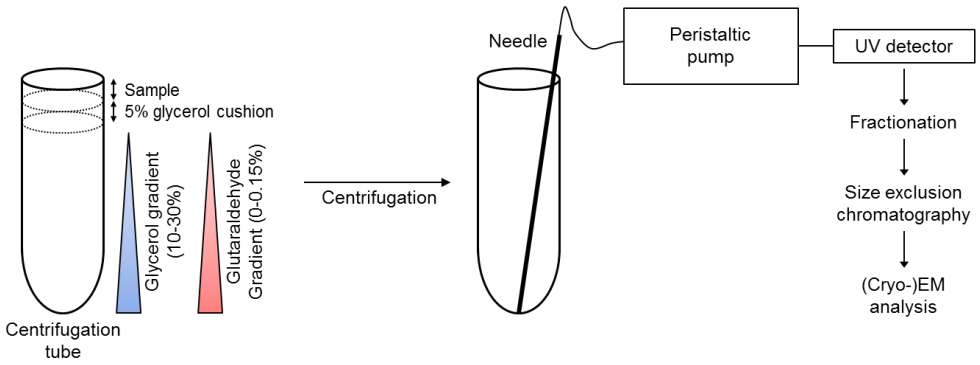

Figure 2-8. **Schematic view of a GraFix experiment.** The GraFix gradient is composed of low percentage of glycerol and fixation agent on the top and high percentage of glycerol and fixation reagent in the bottom (**left**). GraFix gradients are fractionated from bottom to top, cleaned form the excess of glycerol by a SEC and then either used directly for negative-stained electron microscopy or for cryo-electron microscopy (**right**). (Adapted and modified from (Kastner et al., 2008)).

Starting from the optimized affinity chromatography protocol, IMAC coupled to a CaM affinity chromatography, the eluted sample was loaded onto a GraFix gradient. Two glycerol gradients were run in parallel: a control gradient without crosslinker and a fixed gradient. After an ultra-centrifugation run (27,000 rpm for 36.5 hours at 4ºC in a Beckman SW 32 rotor), both gradients were fractionated from bottom to top, 38 fractions of 1mL were collected for each gradient. After quenching of the crosslinking reaction with primary amines (0.1mg/mL lysine as final concentration), the fractions containing proteins were subjected to SDS-PAGE analysis [Fig. 2-9].

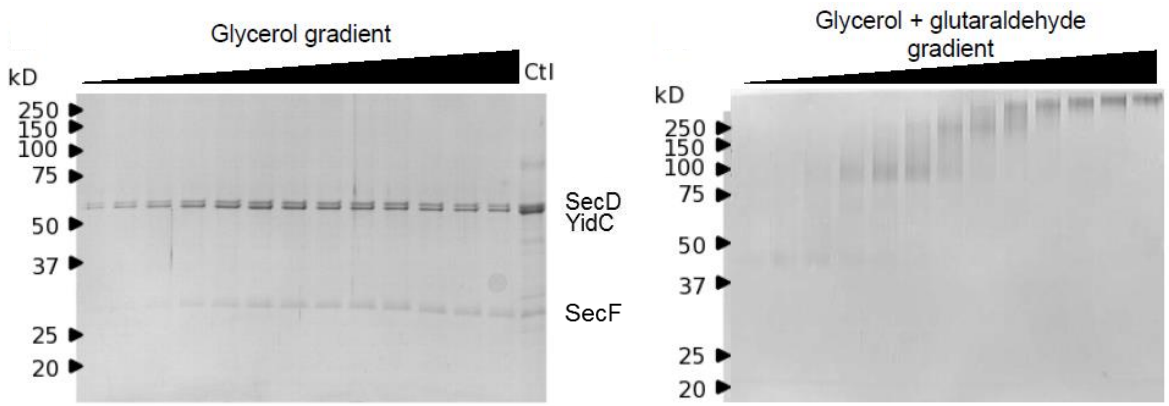

Figure 2-9. **SDS-PAGE analysis of SecDF-YajC-YidC GraFix experiment.** Gradient centrifugation without fixation agent (**left**). Ctl, purified DFYY as a control. Gradient centrifugation with glutaraldehyde as fixation agent (**right**). Glutaraldehyde and glycerol concentrations increase linearly from the left to the right as indicated by the bars.

The GraFix approach was efficient in isolating different species with different subunit stoichiometry especially between YidC and SecD (not crosslinked gradient SDS-PAGE) and

with different size (fixed gradient SDS-PAGE) [Fig. 2-9]. After a concentration step (30kDa Amicon concentrator) of the smallest fractions which still contained all subunits (as judged by Coomassie-staining of the SDS gel containing the fractions control gradient [Fig. 2-9]), the complexes were loaded onto a Superpose 6 SEC column equilibrated with 20mM Hepes-KOH pH8.00, 130mM NaCl, 5mM $Mg(OAc)_2$, 0.03% DDM. The gel filtration was performed in order to further improve the homogeneity, to remove the excess of glutaraldehyde and lysine (which could generate background signal during electron microscopy analysis) and to remove the glycerol which would disturb in cryo-EM experiments. The crosslinked DFYY complex eluted as a single peak [Fig. 2-10].

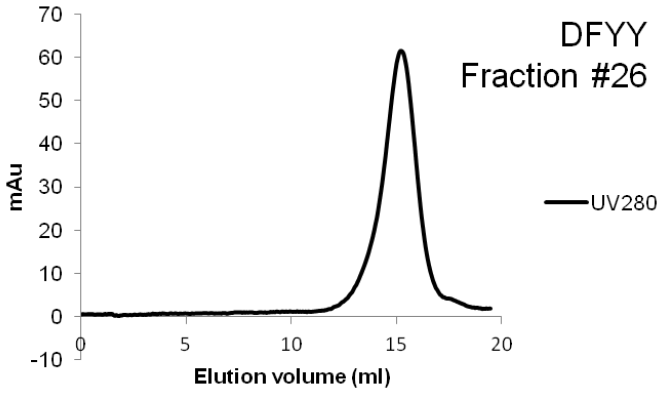

Figure 2-10. **Size exclusion chromatography chromatogram of SecDF-YajC-YidC after GraFix** (Superose 6) in 20mM Hepes-KOH pH8.00, 130mM NaCl, 5mM $Mg(OAc)_2$, 0.03% DDM.

Based on the calibration of our gel filtration column (Superose 6), the fraction #26 corresponds to a complex of a molecular weight of ~180kDa which is the sum of the molecular weight of the subunits of the DFYY membrane protein complex. The peak fraction from the gel filtration was analyzed by negative-stained EM to verify the integrity and the homogeneity of the isolated DFYY sample [Fig. 2-11]. Negative stain EM analysis revealed a homogenous complex with a diameter of about ~12nm. Interestingly, particles isolated by GraFix looked similar in term of shape and size with the “correct size”, not-crosslinked particles observed in figure 7. We concluded that GraFix stabilizes the DFYY complex and at the same time allows purifying sample of a homogenous size.

Since this purification protocol yielded very homogenous DFYY complexes, the same strategy was applied to the holotranslocon complex. Holotranslocon was purified by Ni^{2+}-NTA and calmodulin affinity chromatography and subsequently loaded onto a glycerol and glutaraldehyde gradient. After GraFix, the fractions were analyzed by SDS-PAGE [Fig. 2-12].

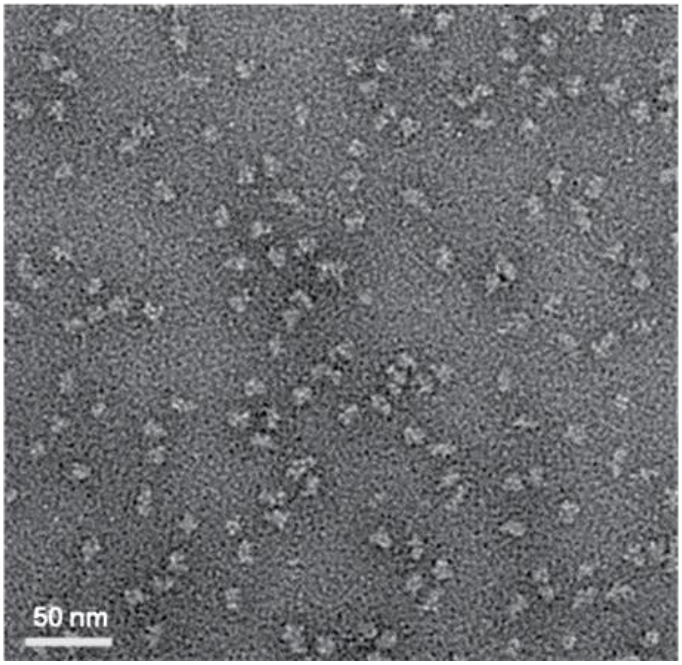

Figure 2-11. **Negative-stained electron microscopy of SecDF-YajC-YidC after GraFix.** The complex was stained with 2% uranyl acetate.

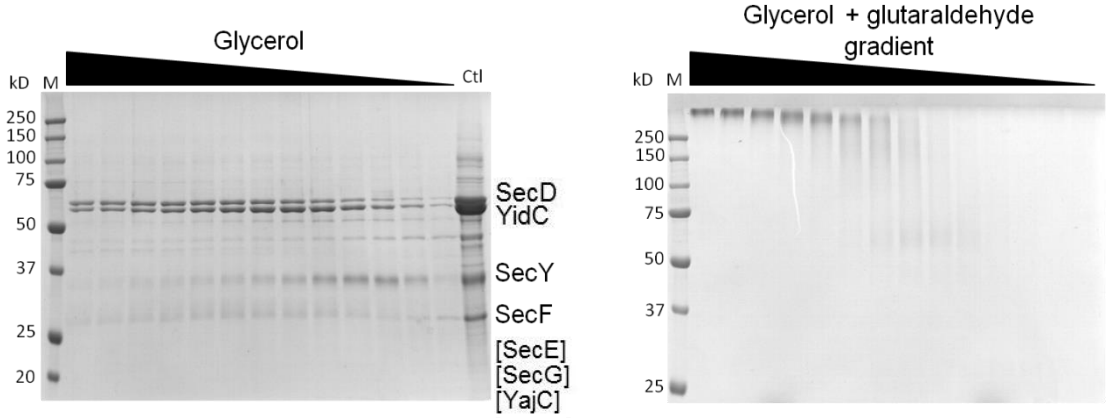

Figure 2-12. **SDS-PAGE analysis of the Holo-translocon GraFix experiment.** Gradient centrifugation without fixation agent (left). M, marker ; Ctl, purified HTL as a control. Gradient centrifugation with glutaraldehyde as fixation agent (right). Glutaraldehyde and glycerol concentrations increase linearly from the left to the right as indicated by the colored bars.

We collected the fractions after GraFix which contained all the subunits as judged by the Commassie-stained SDS gel of non-crosslinking gradient fractions. These were further purified by size exclusion chromatography. Thereby, we were able to isolate a protein complex with a molecular weight of ~250kDa corresponding to the expected size of a HTL complex consisting of one copy of each subunit) [Fig. 2-13].

The fraction of interest was the fraction #23. HTL (~250kDa) was running further into the glyocerol gradient compared to DFYY (fraction #26, ~180kDa). This indicates that meaning that the GraFix gradient is indeed efficient in separating complexes of different molecular

weight which were present in the sample. The homogeneity of the HTL sample was also analyzed by negative stained electron microscopy [Fig. 2-14].

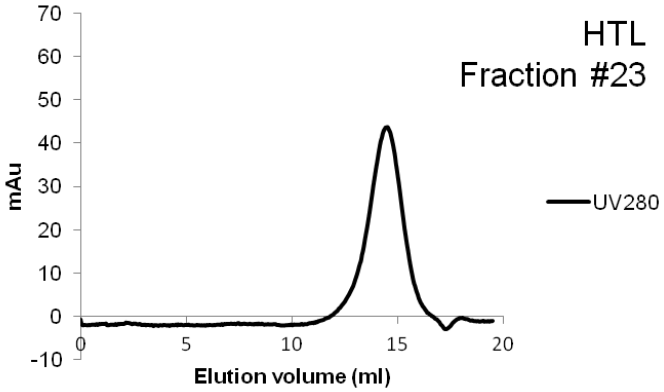

Figure 2-13. **Size exclusion chromatography chromatogram of the Holo-translocon after GraFix** (Superose 6) in 20mM Hepes-KOH pH8.00, 130mM NaCl, 5mM $Mg(OAc)_2$, 0.03% DDM.

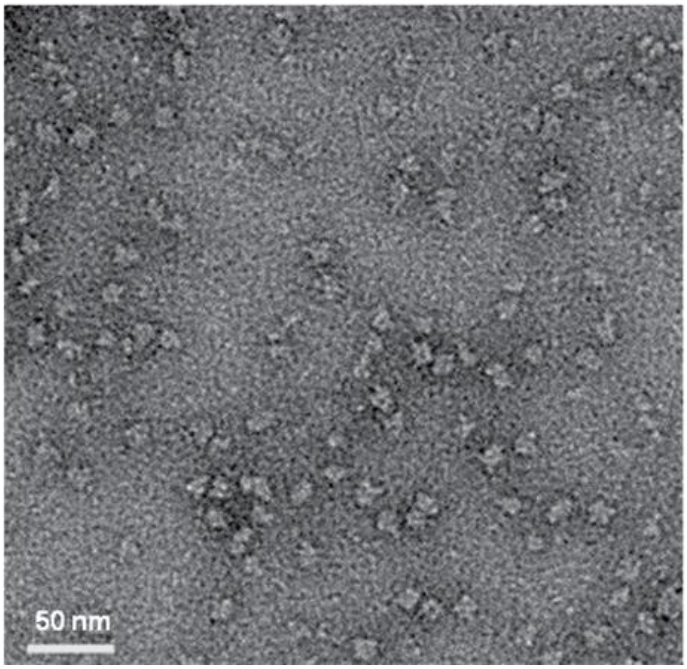

Figure 2-14. **Negative-stained electron microscopy of the Holo-translocon after GraFix.** HTL was stained with 2% uranyl acetate.

After GraFix, the HTL preparation appeared homogeneous. The diameter of the particles is slightly bigger compared to DFYY (~13.5nm versus ~12nm). Subsequently, we used these preparations of homogeneous HTL and DFYY for electron microscopy and 3D image processing (chapter 4).

2-6. Conclusions

During optimization of the purification scheme for holotranslocon we found that this complex is very unstable. High salt and high detergent concentrations lead to irreversible dissociation of the complex into SecYEG and DFYY. In contrast at lower pH values, the DFYY complex was found to be a comparatively stable complex, not sensitive to high detergent concentrations. It eluted as a single peak from the gel filtration column. Nevertheless, the peak fraction from the DFYY complex seemed to be heterogeneous in size according to negative stain EM. We suspected that the grid preparation protocol may interfere with sample integrity, and decided to stabilize our translocation complexes by GraFix. In fact, GraFix and subsequent gel filtration led to homogeneous sample suitable for single particle cryo-EM.

Chapter 3 : Membrane Protein Insertion and Proton-Motive-Force-Dependent Secretion Through the Bacterial Holotranslocon - SecYEG-SecDF-YajC-YidC

Résumé en français / French summary

Le complexe SecYEG est le composant central du système de sécrétion des protéines et d'insertion des protéines membranaires. Ce conduit protéique bactérien interagit avec YidC ainsi que le sous-complexe SecDF-YajC qui sont hautement conservés. Ces derniers facilitent la translocation à l'intérieur mais également à l'extérieur de la membrane. Ensemble, ces protéines forment l'holotranslocon (HTL) que nous avons réussi à surexprimer et purifier avec succès. Au contraire de l'homo-dimère SecYEG, le complexe HTL est un hétéro-dimère composé d'une seule copie chaque sous-complexe, SecYEG et SecDF-YajC-YidC. Les activités de HTL diffèrent de celle du complexe de base SecYEG. HTL est plus efficace durant l'insertion co-traductionnelle de protéine membranaire. De plus, la sécrétion post-traductionnelle de protéine de la membrane externe à tonneau *beta* contrôlée par SecA et la présence d'ATP devient beaucoup plus dépendent de la force proton motrice. À l'évidence, la seconde copie de SecYEG qui est non-essentielle au sein d'un dimère est interchangeable. La modulation de l'activité de la copie de SecYEG translocatrice par l'échange des sous-domaines accessoires SecYEG ou SecDF-YajC-YidC pourrait fournir un moyen d'affiner les capacités de sécrétion ou d'insertion en fonction du substrat. Une modulation similaire pourrait également être exploitée pour la translocation ou l'insertion d'une large gamme de substrats aux travers et dans les membranes eucaryotes, dans le cas du réticulum endoplasmique et des mitochondries.

Publication 2

Membrane Protein Insertion and Proton-Motive-Force-Dependent Secretion Through the Bacterial Holotranslocon - SecYEG-SecDF-YajC-YidC

Authors:
Ryan J. Schulze, Joanna Komar, Mathieu Botte, Sarah Whitehouse, Vicki A.M. Gold, Jelger A. Lycklama à Nijeholt, Karine Huard, Imre Berger, Christiane Schaffitzel and Ian Collinson

Manuscript under review in *Proc. Natl. Acad. Sci. U. S. A.*

Abstract

The SecYEG complex is a central component of the protein secretion and membrane protein insertion apparatus. This bacterial protein channel interacts with the highly conserved YidC and SecDF-YajC sub-complex, which facilitate translocation into and across the membrane. Together, they form the holotranslocon (HTL), which we have successfully over-expressed and purified. In contrast to the homo-dimeric SecYEG, the HTL is a hetero-dimer composed of single copies of SecYEG and SecDF-YajC-YidC. The activities of the HTL differ from the archetypal SecYEG complex. It is more effective in co-translational insertion of membrane proteins and the post-translational secretion of a β-barrelled outer-membrane protein driven by SecA and ATP becomes much more dependent on the proton-motive force. Evidently, the second non-essential copy of SecYEG of the dimer is interchangeable. Modulation of the actively translocating SecYEG copy by exchanging the accessory SecYEG or SecDF-YajC-YidC sub-complexes may provide a means to refine the secretion and insertion capabilities according to the substrate. A similar modularity may also be exploited for the translocation or insertion of a wide range of substrates across and into the endoplasmic reticular and mitochondrial membranes of eukaryotes.

Introduction

The essential SecY/61 complex selectively orchestrates the passage of newly synthesized proteins across and into the cytoplasmic and endoplasmic reticular (ER) membranes of prokaryotes and eukaryotes, respectively. Protein translocation is driven by associated co-translating ribosomes or by specialised energy-transducing factors, such as the bacterial ATPase SecA. The protein-conducting channel is formed by a monomer of the SecYEG complex, encapsulated by two halves of SecY (1). The separation of trans-membrane segments (TMSs) 1-5 from 6-10 along with the displacement of a central plug could help form a channel through the membrane to the outside, as well as laterally into the bilayer (1). SecYEG forms dimers in the membrane (2), required for association and activation of SecA (3-5). However, *in vivo*, the passive SecYEG complex is not rigidly fixed to the translocating copy nor absolutely essential for transport (6).

E. coli inner membranes harbor a 'holotranslocon' (HTL) containing SecYEG and SecDF-YajC (7). YidC is a ubiquitous and essential membrane protein 'insertase' (8, 9), which functions in concert with SecYEG during the biogenesis of many inner membrane (IM) proteins (10-12). In contrast, the insertion of small polypeptides such as the M13 procoat, Pf3 coat protein, and subunit c of the F_1F_O-ATP synthase are thought to occur through YidC alone (13-15). YidC and SecYEG may be bridged in the HTL by a sub- complex consisting of SecD, SecF and YajC (16). SecDF may act by regulating the interaction of SecA with SecYEG (7, 17, 18). Like SecYEG, SecDF is thought to transduce the energy available in the trans-membrane proton-motive force (PMF) to stimulate translocation (19-21), in keeping with other members of the RND superfamily also conferring PMF-driven substrate efflux (22).

We have exploited a novel system that allows the simultaneous over-expression of all seven membrane proteins of the HTL (23). Its purification allows the exploration of unknown aspects of its organisation, activity and bioenergetics, providing new insights of the general secretion and membrane protein insertion machinery.

Results

Production and purification of the HTL: a membrane protein complex of SecYEG- SecDF-YajC-YidC.

By using ACEMBL, we were able to construct a single plasmid encoding all seven subunits (Fig. 1a), allowing for high-level expression of the entire HTL. The complex was purified by Ni^{2+} chromatography followed by size-exclusion combined with an anion exchange step. The HTL eluted as a single symmetrical peak in detergent (*n*-Dodecyl-β-D-maltoside; DDM), characteristic of a single complex (Fig. 1b). All components of the complex but YajC were clearly visible by SDS-PAGE (Fig. 1c). The integrity of the complete complex was verified by applying the sample to a calmodulin column, which retained all seven subunits by virtue of the calmodulin binding peptide (CBP) attached to the C-terminus of YajC (Fig. 1a, d).

Stability of the HTL complex.

A further examination by blue-native (BN)-PAGE revealed one prominent and one diffuse band migrating respectively at ~300 kDa and ~150-200 kDa (Fig. 1e). Both bands were excised and subject to a second dimension denaturing gel. The higher molecular weight (MW) form contained all seven subunits of the HTL (Fig. 1f, lane 1), with a combined mass of ~250 kDa, most likely representing the intact complex. The appearance of the lower MW bands, which also contain all seven subunits (Fig. 1f, lane 2), presumably arises due to the dissociation of the HTL into the SecYEG (~75 kDa) and SecDF-YajC-YidC (~175 kDa) sub-complexes. The dissociation of the HTL complex is dependent on the detergent concentration, reminiscent of the separation of SecYEG homo-dimers into monomers (Fig. 1g)(24). The SecDF-YidC complex had no tendency to self-associate (Fig. 1g).

The intact HTL complex has the same apparent MW as SecYEG dimers (Fig. 1g, *) and, therefore, only contains single copies of SecYEG and SecDF-YajC-YidC. The extraction of tightly bound phospholipids by high detergent concentrations may account for the dissociation of the HTL complex, as in the case of SecYEG dimers (25). Additionally, the integrity of the complex could be directly demonstrated by negative stain electron microscopy (Fig. 2), which revealed the presence of uniformly sized particles of purified HTL complex, as shown in the selected class averages (Fig 2, right).

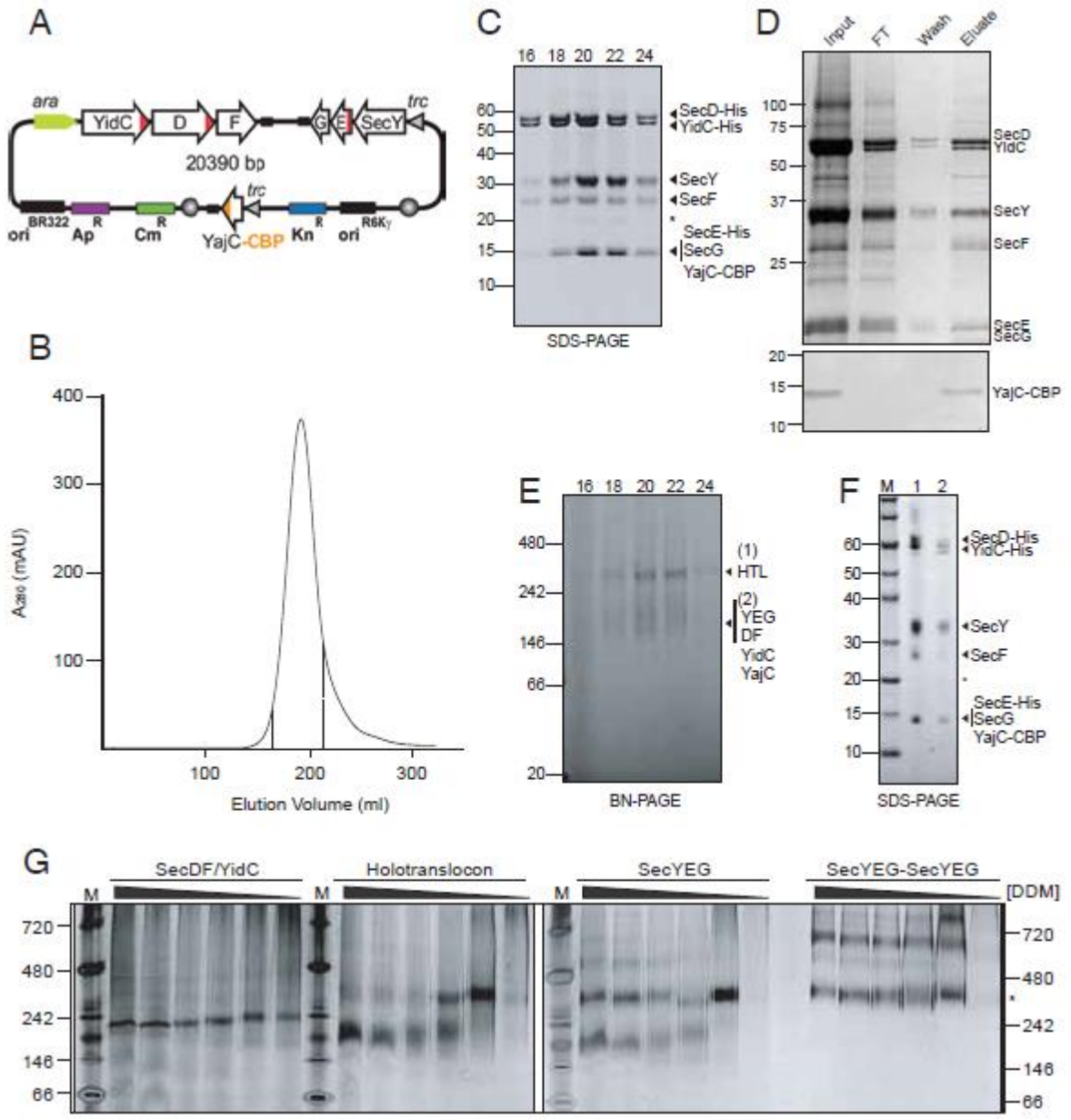

Figure 1. Purification of the *E. coli* HTL. (a) Plasmid map of the HTL construct. (b) Gel Filtration / Ion Exchange elution profile of the HTL. (c) SDS-PAGE representation of peak fractions 16-24 (corresponding to elution volumes 165-215ml of the profile displayed in 1b, dotted lines). (*) represents a proteolytic fragment of SecY (d) SDS- PAGE demonstrating the purification of the entire complex from calmodulin column (above). Detection of the CBP peptide shows that YajC is present in this complex (below). (e) BN-PAGE representation of peak fractions 16-24 from 1b, above. (f) Second dimension SDS-PAGE of gel slices taken from the higher (lane 1) and lower (lane 2) MW complexes seen in 1d. Note that the slight shift in MW for all components of the HTL is the result of a gel slice being placed into the wells for the run. (g) BN-PAGE illustrating the susceptibility of various complexes (SecDF-YidC, HTL, SecYEG, or a covalently-linked dimer of SecYEG (39)) to changes in detergent concentration. 50 ng of complexes purified from C43-overexpressing *E. coli* were resuspended in TSG_{130} buffer containing decreasing concentrations of DDM concentrations from 0.4% to 0%. The asterisk represents migration of the SecYEG tandem dimer.

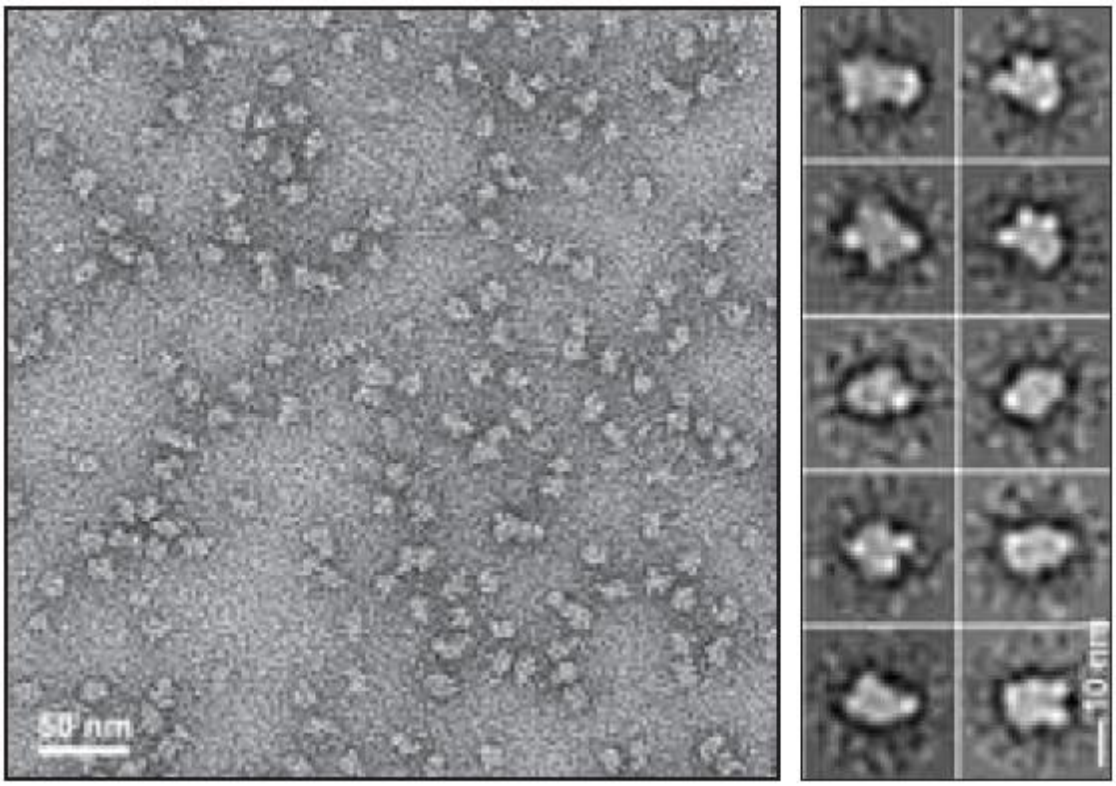

Figure 2. Negative-stain EM of purified HTL Complex. Micrograph of GraFix-treated HTL complexes reveals particles of a diameter of 13-15 nm (top). The 2D class averages of the HTL reveal asymmetric particles composed of several domains (bottom).

Subunit organization of the HTL complex.

We performed in-membrane crosslinking experiments using the photo-inducible Tris-bipyridylruthenium(II) to investigate protein- protein interactions within the HTL complex. SecYEG was used as a control, where as reported previously (4), we observed the formation of SecE-E and SecY-Y products upon crosslinking of inner membrane vesicles (IMVs) over-expressing SecYEG, indicative of the presence of SecYEG dimers (Fig. 3a). When IMVs over-expressing the HTL complex were subjected to the same treatment, they were no longer detected (Fig. 3a). To confirm this result, we used the homo-bifunctional amine-reactive reagent Dithiobis[succinimidyl propionate] (DSP), for *ex vivo* crosslinking of the native membranes prior to HTL purification. In contrast to Tris-bipyridylruthenium(II), which couples neighboring residues without a linker, DSP extends the crosslinking range by virtue of its 12Å spacer arm, allowing for identification of nearby interaction partners. In HTL- and SecYEG- overexpressing membranes, those crosslinks occurring within the SecYEG sub-complex (SecY-E, SecY-G and SecE-G), could be generated with similar efficiency (Fig. 3b, red boxes). Crosslinks at the interface between SecYEG dimers (SecE-E, SecY-E-E and SecY-Y; Fig. 3b, green boxes) were either lost or considerably diminished in the HTL complex.

Notably, new higher-MW products were observed in the crosslinked HTL sample, indicative of contacts between SecYEG and SecDF-YajC-YidC sub-complexes (Fig. 3b, blue boxes). These HTL-specific bands cross-react with SecY, SecE and SecG antibodies and are larger than the corresponding crosslinks with SecY (Fig. 3b; Y-Y, Y-E and Y-G, respectively) and therefore, must have arisen from crosslinks with the higher-MW subunits SecD or YidC. Mass spectroscopy performed on bands excised from the gel (Fig. 3b, *) confirmed the presence of both SecD and YidC. Taken together, the results show that the HTL complex contains only one copy of SecYEG, which contacts SecD and YidC in place of the second copy of SecYEG found in the dimeric form.

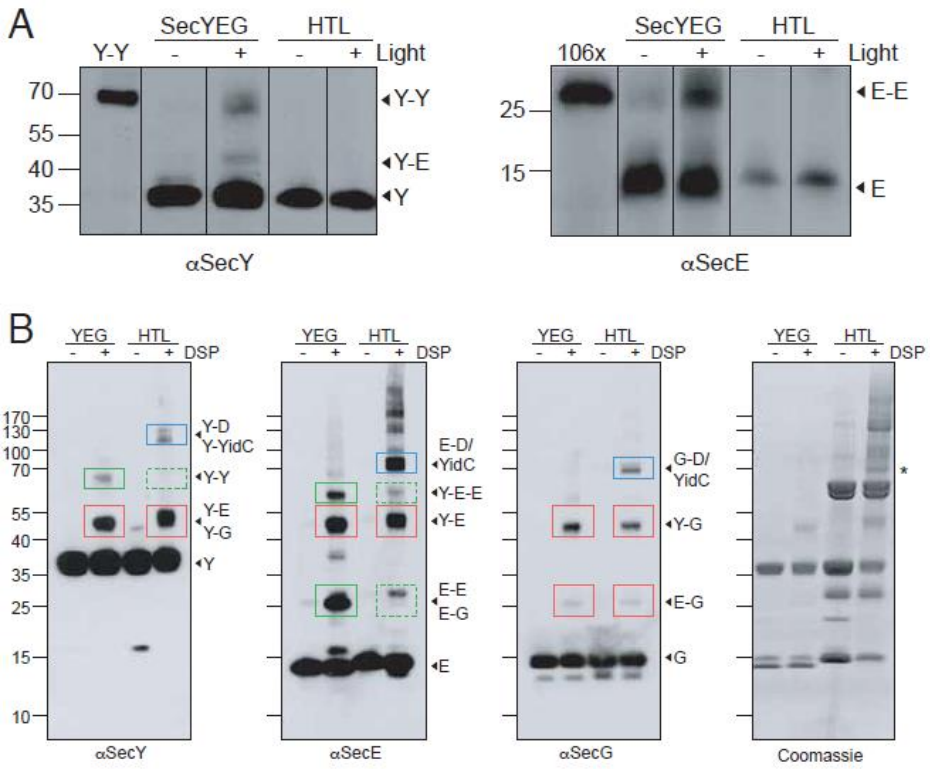

Figure 3. Crosslinking of HTL subunits. (a) Western blots of photo-activatable Tris- bipyridylruthenium(II)-mediated crosslinking (+/- exposure to light radiation) of *E. coli* IMVs overexpressing either SecYEG or HTL. Y-Y represents a purified covalently- linked SecYEG dimer (39). 106x represents a purified SecE-E dimeric version of SecYEG (4). (b) Western blotting of DSP-mediated crosslinking of the same IMVs. Crosslinking adducts preserved between SecYEG and HTL are bounded in red boxes. Those that are eliminated in the HTL are bounded in green boxes. Newly formed adducts are bounded in blue boxes. Bands excised from the Coomassie gel (*) were found by MS of tryptic fragments to contain both YidC and SecD.

Interaction of the HTL complex with SecA.

We analyzed the ability of the HTL complex to associate and activate the motor ATPase SecA for secretion. Both HTL and SecYEG had significantly increased rates of SecA-mediated ATP hydrolysis in the presence of CL (Fig. 4a, compare left and right panels). The association of SecA and SecYEG in the ATP-bound state can be monitored by the quenching of fluorescein- derived SecA in the presence of a non-hydrolyzable analogue (AMPPNP) (4). This same effect was observed upon the addition of the HTL complex (Fig. 4b). The affinity of $SecA_{ATP}$ for HTL is considerably increased (> 10-fold) in the presence of CL. In fact, the K_d was too low to be measured accurately. This effect is also the same for the binding of SecYEG to SecA (Fig. 4b). The results show SecYEG dimers (25) and HTL act on SecA in a very similar CL-dependent fashion.

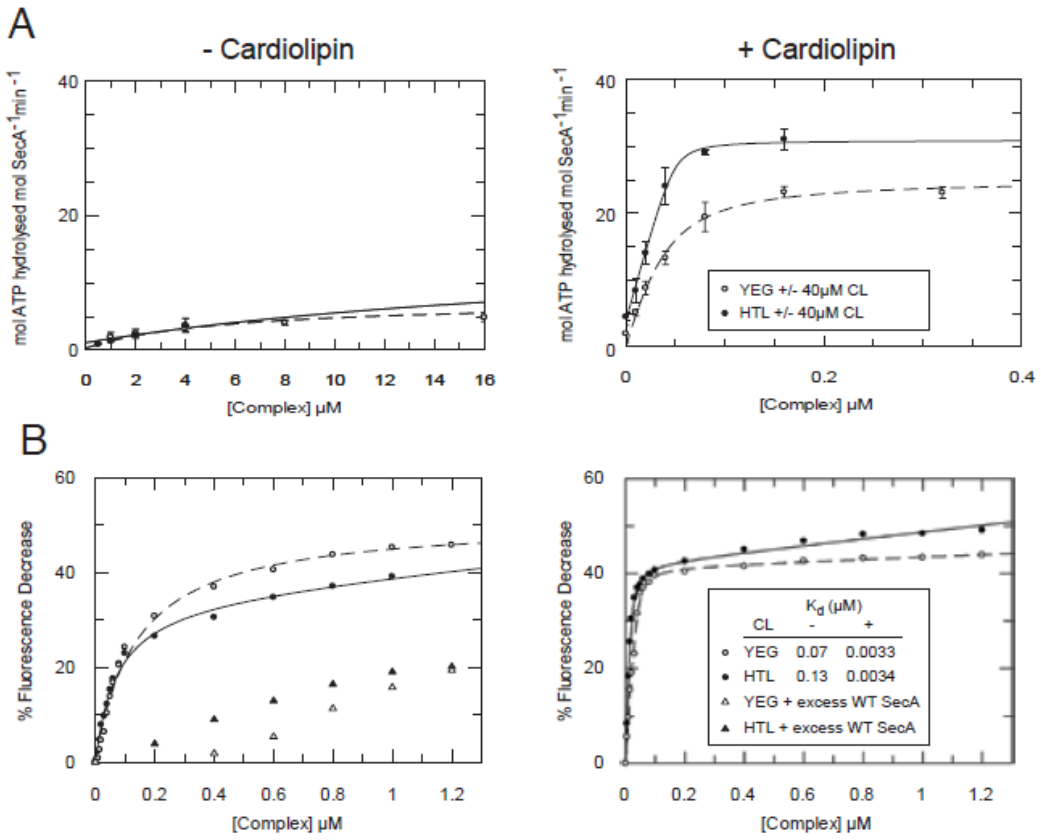

Figure 4. SecYEG- and HTL-mediated stimulation of SecA ATPase activity is enhanced by cardiolipin. (a) Increasing amounts of SecYEG dimer (YEG_2, open circles) or HTL complex (filled circles) were tested for their ability to activate the ATPase activity of SecA (0.3 µM) in the presence or absence of 40 µM cardiolipin. Data are representative of the mean of three independent experiments +/- SD. Data were fit as detailed in the methods. (b) Fluorescence quenching assays using fluorescein-tagged SecA ($SecA_{795Fl}$) and SecYEG or HTL complex in the presence or absence of 40 µM cardiolipin. The inset lists the K_d values determined with and without CL. Note that the values of the K_d in the presence of CL are too low to be determined accurately.

ATP- and PMF-driven protein secretion through the HTL complex.

To assess the functionality of the isolated HTL complex, we examined its ability to transport the outer membrane precursor protein pro-OmpA across a lipid bilayer. Post-translational translocation of pro-OmpA to the interior of proteoliposome vesicles containing either the SecYEG or HTL complex was monitored in the presence and absence of a trans- membrane PMF. For PMF generation, the light-driven proton pump bacteriorhodopsin (BR) was incorporated into proteoliposomes harbouring SecYEG or the HTL. The reconstitution efficiency was assessed by SDS-PAGE (Supplementary Fig. S1). The levels of BR in both sets of proteoliposomes were similar, and the quantities of SecY were consistent with their expected stoichiometries (*i.e.* twice as much in the SecYEG sample, due to the two copies of SecY, compared to one in the HTL). Thus, respective transport activities could therefore be legitimately compared.

The translocation assay was monitored following addition of SecA, ATP and proOmpA, in the presence (+PMF) or absence (-PMF) of a light source. The HTL complex is less effective in ATP-dependent SecA-driven protein secretion, and more dependent on the PMF (Fig. 5a). To verify that the reduced secretion activity of the HTL complex was not the result of an asymmetric reconstitution favoring inwardly-facing cytosolic sites, the sidedness of the vesicles was investigated by exposure to trypsinolysis. (Supplementary Fig. S2). The resulting appearance of a 21 kDa band corresponds to the N-terminal fragment of SecY, due to cleavage in the cytosolic loop between TMSs 6 and 7 (26). In both proteoliposomes containing SecYEG and HTL complexes, SecY was sensitive to proteolysis (Supplementary Fig. S2). Evidently, the reconstitution has favored the orientation with the cytosolic surface facing outwards. Therefore, the observed reduction in secretion activity of the HTL complex is not the result of a reduction in available sites for translocation.

To determine the secretion activity seen for the HTL was not due to dissolution of the $(SecYEG)_1$-(SecDF-YajC-YidC)$_1$ heterodimer and reformation of SecYEG dimers, we performed DSP crosslinking on the proteoliposome samples used for translocation (Fig. 5b). Immunoblotting for SecY mirrors those performed previously on IMVs over- expressing SecYEG and HTL (Fig. 3a). Proteoliposomes containing SecYEG produced SecY-Y and SecY-E-E crosslinks, due to the presence of SecYEG dimers. These crosslinks were not observed in crosslinked proteoliposomes containing the HTL complex (Fig. 5b). Therefore, in these assay conditions, the HTL complex contains single copies of SecYEG and SecDF-YajC-YidC and is competent for secretion of proOmpA.

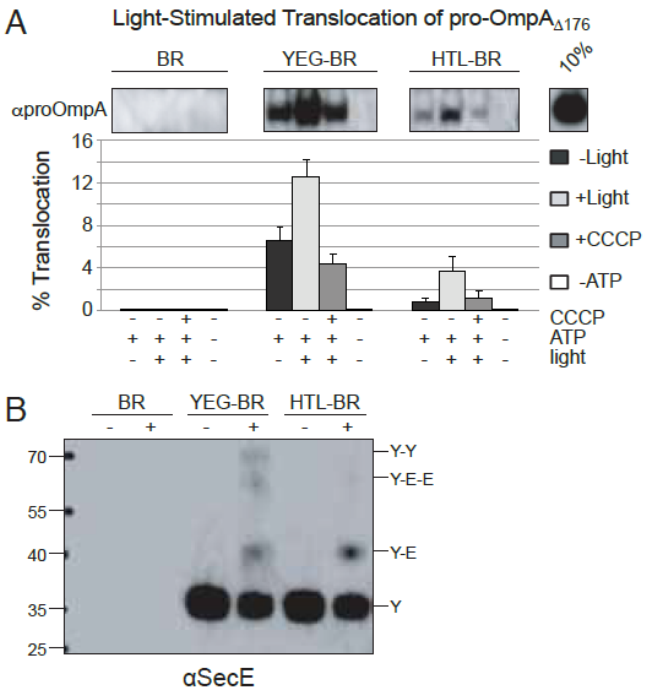

Figure 5. The *E. coli* holo-translocon is competent for protein secretion. (a) *In vitro* translocation assay showing the effect of a light-stimulated PMF on the efficiency of the reaction. SecYEG and HTL proteoliposomes were reconstituted together with BR for the purposes of generating a PMF. The graph shows the fold-change in translocation by SecYEG and the HTL relative to the –PMF condition (in the absence of light). Values represent the mean of four independent experiments +/- SEM. (b) SecY immunoblot of DSP crosslinking of the same proteoliposomes used in 5a, demonstrating that the organization of liposome-incorporated SecYEG and HTL is maintained.

Ribosome binding of HTL and its sub-complexes.

The ability of the HTL complex and its constituents were tested for their ability to associate with the ribosome by co- sedimentation. The HTL complex, SecYEG, YidC and SecDF-YajC-YidC all displayed a preference for ribosomes displaying the nascent trans-membrane helix of FtsQ (27) over non-translating ribosomes (70S) (Fig. 6a). In contrast, SecDF had an equal preference for translating and non-translating ribosomes or the small ribosomal subunit (30S) (Fig. 6a), suggestive of a non-specific interaction. Therefore, the nascent membrane protein probably contacts both SecYEG and YidC.

Using Cy3-labeled SecY at position 148 and 215 (which does not respond to ribosome binding) as a control, we determined the affinity of detergent-solubilized SecYEG and HTL to 70S ribosomes by fluorescence analysis (Fig. 6b). The binding of ribosomes to SecYEG induces conformational changes, which can be monitored by environment sensitive fluorophores at specific locations (28). The increase of Cy3 fluorescence at position 148, located at the periplasmic side of the lateral gate, was used to determine a K_D for HTL (~ 35 nM) and SecYEG (~ 200 nM). Therefore, SecDF-YajC and YidC consolidate the association of the translocon with the ribosome.

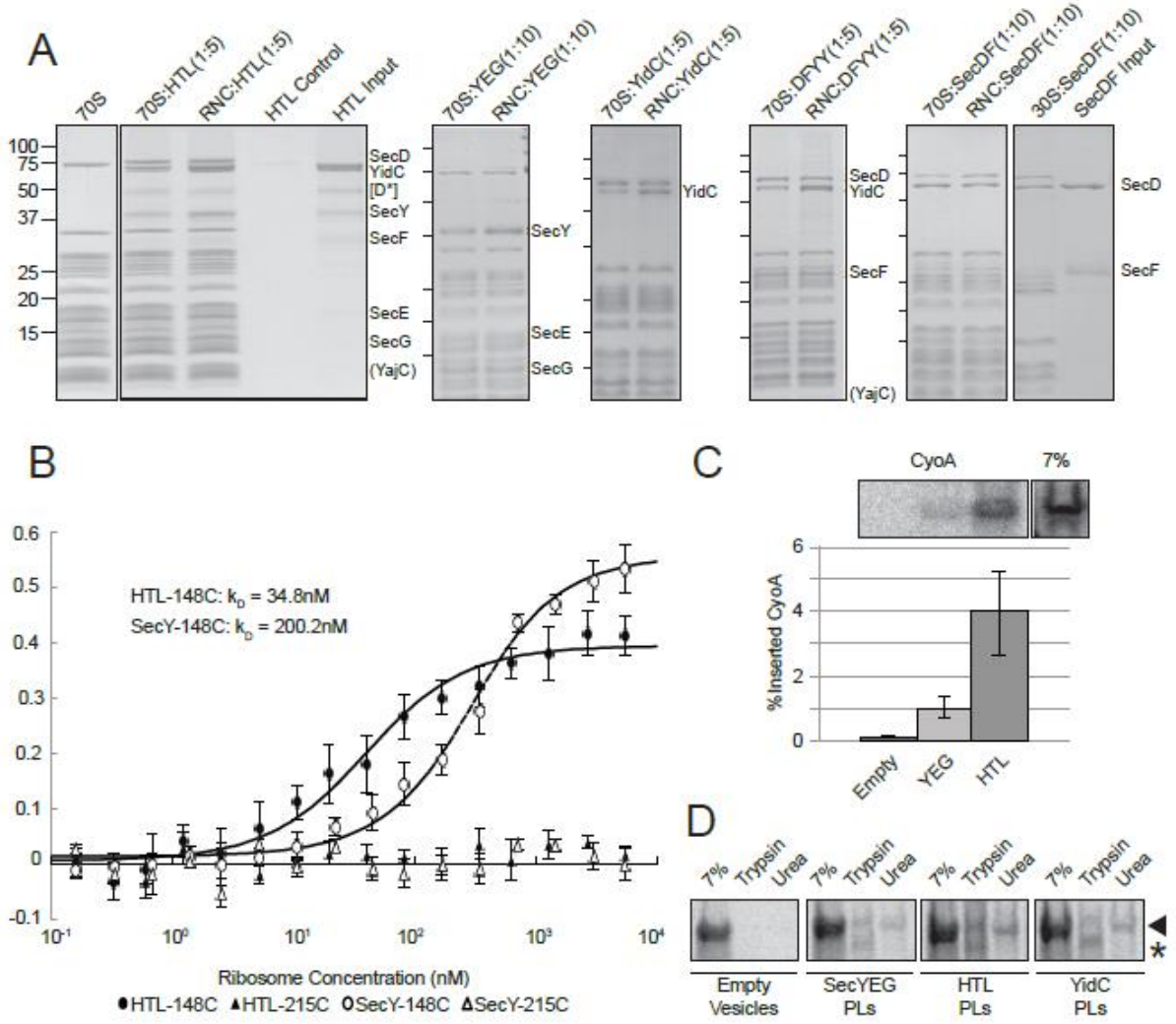

Figure 6. Interaction of the HTL and its sub-complexes with ribosomes. (a) Binding of purified HTL to translating (RNCs) and non-translating ribosomes (70S) analyzed by co-sedimentation experiments. D* is a degradation product of SecD. (b) Binding of detergent-solubilized HTL and SecYEG to 70S ribosomes followed by fluorescence intensity. Constant amounts of SecYEG and HTL containing SecY labelled with Cy3 at positions 148 and 215 were exposed to increasing concentrations of 70S ribosomes leading to an increased fluorescence in the case of SecY labelled at position 148, but not at 215. (c) *In vitro* synthesized *cyoA* mRNA was incubated together with empty liposomes or proteoliposomes containing YEG or the HTL together with an *E. coli* S30 membrane-free cell extract including scSRP (40) to assess incorporation of ^{35}S-labeled CyoA directly into an *in vitro* membrane bilayer. Values represent the mean of four independent experiments +/- SD. (d) Representative phosphorimaging of trypsin/urea- treated ^{35}S-labeled CyoA.

Membrane protein insertion through the HTL complex.

The presence of SecYEG and YidC in the HTL suggests that the complex could be active in membrane protein insertion. Therefore, we compared the capability of SecYEG and the HTL for insertion of a nascent membrane protein, CyoA, into proteoliposomes. CyoA is a polytopic membrane protein subunit of the cytochrome *bo3* oxidase with known

dependencies on YidC and SecYEG for co-translational insertion (29). Successfully incorporated protein was measured by resistance to urea extraction and proteolysis (Figs. 6c and 6d). In comparison to SecYEG proteoliposomes, CyoA was inserted about four-fold more efficiently into proteoliposomes containing the HTL.

Discussion

Our understanding of the integrated process of protein translocation has been restricted by the absence of a pure and stable complex capable of both secretion and membrane protein insertion. Protein secretion is driven through the center of SecYEG (1, 30) and membrane protein insertion through the lateral gate. The partitioning of translocating TMSs into the bilayer is thought to involve YidC (8), which in some cases may act alone (9). However, a physical interaction between SecYEG and YidC has yet to be demonstrated. The nature of this interaction and the mechanism of Sec-dependent membrane protein insertion have yet to be addressed. This work resolves this problem in the production, purification and functional reconstitution of a complex containing both SecYEG and YidC, as well as the accessory sub-complex SecDF-YajC - otherwise known as the holotranslocon (HTL). The concomitant over-expression of all seven constituents of the HTL complex seems to have been a prerequisite for obtaining intact complex. YidC was most likely incorporated as a component of the previously identified SecDF-YajC-YidC sub-complex (16). We show that the HTL is a hetero-dimeric assembly of single copies of this sub-complex and SecYEG (Fig. 7).

Crosslinking experiments have localised YidC to the lateral gate of SecY (TMSs 2b, 3, 7; (12)), which also contacts translocating TMSs as they emerge from the translocon (10, 11, 31). We also show crosslinks between SecD/YidC and SecY, E and G. These findings, together with a reported functional interaction between SecG and SecDF-YajC (32), are suggestive of an interface involving the N-terminal half of SecY (TMS 1 - 5), SecE and SecG (Fig. 7).

A comparison of the activities of HTL- and SecYEG-containing proteoliposomes suggests that the HTL complex is less capable of protein secretion, but much more responsive to the PMF. The determinants and mechanistic basis governing this stimulation are not immediately clear. The core SecYEG complex itself couples the PMF to translocation (20). The increased dependence of the HTL on the PMF may result from dual effects of SecYEG and SecDF. The HTL complex is more proficient in co- translational membrane protein insertion compared to SecYEG alone. The increased efficiency afforded by the presence of YidC in the HTL complex may be critical for rapid protein assembly, membrane

biogenesis and competitive survival. The different dependencies of SecYEG and HTL for secretion and insertion are presumably selected according to the specific requirements of the translocation substrate. Moreover, the capabilities of the HTL for both secretion and insertion may be critical for the translocation of membrane proteins containing large extracellular domains.

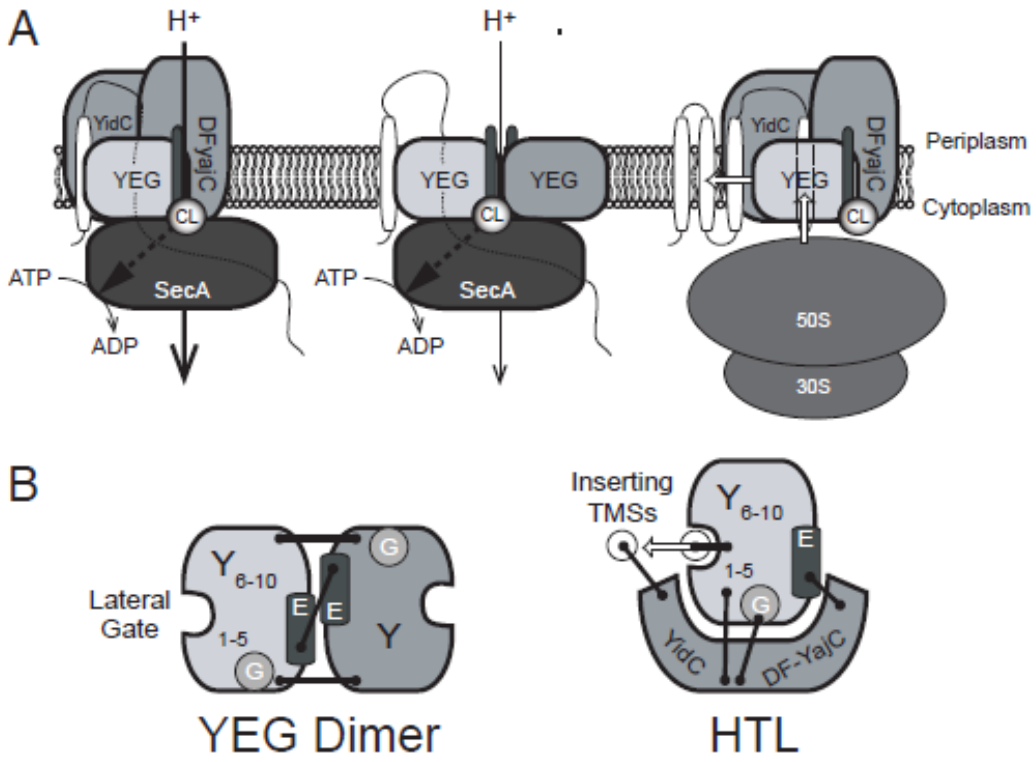

Figure 7. Model for structural organization and activity of the HTL. (a) The SecYEG translocon can associate with SecDF-YajC-YidC (left) to promote protein transport in a SecA-dependent fashion. This translocation reaction can be stimulated by the presence of a PMF and the anionic phospholipid cardiolipin. SecYEG dimers (middle), arranged in a back-to-back orientation via SecE-E interactions, are capable of mediating the same reaction, but the effect of the PMF is less. Membrane protein integration (right) may preferentially use the SecYEG-SecDF-YajC-YidC setup (the holo-translocon) for insertion of newly-synthesized transmembrane helices directly into the lipid bilayer. (b) Top view of proposed interactions for the YEG dimer and holo-translocon. Black bars represent subunit crosslinks.

Different translocons may form either from single copies of SecYEG and SecDF-YajC-YidC (HTL) or two copies of SecYEG (Fig. 7) or of YidC alone. The estimated number of copies of SecYE (300-400 copies/cell), SecDF (30 copies/cell) (33) and YidC (2700 copies/cell) (34) are very different. Thus, a typical cell might contain up to 5 copies of SecYEG dimers for every SecYEG-(SecDF-YajC-YidC) complex. The need for a large (100-fold) excess of YidC is unclear; it may in part be required for its Sec- independent activity.
The dynamic exchange of the accessory complexes bound to SecYEG may provide a means

to modulate translocation activity (Fig. 7) and the composition of the membrane and envelope during different stages of growth or upon exposure to different environmental conditions. Similarly, the eukaryotic Sec61 complex and mitochondrial import machinery are likely to associate with a number of different accessory factors tailored to the specific needs of folding, assembly and modification.

Materials and Methods

Strains, Plasmids and Antisera.

E. coli strain C43(DE3) was used for overexpression of the HTL components and was a gift from Sir John Walker (MRC Mitochondrial Biology Unit, Cambridge). The expression vectors for SecYEG and SecDF-YidC-YajC (DFYY) were from our lab collection (35). The plasmids for SecDF-YidC and covalently-linked SecYEG dimer expression were gifts from Franck Duong (University of British Columbia, Vancouver, Canada). Mouse monoclonal antibodies to SecY, E, and G were from our laboratory collection.

Enzymes and Chemicals.

Cardiolipin was obtained from Avanti Polar Lipids. *n*- Dodecyl-β-D-maltoside (DDM) was from Glycon Biochemicals GmbH (Luckenwalde, Germany). Unless noted otherwise, all other reagents used in this study were from Sigma-Aldrich (St. Louis, MO, USA).

Construction of the pACEMBL:HTL expression plasmid.

The HTL expression plasmid (Fig. 1a) was constructed using the ACEMBL expression system (23). (See SI Materials and Methods for full details).

Purification of SecYEG, SecA, proOmpA and SecDF-YidC.

SecYEG, SecA and proOmpA proteins were purified according to well-established procedures (36). SecDF- YidC was purified in the same way as SecYEG by Ni^{2+}-chelating, anion exchange and size exclusion chromatography.

Purification of the HTL.

Freshly transformed *E. coli* C43(DE3) containing pACEMBL:HTL were grown in 2xYT broth with antibiotics to an OD_{600} of 0.8, prior to 3 h of induction using 1 mM IPTG and 0.2 % (w/v) arabinose. Following centrifugation, cell pellets were broken at 25 kpsi using a cell

disruptor (Constant Systems, Ltd., Daventry, UK) in TSG_{130} buffer (20 mM Tris-Cl, pH 8.0, 130 mM NaCl, 10 % (v/v) glycerol). Membranes were collected by and solubilized by rotation in TSG_{130} buffer containing 2 % (w/v) DDM for 1h at 4°C. The DDM-soluble fraction was clarified by further centrifugation and applied to a Chelating Ni^{2+}-Sepharose Fast Flow column (GE Healthcare) pre-equilibrated with TSG_{130} + 0.1 % DDM. The resin bed was washed with ten column volumes of buffer containing 30 mM imidazole prior to elution with the same buffer containing 500 mM imidazole. Peak fractions were loaded onto a Superdex 200, 26/60 gel filtration column (GE Healthcare) placed in-line with a Q-sepharose ion exchange column equilibrated in TSG_{130} + 0.05 % DDM. A well-defined A_{280} peak eluted at approximately 190 ml and was concentrated in a 50 kDa-MW cut-off centrifugation filter (Amicon) to ~10 mg/ml, using an experimentally determined molar extinction coefficient of ε_{HTL} = 497,000 M^{-1} cm^{-1}.

Cy3 labelling of HTL and SecYEG.

Membranes containing over-expressed cysteine mutants of SecYEG and HTL were incubated with 2 mM TCEP for 15 min. on ice. Subsequently, Cy3 maleimide (Lumiprobe) was added at a concentration of 1 mM and incubated for 1 hour at 4°C in the dark. The reaction was quenched by adding 10 mM reduced glutathione. HTL and SecYEG were then purified as before.

Blue-Native PAGE analysis.

To analyze the effect of detergent concentration on the oligomeric states of the HTL, SecYEG, SecDF-YidC, and YidC, we incubated 50 ng of each complex in TSG_{130} buffer containing decreasing detergent concentrations on ice for 20 min. Coomassie G-250 was then added to a final concentration of 0.025 % prior to loading onto 4-16% Bis-Tris NativePAGE gels (Invitrogen, Carlsbad, CA). Bands were visualized by silver stain (SilverQuest Staining Kit, Invitrogen).

***In vivo* and *in vitro* crosslinking.**

Analysis of inter-subunit organization within the HTL was probed using Tris-bipyridylruthenium(II) (as described (4)) or DSP. DSP crosslinking was performed in IMVs containing overexpressed SecYEG or HTL in HSG_{130} (50mM HEPES, pH 7.5, 130 mM NaCl, 10 % glycerol) buffer. IMVs were isolated as in (4). DSP was then added to the IMVs at a final concentration of 150 µM before incubation at room temperature for 20 min. The reaction was quenched by addition of Tris-Cl, pH 8.0 to a final concentration of 50 mM.

The crosslinked SecYEG or HTL was then examined by Western blot directly from IMVs or by further purification as above.

SecA ATPase Stimulation.

SecYEG- or HTL-mediated stimulation of the SecA ATPase was measured by titrating in increasing concentrations of each complex into solutions of SecA, as has been previously described (36), in the presence or absence of 40 µM cardiolipin. See SI Materials and Methods for data analysis.

Affinity measurements of SecA to either SecYEG or HTL by quenching of an extrinsic fluorescent probe on SecA.

SecYEG or HTL were titrated into solutions of fluorescently labeled $SecA_{A795C}$ ($SecA_{795Fl}$) as indicated. Fluorescence assays were performed in 20 mM Tris, (pH 8.0), 130 mM NaCl, 10 % glycerol, 2 mM $MgCl_2$, 0.02 % DDM, 1 mM AMPPNP and 10 nM $SecA_{795Fl}$. $SecA_{795Fl}$ fluorescence quenching was monitored using a Jobin Yvon Fluorolog (Horiba Scientific), at an excitation wavelength of 495 nm and emission wavelength of 515 nm. 40 µM cardiolipin was incorporated into the assay buffer where required, and SecYEG or HTL stocks were incubated with 40 µM cardiolipin for one hour prior to titration. Specificity of the quenching of $SecA_{795Fl}$ was assessed by competition for SecYEG or HTL binding using 1 µM wild-type SecA. See SI Materials and Methods for data analysis.

Co-reconstitution of BR with translocation machinery.

For *in vitro* generation of a PMF in proteoliposomes, bacteriorhodopsin (BR) from *Halobacterium halobium* purple membranes was co-reconstituted together with the HTL or SecYEG. Purple membranes were purified by standard methods (37) (See SI Materials and Methods for full details). Protein translocation was then established into the vesicles by standard methods (36) for 15 minutes at RT, either in the dark or 10 cm away from a saturating light source from a Kodak slide projector fitted with a yellow filter for the generation of a PMF. Carbonyl cyanide *m*-chlorophenyl hydrazine (CCCP) was used at a final concentration of 50 µM to collapse the PMF.

***In vitro* translocation assay.**

The protein transport activity of the HTL or SecYEG was analyzed as described (36).

Ribosome Binding Assays.

Binding of purified SecYEG, HTL, YidC, SecDF or DF- YajC-YidC, to ribosome nascent chain complexes (RNCs) displaying the FtsQ transmembrane helix (27) and to 70S non-translating ribosomes was analyzed by co- sedimentation experiments. In all experiments, excess of translocon (sub)complexes compared to ribosomes was used (see Fig. 6a).

Affinity measurements of either SecYEG or HTL to 70S by fluorescence analysis.

100 nM Cy3-labelled cysteine mutants of HTL or SecYEG in 50 mM HEPES/KOH pH 7.5; 100 mM $KOAc_2$; 20 mM $MgOAc_2$; 10% glycerol; 0.03% DDM was mixed 1:1 with 0.3 nM to 11 µM 70S ribosomes in 20 mM HEPES/KOH pH 7.5; 20 mM $MgOAc_2$; 30 mM NH_4Cl; 1 mM DTT in a volume of 30 µl. Fluorescence was measured using a Monolith NT.115 and data was analysed using the supplied software (Nanotemper, Germany). Each experiment was repeated 4-fold and the fluorescence was normalized by division through the average of the first four data points.

Negative-stain EM and image processing.

Detergent-solubilized, purified HTL complexes were subjected to GraFix (38) and subsequently analyzed by negative-stain EM. (See SI Materials and Methods for full details).

***In vitro* transcription/translation/insertion assay.**

E. coli cytochrome *bo3* oxidase subunit CyoA was chosen as a substrate for monitoring co-translational insertion into proteoliposomes. mRNA transcripts were generated using T7 RNA polymerase by *in vitro* transcription from PCR products containing *cyoA* downstream of a T7 promoter. These mRNAs were subsequently used in a coupled *in vitro* translation/insertion assay. (See SI Materials and Methods for full details).

Acknowledgements

We are very grateful to Dr John Bason (MRC-Mitochondrial Biology Unit, Cambridge, UK) for advice with the reconstitution of BR, and Sir John Walker (MRC-Mitochondrial Biology Unit, Cambridge, UK) for the *E. coli* C43 expression strain. Our gratitude also goes to Prof Franck Duong (University of Bristish Columbia, Vancouver, Canada) for SecDF-YidC and SecY-Y over-expression constructs. We thank Dr Alice Robson (University of Bristol) for assistance with kinetic analysis. This work was supported by a Royal Society Leverhulme Research Fellowship (to IC) and a BBSRC project grant (BB/F007248/1 to IC). CS is supported by contract research ‘Methoden für die Lebenswissenschaften’ of the Baden-

Württemberg Stiftung, by the *Agence Nationale* de la Recherche (HOLOTRANS project, JC09_471873) and an ERC Starting Grant (281331).

Author Contribution

RS, IB, CS and IC designed the experiments. RS, JK, SW, VG, MB, KH, JL, CS, and IC performed the experiments. HTL plasmid construction was performed by CS, MB, KH, and IB. Data was analyzed by RS, JK, VG, IB, CS and IC. RS, IB, CS, and IC wrote the manuscript. Requests for ACEMBL-system based expression reagents should be directed to Imre Berger (iberger@embl.fr).

References

1. Van den Berg B, Clemons WMJ, Collinson I, Modis Y, Hartmann E, Harrison SC, Rapoport TA (2004) X-ray structure of a protein-conducting channel. *Nature* 427:36–44.
2. Breyton C, Haase W, Rapoport TA, Kühlbrandt W, Collinson I (2002) Three-dimensional structure of the bacterial protein-translocation complex SecYEG. *Nature* 418:662–665.
3. Osborne AR, Rapoport TA (2007) Protein translocation is mediated by oligomers of the SecY complex with one SecY copy forming the channel. *Cell* 129:97–110.
4. Deville K, Gold VA, Robson A, Whitehouse S, Sessions RB, Baldwin SA, Radford SE, Collinson I (2011) The oligomeric state and arrangement of the active bacterial translocon. *J. Biol. Chem.* 286:4659–4669.
5. Dalal K, Chan CS, Sligar SG, Duong F (2012) Two copies of the SecY channel and acidic lipids are necessary to activate the SecA translocation ATPase. *Proc. Natl. Acad. Sci. U. S. A.* 109:4104–4109.
6. Park E, Rapoport TA (2012) Bacterial protein translocation requires only one copy of the SecY complex *in vivo*. *J. Cell. Biol.* 198:881–893.
7. Duong F, Wickner W (1997) Distinct catalytic roles of the SecYE, SecG and SecDFyajC subunits of preprotein translocase holoenzyme. *EMBO J.* 16:2756–2768.
8. Scotti PA, Urbanus ML, Brunner J, de Gier JW, von Heijne G, van der Does C, Driessen AJ, Oudega B, Luirink J (2000) YidC, the *Escherichia coli* homologue of mitochondrial Oxa1p, is a component of the Sec translocase. *EMBO J.* 19:542–549.
9. Samuelson JC, Chen M, Jiang F, Moller I, Wiedmann M, Kuhn A, Phillips GJ, Dalbey RE (2000) YidC mediates membrane protein insertion in bacteria. *Nature* 406:637–641.
10. Beck K, Eisner G, Trescher D, Dalbey RE, Brunner J, Müller M (2001) YidC, an assembly site for polytopic *Escherichia coli* membrane proteins located in immediate proximity to the SecYE translocon and lipids. *EMBO Rep.* 2:709–714.
11. Urbanus ML, Scotti PA, Fröderberg L, Saaf A, de Gier JW, Brunner J, Samuelson JC, Dalbey RE, Oudega B, Luirink J (2001) Sec-dependent membrane protein insertion: sequential interaction of nascent FtsQ with SecY and YidC. *EMBO Rep.* 2:524–529.
12. Sachelaru I, Petriman NA, Kudva R, Kuhn P, Welte T, Knapp B, Drepper F, Warscheid B, Koch HG (2013) YidC occupies the lateral gate of the SecYEG translocon and is sequentially displaced by a nascent membrane protein. *J. Biol. Chem.* 288:16295-16307.
13. Samuelson JC, Jiang F, Yi L, Chen M, de Gier JW, Kuhn A, Dalbey RE (2001)

Function of YidC for the insertion of M13 procoat protein in *Escherichia coli*: translocation of mutants that show differences in their membrane potential dependence and Sec requirement. *J. Biol. Chem.* 276:34847–34852.

14. Chen M, Samuelson JC, Jiang F, Müller M, Kuhn A, Dalbey RE (2002) Direct interaction of YidC with the Sec-independent Pf3 coat protein during its membrane protein insertion. *J. Biol. Chem.* 277:7670–7675.
15. van der Laan M, Bechtluft P, Kol S, Nouwen N, Driessen AJ (2004) F1F0 ATP synthase subunit c is a substrate of the novel YidC pathway for membrane protein biogenesis. *J. Cell. Biol.* 165:213–222.
16. Nouwen N, Driessen AJ (2002) SecDFyajC forms a heterotetrameric complex with YidC. *Mol. Microbiol.* 44:1397–1405.
17. Duong F, Wickner W (1997) The SecDFyajC domain of preprotein translocase controls preprotein movement by regulating SecA membrane cycling. *EMBO J.* 16:4871–4879.
18. Economou A, Pogliano JA, Beckwith J, Oliver DB, Wickner W (1995) SecA membrane cycling at SecYEG is driven by distinct ATP binding and hydrolysis events and is regulated by SecD and SecF. *Cell* 83:1171–1181.
19. Tsukazaki T, Mori H, Echizen Y, Ishitani R, Fukai S, Tanaka T, Perederina A, Vassylyev DG, Kohno T, Maturana AD *et al.* (2011) Structure and function of a membrane component SecDF that enhances protein export. *Nature* 474:235–238.
20. Brundage L, Hendrick JP, Schiebel E, Driessen AJ, Wickner W (1990) The purified *E. coli* integral membrane protein SecY/E is sufficient for reconstitution of SecA-dependent precursor protein translocation. *Cell* 62:649–657.
21. Arkowitz RA, Wickner W (1994) SecD and SecF are required for the proton electrochemical gradient stimulation of preprotein translocation. *EMBO J.* 13:954-963.
22. Tseng TT, Gratwick KS, Kollman J, Park D, Nies DH, Goffeau A, Saier MHJ (1999) The RND permease superfamily: an ancient, ubiquitous and diverse family that includes human disease and development proteins. *J. Mol. Microbiol. Biotechnol.* 1:107–125.
23. Bieniossek C, Nie Y, Frey D, Olieric N, Schaffitzel C, Collinson I, Romier C, Berger P, Richmond TJ, Steinmetz MO *et al.* (2009) Automated unrestricted multigene recombineering for multiprotein complex production. *Nat. Methods* 6:447-450.
24. Bessonneau P, Besson V, Collinson I, Duong F (2002) The SecYEG preprotein translocation channel is a conformationally dynamic and dimeric structure. *EMBO J.* 21:995–1003.
25. Gold VA, Robson A, Bao H, Romantsov T, Duong F, Collinson I (2010) The action of cardiolipin on the bacterial translocon. *Proc. Natl. Acad. Sci. U. S. A.* 107:10044–10049.

26. Akiyama Y, Ito K (1990) SecY protein, a membrane-embedded secretion factor of *E. coli*, is cleaved by the ompT protease *in vitro*. *Biochem. Biophys. Res. Commun.* 167:711–715.
27. Schaffitzel C, Ban N (2007) Generation of ribosome nascent chain complexes for structural and functional studies. *J. Struct. Biol.* 158:463–471.
28. Lycklama à Nijeholt JA, Wu ZC, Driessen AJ (2011) Conformational dynamics of the plug domain of the SecYEG protein-conducting channel. *J. Biol. Chem.* 286:43881–43890.
29. du Plessis DJ, Nouwen N, Driessen AJ (2006) Subunit a of cytochrome o oxidase requires both YidC and SecYEG for membrane insertion. *J. Biol. Chem.* 281:12248–12252.
30. Cannon KS, Or E, Clemons WMJ, Shibata Y, Rapoport TA (2005) Disulfide bridge formation between SecY and a translocating polypeptide localizes the translocation pore to the center of SecY. *J. Cell. Biol.* 169:219–225.
31. Klenner C, Kuhn A (2012) Dynamic disulfide scanning of the membrane-inserting Pf3 coat protein reveals multiple YidC substrate contacts. *J. Biol. Chem.* 287:3769-3776.
32. Kato Y, Nishiyama K, Tokuda H (2003) Depletion of SecDF-YajC causes a decrease in the level of SecG: implication for their functional interaction. *FEBS Lett.* 550:114–118.
33. Pogliano KJ, Beckwith J (1994) Genetic and molecular characterization of the *Escherichia coli* secD operon and its products. *J. Bacteriol.* 176:804–814.
34. Urbanus ML, Fröderberg L, Drew D, Björk P, de Gier JW, Brunner J, Oudega B, Luirink J (2002) Targeting, insertion, and localization of *Escherichia coli* YidC. *J. Biol. Chem.* 277:12718–12723.
35. Collinson I, Breyton C, Duong F, Tziatzios C, Schubert D, Or E, Rapoport T, Kühlbrandt W (2001) Projection structure and oligomeric properties of a bacterial core protein translocase. *EMBO J.* 20:2462–2471.
36. Robson A, Gold VA, Hodson S, Clarke AR, Collinson I (2009) Energy transduction in protein transport and the ATP hydrolytic cycle of SecA. *Proc. Natl. Acad. Sci. U. S. A.* 106:5111–5116.
37. Oesterhelt D, Stoeckenius W (1974) Isolation of the cell membrane of *Halobacterium halobium* and its fractionation into red and purple membrane. *Methods Enzymol.* 31:667–678.
38. Kastner B, Fischer N, Golas MM, Sander B, Dube P, Boehringer D, Hartmuth K, Deckert J, Hauer F, Wolf E *et al.* (2008) GraFix: sample preparation for single- particle electron cryomicroscopy. *Nat. Methods* 5:53–55.
39. Duong F (2003) Binding, activation and dissociation of the dimeric SecA ATPase at the

dimeric SecYEG translocase. *EMBO J.* 22:4375–4384.

40. Estrozi LF, Boehringer D, Shan SO, Ban N, Schaffitzel C (2011) Cryo-EM structure of the *E. coli* translating ribosome in complex with SRP and its receptor. *Nat. Struct. Mol. Biol.* 18:88–90.

Supplementary Information (Materials and Methods) – Schulze *et al.*

Supplementary Figures

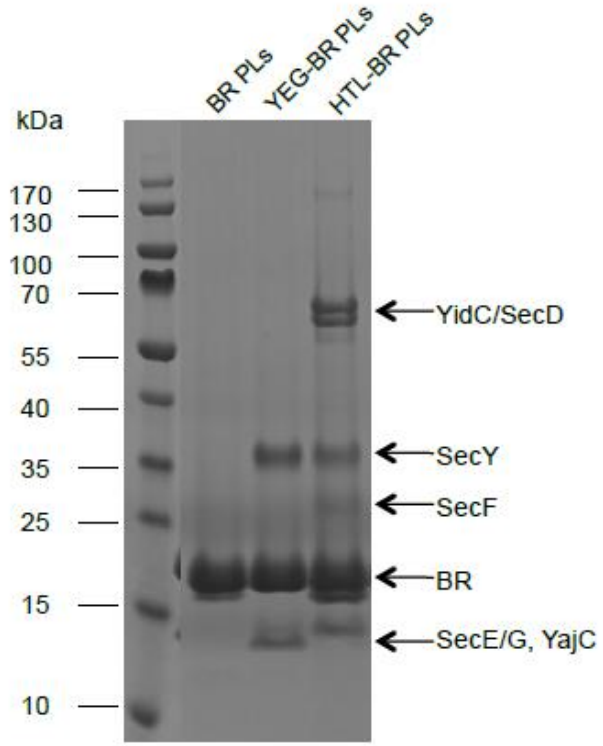

Figure S1. Composition of proteoliposomes used for *in vitro* translocation and *in vitro* insertion experiments. Aliquots of proteoliposomes used for the translocation/insertion experiments were solubilized in LDS sample loading buffer and subjected to SDS-PAGE on 4-20% Bis-Tris gels. Proteins were visualized by Coomassie staining. Note that migration of SecE is slightly higher in the HTL construct compared to the SecYEG construct due to slight differences in sequences of the affinity tags between the two.

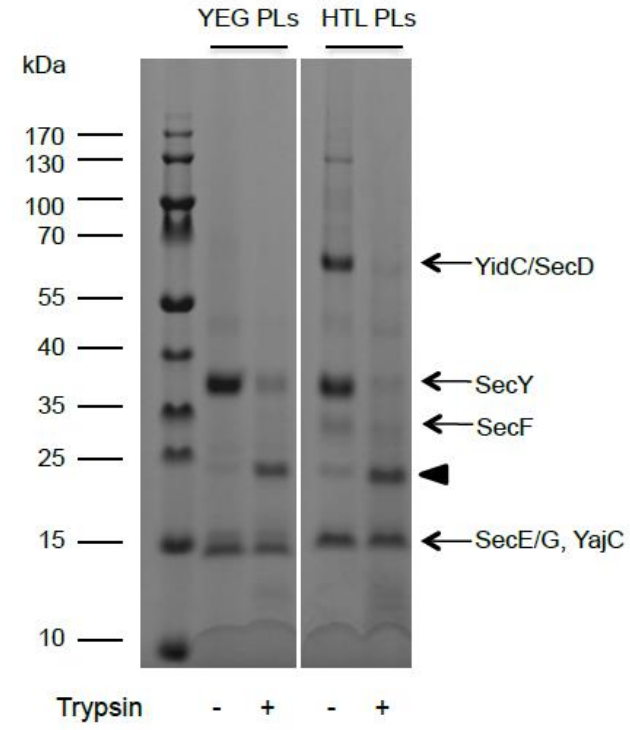

Figure S2. Orientation of complexes in proteoliposomes. Aliquots of SecYEG- and HTL-containing proteoliposomes were treated with trypsin and subjected to SDS-PAGE followed by Coomassie staining. The generated proteolysis fragment is indicated by a black arrowhead.

Construction of the pACEMBL:HTL expression plasmid.

The pACEMBL:HTL plasmid was constructed using the ACEMBL system {Bieniossek et al., 2009, Nat Methods}. The plasmid consists of the pACE acceptor and the pDC and pDK donor vectors combined by Cre-loxP fusion (LoxP, grey circles). A polycistron encoding for YidC, SecD (D), SecF (F) with an arabinose promoter (ara, lime green) has been subcloned into pACE. A second polycistron encoding for SecY, SecE (E) and SecG (G) with a trc promoter (trc, grey triangles) has been cloned into pDC. Calmodulin-binding protein (CBP)-tagged YajC under the control of the trc promoter was cloned into pDK. In Fig. 1a, transcriptional terminators are shown as small black rectangles. The position of hexahistidine-tags in YidC, SecD and SecE are indicated in red and the CBP-tag of YajC is indicated in orange. Origins of replication (BR322 and R6Kγ) are indicated by large black rectangles. Antibiotic resistance genes confer resistance to the following antibiotics: Ap (ampicillin, purple), Cm (chloramphenicol, green), and Kn (kanamycin, blue) (Fig. 1a).

SecA ATPase Stimulation.

The data in the absence of CL were fitted to the one-site weak binding equation (Equation 1):

$$v = \frac{B_{max}.[L]}{K_d + [L]}$$

(Eq. 1)

where [*L*] is the total concentration of ligand (SecYEG or HTL), *v* is the enzyme velocity, B_{max} is the total capacity of SecA-ligand, and K_d is the dissociation constant. Data recorded in the presence of CL were fitted to a one site tight binding equation with *background* (basal activity in the absence of SecYEG or HTL) (Equation 2):

$$v = B_{max}.\frac{[L] + [E_o] + K_d - \sqrt{([L] + [E_o] + K_d)^2 - 4[E_o][L]}}{2[E_o]} + Background$$

(Eq. 2)

where *v* is equal to enzyme velocity, B_{max} is the total capacity of SecA-ligand, [*L*] is the total ligand (*i.e.* SecYEG or HTL) concentration, [E_O] is the total SecA concentration and K_d is the dissociation constant for SecA-ligand.

Affinity measurements of SecA to either SecYEG or HTL by quenching of an extrinsic fluorescent probe on SecA.

SecYEG data measured in the absence of CL were fitted to the one-site weak binding equation (Equation 3):

$$F = \frac{F_{max}.[L]}{K_d + [L]}$$

(Eq. 3)

where [*L*] is the total concentration of ligand (SecYEG or HTL), *F* is the fluorescence change, F_{max} is the maximum fluorescence quench, and K_d is the dissociation constant. HTL data recorded in the absence of CL were fitted to the one-site weak binding equation with a linear component (*m*) (Equation 4):

$$F = \frac{F_{max}.[L]}{(K_d + [L]) + m.[L]}$$

(Eq. 4)

HTL and YEG data in the presence of CL were fitted to a one site tight binding equation with linear phase (Equation 5):

$$F = F_{max}.\frac{[L] + [E_o] + K_d - \sqrt{([L] + [E_o] + K_d)^2 - 4.[E_o].[L]}}{2.[E_o]} + m.[L]$$

(Eq. 5)

where *F* is the fluorescence change, [*L*] is the concentration of ligand, [E_O] is the total SecA concentration, K_d is the dissociation constant, *m* is the linear component, and F_{max} is the maximum signal change.

Co-reconstitution of BR with translocation machinery.

BR membranes were purified by standard methods {Oesterhelt and Stoeckenius, 1974, Methods Enzymol, 31, 667-78} and solubilized with 2 % Triton X-100 for 72 h at 21°C. Proteoliposomes were made by combining BR (0.22 mg/ml = 8.9 mM) together with either SecYEG (0.22 mM - dimer) or HTL (0.22 mM) and *E. coli* total polar lipids: hen egg PC (3:1 ratio; 2.9 mg/ml) in the presence of 0.25 % Triton X-100 in liposome buffer (20 mM Tris-Cl, 50 mM KCl, 2 mM $MgCl_2$) at 23°C in total darkness. The vesicles were then reconstituted by the removal of detergent via adsorption to polystyrene Bio-beads SM-2 Adsorbent (Bio-Rad), pelleted by ultra-centrifugation and reconstituted in liposome buffer together with purified BR (90 µM), SecYEG (2.3 µM dimers) or the HTL complex (2.3 µM).

Negative-stain EM and image processing.

Detergent-solubilized, purified HTL complexes were subjected to GraFix {Kastner et al., 2008, Nat Methods, 5, 53-5} and subsequently analyzed by negative-stain EM. The complexes were absorbed onto carbon film for 30 s, followed by negative staining with 2% uranyl acetate for 30 s. 150 micrographs of the complex were recorded under low dose conditions with a bottom mounted Orios SC600 camera (Gatan Inc.) in a Jeol 1200EX II transmission electron microscope running at 100 kV at a magnification of 40,000x (pixel size of 1.7Å). A total of 8,000 individual HTL complexes were selected with Boxer (EMAN) {Ludtke et al., 1999, J Struct Biol, 128, 82-97} from the micrographs and processed with IMAGIC-5 (Image Science) {van Heel et al., 1996, J Struct Biol, 116, 17-24}. After a first "reference-free" alignment procedure, the particles were iteratively subjected to multivariate statistical analysis and classification. Selected 2D class averages were used as reference images for the subsequent rounds of alignment resulting in 300 2D class averages {van Heel and Frank, 1981, Ultramicroscopy, 6, 187-94}. Characteristic class averages are shown in Fig. 2.

Trypsin proteolysis.

SecYEG and HTL proteoliposomes were subjected to proteolysis using trypsin (15 µg/µl) at a ratio of 2:1. The reactions were incubated at room temperature for 20 minutes, solubilised in LDS sample buffer and subsequently run on SDS-PAGE followed by Coomassie blue staining.

***In vitro* transcription/translation/insertion assay.**

E. coli cytochrome *bo3* oxidase subunit CyoA was chosen as a substrate for monitoring co-translational insertion into proteoliposomes. mRNA transcripts were generated using T7 RNA polymerase by *in vitro* transcription from PCR products containing *cyoA* downstream of a T7 promoter. These mRNAs were subsequently used in a coupled *in vitro* translation/insertion assay. Briefly, 8 µg of mRNA transcript was translated using an *E. coli* membrane-free cell extract {Schaffitzel and Ban, 2007, J Struct Biol, 158, 463-71} in the presence of *E. coli* scSRP {Estrozi et al., 2011, Nat Struct Mol Biol, 18, 88-90} and proteoliposomes containing BR +/- SecYEG or the HTL complex. The nascent polypeptides were detected by incorporation of radiolabeled ^{35}S-methionine. To assay for membrane insertion, the *in vitro* translation reaction was allowed to proceed in the presence of the same proteoliposomes used for the *in vitro* translocation assays. Following a 90 min coupled translation/insertion at room temperature, the proteoliposomes were purified by sucrose flotation and treated with 5M urea for 20 min on ice. The urea-washed proteoliposomes were then pelleted and

resuspended in SDS-PAGE sample buffer and loaded onto a 4-15% Bis-Tris PAGE gel. Radioactive material was identified by phosphorimaging.

Chapter 4 : Cryo-EM Structure of the SecYEG-SecDFYajC-YidC Holotranslocon complex

Résumé en français / French summary

L'existence d'un supercomplexe SecYEG-SecDFYajC-YidC chez *Escherichia coli* a été démontrée il y a plus d'une dizaine d'années. Ce complexe de protéines membranaires n'a cependant pu être analysé biochimiquement ou structuralement dû à la faible quantité d'échantillon hétérogène extrait de la membrane. Nous avons établi la production et la purification de ce complexe holotranslocon et l'avons utilisé pour une étude de cryo-microscopie électronique des particules isolées. La structure a été affinée à une résolution de 10.5 Å ce qui nous a permis de placer les structures cristallines à haute résolution des sous-complexes et domaines dans la densité. Le modèle quasi atomique révèle pour la première fois l'organisation moléculaire de SecYEG, SecDF-YajC et YidC au sein de complexe holotranslocon et explique les données biochimiques et de réticulation existantes. Basée sur nos données, nous suggérons un modèle expliquant comment le domaine accessoire de l'holotranslocon assiste la translocation des séquences hydrophiles et l'intégration des domaines transmembranaires dans la bicouche lipidique. Nous suggérons que l'holotranslocon fournit un environnement de protection pour le repliement des domaines transmembranaire polytopiques.

Manuscript

Cryo-EM Structure of the SecYEG-SecDFYajC-YidC Holotranslocon Complex

Manuscript in preparation

Abstract

The existence of a SecYEG-SecDFYajC-YidC supercomplex in *Escherichia coli* has been demonstrated more than a decade ago (Duong & Wickner, 1997, Scotti et al., 2000). The membrane protein complex could however not been biochemically or structurally analyzed due to the poor amount of heterogenous sample extracted from the membrane. We established the production and purification of this holotranslocon complex and used it for single particle cryo-electron microscopy. The structure was refined to 10.5 Å resolution which allowed to place the high-resolution crystal structures of the subcomplexes and domains into the density. The quasi-atomic model reveals for the first time the molecular organization of SecYEG, SecDF-YajC and YidC in the holotranslocon complex and explains the existing biochemical and crosslinking data. Based on our data, we suggest a model on how the accessory domains in the holotranslocon support translocation of hydrophilic sequences and integration of transmembrane domains into the lipid bilayer. We suggest that the holotranslocon provides a protected environment for the folding of polytopic transmembrane domains.

Introduction

One third of all proteins in a cell are translocated into or across a membrane. In *Escherichia coli*, this is accomplished by the universally conserved heterotrimeric SecYEG protein-conducting channel (Dalbey et al., 2011; Driessen & Nouwen, 2008; Luirink et al., 2012; Rapoport, 2008; Van den Berg et al., 2004). The crystal structures of SecYEG reveal that the ten transmembrane helices (TMHs) of SecY form the central pore through which hydrophilic parts of substrates are translocated (Ito, 1990; Van den Berg et al., 2004; Zimmer et al., 2008). SecY helices adopt the shape of a clam shell which can open. Thus, signal sequences and TMHs of the translocation substrates can be integrated into the lateral gate of SecY from where they can partition into the lipid bilayer (Hizlan et al., 2012; Van den Berg et al., 2004). Membrane proteins are translocated co-translationally (Ulbrandt et al., 1997). In this case, the ribosomal tunnel exit is aligned with the translocation pore (Becker et al., 2009; Beckmann et al., 2001; Frauenfeld et al., 2011; Mitra et al., 2005). Exported proteins mostly are translocated post-translationally requiring ATP and the ATPase SecA which forms a complex with SecYEG (Brundage et al., 1990; Hartl et al., 1990; Zimmer et al., 2008). Protein secretion can be enhanced by the proton motive force (PMF) (Brundage et al., 1990; Driessen, 1992; Schiebel et al., 1991; Shiozuka et al., 1990). SecE and SecG do not participate directly in translocation but are important for the integrity and stability of SecY.
Protein translocation additionally requires the membrane proteins SecD, SecF, YajC and YidC which associate with SecYEG forming the 'holotranslocon' (Duong & Wickner, 1997a; Scotti et al., 2000) SecYEG, SecDF and YidC are essential for cell viability (K. J. Pogliano & J. Beckwith, 1994). In inverted membrane vesicles, SecD and SecF can enhance translocation via SecYEG by using the PMF (Tsukazaki et al., 2011). SecDF have been suggested to prevent backsliding of translocation substrates (Duong & Wickner, 1997b) and to facilitate substrate release in the periplasm (Matsuyama et al., 1993; Tsukazaki et al., 2011). In the structure of *Thermus thermophilus* SecDF, the six transmembrane (TM) helices of SecD and of SecF are arranged pseudo-symmetrically (Tsukazaki et al., 2011). The TMH domain arrangement resembles the TM region of AcrB (Murakami et al., 2006) indicating a similar proton transport mechanism for SecD. The P1base domain of SecD and the periplasmic domain (P4) of SecF form pseudo-symmetric, anti-parallel beta-sheets (Tsukazaki et al., 2011). Deletion of the P1-head domain, which is implicated in substrate release (Matsuyama et al., 1993), interferes with proton transport. This suggests that substrate binding and conformational changes in the P1 head are linked to proton flow through the TM part of SecDF (Tsukazaki et al., 2011). SecDF forms a tight complex with the small 11 kDa protein, YajC of unknown function which consists of one TM helix and a C-terminal, cytoplasmic domain (Fang & Wei, 2011). YajC has been suggested to bridge

SecYEG and SecDF complexes structurally or functionally in absence of SecG (Duong & Wickner, 1997a).

YidC is essential for the insertion and folding of inner membrane proteins (Samuelson et al., 2000; van der Laan et al., 2005). YidC contains six TM helices and a large periplasmic domain. The C-terminal five TM helices are conserved in mitochondria and chloroplasts and are responsible for the Sec-independent translocase activity of YidC (Jiang et al., 2002; van Bloois et al., 2005). In complex with SecYEG, YidC is suggested to bind TM helices which leave the lateral gate of SecY and to assist in membrane protein folding (Nagamori et al., 2004; Urbanus et al., 2001; Zhu et al., 2013) and complex assembly (van der Laan et al., 2003). The periplasmic domain of YidC adopts a beta-supersandwich fold and contains a cleft implicated in binding of translocation substrates (Oliver & Paetzel, 2008; Ravaud et al., 2008). The YidC TM region has been studied by electron microscopy (EM) (Kohler et al., 2009; Lotz et al., 2008). YidC forms a stable complex with SecDFYajC (Nouwen & Driessen, 2002). In contrast, its interaction with SecYEG seems to be weak and dynamic (Sachelaru et al., 2013). However, in the presence of SecDFYajC, a stable complex can be immuneprecipitated (Duong & Wickner, 1997a) .

Here, we present the cryo-electron microscopy structure of the SecYEG-SecDFYajC-YidC holotranslocon complex at 10.5 Å resolution providing important, unprecedented insights in the architecture of the complex and the functional interplay of the subunits during translocation.

Results

Using the Acembl system (Bieniossek et al., 2009), we generated an *E. coli* plasmid for overexpression of all seven membrane proteins forming the holotranslocon. The n-Dodecyl β-D-Maltopyranoside (DDM)-solubilized SecYEG-SecDFYajC-YidC complex was purified by two affinity chromatography steps (Supplementary Fig. 1a). Size-exclusion chromatography and analytical ultracentrifugation indicated a molecular weight of ~250 kDa of the complex and 0.5g DDM bound per 1g protein (Supplementary Fig. 1b,c) corresponding to one copy each of SecYEG, SecDF and YidC in the complex. The cryo-EM structure of the holotranslocon refined to 10.5 Å resolution (‘gold-standard’ method (Scheres & Chen, 2012) and Fourier shell correlation criterion 0.5; Supplementary Fig. 2). The structure reveals a complex with dimensions of 114 Å x 106 Å x 92 Å with numerous cavities and protrusions (Fig. 1). We placed the available crystal structures of SecYEG (Van den Berg et al., 2004), SecDF (Tsukazaki et al., 2011), YajC (Törnroth-Horsefield et al., 2007) and of the periplasmic domain of YidC (Ravaud et al., 2008) as rigid bodies into the density. Thus, we

generated a quasi-atomic model corresponding to ~70% of the molecular weight of the holotranslocon (Fig. 1).

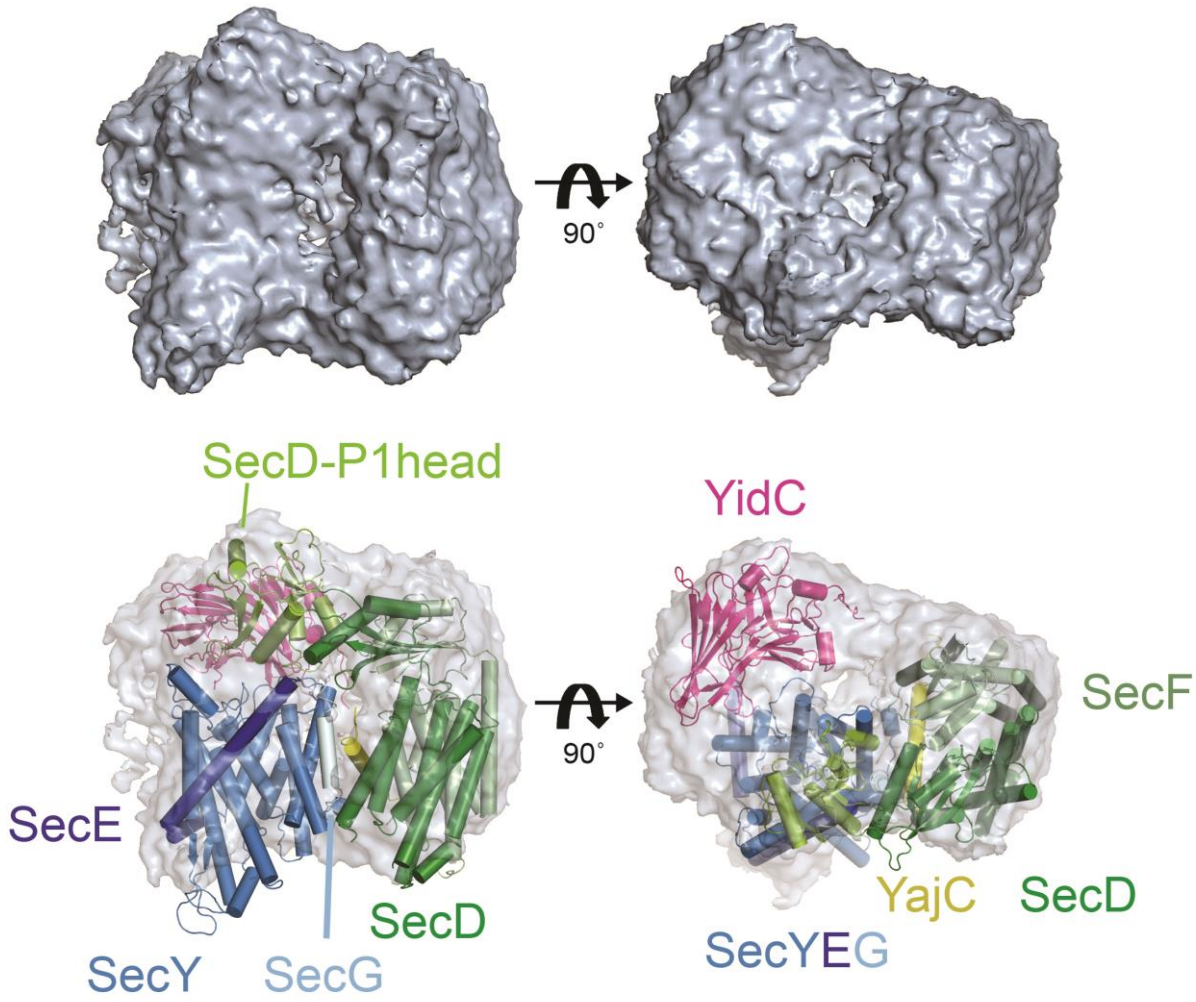

Figure 1. Structure of the *E. coli* SecYEG-SecDFYajC-YidC holotranslocon complex. The cryo-EM structure (top) is displayed in a side view (left) from the plane of the membrane and from the periplasm (right). The quasi-atomic model of holotranslocon is shown below. The cryo-EM density is depicted in transparent grey; SecY is coloured marine, SecE dark blue, SecG in cyan, SecD in green, SecF in light green and the periplasmic domain of YidC in magenta.

SecDFYajC and YidC have been shown to form a stable complex in *E. coli* (Nouwen & Driessen, 2002) (Supplementary Fig. 1). We calculated an independent EM reconstruction of this subcomplex (DFYY) in order to identify the position of SecYEG in the holotranslocon structure (Fig. 2, Supplementary Fig. 3). The EM reconstruction of DFYY could be placed into the holotranslocon reconstruction with a correlation coefficient of 0.975 indicating that the DFYY complex is rigid and does not undergo major conformational changes upon SecYEG docking (Fig. 2).

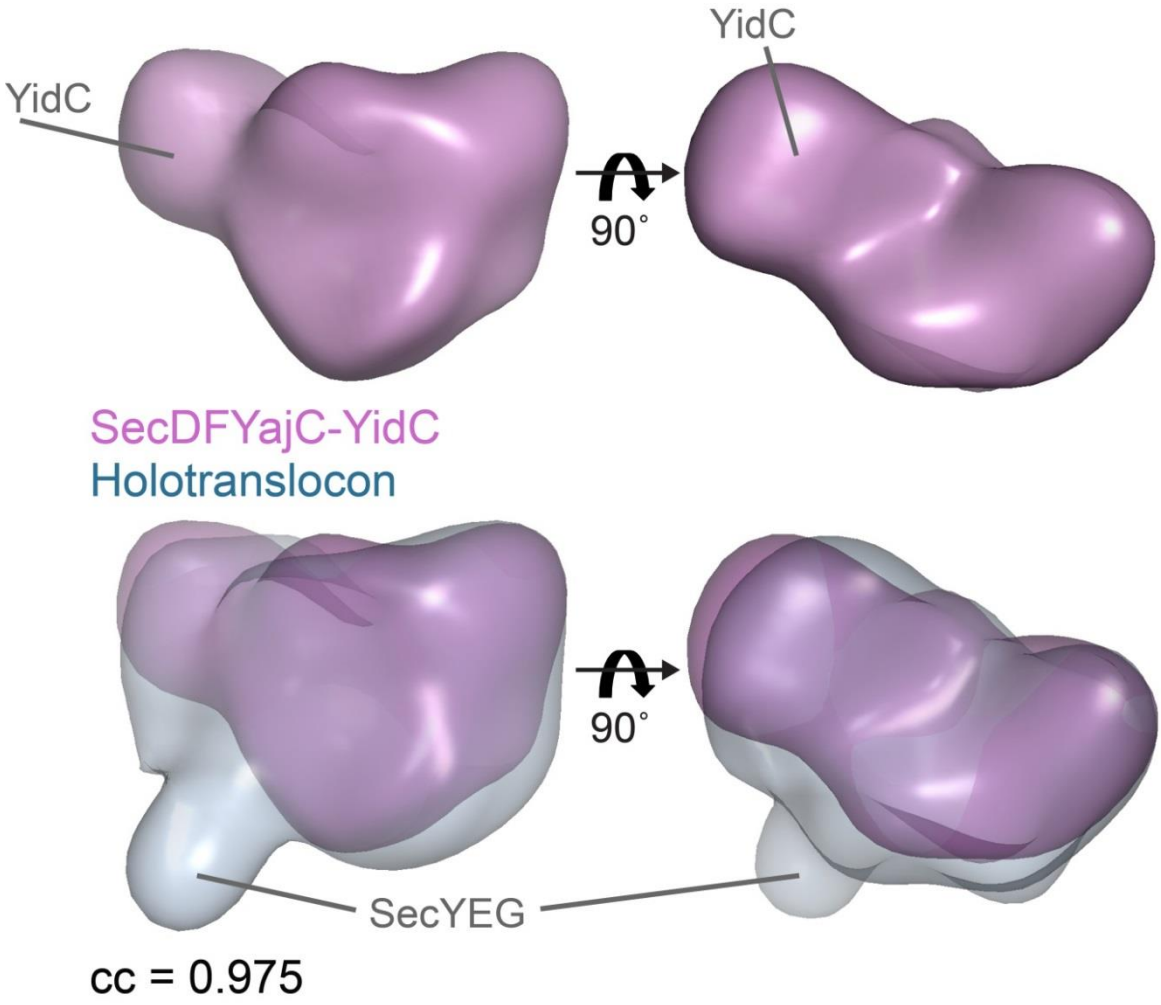

Figure 2. Localization of SecYEG in the Holotranslocon Complex. EM reconstruction of SecDFYajC-YidC (purple, above) in a view from the plane of the membrane (left) and from the periplasmic side (right). The SecDFYajC-YidC complex can be placed into the holotranslocon density (lightblue) with a correlation coefficient of 0.975 (below) indicating a very similar domain architecture of SecD, SecF, YajC and YidC in both complexes. The localization of SecYEG in the holotranslocon density is indicated.

Next, we analyzed the structural heterogeneity of the holotranslocon complex. The 3D variance map of the holotranslocon reconstruction indicates that the flexibility of the complex is highest in the SecYEG part (Supplementary Fig. 4). Furthermore, the map displaying the local resolution shows that the resolution is lower in the region of high variance which includes the SecYEG density (Supplementary Fig. 5). In agreement with this, we observed that the density corresponding to SecYEG is somewhat too small to accommodate the complete SecYEG crystal structure (Fig. 1). using 3D-classification by maximum-likelihood (Scheres et al., 2008) and multi-reference 3D angular refinement (Penczek et al., 2011), we could not detect clearly distinct SecYEG conformations in the holotranslocon complex.

Therefore, we assume that SecYEG binding to SecDFYajC-YidC is flexible and dynamic. Despite the fact that bacterial SecYEG complexes have been crystallized (Tsukazaki et al., 2008; Zimmer et al., 2008), we decided to fit the *Methanococcus jannaschii* SecYβγ structure (Van den Berg et al., 2004) into the holotranslocon density because it represents the inactive translocon where the channel is sealed with a small α-helix of SecY, named the plug.

To localize the position of YidC in the holotranslocon, we purified the SecYEG-SecDFYajC complex (ΔYidC) and calculated a 3D reconstruction using negative stain EM data (Fig. 3; Supplementary Fig. 6). A significant conformational change is observed in the ΔYidC complex compared to the holotranslocon structure (Fig. 3). This hampers the superimposition of the two 3D EM reconstructions. We observe a new connection between SecYEG and the remaining density (Fig. 3) and a small domain appears in the density which has not been observed before. In the ΔYidC reconstruction, we cannot detect the large domain positioned above SecYEG. Therefore, we attribute this density to the YidC periplasmic domain P1 (Fig 1). In fact, the crystal structure of the YidC P1 domain can be placed with high confidence into this density (see below).

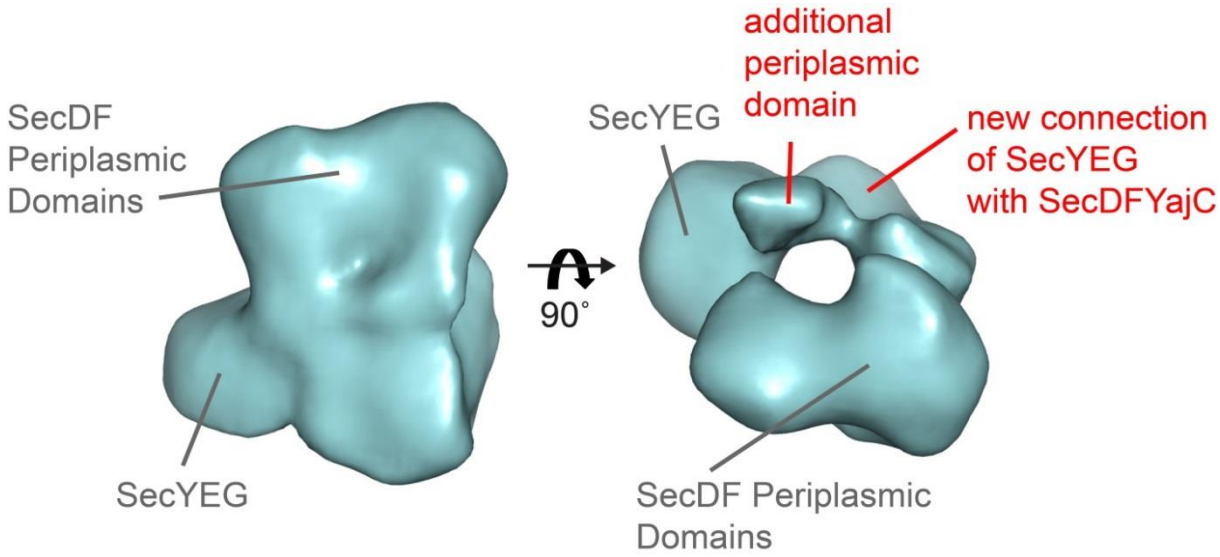

Figure 3. EM reconstruction of the SecYEG-SecDFYajC complex in a side view (left) and a view from the periplasm (right). The SecYEG density is more ordered compared to the holotranslocon and forms a new connection with the remaining density attributed to SecDFYajC. Additional density is detected on the periplasmic site of the complex positioned above SecYEG.

After localization of SecYEG and YidC in the holotranslocon map (Fig. 2 and Fig. 3), we placed the crystal structure of *Th. termophilus* SecDF (Tsukazaki et al., 2011) into the cryo-EM density (Fig. 4a). While SecF and the transmembrane region of SecD fit well into the density, the periplasmic domain P1 of SecD sticks out of the density. SecD-P1 consists of a

P1base with a ferredoxin-like fold and a P1head domain (Tsukazaki et al., 2011). A rotation of this domain and of the TMH1 of ~120 degrees around a hinge region between the P1 domain and TMH2 of SecD is required to fit this domain into the EM density (Fig. 4b). This conformational change disrupts the antiparallel beta-sheet connecting SecD P1 with the periplasmic domain P4 of SecF. Both, the P1base and the P4 domain adopt ferredoxin-like folds (Tsukazaki et al., 2011). Closer inspection of the P1-P4 domain interactions revealed that the five hydrogen bonds between SecD and SecF stabilizing the beta sheet have an average length of 3.36 Å indicating a rather week interaction of the two ferredoxin-like folds. For comparison, the beta-sheet-forming H-bonds within the ferredoxin-like folds of P1base and of P4 have an average length of 2.71 Å (Tsukazaki et al., 2011). Thus, it is conceivalbe that the periplasmic domains of SecD and SecF do not form a continuous beta-sheet in the holotranslocon complex. Furthermore, such a rather drastic conformational change with high activation energy may explain why it is not possible to reconstitute SecYEG-SecDFYajC complexes from the isolated subcomplexes.

As a result of the P1 rotation, the P1head domain is positioned above the translocation channel formed by SecY (Fig. 4a). As described above, the P1head has been suggested to play an important role in catalyzing protein translocation, possibly by binding the translocated polypeptide and by assisting the peptide release from the translocase (Matsuyama et al., 1993; Nouwen et al., 2005; Tsukazaki et al., 2011). The P1head domain was reported to adopt at least two conformations, an F- and an I-form which are related to each other by a 120 degree rotation around the loops connecting the P1base and P1head domains (Tsukazaki et al., 2011). The F-form of P1 fits into the holotranslocon density while the I-form clearly sticks out of the density (Supplementary Fig. 7). Superimposition of the F- and I-form of the P1head domain (Supplementary Fig. 7) suggests that there is no sterical hindrance in the holotranslocon complex to adopt the I-Form, and thus both conformations could be adopted during protein translocation. In the cryo-EM structure, we visualized the more compact F-Form of the SecD P1head domain where the P1base and the P1head domain of SecD are positioned above SecY, SecE and SecG. This placement is supported by crosslinking and complementation experiments (Schulze et al., submitted; (Kato et al., 2003)).

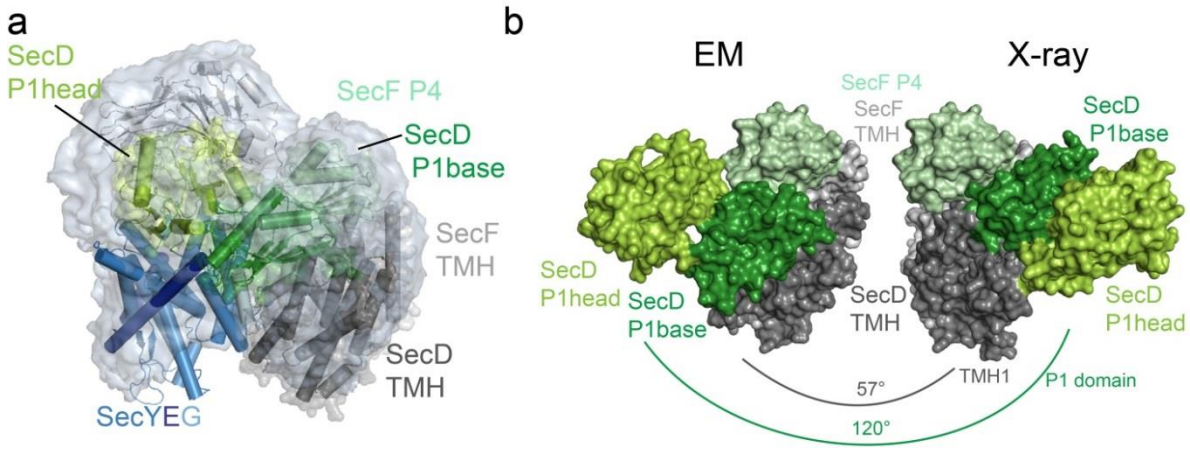

Figure 4. Fitting of the Crystal Structure of SecDF into the Holotranslocon Complex (Model 1). **(a)** Quasi atomic model showing the fitting of SecD and SecF domains into the EM density (grey). The transmembrane helices of SecD (dark grey) are in in contact with SecG and YajC. The periplasmic domain (P1) of SecD (dark green) is positioned above SecYEG such that the P1 head domain (greenyellow) is placed directly above the translocation channel formed by SecY (marine). **(b)** Comparison of the SecDF conformation in the quasi atomic model (left) with the SecDF crystal structure from *Thermus thermophilus* (Tsukazaki et al., 2011). The periplasmic domain (green and greenyellow) and the first transmembrane helix (TMH1) of SecD need to be rotated by 120° and 57° respectively to fit the density. The SecF (lightgrey and lightgreen) conformation remains virtually the same.

YajC was included in the holotranslocon expression construct because it may bridge the two SecYEG and SecDF subcomplexes (Duong & Wickner, 1997a). However, we did not observe any stabilizing effect of YajC during solubilization and purification of holotranslocon complexes. The only structural information available on YajC is the N-terminal TM helix spanning from the periplasma into the cytosol. The TM helix of YajC was crystallized in complex with the multidrug transporter AcrB which is homologous to SecDF (Törnroth-Horsefield et al., 2007; Tsukazaki et al., 2011). The copy number of YajC in holotranslocon is unknown as the 10 kDa protein is too small to confidently determine its stoichiometry by analytical ultracentrifugation (Supplementary Fig. 1c). In analogy to the AcrB-YajC complex, we assumed one copy of YajC bound to SecDF and fitted the YajC TM helix by superimposition of the crystal structures of the SecDF and the AcrB transmembrane regions (Törnroth-Horsefield et al., 2007; Tsukazaki et al., 2011). This places YajC at the interface between SecDF and SecYEG which is in agreement with a previous observation from Duong & Wickner (1997) where YajC could be co-immunoprecipitated with SecDF and with SecYEG. According to this placement, the cytoplasmic domain of YajC would be close to SecF. In fact, we observe unfilled density in the cytoplasm in this region.

The crystal structure of the periplasmic domain P1 of *E. coli* YidC (Oliver & Paetzel, 2008; Ravaud et al., 2008) could be unambiguously placed into the density located above the SecYEG translocon (Fig. 5a, cc = 0.925). In the YidC P1 crystal structure, a polyethylene

glycol (PEG) molecule was found in an elongated cleft containing many hydrophobic, conserved residues (Ravaud et al., 2008). It was suggested that this may be a binding pocket for translocation substrates. In fact, the YidC P1 domain is positioned in the holotranslocon complex such that it could interact with hydrophobic stretches of the translocated polypeptide (Fig. 5a).

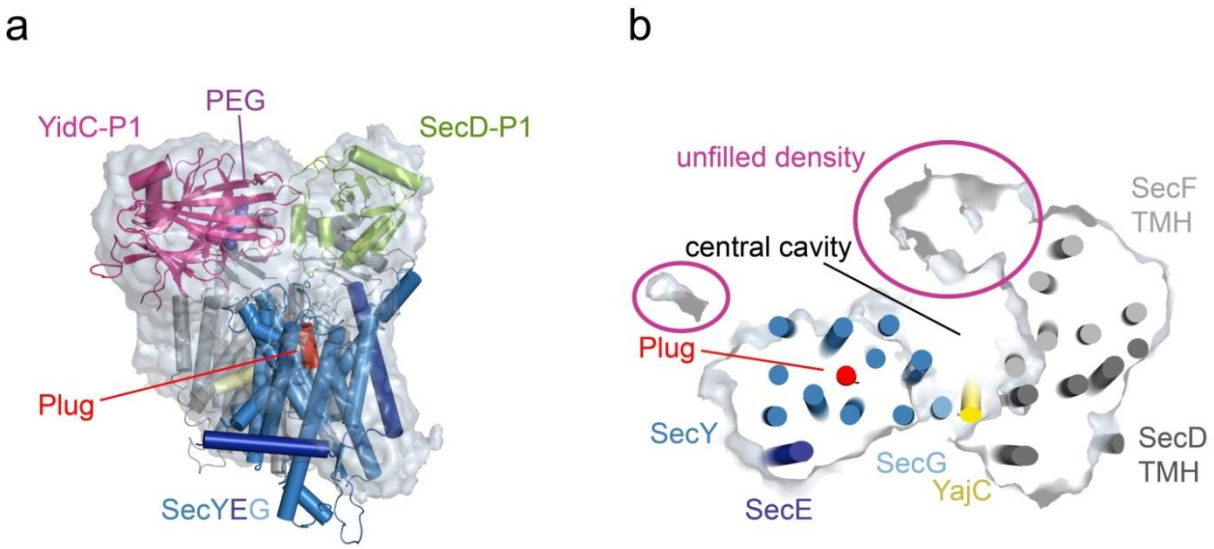

Figure 5. YidC placement in the holotranslocon complex. (a) Side view of the holotranslocon complex from the plane of the membrane. The crystal structure of the periplasmic domain of *E. coli* YidC (magenta) (Oliver & Paetzel, 2008; Ravaud et al., 2008) could be unambiguously placed into the cryo-EM density (cc = 0.93) next to the SecYEG translocation channel (blue) (Van den Berg et al., 2004) which in its inactive state is sealed by the plug helix of SecY (in red). The PEG molecule bound to YidC in a putative substrate-binding cleft (Ravaud et al., 2008) is depicted in purple spheres. **(b)** Slap in the plane of the membrane shown from the periplasmic site. Unfilled density is identified connected to the transmembrane helices of SecF (light grey) and YajC (yellow) and *vis-à-vis* the lateral gate of SecYEG. A central cavity is detected in the center of the complex.

Together, the periplasmic domains of SecD, SecF and YidC form a ring-like arrangement in the holotranslocon complex (Fig. 1). In the membrane the TM domains are forming a U-shape and a central cavity is observed (Fig. 5b). Next to the TM domains of SecF and YajC and *vis-à-vis* of the SecY channel, additional density is detected. This unfilled density is connected to the YidC periplasmic domain and contacts SecY close to the cytoplasm. It could well be that this density corresponds to the TM region of YidC of which a high resolution structure is not available. In support of this, crosslinks of the cytoplasmic C-terminus of YidC to SecF, YajC and SecY (but not SecD) have been reported recently (Sachelaru et al., 2013)(Supplementary Table 1).

Smaller unfilled density corresponding to one or two TM helices is observed next to the SecYEG complex (Fig. 5b). This density is close to SecYEG and to the YidC periplasmic domain. Therefore, it could be allocated to TM helices 1 and 2 of SecE or to TM helix 1 of

YidC. We favor the latter option because in the EM reconstruction of DFYY we observe a similar density at high contour level (Supplementary Fig. 8). In support of this, in the projection map of *E. coli* one helix of YidC was positioned rather distant from the other helices (Lotz et al., 2008) indicating that TM1 likely is not tightly connected to the C-terminal conserved TM part of YidC.

Discussion

Here, we present the cryo-EM structure of the holotranslocon complex which has been discovered 15 years ago by radio-immunoprecipitation (Duong & Wickner, 1997a). Since then, translocation by SecYEG and YidC alone has been extensively studied biochemically, and crystal structures were reported for a major part of the subunits forming the holotranslocon. Nevertheless, the holotranslocon itself and its subcomplexes (SecDFYajC-YidC and SecYEG-SecDFYajC as well as SecYEG-YidC) have not been analyzed thoroughly, likely due to the difficulty to prepare these complexes in sufficient quality and quantity. Accordingly, the impact of the holotranslocon on protein translocation remained enigmatic.

We were able to place all the available crystal structures into the holotranslcon density to generate a testable quasi-atomic model. The position of SecYEG and of the YidC perimplasmic domain was determined by reconstitution of subcomplexes lacking these proteins (DFYY and ΔYidC maps, Figs.2 and 4). Importantly, the quasi-atomic model we present here is in agreement with the reported protein-protein interactions of SecYEG, SecDF, YajC and YidC (Supplementary Table 1). In particular, SecYEG-YidC complexes could be co-immunoprecipitated (Boy & Koch, 2009). More recently, it has been reported that YidC crosslinks to the lateral gate transmembrane helices of SecYEG (Sachelaru et al., 2013) and that the transmembrane helices of nascent membrane proteins can be crosslinked first to the lateral gate and later to YidC (Urbanus et al., 2001) (Fig 6a). In our quasi atomic model, the unfilled TM part (Fig. 5b) which could be attributed to the YidC conserved TM region is juxtaposed to the SecYEG lateral gate. This placement also is in agreement with the suggestion that YidC mediates folding and assembly of polytopic membrane proteins (Beck et al., 2001) and membrane protein complexes (van der Laan et al., 2003). We observe an unfilled cavity in the plane of the membrane, surrounded by proteins (SecY, SecDF and likely the YidC conserved TM region) which very likely is filled with lipids. This may suggest that the holotranslocon provides a protected environment for the nascent membrane proteins that exit laterally from the SecY translocation channel for folding and assembly (Fig. 6b), thus preventing aggregation of the newly synthesized TM helices with other membrane proteins. Furthermore, if the membrane protein fails to fold correctly, YidC

could direct it to the FtsH-HflK/C protease complex for degradation (van Bloois et al., 2008; van Stelten et al., 2009), thus allowing for quality control.

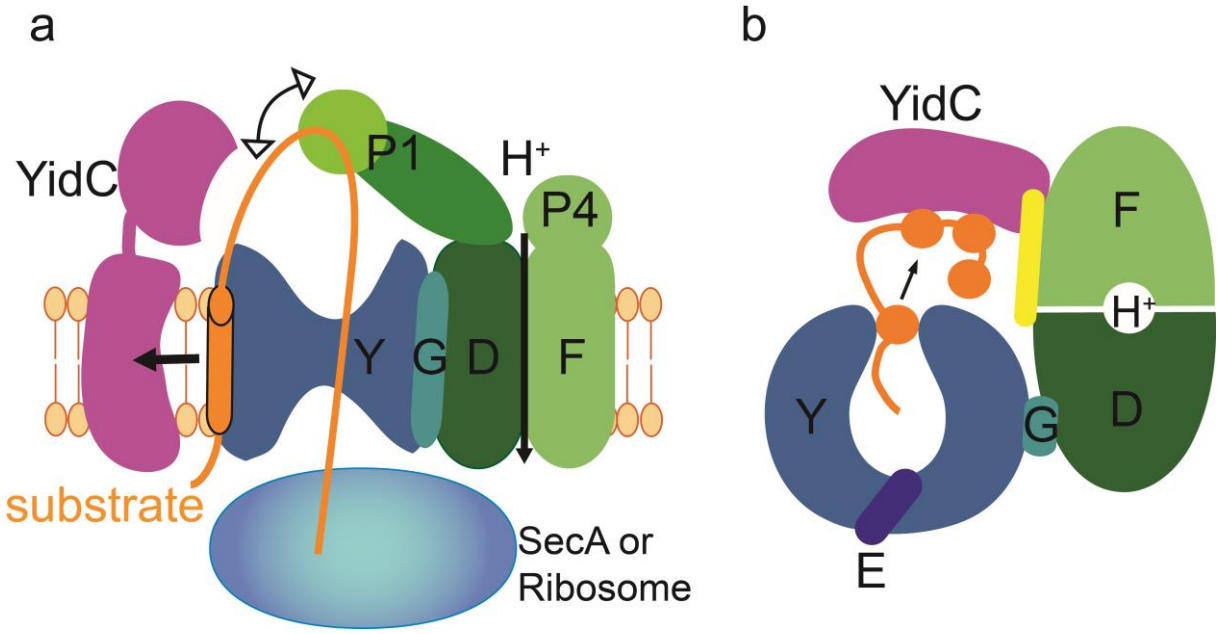

Figure 6. Model of protein translocation catalyzed by the holotranslocon. (a) Protein translocation through SecYEG driven by the proton motive force (PMF) and SecDF. The periplasmic domain of YidC and the head domain of SecD are positioned such that they can interact with translocation substrates and prevent backsliding of the polypeptide through the SecYEG translocation channel. In the cytoplasm, translocation is energized by SecA ATPase or the ribosome. **(b)** Membrane protein integration and folding can occur at the interface between the SecY lateral gate and YidC in a protected lipid-holotranslocon environment where transmembrane helices accumulate until they can fold into a domain. Membrane protein insertion could also be energized by the PMF and SecDF. SecDF is colored in green, SecYEG in blue colors, YajC in yellow, YidC in magenta and the translocation substrate in orange.

The role of the periplasmic domain of YidC is enigmatic. In fact, large parts of the N-terminus of YidC (TMH1 and most of P1) can be deleted without affecting *E. coli* cell growth and membrane protein insertion (Xie et al., 2006). YidC P1 has been crosslinked to SecD (Sachelaru et al., 2013) and was co-purified with SecF (Xie et al., 2006). However, the presence of SecD in the immunoprecipitate was not tested in the Western blots (Xie et al., 2006), thus an interaction of YidC P1 with SecDF cannot be excluded. The ring-like arrangement of the periplasmic domains of SecD, SecF and YidC (Fig. 1) agrees with these findings. Moreover, we assume that the periplasmic domains of YidC and SecD are flexibly arranged to each other and to the membrane part of the complex.

In a recent study, we reported crosslinks of SecD and YidC to SecY, SecE and SecG respectively (Schulze et al., submitted) (Supplementary Table 1). According to our quasi-

atomic model, both periplasmic domains are positioned above SecYEG (Fig. 5a) and thus could flexibly interact with the periplasmic parts of SecYEG. This position would also allow SecD P1head and YidC P1 to interact with the translocated polyproteins (Fig. 6a) emerging from the SecY channel. A role for SecD P1head in supporting later steps of protein translocation (J. A. Pogliano & J. Beckwith, 1994) by using the PMF (Schiebel et al., 1991; Tsukazaki et al., 2011) and in facilitating substrate release in the periplasma (Matsuyama et al., 1993) has been suggested previously. The placement of YidC close to the SecY translocation pore (this study) and the discovery of a hydrophobic cleft in YidC which could accommodate an unpolar, unfolded polypeptide (Ravaud et al., 2008) hints at a role for YidC P1 in facilitating translocation across the membrane. Moreover, the P1 domain of YidC could contribute to stabilize the SecYEG-YidC interaction.

Crosslinking of the C-terminus of YidC to SecF (and not to SecD) (Sachelaru et al., 2013) supports the placement of SecF next to YidC. Furthermore, SecG which is placed at the interface between SecD and SecYEG in our quasi-atomic model can be functionally complemented by SecDF (Kato et al., 2003) and crosslinked to SecD (but not SecF) (Schulze et al., submitted). This supports the placement of the SecD TM region next to SecG (Fig. 1). Nevertheless, this placement is not unambiguous: The TM region of SecDF is pseudosymmetric (Tsukazaki et al., 2011) and therefore, the opposite fitting is equally possible (i.e. the TM region of SecF at the interface to SecYEG and the TM region of SecD at the interface to the TM region of YidC). Additional crosslinking experiments are required to provide stronger support for our current model.

The SecD P1 domain of *E. coli* is 180 amino acids longer than the P1 domain in the crystal structure from *Th. thermophilus*. These insertions are positioned in the linker after TMH1 (residue 34-119) after the first beta sheet-forming sequence (strand 144-223) and between beta-sheet strand 8 and 9 (residue 370-388) (Supplementary Fig. 9). These insertions likely add flexibility to the *E. coli* P1 domain and may occupy currently unfilled density in the periplasmic part of the structure in vicinity of the P1base and above the SecY translocation channel (Fig. 1, Fig. 4a).

The fact that the density of SecYEG is smaller than expected indicates that SecYEG interacts flexibly with SecDFYajC and YidC. Moreover, the interaction with SecDFYajC-YidC could induce conformational changes in SecYEG, similar to the ‘pre-open state’ of SecYEG which is adopted upon interaction with SecA (Zimmer et al., 2008). Future studies will need to address the dynamics of the holotranslocon during co-and post-translational translocation.

Furthermore, the physiological role of the holotranslocon needs to be addressed in future. The cellular copy numbers of SecDF (~30 copies), SecYEG (~300) and YidC (~2000) (K. J. Pogliano & J. Beckwith, 1994) suggests that the holotranslocon is not required for translocation of all substrates. Holotranslocon could exist in the membrane as a preformed

translocation complex which is necessary for the translocation of a special subset of proteins. Alternatively, SecDFYajC-YidC could be recruited by SecYEG during translocation to support translocation. Finally, SecDF could be required to establish the SecYEG-YidC interaction and then be released. In support of this, it has been observed in a blue native gel analysis that SecDF stabilized the SecYEG-YidC interaction without being permanently associated with the SecYEG-YidC complex (Boy & Koch, 2009).

The work and the holotranslocon model presented here (Figs. 1,6) provide a framework for future experiments. Structure-based mutational studies and more specific crosslinking experiments are now possible to further clarify the impact of the holotranslocon on membrane protein insertion and protein secretion.

METHODS

Production and Purification of Holotranslocon Complex and Subcomplexes

The HTL expression plasmid pACEMBL_HTL3 was generated using the ACEMBL expression system (Bieniossek et al., 2009). It consists of the pACE acceptor vector with a polycistron encoding for YidC, SecD (D), SecF (F) with an arabinose promoter, the pDC donor vector encoding for SecY, SecE (E) and SecG (G) with a trc promoter, and the pDK donor vector encoding YajC fused with a calmodulin-binding protein (CBP)-tag with a trc promoter. The ACEMBL acceptor and donor vectors were combined by Cre-loxP fusion to yield pACEMBL_DFYY and pACEMBL_HTL3. pACEMBL_HTL3ΔYidC was generated by deletion of the YidC gene from the pACEMBL_HTL3 expression plasmid.

E. coli BL21(DE3) Star was transformed with pACEMBL_HTL3, pACEMBL_HTL3ΔYidC and pACEMBL_DFYY respectively, and grown in 2xYT medium containing 50 µg/ml ampicillin, 30 µg/ml kanamycin, and 34 µg/ml chloramphenicol to an OD_{600} of 0.8, prior to 3 h of induction using 0.5 mM IPTG and 0.2% (w/v) arabinose. Following centrifugation, the cells were broken at 18 kpsi using a microfluidizer in the presence of HSGM buffer (20 mM Hepes-KOH, 130 mM NaCl, 5 mM $Mg(OAc)_2$, 10 % (v/v) glycerol, pH 8.0). The membranes were collected by ultracentrifugation (150,000 x g, 1.5 h, 4°C, Ti70 rotor) of the lysate and solubilized in HSGM buffer containing 1.5% DDM (Glycon, Germany) for 2 h by rotation at 4°C. After centrifugation (150,000 x g, 1 h, 4°C, Ti70 rotor), the supernatant was loaded onto a chelating Ni^{2+}-Sepaharose Fast Flow (GE Healthcare) column equilibrated with HSGM containing 10 mM imidazole and 0.1% DDM.

After a high salt wash (20 mM Hepes-KOH, 500 mM NaCl, 5 mM $Mg(OAc)_2$, 10 % (v/v) glycerol, 10 mM imidazole, 0.1% DDM, pH 8.0) and a wash with HSGM containing 40 mM imidazole and 0.1% DDM, the HTL complex was eluted with HSGM containing 300 mM imidazole and 0.1% DDM. The eluted protein was transferred into CBP buffer (50 mM

Hepes-KOH, 130 mM NaCl, 10% glycerol, 2 mM $CaCl_2$, 0.03% DDM, pH 8.0) using a desalting column (GE Healthcare) and loaded over night onto a gravity-flow calmodulin affinity column (Stratagene). After washing (CBP buffer with 0.2 mM $CaCl_2$), HTL was eluted with CBP elution buffer (50 mM Hepes-KOH, 400 mM NaCl, 3% glycerol, 2 mM EGTA, 0.03% DDM, pH 8.0).

For electron microscopy and biophysical characterization, the complexes were stabilized by mild glutaraldehyde crosslinking in a glycerol gradient (Kastner et al., 2008). Briefly HTL was loaded onto a 40 ml glycerol gradient from 10% to 30% glycerol and from 0 to 0.15% glutaraldehyde in HSGM buffer with 0.03% DDM and centrifuged for 36.5h at 83,000 x g and 4°C (SW32 rotor, Beckman Coulter). The fraction containing HTL was supplemented with 100 µg of lysine to stop the crosslinking reaction and concentrated using a concentrator with a molecular weight cut-off of 30 kDa (Amicon). The concentrated fraction was further purified using a Superose 6 column equilibrated in HSMD buffer (20 mM Hepes-KOH, 130 mM NaCl, 2 mM $Mg(OAc)_2$, 0.03% DDM, pH 8.0). The molar extinction coefficient of HTL was experimentally determined to be ε_{HTL} = 497 000 M^{-1} cm^{-1} (Schulze et al., submitted). Purified protein samples are shown in Supplementary Figs. 1 and 6 (HTL3, DFYY, and DeltaYidC). Negative-stain EM and 2D class averages drove optimization of the purification procedure, confirmed the homogeneity of the complexes and their similarity.

Analytical Ultracentrifugation

A Beckman XL-I analytical ultracentrifuge and an An-60Ti rotor (Beckman Coulter) with 12 mm optical path length cell equipped with sapphire windows were used for analytical ultracentrifugation. Absorbance at 280 nm and interference profiles were measured for 16 hours at 35,000 rpm and 10 °C. Analysis was done in terms of continuous size-distribution (c(s)) with the Sedfit program (Schuck & Rossmanith, 2000), considering 200 particles with sedimentation coefficients, s, between 0.1 and 20 S, with a frictional ratio of 1.3 and a partial specific volume intermediate between that of the protein and that of the detergent used. The parameters used were 0.74 and 0.83 for the partial specific volumes of the proteins and the β-dodecylmaltoside (β-DDM) (Salvay et al., 2007), respectively; and 0.187 and 0.143 for the refractive index increment of the proteins and the β-DDM) (Salvay et al., 2007), respectively. A regularization procedure was also applied with a confidence level of 0.68. Sample density and viscosity were 1.007 g/mL and 1.35 mPa.s, respectively, as determined with Sednterp.

Random Conical Tilt Reconstructions

Holotranslocon and two subcomplexes (SecDFYajC-YidC and SecYEG-SecDFYajC) at 0.15 mg/ml were absorbed to carbon film for 30 s, followed by a negative staining with 1% uranyl acetate for 30 s. 300 micrographs were recorded at room temperature on a Biotwin Ice

CM120 electron microscope (FEI) at a magnification of 71,550 × and a defocus of ~2 µm at 120kV, using a 4k × 4k CCD camera. Two consecutive images of the same area were taken at 45° and 0° tilt angles under low-dose conditions. Contrast transfer function was analyzed and corrected using the bctf tool included in the Bsoft package (Heymann & Belnap, 2007). Around 15,000 HTL, 12000 DFYY and 10,000 DeltaYidC tilt pairs were selected manually by using the program tiltpicker (Voss et al., 2009). Untilted images were aligned by using iteratively refined classes as references and subsequent multivariance statistical analysis (MSA) for classification into 400 classes using IMAGIC-5 software (van Heel et al., 1996) and XMIPP (Scheres et al., 2005). 400 volumes were calculated from the 2D classes and were averaged using XMIPP MLtomo (Scheres et al., 2009) to compensate for the missing cone, resulting ten RCT reconstructions for each sample. Two volumes of each sample were subjected to further refinement cycles through projection matching with the Spider software suite (Frank et al., 1996), additionally including 15,000 untilted images for HTL (Supplementary Fig. 3)(Fig. 2).

Cryo-EM and Image Processing

Purified HTL (0.15 mg/ml) was applied to a thin carbon foil sustained by a holey carbon grid (Quantifoil^{TM} 2/2) and plunge-frozen in liquid ethane with controlled temperature and humidity (Vitrobot^{TM}, FEI). Samples were imaged under low-dose conditions (~10 e^{-} $Å^{-2}$) at a magnification of 78000 × on a Polara cryo-transmission electron microscope (FEI) at 100 kV. 2500 Images were recorded on a 4k x 4k CCD camera at 1.4 Å/px and coarsened tree times resulting in a final pixel size of 4.2Å before analysis on the specimen. The contrast transfer function of the microscope was determined for each micrograph using the Bsoft program (Heymann & Belnap, 2007), and the image phases were flipped accordingly. Using the EMAN2 software package, 61000 particles were boxed (Tang et al., 2007). The HTL RCT reconstruction was used as the starting model for calculation of the 3D reconstruction from cryo-EM data using Xmipp, Imagic and Spider. Maximum likelihood 3D refinement was used in Xmipp (Scheres et al., 2007). In parallel, SPIDER was used to generate reference projection of the RCT volume, to align those references against the experimental images and the BP RP program of SPIDER was used to reconstruct the refined volume (Shaikh et al., 2008). For IMAGIC refinement, the threed-forward program was used to generate reference projections followed by the M-R-A program to generate the aligned images and the true-threed-reconstruct program to back project the aligned images (van Heel et al., 1996). The fully deconvoluted images (used for the final reconstruction) and the phase flipped images (used for the projection matching cycle) were band-pass filtered between 200 and 15 Å, respectively.

The resolution of the structure was determined according to the gold-standard Fourier schell correlation at the (FSC) = 0.5 cut-off (Scheres & Chen, 2012) and the final reconstruction was filtered accordingly (Supplementary Fig. 2).

3D variance analysis of HTL structure

3D variance map was calculated to assess the heterogeneity of the HTL complex by hypergeometrically stratified resampling (HGSR) implemented in SPARX (Penczek et al., 2011). The 60,984 particles where assigned to 211 angular region using an angular step size of 10°. 10,000 volumes were reconstructed from 9284 randomly chosen images of the CTF corrected HTL dataset (15.2 % of the complete dataset) using the Euler-angles defined in the last asymmetric refinement cycle by projection matching. The volumes were low-pass filtered to 14.58 Å and the variance was computed. The HTL map was colored based on the local variance using the "Surface color" tool implemented in Chimera UCSF (Pettersen et al., 2004) (Supplementary Fig. 4).

Variability analysis was also performed in Xmipp (Scheres et al., 2007). The dataset was split into ten datasets and ten independent volumes were reconstructed using the final HTL reconstruction as starting volume. The ten volumes were then subjected to Maximum likelihood 3D refinement until convergence. The ten refined reconstructions were then compared visually in Chimera UCSF (Pettersen et al., 2004).

Local resolution estimation

The local resolution estimation was performed on the final HTL reconstruction using the "blocres" program implemented in the bsoft package (Heymann & Belnap, 2007; Heymann et al., 2008). The dataset was split randomly into two halves in order to obtain two reconstructions. The two reconstructions were used to estimate the local resolution. The HTL map was colored based on the local resolution estimation using the "Surface color" tool implemented in Chimera UCSF (Pettersen et al., 2004).

Generation of the quasi-atomic model of holotranslocon

The quasi-atomic model of the *E. coli* holotranslocon complex was generated using the crystal structures of *M. jannaschii* SecYβγ (Van den Berg et al., 2004), SecDF from *Thermus thermophilus* (Tsukazaki et al., 2011), *E. coli* YidC P1 (Ravaud et al., 2008) and YajC (Törnroth-Horsefield et al., 2007). The structures were placed into the EM map with UCSF Chimera (Pettersen et al., 2004). The N-terminus of SecD (TMH1 and periplasmic domain) was placed independently from the SecD TMH2-6 region in Chimera, and the corresponding residues were connected afterwards again using pymol (DeLano Scientific). The resulting model was energy minimized in CNS Version 1.0 (Brunger et al., 1998). The figures were

generated with PyMOL (DeLano Scientific). In the rendering of the EM maps, the density cutoffs were set for the display of envelopes that represent ~110% of the a priori estimated volume for the translocation complexes.

REFERENCES

Beck, K., Eisner, G., Trescher, D., Dalbey, R. E., Brunner, J., & Müller, M. (2001). YidC, an assembly site for polytopic *Escherichia coli* membrane proteins located in immediate proximity to the SecYE translocon and lipids. *EMBO Rep.,* **2**, 709-714.

Becker, T., Bhushan, S., Jarasch, A., Armache, J. P., Funes, S., Jossinet, F., Gumbart, J., Mielke, T., Berninghausen, O., Schulten, K., Westhof, E., Gilmore, R., Mandon, E. C., & Beckmann, R. (2009). Structure of monomeric yeast and mammalian Sec61 complexes interacting with the translating ribosome. *Science,* **326**, 1369-1373.

Beckmann, R., Spahn, C. M., Eswar, N., Helmers, J., Penczek, P. A., Sali, A., Frank, J., & Blobel, G. (2001). Architecture of the protein-conducting channel associated with the translating 80S ribosome. *Cell,* **107**, 361-372.

Bieniossek, C., Nie, Y., Frey, D., Olieric, N., Schaffitzel, C., Collinson, I., Romier, C., Berger, P., Richmond, T. J., Steinmetz, M. O., & Berger, I. (2009). Automated unrestricted multigene recombineering for multiprotein complex production. *Nat. Methods,* **6**, 447-450.

Boy, D., & Koch, H. G. (2009). Visualization of distinct entities of the SecYEG translocon during translocation and integration of bacterial proteins. *Mol. Biol. Cell.,* **20**, 1804-1815.

Brundage, L., Hendrick, J. P., Schiebel, E., Driessen, A. J., & Wickner, W. (1990). The purified *E. coli* integral membrane protein SecY/E is sufficient for reconstitution of SecA-dependent precursor protein translocation. *Cell,* **62**, 649-657.

Brunger, A. T., Adams, P. D., Clore, G. M., DeLano, W. L., Gros, P., Grosse-Kunstleve, R. W., Jiang, J. S., Kuszewski, J., Nilges, M., Pannu, N. S., Read, R. J., Rice, L. M., Simonson, T., & Warren, G. L. (1998). Crystallography & NMR system: A new software suite for macromolecular structure determination. *Acta. Crystallogr. D. Biol. Crystallogr.,* **54**, 905-921.

Dalbey, R. E., Wang, P., & Kuhn, A. (2011). Assembly of bacterial inner membrane proteins. *Annu. Rev. Biochem.,* **80**, 161-187.

Driessen, A. J. (1992). Precursor protein translocation by the *Escherichia coli* translocase is directed by the protonmotive force. *EMBO J.,* **11**, 847-853.

Driessen, A. J., & Nouwen, N. (2008). Protein translocation across the bacterial cytoplasmic membrane. *Annu. Rev. Biochem.,* **77**, 643-667.

Duong, F., & Wickner, W. (1997a). Distinct catalytic roles of the SecYE, SecG and SecDFyajC subunits of preprotein translocase holoenzyme. *EMBO J.,* **16**, 2756-2768.

Duong, F., & Wickner, W. (1997b). The SecDFyajC domain of preprotein translocase controls preprotein movement by regulating SecA membrane cycling. *EMBO J.,* **16**, 4871-4879.

Fang, J., & Wei, Y. (2011). Expression, purification and characterization of the *Escherichia coli* integral membrane protein YajC. *Protein Pept. Lett.,* **18**, 601-608.

Frank, J., Radermacher, M., Penczek, P., Zhu, J., Li, Y., Ladjadj, M., & Leith, A. (1996). SPIDER and WEB: processing and visualization of images in 3D electron microscopy and related fields. *J Struct. Biol.,* **116**, 190-199.

Frauenfeld, J., Gumbart, J., Sluis, E. O., Funes, S., Gartmann, M., Beatrix, B., Mielke, T., Berninghausen, O., Becker, T., Schulten, K., & Beckmann, R. (2011). Cryo-EM structure of the ribosome-SecYE complex in the membrane environment. *Nat. Struct. Mol. Biol.,* **18**, 614-621.

Hartl, F. U., Lecker, S., Schiebel, E., Hendrick, J. P., & Wickner, W. (1990). The binding cascade of SecB to SecA to SecY/E mediates preprotein targeting to the *E. coli* plasma membrane. *Cell,* **63**, 269-279.

Heymann, J. B., & Belnap, D. M. (2007). Bsoft: image processing and molecular modeling for electron microscopy. *J. Struct. Biol.,* **157**, 3-18.

Heymann, J. B., Cardone, G., Winkler, D. C., & Steven, A. C. (2008). Computational resources for cryo-electron tomography in Bsoft. *J. Struct. Biol.,* **161**, 232-242.

Hizlan, D., Robson, A., Whitehouse, S., Gold, V. A., Vonck, J., Mills, D., Kühlbrandt, W., & Collinson, I. (2012). Structure of the SecY complex unlocked by a preprotein mimic. *Cell Rep.,* **1**, 21-28.

Ito, K. (1990). Structure, function, and biogenesis of SecY, an integral membrane protein involved in protein export. *J. Bioenerg. Biomembr.,* **22**, 353-367.

Jiang, F., Yi, L., Moore, M., Chen, M., Rohl, T., Van Wijk, K. J., De Gier, J. W., Henry, R., & Dalbey, R. E. (2002). Chloroplast YidC homolog Albino3 can functionally complement the bacterial YidC depletion strain and promote membrane insertion of both bacterial and chloroplast thylakoid proteins. *J. Biol. Chem.,* **277**, 19281-19288.

Kastner, B., Fischer, N., Golas, M. M., Sander, B., Dube, P., Boehringer, D., Hartmuth, K., Deckert, J., Hauer, F., Wolf, E., Uchtenhagen, H., Urlaub, H., Herzog, F., Peters, J. M., Poerschke, D., Luhrmann, R., & Stark, H. (2008). GraFix: sample preparation for single-particle electron cryomicroscopy. *Nat. Methods,* **5**, 53-55.

Kato, Y., Nishiyama, K., & Tokuda, H. (2003). Depletion of SecDF-YajC causes a decrease in the level of SecG: implication for their functional interaction. *FEBS Lett.,* **550**, 114-118.

Kohler, R., Boehringer, D., Greber, B., Bingel-Erlenmeyer, R., Collinson, I., Schaffitzel, C., & Ban, N. (2009). YidC and Oxa1 form dimeric insertion pores on the translating ribosome. *Mol. Cell.,* **34**, 344-353.

Lotz, M., Haase, W., Kühlbrandt, W., & Collinson, I. (2008). Projection structure of yidC: a conserved mediator of membrane protein assembly. *J. Mol. Biol.,* **375**, 901-907.

Luirink, J., Yu, Z., Wagner, S., & de Gier, J. W. (2012). Biogenesis of inner membrane proteins in *Escherichia coli*. *Biochim. Biophys. Acta.,* **1817**, 965-976.

Matsuyama, S., Fujita, Y., & Mizushima, S. (1993). SecD is involved in the release of translocated secretory proteins from the cytoplasmic membrane of *Escherichia coli*. *EMBO J.,* **12**, 265-270.

Mitra, K., Schaffitzel, C., Shaikh, T., Tama, F., Jenni, S., Brooks, C. L., 3rd, Ban, N., & Frank, J. (2005). Structure of the *E. coli* protein-conducting channel bound to a translating ribosome. *Nature,* **438**, 318-324.

Murakami, S., Nakashima, R., Yamashita, E., Matsumoto, T., & Yamaguchi, A. (2006). Crystal structures of a multidrug transporter reveal a functionally rotating mechanism. *Nature,* **443**, 173-179.

Nagamori, S., Smirnova, I. N., & Kaback, H. R. (2004). Role of YidC in folding of polytopic membrane proteins. *J. Cell. Biol.,* **165**, 53-62.

Nouwen, N., & Driessen, A. J. (2002). SecDFyajC forms a heterotetrameric complex with YidC. *Mol. Microbiol.,* **44**, 1397-1405.

Nouwen, N., Piwowarek, M., Berrelkamp, G., & Driessen, A. J. (2005). The large first periplasmic loop of SecD and SecF plays an important role in SecDF functioning. *J. Bacteriol.,* **187**, 5857-5860.

Oliver, D. C., & Paetzel, M. (2008). Crystal structure of the major periplasmic domain of the bacterial membrane protein assembly facilitator YidC. *J. Biol. Chem.,* **283**, 5208-5216.

Penczek, P. A., Kimmel, M., & Spahn, C. M. (2011). Identifying conformational states of macromolecules by eigen-analysis of resampled cryo-EM images. *Structure,* **19**, 1582-1590.

Pettersen, E. F., Goddard, T. D., Huang, C. C., Couch, G. S., Greenblatt, D. M., Meng, E. C., & Ferrin, T. E. (2004). UCSF Chimera--a visualization system for exploratory research and analysis. *J. Comput. Chem.,* **25**, 1605-1612.

Pogliano, J. A., & Beckwith, J. (1994). SecD and SecF facilitate protein export in *Escherichia coli*. *EMBO J.,* **13**, 554-561.

Pogliano, K. J., & Beckwith, J. (1994). Genetic and molecular characterization of the *Escherichia coli* secD operon and its products. *J. Bacteriol.,* **176**, 804-814.

Rapoport, T. A. (2008). Protein transport across the endoplasmic reticulum membrane. *FEBS J.,* **275**, 4471-4478.

Ravaud, S., Stjepanovic, G., Wild, K., & Sinning, I. (2008). The crystal structure of the periplasmic domain of the *Escherichia coli* membrane protein insertase YidC contains a substrate binding cleft. *J. Biol. Chem.,* **283**, 9350-9358.

Sachelaru, I., Petriman, N. A., Kudva, R., Kuhn, P., Welte, T., Knapp, B., Drepper, F., Warscheid, B., & Koch, H. G. (2013). YidC occupies the lateral gate of the SecYEG translocon and is sequentially displaced by a nascent membrane protein. *J. Biol. Chem.,* **288**, 16295-16307.

Salvay, A. G., Santamaria, M., le Maire, M., & Ebel, C. (2007). Analytical ultracentrifugation sedimentation velocity for the characterization of detergent-solubilized membrane proteins Ca++-ATPase and ExbB. *J. Biol. Phys.,* **33**, 399-419.

Samuelson, J. C., Chen, M., Jiang, F., Moller, I., Wiedmann, M., Kuhn, A., Phillips, G. J., & Dalbey, R. E. (2000). YidC mediates membrane protein insertion in bacteria. *Nature,* **406**, 637-641.

Scheres, S. H., & Chen, S. (2012). Prevention of overfitting in cryo-EM structure determination. *Nat. Methods,* **9**, 853-854.

Scheres, S. H., Gao, H., Valle, M., Herman, G. T., Eggermont, P. P., Frank, J., & Carazo, J. M. (2007). Disentangling conformational states of macromolecules in 3D-EM through likelihood optimization. *Nat. Methods,* **4**, 27-29.

Scheres, S. H., Melero, R., Valle, M., & Carazo, J. M. (2009). Averaging of electron subtomograms and random conical tilt reconstructions through likelihood optimization. *Structure,* **17**, 1563-1572.

Scheres, S. H., Nunez-Ramirez, R., Sorzano, C. O., Carazo, J. M., & Marabini, R. (2008). Image processing for electron microscopy single-particle analysis using XMIPP. *Nat. Protoc.,* **3**, 977-990.

Scheres, S. H., Valle, M., & Carazo, J. M. (2005). Fast maximum-likelihood refinement of electron microscopy images. *Bioinformatics,* **21 Suppl 2**, ii243-244.

Schiebel, E., Driessen, A. J., Hartl, F. U., & Wickner, W. (1991). Delta mu H+ and ATP function at different steps of the catalytic cycle of preprotein translocase. *Cell,* **64**, 927-939.

Schuck, P., & Rossmanith, P. (2000). Determination of the sedimentation coefficient distribution by least-squares boundary modeling. *Biopolymers,* **54**, 328-341.

Scotti, P. A., Urbanus, M. L., Brunner, J., de Gier, J. W., von Heijne, G., van der Does, C., Driessen, A. J., Oudega, B., & Luirink, J. (2000). YidC, the *Escherichia coli* homologue of mitochondrial Oxa1p, is a component of the Sec translocase. *EMBO J.,* **19**, 542-549.

Shaikh, T. R., Gao, H., Baxter, W. T., Asturias, F. J., Boisset, N., Leith, A., & Frank, J. (2008). SPIDER image processing for single-particle reconstruction of biological macromolecules from electron micrographs. *Nat. Protoc.,* **3**, 1941-1974.

Shiozuka, K., Tani, K., Mizushima, S., & Tokuda, H. (1990). The proton motive force lowers the level of ATP required for the *in vitro* translocation of a secretory protein in *Escherichia coli*. *J. Biol. Chem.,* **265**, 18843-18847.

Tang, G., Peng, L., Baldwin, P. R., Mann, D. S., Jiang, W., Rees, I., & Ludtke, S. J. (2007). EMAN2: an extensible image processing suite for electron microscopy. *J. Struct. Biol.,* **157**, 38-46.

Törnroth-Horsefield, S., Gourdon, P., Horsefield, R., Brive, L., Yamamoto, N., Mori, H., Snijder, A., & Neutze, R. (2007). Crystal structure of AcrB in complex with a single transmembrane subunit reveals another twist. *Structure,* **15**, 1663-1673.

Tsukazaki, T., Mori, H., Echizen, Y., Ishitani, R., Fukai, S., Tanaka, T., Perederina, A., Vassylyev, D. G., Kohno, T., Maturana, A. D., Ito, K., & Nureki, O. (2011). Structure and function of a membrane component SecDF that enhances protein export. *Nature,* **474**, 235-238.

Tsukazaki, T., Mori, H., Fukai, S., Ishitani, R., Mori, T., Dohmae, N., Perederina, A., Sugita, Y., Vassylyev, D. G., Ito, K., & Nureki, O. (2008). Conformational transition of Sec machinery inferred from bacterial SecYE structures. *Nature,* **455**, 988-991.

Ulbrandt, N. D., Newitt, J. A., & Bernstein, H. D. (1997). The *E. coli* signal recognition particle is required for the insertion of a subset of inner membrane proteins. *Cell,* **88**, 187-196.

Urbanus, M. L., Scotti, P. A., Fröderberg, L., Saaf, A., de Gier, J. W., Brunner, J., Samuelson, J. C., Dalbey, R. E., Oudega, B., & Luirink, J. (2001). Sec-dependent membrane protein insertion: sequential interaction of nascent FtsQ with SecY and YidC. *EMBO Rep.,* **2**, 524-529.

van Bloois, E., Dekker, H. L., Fröderberg, L., Houben, E. N., Urbanus, M. L., de Koster, C. G., de Gier, J. W., & Luirink, J. (2008). Detection of crosslinks between FtsH, YidC, HflK/C suggests a linked role for these proteins in quality control upon insertion of bacterial inner membrane proteins. *FEBS Lett.,* **582**, 1419-1424.

van Bloois, E., Nagamori, S., Koningstein, G., Ullers, R. S., Preuss, M., Oudega, B., Harms, N., Kaback, H. R., Herrmann, J. M., & Luirink, J. (2005). The Sec-independent function of *Escherichia coli* YidC is evolutionary-conserved and essential. *J. Biol. Chem.,* **280**, 12996-13003.

Van den Berg, B., Clemons, W. M., Jr., Collinson, I., Modis, Y., Hartmann, E., Harrison, S. C., & Rapoport, T. A. (2004). X-ray structure of a protein-conducting channel. *Nature,* **427**, 36-44.

van der Laan, M., Nouwen, N. P., & Driessen, A. J. (2005). YidC--an evolutionary conserved device for the assembly of energy-transducing membrane protein complexes. *Curr. Opin. Microbiol.,* **8**, 182-187.

van der Laan, M., Urbanus, M. L., Ten Hagen-Jongman, C. M., Nouwen, N., Oudega, B., Harms, N., Driessen, A. J., & Luirink, J. (2003). A conserved function of YidC in the biogenesis of respiratory chain complexes. *Proc. Natl. Acad. Sci. U. S. A.,* **100**, 5801-5806.

van Heel, M., Harauz, G., Orlova, E. V., Schmidt, R., & Schatz, M. (1996). A new generation of the IMAGIC image processing system. *J. Struct. Biol.,* **116**, 17-24.

van Stelten, J., Silva, F., Belin, D., & Silhavy, T. J. (2009). Effects of antibiotics and a proto-oncogene homolog on destruction of protein translocator SecY. *Science,* **325**, 753-756.

Voss, N. R., Yoshioka, C. K., Radermacher, M., Potter, C. S., & Carragher, B. (2009). DoG Picker and TiltPicker: software tools to facilitate particle selection in single particle electron microscopy. *J. Struct. Biol.,* **166**, 205-213.

Xie, K., Kiefer, D., Nagler, G., Dalbey, R. E., & Kuhn, A. (2006). Different regions of the nonconserved large periplasmic domain of *Escherichia coli* YidC are involved in the SecF interaction and membrane insertase activity. *Biochemistry,* **45**, 13401-13408.

Zhu, L., Kaback, H. R., & Dalbey, R. E. (2013). YidC--a molecular chaperone for LacY protein folding via the SecYEG machinery. *J. Biol. Chem*.

Zimmer, J., Nam, Y., & Rapoport, T. A. (2008). Structure of a complex of the ATPase SecA and the protein-translocation channel. *Nature,* **455**, 936-943.

SUPPLEMENTARY INFORMATION

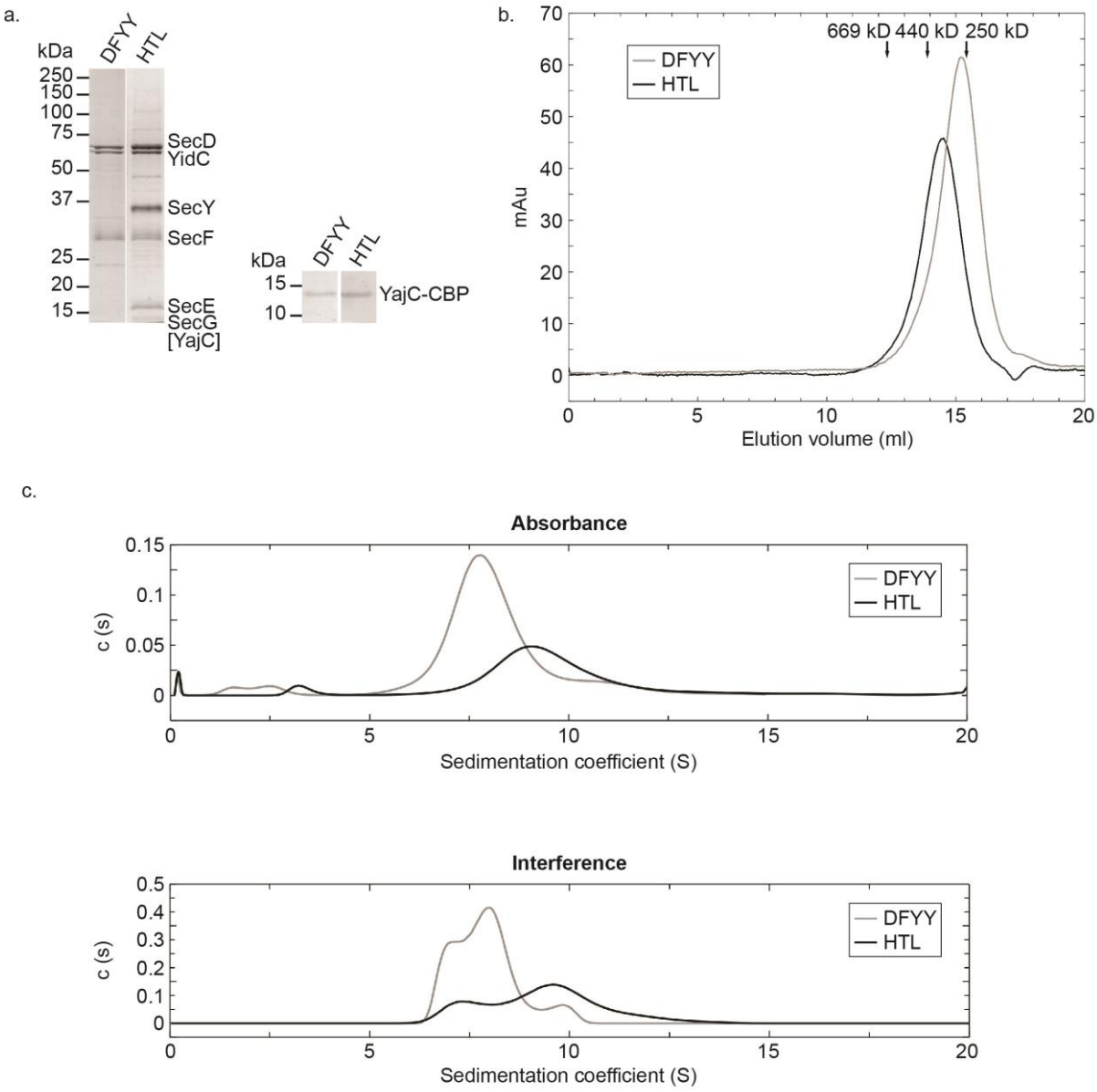

Supplementary Figure 1. Purification and biophysical characterization of holotranslocon and SecDF-YajC-YidC complexes. (a) Coomassie-stained SDS-PAGE of the holo-translocon (HTL) and SecDF-YajC-YidC (DFYY) (left). Detection of the CBP-tagged YajC protein by Western blotting using biotinylated calmodulin and a streptavidin-horseradish peroxidase conjugate (right). **(b)** Superose6 gel filtration profile of HTL and DFFY stabilized by the GraFix method (Kastner et al., 2008). The elution volume of proteins which were used for calibration is indicated by arrows. **(c)** Analysis of sedimentation velocity of HTL and DFYY prepared by the GraFix method. The left panel presents the absorbance c(S) distribution whereas the right panel presents the interference c(S) distribution. HTL is represented as a black line and DFYY is represented as a grey line.

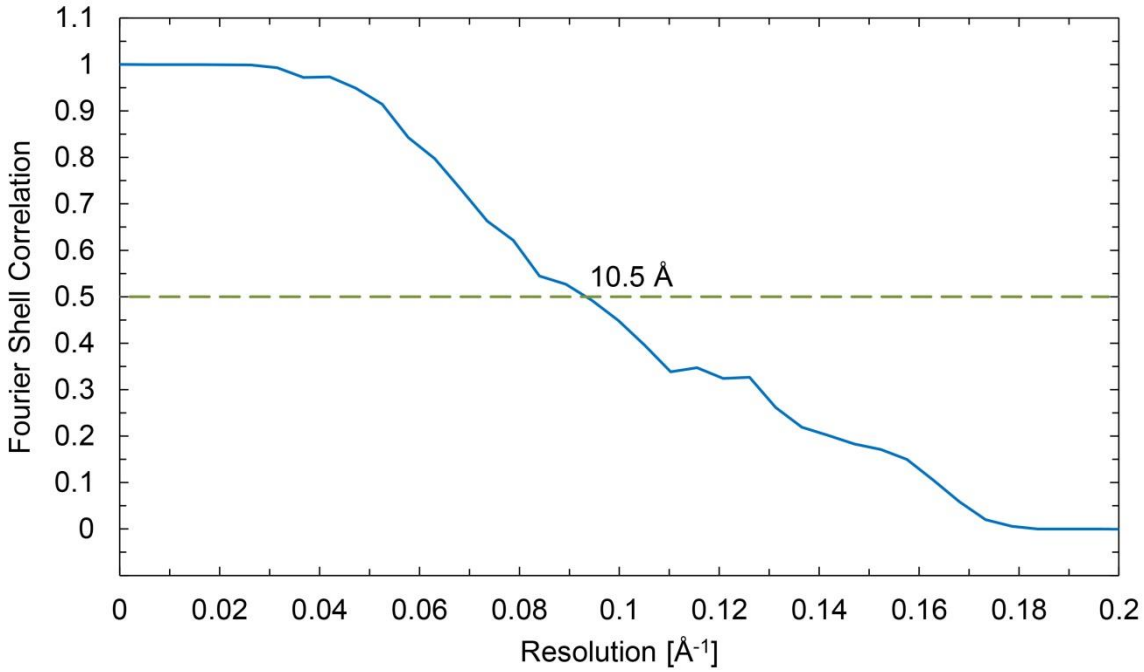

Supplementary Figure 2. Gold-standard FSC curve of the cryo-EM holotranslocon structure. The Fourier Shell Correlation (FSC) curve was determined using the 'gold standard method' (Scheres & Chen, 2012). 60,000 particles were split randomly into two halves, and the corresponding reconstructions were refined independently. FSC=0.5 indicates a resolution of 10.5 Å (dotted green line).

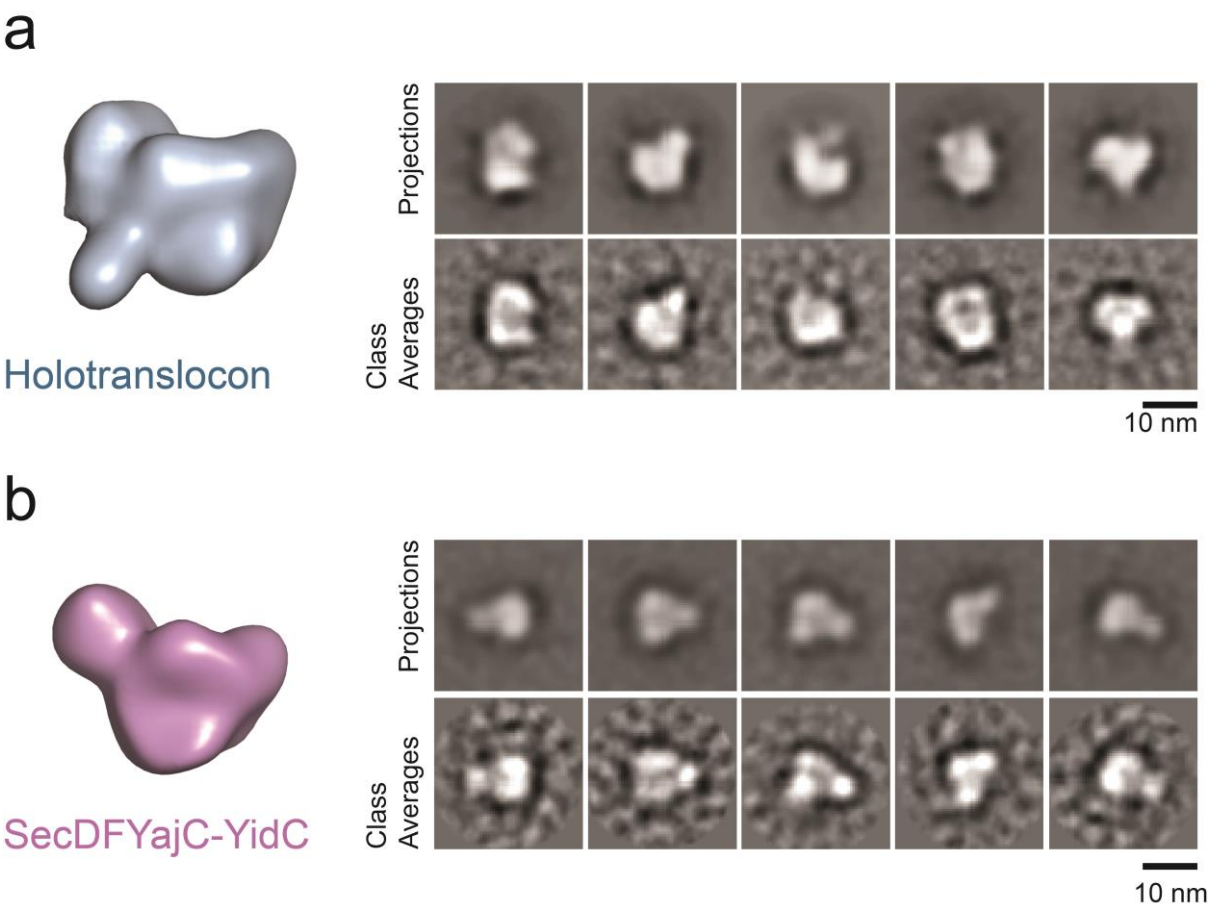

Supplementary Figure 3. Random conical tilt (RCT) reconstructions of **(a)** holotranslocon, **(b)** SecDFYajC-YidC (DFYY). A front view is shown for all maps (left). The projections of the maps are shown above the corresponding 2D class averages obtained by 2D multivariate statistical analysis (MSA) of the negative stain EM data (right).

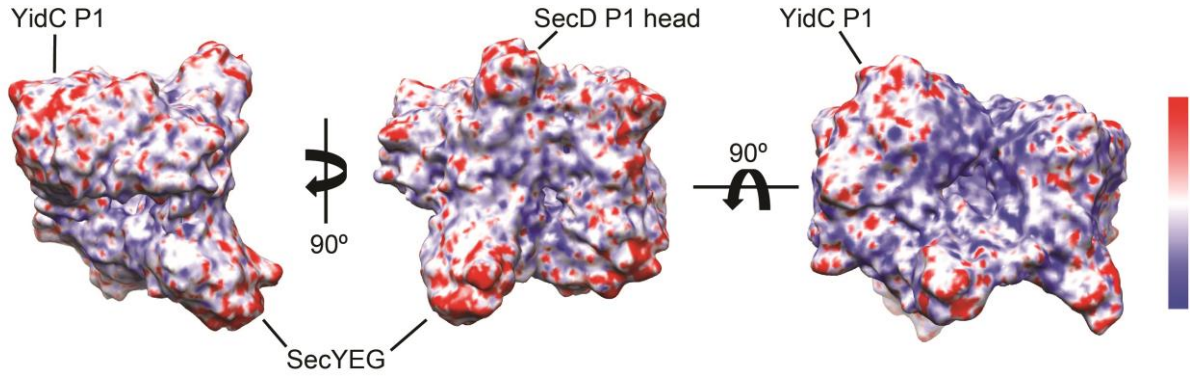

Supplementary Figure 4. 3D variance map of the holo-translocon reconstruction. 10,000 hypergeometrically stratified resampled (HGSR) volumes were generated using SPARX (Penczek et al., 2011). The volumes were then subjected to principal component analysis (PCA) to determine the variable regions of the HTL. **Left:** front view from the plane of the membrane; **middle:** side view of the holotranslocon complex; **right:** view from the periplasma on the holotranslocon. Highly homogeneous regions (lower voxel variances) are coloured in blue, flexible or heterogeneous regions (higher voxel variances) are displayed in red. The surface representations were prepared in Chimera (Pettersen et al., 2004).

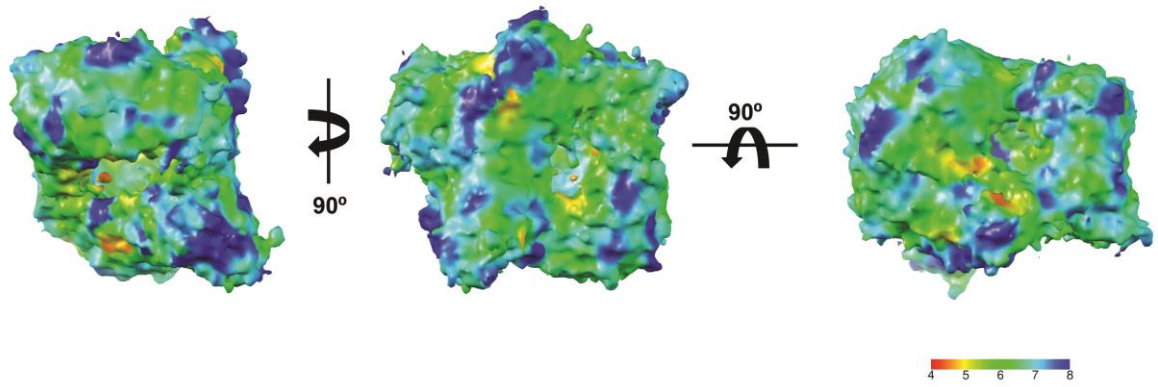

Supplementary Figure 5. Local resolution estimation of the holo-translocon cryo-EM reconstruction. The local resolution has been measured using the blocres program implemented in the bsoft package (Heymann & Belnap, 2007; Heymann et al., 2008) explaining the differences in numbers compared to Supplementary Fig. 2. **Left:** front view from the plane of the membrane; **middle:** side view of the holotranslocon complex; **right:** view from the periplasma on the holotranslocon. The map is colored based on the calculated local resolution from 4 Å (red) to 8 Å (dark blue).

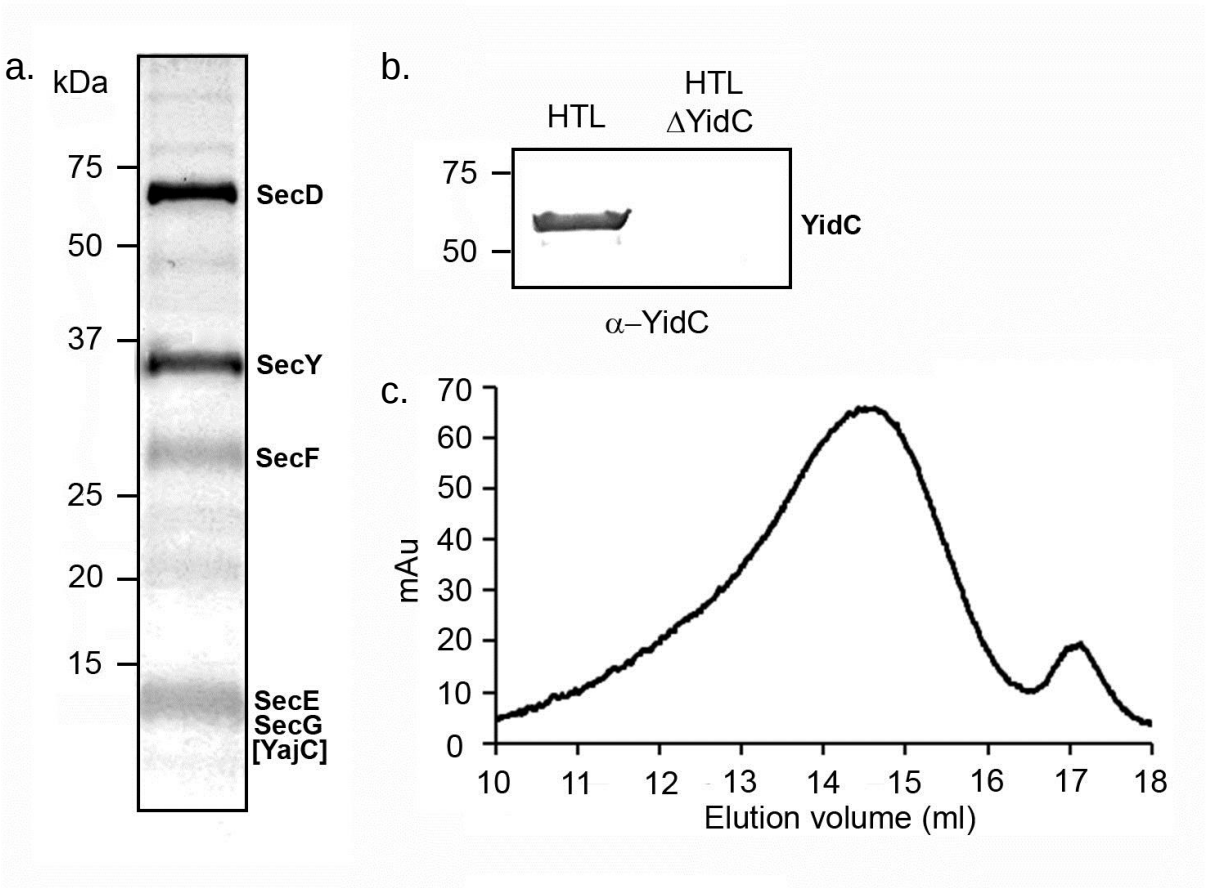

Supplementary Figure 6. Characterization of the SecYEG-SecDFYajC complex. (a) Commassie-stained SDS gel of the purified SecYEG-SecDFYajC complex, **(b)** western blot using an anti-YidC antibody, **(c)** Superose6 gel filtration profile of the crosslinked SecYEG-SecDFYajC complex.

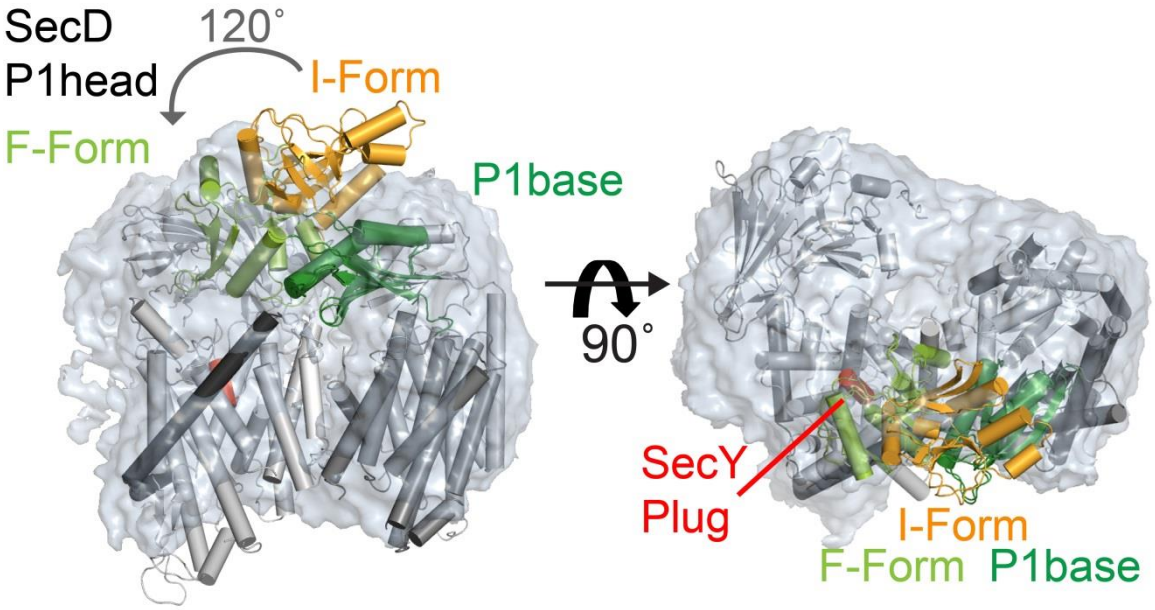

Supplementary Figure 7. Fitting of the F- and the I-conformation of the SecD P1head domain into the holotranslocon density. (a) F-form (greenyellow) and I-Form (orange) of the P1head domain shown in a side view from the plane of the membrane; **(b)** and shown in a view from the periplasma. The I-form model was generated by superimposition of the SecD P1base (forest) from the crystal structure of the periplasmic domain of SecD (3AQO, (Tsukazaki et al., 2011)) with the SecD P1base of the quasi-atomic model of holotranslocon (this study). Both conformations position the P1head domain very close to the protein conducting channel which in the quasi-atomic model is sealed by the plug (red).

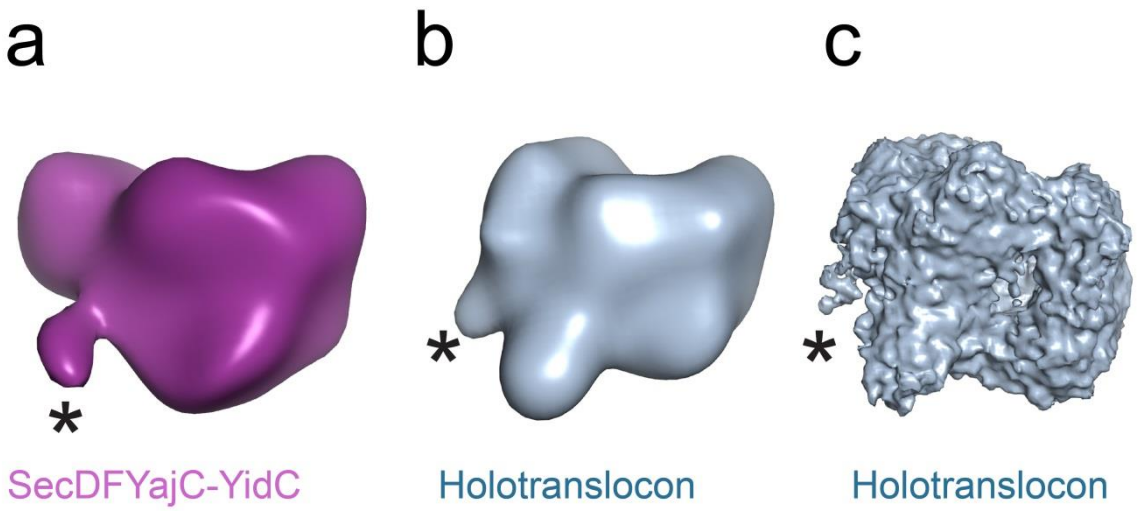

Supplementary Figure 8. Unfilled density next to the YidC periplasmic domain (a) in the SecDFYajC-YidC EM reconstruction, (b) in the holotranslocon EM reconstruction and (c) in the holotranslocon cryo-EM structure. All maps are displayed at a higher contour level to visualize the extra density (marked with a star).

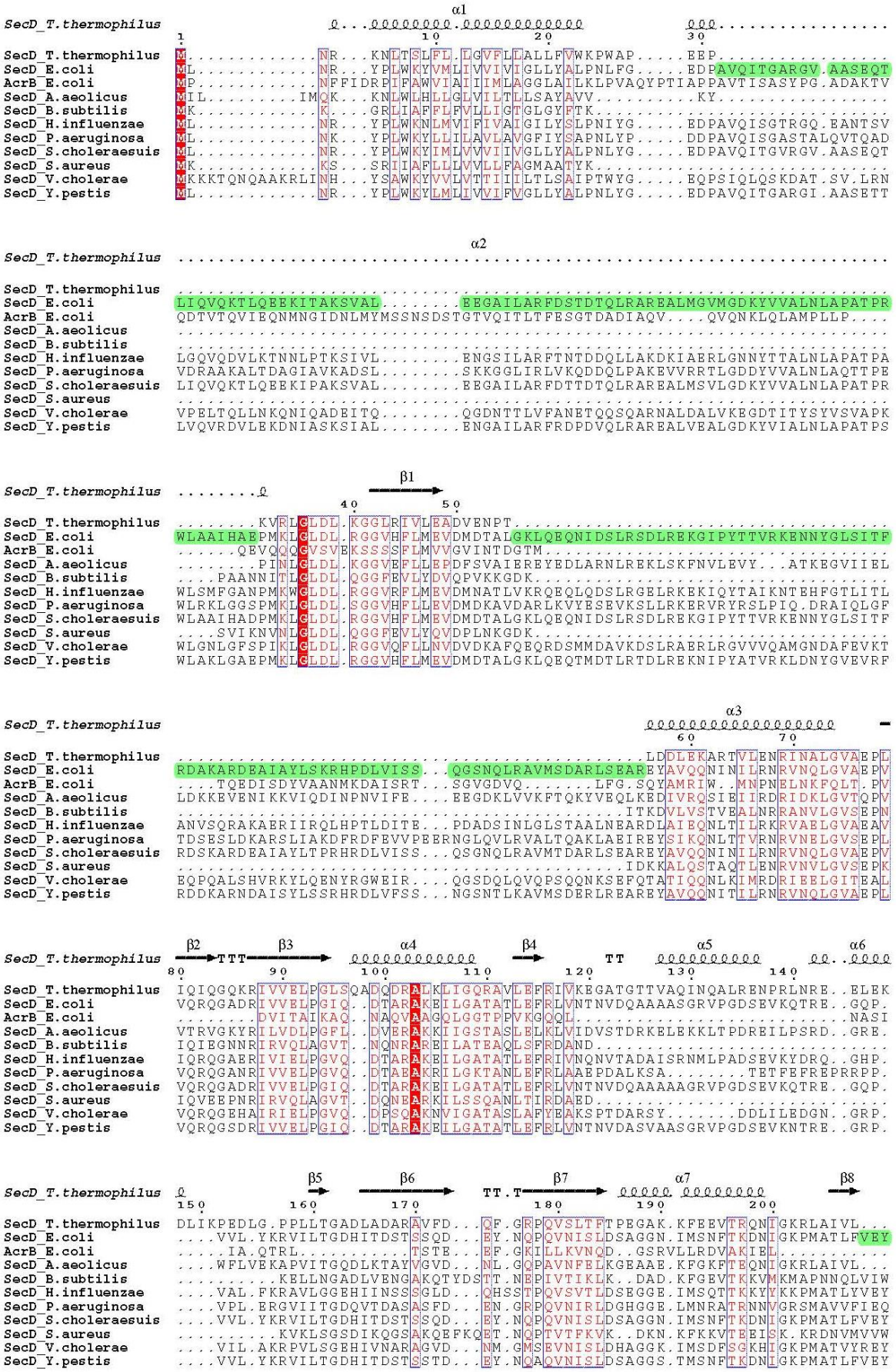
SecD_T.thermophilus
SecD_T.thermophilus
SecD_E.coli
AcrB_E.coli
SecD_A.aeolicus
SecD_B.subtilis
SecD_H.influenzae
SecD_P.aeruginosa
SecD_S.choleraesuis
SecD_S.aureus
SecD_V.cholerae
SecD_Y.pestis

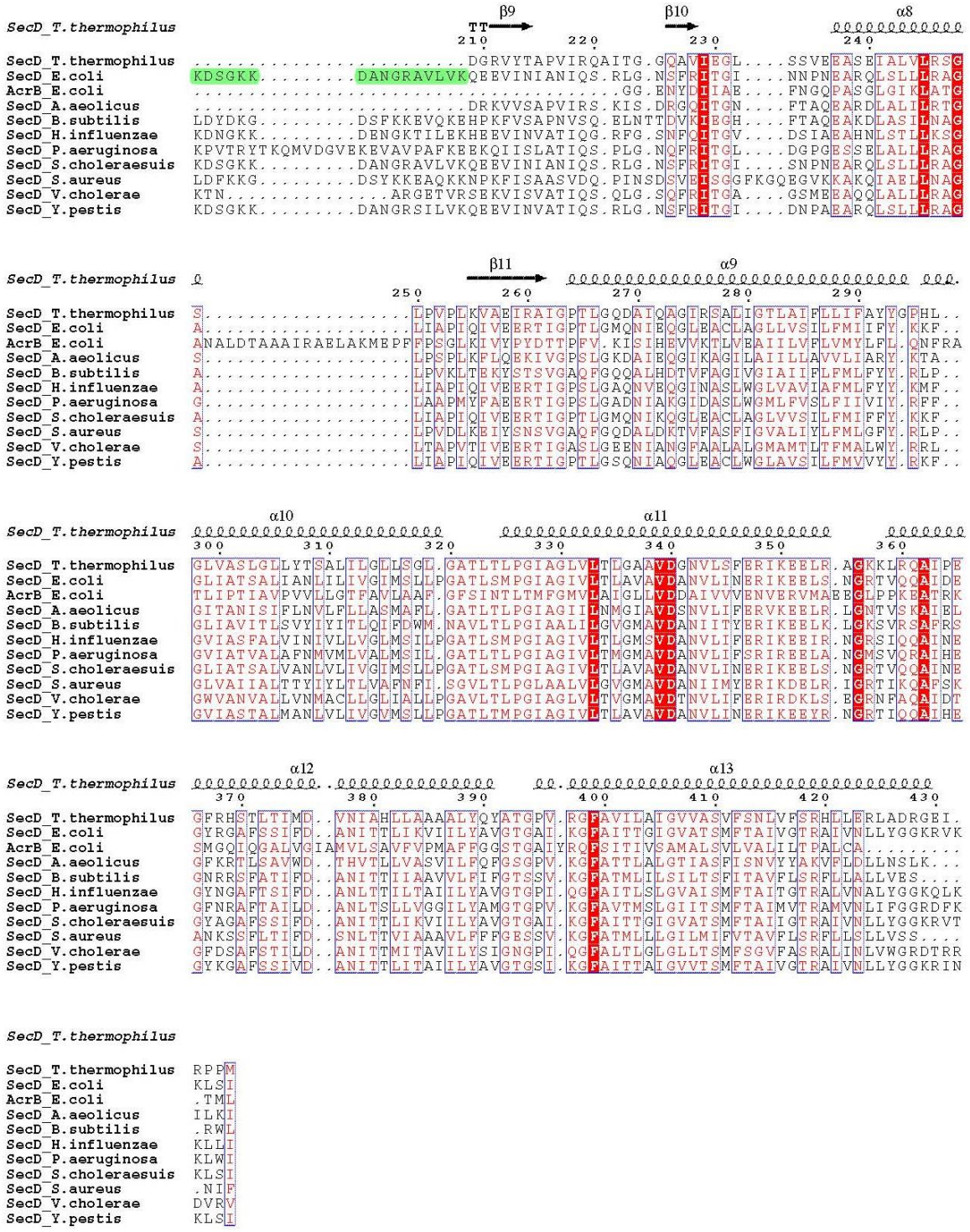

Supplementary Figure 9. Multiple sequence alignment of SecD. The global alignment of the different SecD sequences was performed using the T-coffee package (Notredame et al., 2000). The alignment of the sequences with the secondary structure was performed using the ESPript program (Gouet et al., 1999). Identical residues are indicated with white letters on a red box, similar residues are red letters in a white box, variable residues are represented by black letters, and dots represent gaps. The parts of the *E. coli* sequence highlighted in green represent the additional amino acids compare to the *Th. thermophilus* sequence. The secondary structure based on the available crystal structure (PDB code: 3AQP) is shown on top of the alignment. α: α-helix; β: β-sheet; T: β-turns/coils. The numbering corresponds to the sequence of *T. thermophilus* SecD domain.

Protein 1	Protein 2	Involved residues	Experimental approach	Reference
YidC	SecF	YidC 215-265	Co-immunoprecipitation *	Xie et al., *Biochemistry* 2006
YidC	SecYEG	n/a	Co-immunoprecipitation	Scotti et al., *EMBO J*. 2000; Boy & Koch, *Mol. Biol. Cell* 2000
YidC	SecY	SecY TM2b, TM3, TM7, TM8	Crosslinking studies	Sachelaru et al., *J. Biol. Chem.* 2013
YidC	SecD YajC SecG	YidC 249 [located in P1 domain]	Crosslinking studies	Sachelaru et al., *J. Biol. Chem.* 2013
YidC	SecF YajC SecY	YidC 540 [cytoplasmic C-terminus]	Crosslinking studies	Sachelaru et al., *J. Biol. Chem.* 2013
YajC	SecDF	n/a	Co-immunoprecipitation	Duong & Wickner, *EMBO J.* 1997
YajC	SecYEG	n/a	Co-immunoprecipitation	Duong & Wickner, *EMBO J.* 1997
SecY	SecD YidC	n/a	Crosslinking studies	Schulze et al., submitted 2013
SecE	SecD YidC	n/a	Crosslinking studies	Schulze et al., submitted 2013
SecG	SecD YidC	n/a	Crosslinking studies	Schulze et al., submitted 2013
SecG	SecDF-YajC	n/a	Crosslinking studies and depletion studies	Kato et al., *FEBS Lett.* 2003

Supplementary Table 1: Reported protein-protein interactions of SecYEG, SecDF, YajC and YidC. n/a stands for not available information.

SUPPLEMENTARY REFERENCES

Boy, D., & Koch, H. G. (2009). Visualization of distinct entities of the SecYEG translocon during translocation and integration of bacterial proteins. *Mol. Biol. Cell.,* **20**, 1804-1815.

Duong, F., & Wickner, W. (1997a). Distinct catalytic roles of the SecYE, SecG and SecDFyajC subunits of preprotein translocase holoenzyme. *EMBO J.,* **16**, 2756-2768.

Gouet, P., Courcelle, E., Stuart, D. I., & Metoz, F. (1999). ESPript: analysis of multiple sequence alignments in PostScript. *Bioinformatics,* **15**, 305-308.

Heymann, J. B., & Belnap, D. M. (2007). Bsoft: image processing and molecular modeling for electron microscopy. *J. Struct. Biol.,* **157**, 3-18.

Heymann, J. B., Cardone, G., Winkler, D. C., & Steven, A. C. (2008). Computational resources for cryo-electron tomography in Bsoft. *J. Struct. Biol.,* **161**, 232-242.

Kastner, B., Fischer, N., Golas, M. M., Sander, B., Dube, P., Boehringer, D., Hartmuth, K., Deckert, J., Hauer, F., Wolf, E., Uchtenhagen, H., Urlaub, H., Herzog, F., Peters, J. M., Poerschke, D., Luhrmann, R., & Stark, H. (2008). GraFix: sample preparation for single-particle electron cryomicroscopy. *Nat. Methods,* **5**, 53-55.

Kato, Y., Nishiyama, K., & Tokuda, H. (2003). Depletion of SecDF-YajC causes a decrease in the level of SecG: implication for their functional interaction. *FEBS Lett.,* **550**, 114-118.

Notredame, C., Higgins, D. G., & Heringa, J. (2000). T-Coffee: A novel method for fast and accurate multiple sequence alignment. *J. Mol. Biol.,* **302**, 205-217.

Penczek, P. A., Kimmel, M., & Spahn, C. M. (2011). Identifying conformational states of macromolecules by eigen-analysis of resampled cryo-EM images. *Structure,* **19**, 1582-1590.

Pettersen, E. F., Goddard, T. D., Huang, C. C., Couch, G. S., Greenblatt, D. M., Meng, E. C., & Ferrin, T. E. (2004). UCSF Chimera--a visualization system for exploratory research and analysis. *J. Comput. Chem.,* **25**, 1605-1612.

Sachelaru, I., Petriman, N. A., Kudva, R., Kuhn, P., Welte, T., Knapp, B., Drepper, F., Warscheid, B., & Koch, H. G. (2013). YidC occupies the lateral gate of the SecYEG translocon and is sequentially displaced by a nascent membrane protein. *J. Biol. Chem.,* **288**, 16295-16307.

Scheres, S. H., & Chen, S. (2012). Prevention of overfitting in cryo-EM structure determination. *Nat. Methods,* **9**, 853-854.

Scotti, P. A., Urbanus, M. L., Brunner, J., de Gier, J. W., von Heijne, G., van der Does, C., Driessen, A. J., Oudega, B., & Luirink, J. (2000). YidC, the *Escherichia coli* homologue of mitochondrial Oxa1p, is a component of the Sec translocase. *EMBO J.,* **19**, 542-549.

Tsukazaki, T., Mori, H., Echizen, Y., Ishitani, R., Fukai, S., Tanaka, T., Perederina, A., Vassylyev, D. G., Kohno, T., Maturana, A. D., Ito, K., & Nureki, O. (2011). Structure and function of a membrane component SecDF that enhances protein export. *Nature,* **474**, 235-238.

Xie, K., Kiefer, D., Nagler, G., Dalbey, R. E., & Kuhn, A. (2006). Different regions of the nonconserved large periplasmic domain of *Escherichia coli* YidC are involved in the SecF interaction and membrane insertase activity. *Biochemistry*, **45**, 13401-13408.

Chapter 5 : Other experiments

Résumé en français / French summary

Dans ce chapitre, nous avons utilisé différentes approches méthodologiques afin d'analyser les interactions protéine-protéine au sein du complexe holotranslocon. De plus, nous avons voulu identifier les interactions possible entre l'holotranslocon et de nouveau partenaires ainsi qu'étudier la fonction de l'holotranslocon *in vivo*.

Dans un premier temps, nous avons étudié l'architecture de l'holotranslocon et les interfaces protéine-protéine entre différentes sous-unités constituant le complexe HTL par spectrométrie de masse native et par une réaction de réticulation couplée à de la spectrométrie de masse. Malheureusement, la spectrométrie de masse est difficile à appliquer à des protéines membranaires et par conséquent, ces deux approches nécessiteront des efforts supplémentaire afin d'optimiser les conditions expérimentales et la configuration des instruments.

Dans le but d'étudier davantage l'interaction entre le complexe HTL et le ribosome qui a été mis en évidence dans le chapitre 3, nous avons utilisé un complexe ribosome-HTL pour une analyse par cryo-microscopie électronique. Une reconstruction 3D préliminaire montre une densité supplémentaire proche de la sortie du tunnel du ribosome qui est le site présumé d'interaction avec l'holotranslocon.

Ensuite, nous avons reconstitué l'holotranslocon dans des nanodisques. Les nanodisques sont des particules de forme discoïdale formés d'une bicouche lipidique pouvant contenir une protéine membranaire. Les nanodisques-HTL vont nous permettre de visualiser HTL dans son environnement membranaire natif. Nous avons reconstitué avec succès SecYEG dans des nanodisques, nous permettant d'envisager la reconstitution du complexe HTL ainsi que son étude avec des partenaires de liaison par cryo-microscopie électronique.

Enfin, nous avons procédé à une analyse protéomique de cellules d'*E. coli* appauvries en SecDF dans le but d'identifier des substrats dont la translocation serait dépendante de la présence de force proton motrice. La translocation de ces substrats dépendrait de l'holotranslocon car SecD et SecF ne sont pas des translocases mais agissent en complexe avec YidC et/ou SecYEG. Par trypsinisation et spectrométrie de masse, nous avons obtenu une liste de protéines membranaires qui ont été affectées par l'absence de SecDF. Maintenant, ces substrats potentiels de SecDF/HTL doivent être validés par des expériences de translocation *in vitro*.

5-1. Native mass spectrometry study of the holotranslocon and its subcomplexes

In recent years, mass spectrometry made significant contribution to structure elucidation of non-covalent protein assemblies (Sharon et al., 2007; van den Heuvel & Heck, 2004). Nanoelectrospray mass spectrometry was applied to a micellar solution of a heteromeric ABC (ATP-binding cassette) transporter, a membrane protein complex comprising transmembrane and cytoplasmic subunits (Barrera et al., 2008) and to V-type ATPases (Zhou et al., 2011). The mass spectra of these detergent solubilized membrane protein complexes reveal the subunit stoichiometry and architecture of the complexes by identification of subcomplexes. Moreover, tightly bound lipids were identified. In light of the long-standing difficulties to study membrane protein complexes by mass spectroscopy, these studies present a significant methodological advance.

Therefore, we aimed to investigate the subunit stoichiometry and architecture of the holotranslocon by nanoelectrospray mass spectrometry in collaboration with Carol V. Robinson (Oxford). The technique couples electrospray ionization to mass spectrometry and provides information about the composition, topological arrangements, dynamics and structural properties of protein complexes. Obtaining such structural information about a seven-membered membrane protein complex would present both, a methodological and a scientific breakthrough. The main difficulty when applying this technology is to provide sufficient energy to the detergent-solubilized complexes in order to remove all the detergent molecules and to make these complexes fly in the vacuum of the mass spectrometer.

As a pilot experiment, we first analyzed the core translocon complex SecYEG as it is the most stable subcomplex of the holotranslocon. Purified SecYEG (Mitra et al., 2005) in native MS buffer (2mM Hepes-KOH pH7.00, 200mM NH_4Ac, 10mM $Mg(OAc)_2$, 0.03% DDM) was sent to the laboratory of Carol Robinson for the native MS analysis. The SecYEG complex was flying, and we were able to obtain a mass spectrogram [Fig. 5-1]. After analysis, several peaks corresponding to (sub)complexes and subunits of SecYEG were identified. The SecYEG complex as well as SecY and SecG monomers were found; SecE was not detected. Surprisingly, we were able to detect two additional subcomplexes of SecYEG, SecEG and SecYG. Based on genetic data and the crystal structures of Sec complexes (Douville et al., 1994; Frauenfeld et al., 2011; Nishiyama et al., 1994; Tsukazaki et al., 2008; Zimmer et al., 2008), the formation of the SecEG and SecYG was not anticipated; in contrast SecYE complexes were described in the literature (Brundage et al., 1990; Douville et al., 1994).

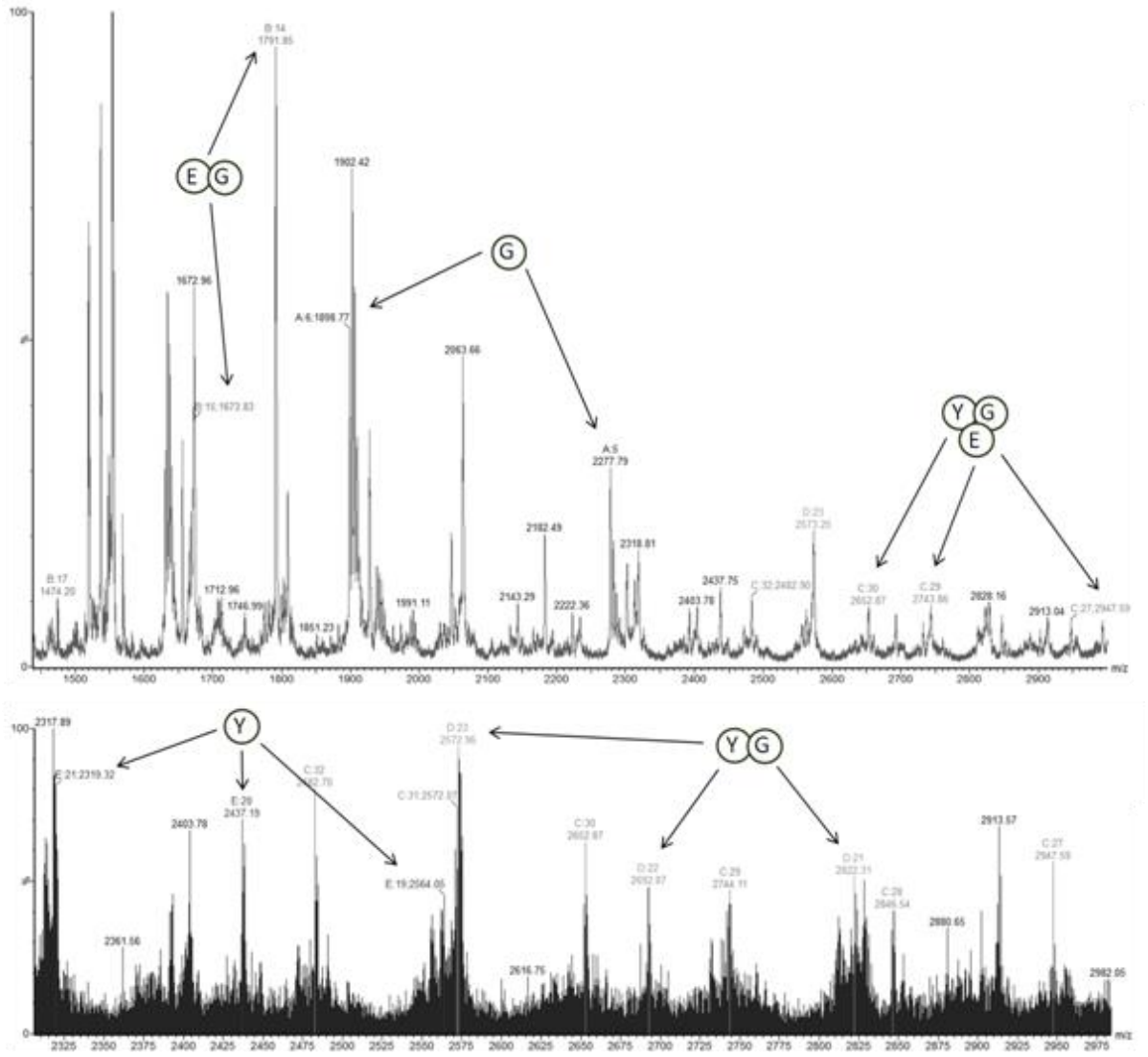

Figure 5-1. **Native mass spectra of DDM-solubilized SecYEG complex.** The sample was buffer-exchanged with 200nM ammonium acetate pH 7.4 supplemented with 0.03% DDM. Subsequently, the sample was loaded onto capillaries. Mass spectra were acquired on a quadropole time-of-flight (Waters) modified for the transmission of high mass to charge. The following parameters were used for the acquisition: 1.7kV for the capillary and 100-200V for the cone. The backing pressure was set between 5-10 mbar to enhance the transmission of high molecular weight species. The protein was released from the micelle using a collision energy of 150-200V and argon or SF6 as collision gas at a pressure of $9x10^{-4}$ mBar. Data analyses were performed using the MassLynx software (Waters).

This was the first time that a complex between SecE and SecG has been shown. Similarly, a SecYG complex was rather unexpected but could be explained based on the X-ray structure of the bacterial SecYEG complex where SecG contacts the N-terminal five alpha helices of SecY [Fig. 5-2] (Zimmer et al., 2008).

Unfortunately, when the same experiment was performed with purified HTL by Ni^{2+}-NTA and by calmodulin affinity chromatography, no protein could be detected by MS. This complex apparently could not be transferred into the vacuum.

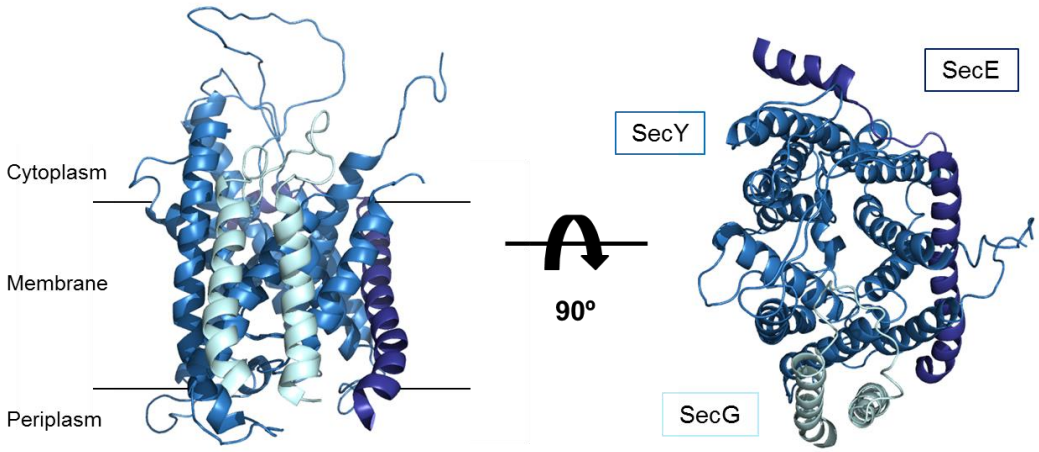

Figure 5-2. **Crystal structure of SecYEG.** View of the SecYEG complex from the membrane plan (**left**). The membrane bilayer is represented by the black lines. Cytoplasmic view of the SecYEG complex (**right**). SecY is represented in light blue, SecE in dark blue and SecG in cyan. (PDB code: 3DIN (Zimmer et al., 2008)).

To obtain information about the molecular weight and the stoichiometry of the HTL complex, we decided to repeat the experiment using crosslinked HTL. Again we used glutaraldehyde crosslinked SecYEG complex as a positive control. Unfortunately neither the crosslinked SecYEG nor the crosslinked HTL could be detected by MS indicating that glutaraldehyde crosslinking interferes with ionization of the protein complexes. Furthermore we speculate that even with very high energy, it is close to impossible to remove the detergent belt from crosslinked membrane protein complexes.

Subsequently, we tested detergent–solubilized SecDF-YajC-YidC (sub)complex for native MS. But again, no proteins could be detected by MS. We were expecting to see at least some of the individual subunits (e.g. YidC alone), but no signal could be detected at all from the SecDF-YajC-YidC subcomplex. We speculate that the micelles were probably too robust, even at maximum collision energy and with SF6 instead of Argon. The main limitation in that study was an experimental limitation. The major problem in this experiment is that the maximum energy provided was not sufficiently high to remove the detergent molecules from the HTL and DFYY complexes. In order to overcome this problem, the laboratory of Carol Robinson is currently developing a laser to activate the micelles in the gas phase. This laser activation then should provide sufficient energy and thus allow analysis of the SecDF-YajC-YidC subcomplex and the holotranslocon by native MS.

Because of the technical problems to overcome in order to transfer the entire HTL complex into the vacuum of the mass spectrometer, we did not further pursue native mass spectrometry with HTL. Instead, we obtained the molecular weight and subunit stoichiometry of the HTL by analytical ultracentrifugation (chapter 4). Further, we decided to study the protein-protein interaction network within the HTL complex by crosslinking mass spectrometry.

5-2. Crosslinking mass spectrometry

Obtaining crystal structures of multi-protein complexes is already challenging, for trans-membrane complexes it is rarely yielding success. An alternative to this is to combine structural data from any source and combine it in an integrated structural biology approach (Alber et al., 2007). Crosslinking/mass spectrometry (CLMS) has yielded distance constraints that allowed placing individual subunits within the larger context of a multi-protein complex, e.g. the proteasome (Lasker et al., 2012).

The aim of the CLMS approach is to identify and quantify the interactions and the accurate sites of protein-protein interaction (Back et al., 2003). It makes use of specific chemical crosslinking, tryptic digest and subsequent analysis by mass spectrometry. Novel computer algorithms automatically interpret the mass spectrometric data and identify crosslinked peptides.

We applied CLMS to the HTL in collaboration with Juri Rappsilber's laboratory at Edinburgh University. The main drawback of this approach was that we had to use specific chemical crosslinkers which yield crosslinking products of a defined mass (rather than glutaraldehyde) that can subsequently be identified by the algorithms developed in the laboratory of Juri Rappsilber [Fig. 5-3]. These crosslinkers are directed against lysines (amine groups) which are under-represented in the transmembrane part. Thus, we can expect to obtain mostly information about the interactions of the periplasmic and cytoplasmic domains and loops within the holotranslocon.

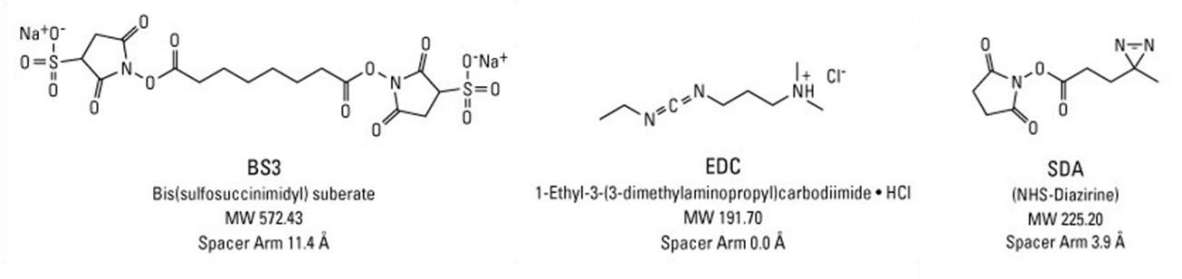

Figure 5-3. **Crosslinkers compatible with mass spectrometry analysis.** BS3 is a homo-bifunctional amine-to-amine crosslinker (**left**); EDC can mediate carboxyl-to-amine crosslinking (**middle**); SDA combines amine-reactive chemistry with photo-activatable diazirine-based conjugation, thus crosslinking amine-containing molecules to nearly any other functional group (**right**). The molecular weight is indicated in Da, and the spacer arm is specified for each crosslinker.

The first crosslinking experiment was performed with the BS3 crosslinking agent which is a homo-bifunctional amine-reactive crosslinker. After Ni2+-NTA and calmodulin affinity chromatography, the purified HTL (in HSGM buffer supplemented with 0.03% DDM) was

mixed with different amounts of BS3 in order to determine the optimal ratio for the reaction. After quenching the reaction by addition of 30% (v/v) saturated Ammonium bicarbonate for 45 min on ice, the different conditions were analyzed by SDS-PAGE [Fig. 5-4].

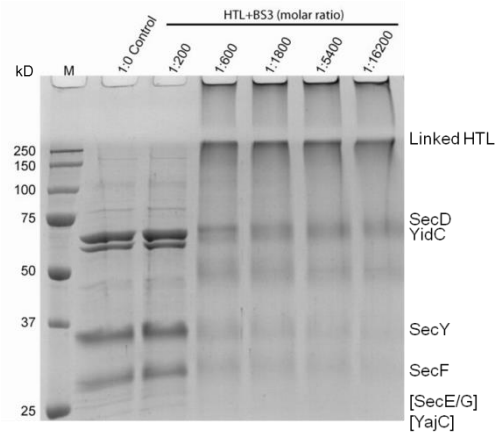

Figure 5-4. **Titration of the BS3 crosslinker to determine the optimal protein to crosslinker ratio for the reaction.** Crosslinked products were analyzed on a Coomassie-stained SDS-PAGE gel. Purified HTL without BS3 was used as a control. Based on the gel a molar ration of 1:600 was chosen for HTL crosslinking.

As shown by SDS-PAGE analysis [Fig. 5-4], formation of a high molecular weight complex was observed running at the top of the gel and in the wells. Based on this result, we choose the molar ratio 1 HTL and 600 BS3 crosslinker molecules for the large-scale crosslinking reaction. This ratio was the best compromise in order to obtain a good yield of crosslinked HTL complexes without oversaturating the reaction which may result in more unspecific crosslinking products (false positives). The sample in a NuPAGE® Novex® 3-8% tris-acetate gel was sent to the Rappsilber laboratory. The band corresponding to the linked complex was isolated, subjected to tryptic digestion followed by mass spectrometry analysis. We identified a number of crosslinking products [Fig. 5-5].

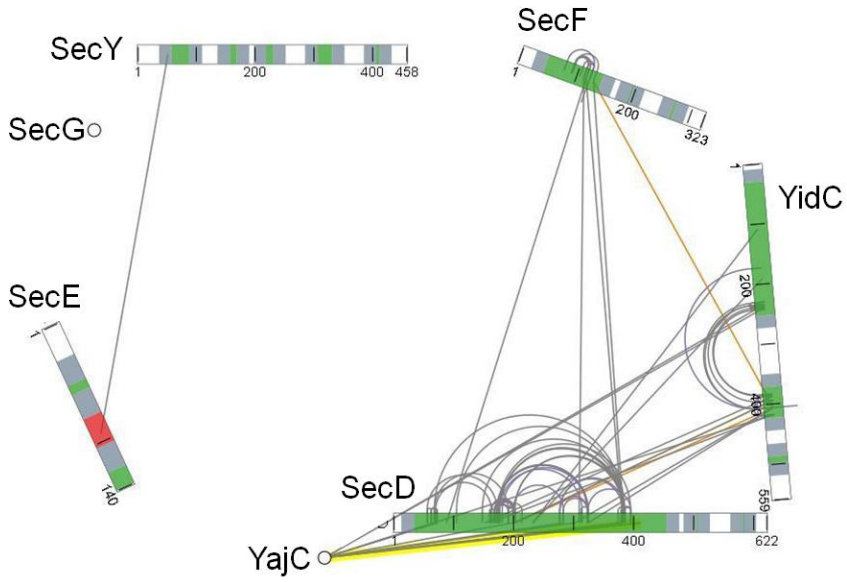

Figure 5-5. **Crosslinking MS data of the detergent-solubilized holo-translocon complex using BS3 as crosslinking agent.** Transmembrane regions are shown in grey, cytoplasmic domains in white, periplasmic domains in green, amphipathic helix of SecE in red, and crosslinks are depicted as grey lines.

Several of identified crosslinks occur between residues within a subunit, in particular in the SecD periplasmic domain. Unfortunately, we also observe crosslinks between periplasmic and cytoplasmic domains. This is a sign of either aggregation or a problem of specificity of the BS3 crosslinker which has a rather long spacer arm (11.4 Å).

In order to address this problem, we repeated the experiment using a different crosslinking agent which would crosslink direct, specific interactions. The EDC is a "zero length" crosslinker [Fig. 5-3]. This homo-bifunctional crosslinker reacts with residues which are in very close proximity. Unfortunately, the reaction with EDC was not leading to any specific crosslinking products which could be observed by SDS-PAGE analysis. Next, we opted for SDA [Fig. 5-3], a photo-activatable crosslinker which has a spacer arm of 3.9 Å and crosslinks an amine residue to any amino acid side chain or peptide backbone upon activation with long-wave UV light (330-370nm). After Ni2+-NTA and calmodulin affinity chromatography, purified HTL (in HSGM buffer supplemented with 0.03% DDM) was mixed with SDA in a molar ratio of 4:1 and 8:1. After UV activation, the sample was loaded on a Novex® 4-12% tris-glycine gel for analysis [Fig. 5-6].

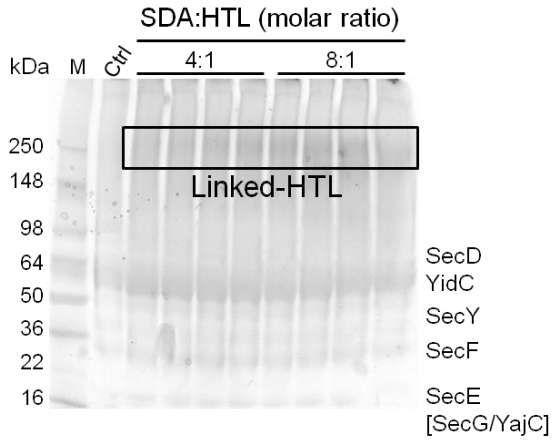

Figure 5-6. **Titration of the SDA crosslinker to obtain efficient crosslinking of the holo-translocon.** A molar ratio of 4:1 and 8:1 of SDA and HTL was chosen. After UV-crosslinking, the products were analyzed on a Coomassie-stained SDS-PAGE gel. Purified HTL without SDA was used as a control.

The SDA crosslinking product corresponded to the expected size for the HTL complex (~250 kDa). This species was subjected to tryptic digestion and mass spectrometry analysis of the digested peptide. Crosslinked peptides were identified and a map of the interaction was generated [Fig. 5-7].

The specificity was increased with the SDA crosslinker compared to the BS3 crosslinking agent, i.e. we observed less crosslinks with SDA. The results showed the same types of crosslink. We observed intrasubunit crosslinks in SecD mostly, and intersubunit crosslinks between SecDF-YidC. Again, crosslinks between cytoplasmic and periplasmic residues were observed, indicating a high rate of false positives.

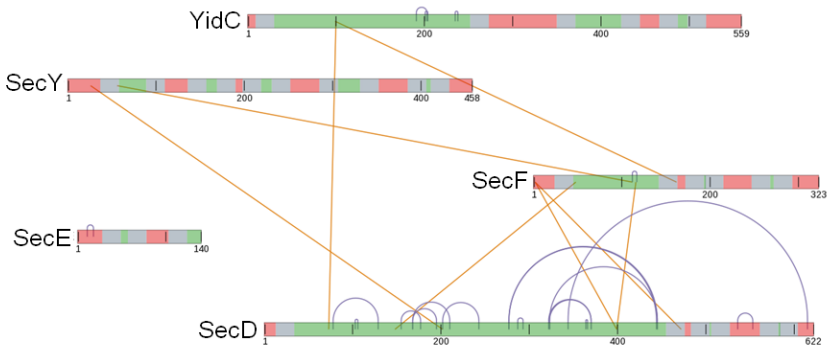

Figure 5-7. **Crosslinking MS data of the detergent-solubilized holo-translocon using the photo-activatable crosslinker SDA.** Transmembrane regions are shown in grey, periplasmic domains in green, cytoplasmic domains in red, and crosslinks are represented as lines (orange: between proteins; blue: within proteins).

In order to avoid the unspecific (false) crosslinks obtained by the approach described above using detergent-solubilized HTL, we next will crosslink the complex in the membrane (in spheroplasts) and purify HTL afterwards via the His-tags using IMAC affinity purification. Thereby, we expect to minimize artefacts and thus to be in a position to identify the interface between the different subunits of this complex, at least in the periplasm.

5-3. Ribosome-bound complexes

As described in chapter 3, a ribosome-holotranslocon complex can be isolated but this complex had never been observed by cryo-electron microscopy. In order to perform a cryo-EM study on this complex, we had first to determine the concentration of ribosome and HTL, as well as the best molar ratio of HTL and ribosome nascent chain complexes (RNCs) in order to observe efficient complex formation. To this end, ribosomes were incubated with different molar ratios of purified holotranslocon complex in ribosome binding buffer (20mM Hepes-KOH pH7.5, 100 mM NaCl, 10 mM $Mg(OAc)_2$, 0.03% DDM). After incubation on ice, the reaction mixtures were centrifuged through a 0.5M sucrose cushion (in ribosome binding buffer) (55000 rpm, 3 hours, 4ºC, TLA 55 rotor). After ultracentrifugation, the supernatant was discarded and the ribosomal pellet was resuspended and analyzed by SDS-PAGE [Fig. 5-8]. 10 µg of ribosomes were loaded in each well of the gel. As a control, the corresponding amount of purified holotranslocon for a 1:1 molar ratio binding has been loaded. As shown on the Coomassie-stained gel, the ratio 1:5 appears to lead to a 1:1 binding of HTL to RNC; thus this is the minimal excess of HTL to be used for complex formation. For grid preparation, a 20-fold molar excess of HTL was chosen to ensure efficient complex formation, i.e. that most of the ribosomes are in complex with a HTL. RNC-HTL complexes (110 nM) were loaded on a holey carbon grid (Quantifoil™ 2/2) precoated with a thin carbon

foil. Grids incubated with the sample were plunge-frozen in liquid ethane using a Vitrobot™ system (FEI). Cryo-EM data were collected on a Titan Krios cryo-TEM (FEI) at EMBL-Heidelberg under low-dose conditions (20 $e^{-}Å^{-2}$) at 200kV and with a calibrated pixel size of 1.4 Angstrom [Fig. 5-8]. Around 5000 micrographs were collected. The analysis of the electron microscopy images and structure calculation will be performed by another PhD student in the laboratory. Preliminary results show additional density next to the polypeptide exit tunnel of the ribosome which is the expected binding site of the translocon. After structure determination, the detergent-solubilized HTL structure (described in chapter 4) will be compared to the ribosome-HTL structure in order to observe any rearrangement within the membrane protein complex upon binding to the ribosome nascent chain complex.

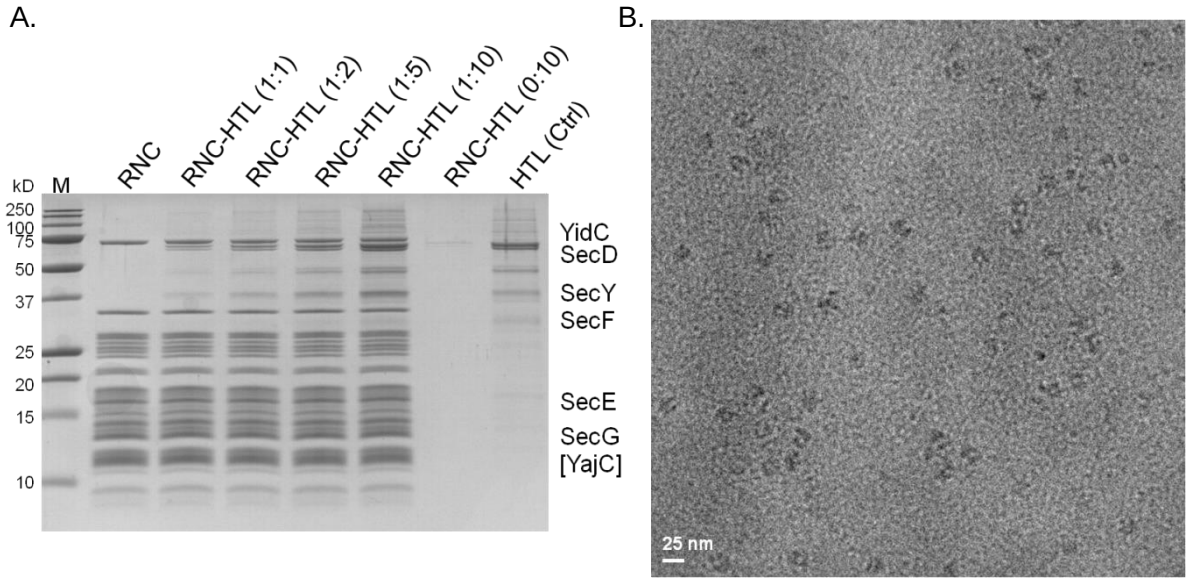

Figure 5-8. **Ribosome-holo-translocon complex. A.** Binding of purified HTL3 to RNCs analyzed by ribosomal pelleting through a sucrose cushion. As a control, RNC and HTL3 were loaded alone; HTL3 did not migrate through the sucrose cushion in absence of ribosomes; purified HTL3 (not centrifuged) was loaded for comparison. The molar ratio used in the binding assay is indicated in brackets. **B.** Cryo-EM micrograph of the ribosome-HTL complex recorded on a CCD at 200KV.

5-4. Reconstitution of translocation complexes into nanodiscs

Membrane proteins can be studied either in a detergent-solubilized state or in a native-like environment. To mimic this native environment, one can use either bicelles (Faham & Bowie, 2002) or nanodiscs. The latter approach has been developed during the last decade (Bayburt et al., 2002). The Sligar laboratory engineered the nanodiscs based on the apolipoprotein A-1 (Bayburt et al., 2002). This plasma lipoprotein is an amphipathic α-helical protein which has the capacity to bind to the hydrophobic tail of the lipids. Based on this protein, they developed a membrane scaffold protein (MSP). In addition, phospholipids

have the tendency to self-assemble into a bilayer. Therefore, if two MSP proteins are in presence of phospholipids, each MSP will interact with the hydrophobic part of one leaflet of the lipid bilayer and this will induce the formation of a disc-like particle. The size of the disc is determined by the length of the MSP. In order to control the diameter of the nanodisc particles, membrane scaffold proteins (MSPs) of different sizes have been developed based on the apolipoprotein A−I (Denisov et al., 2004). To reconstitute a membrane protein into a nanodisc, the detergent-solubilized membrane protein is mixed with phospholipids and MSP. The ratio for the reconstitution has to be experimentally determined and optimized. The critical step in nanodisc formation is the removal of the detergent. Bio-Beads® (Bio-Rad) are used for this process. These are macroporous polystyrene beads which have the capacity to adsorb the detergent from a solution (Bio-Rad). Therefore, upon removal of the detergent using Bio-Beads®, the membrane protein assembles with phospholipids into a discoidal lipid bilayer. The size of the disc is determined by the length of the MSP. Therefore, in case of reconstitution of large membrane protein complex, the size of the MSPs used has to be adjusted. This technique has several advantages (i) it keeps the membrane protein soluble without any detergent in the buffer; (ii) the membrane protein stays in a native-like membrane environment, i.e. in a lipid bilayer; (iii) it allows the control of the oligomeric state of a membrane protein complex: e.g. monomers can be separated from dimers.

To reconstitute HTL into nanodiscs, we first had to produce MSP which contains a histidine-tag for affinity chromatography. We expressed MSP-1 (the smallest available MSP protein) in *E. coli* BL21 (DE3) STAR cells. The cells were grown in 2xYT medium at 37ºC. Expression of the proteins of interest was induced by addition of 1mM IPTG at OD_{600nm} of 1. After 3 hours of induction, cells were harvested and resuspended in a MSP lysis buffer (20mM Tris-HCl pH7.5, 1% Triton X-100). The cells were sonicated 3 to 4 times for 1 minute and centrifuged at 17,000-20,000 x g for 20-30 min. Subsequently, the lysate was loaded onto a Ni^{2+}-NTA affinity column and washed with MSP washing buffer (40mM Tris-HCl pH 8.00, 300mM NaCl, 1% Triton X-100). A second wash was performed with a cholate buffer (40mM Tris-HCl pH8.00, 300mM NaCl, 50mM cholate, 20mM imidazole) followed by a final wash step (40mM Tris-HCl pH8.00, 300mM NaCl, 50mM imidazole). MSP was eluted with MSP elution buffer (40mM Tris-HCl pH8.00, 300mM NaCl, 500mM imidazole) (Bayburt et al., 2002). The protein in the elution fraction was analyzed by SDS-PAGE [Fig. 5-9].

After a single affinity chromatography step [Fig. 5-9], the purity of MSP was sufficient to continue with reconstitution experiments into nanodiscs.

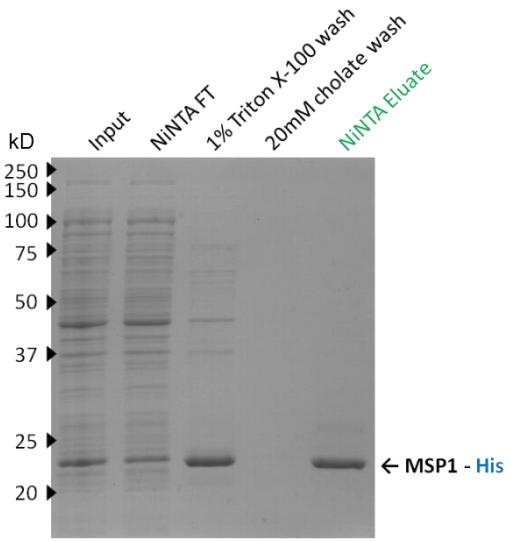

Figure 5-9. **Ni^{2+} affinity chromatography purification of MSP-1.** Coomassie-stained SDS-PAGE gel showing the protein composition of the different purification steps. The position of the purified MSP-1 protein is indicated by an arrow. Marker sizes are indicated in kDa. FT, flow through.

As a control, we first incorporated a monomeric SecYEG into nanodiscs. As described in the literature (Alami et al., 2007), we mixed SecYEG, MSP1 and solubilized lipids (*E. coli* extracted polar lipids [Avanti Polar Lipids] in resuspension buffer [20mM Hepes-KOH pH7.5, 100mM KOAc, 6mM $Mg(OAc)_2$, 1mM DTT, 25mg/mL cholate]) in a molar ratio of 1:4:100 in reconstitution buffer (20mM Hepes-KOH pH7.5, 100mM KOAc, 6mM $Mg(OAc)_2$, 1mM DTT, 0.1% DDM). The self-assembly of SecYEG into nanodiscs was initiated by addition of Bio-Beads® (Bio-Rad). After removal of the Bio-Beads®, the reconstitution mixture was loaded onto a size exclusion chromatography column (S200 10/30) equilibrated with nanodisc gel filtration buffer (20mM Hepes-KOH pH7.5, 100mM KOAc, 6mM $Mg(OAc)_2$, 1mM DTT, 10% glycerol) [Fig. 5-10].

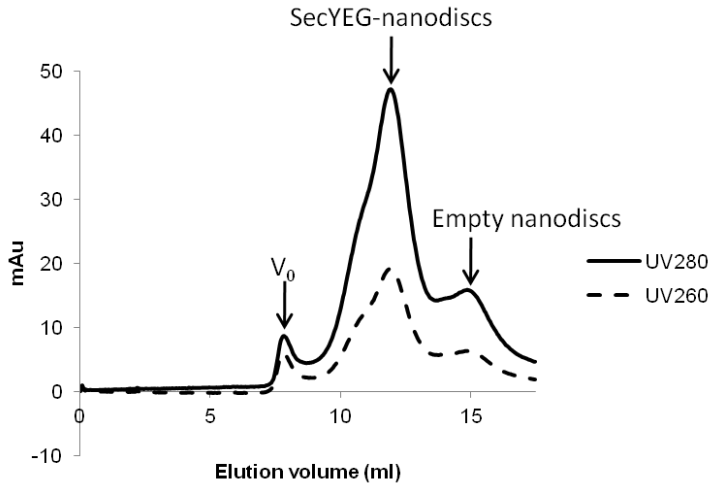

Figure 5-10. **Size exclusion chromatogram of reconstituted nanodisc-SecYEG translocon.** Using a S200 10/30 column and nanodisc gel filtration buffer.

We were able to separate different species by gel filtration. Based on the calibration of our column and on the molecular weight of the expected nanodisc complexes, we identified possible SecYEG-nanodiscs and empty nanodiscs. The corresponding fractions were analyzed by SDS-PAGE [Fig. 5-11].

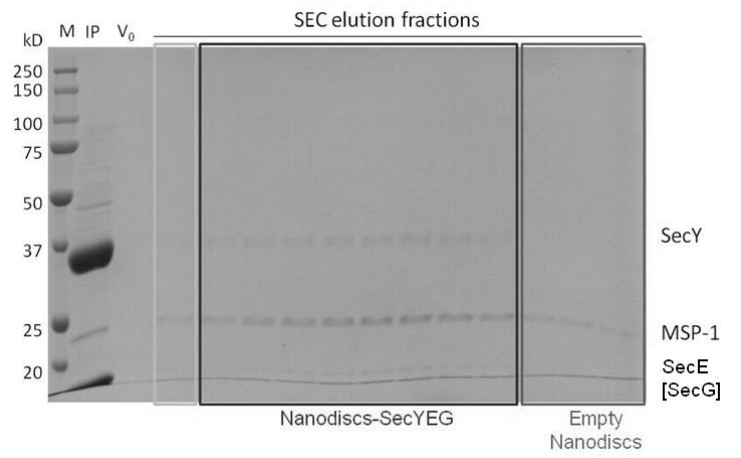

Figure 5-11. **SDS-PAGE analysis of the SecYEG translocon reconstituted in nanodiscs.** After gel filtration, protein containing fractions were loaded onto a SDS-PAGE gel and Coomassie-stained. SecYEG-containing and empty nanodiscs are indicated by boxes.

The analyzed fractions show the expected pattern. The SecYEG-nanodiscs contained SecY, SecE, SecG and MSP-1. Considering the fact that 2 MSP-1 proteins are necessary to form a nanodisc particle, the band intensities observed in SDS-PAGE analysis indicates the incorporation of one SecYEG complex per nanodisc particle. Based on these results, we decided to analyze the fraction containing SecYEG-nanodiscs by negative-stain EM [Fig. 5-12].

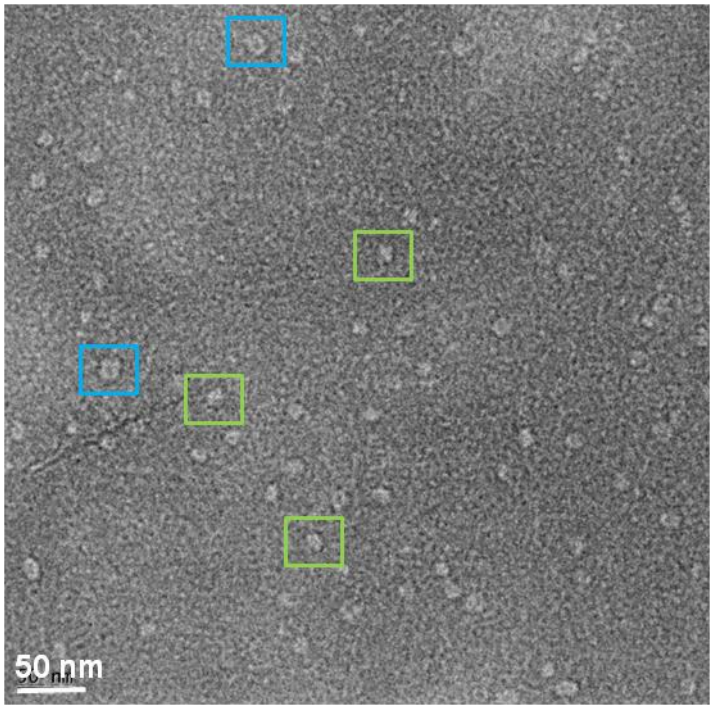

Figure 5-12. **Negative-stained electron microscopy of nanodiscs containing SecYEG.** The sample was stained with 2% uranyl acetate. Colored squares highlight two different sizes of nanodiscs.

Two different sizes of nanodisc particles were observed as shown on the electron microscope micrograph [Fig. 5-12]. The fractions containing empty nanodiscs were also analyzed by EM and a different behavior was observed: Contrary to the nanodiscs containing SecYEG complex, empty nanodisc were observed to interact with the carbon of the grid via the edge of the nanodisc. Obviously, there is a difference in hydrophobicity between empty and protein-containing nanodiscs leading to different adsorption to the carbon foil during grid preparation and thus to different preferential views in EM.

Subsequently, reconstitution experiments were performed with the DFYY and the HTL complexes. The first experiments were not successful. Likely, the nanodisc formed by MSP1 is too small to incorporate DFYY with 19 transmembrane helices and HTL with 34 transmembrane helices. Thus, a larger variant of MSP is required in order to incorporate the supplementary transmembrane helices. In addition to the increased diameter, the reconstitution reaction with lipids and MSP variant will need optimization. If too many lipids are added, the insertion of the membrane protein complexes could be disfavored because of lacking space within the nanodisc. This project will be continued by another PhD student in our laboratory. The ultimate aim is to determine by single particle cryo-EM the structure of a ribosome-nanodisc HTL complex, similarly to the RNC-SecYEG nanodisc complex structure described previously by the Beckmann laboratory (Frauenfeld et al., 2011). Such a structure would be closer to the native HTL in the plasma membrane and could represent an actively translocating complex with a substrate in the translocation pore.

5-5. Proteomic study on SecDF knock-out *E.coli* strain

The exact role of SecDF-YajC during translocation is enigmatic. Cellular copy numbers indicate that there are only 30-50 molecules of SecDF in the cell, in comparison to ~500 copies of SecYEG and 2500 copies of YidC (Matsuyama et al., 1992; K. J. Pogliano & J. Beckwith, 1994; Schatz et al., 1991; Urbanus et al., 2002). Based on these data, it is unlikely that the holotranslocon is responsible for, or involved in the membrane protein integration (or protein export) of all translocated proteins. We hypothesize that SecDF-YajC-YidC are recruited by SecYEG to translocate certain substrates for instance by accelerating translocation by coupling it to the proton motif force (Arkowitz & Wickner, 1994; J. A. Pogliano & J. Beckwith, 1994; Tsukazaki et al., 2011).

In order to identify such holotranslocon substrates, we decided to perform a proteomic study to find out whether SecDF-YajC was required for the translocation of specific substrates. The main difficulties in this study came from the fact that all the subunits of the holotranslocon are vital to the cell. As a consequence, it is difficult to determine if there is any

requirement of a certain subunit for the translocation of a specific substrate. To overcome this problem, we used a conditional SecDF expression strain (Economou et al., 1995). In *E. coli* strain JP352, the chromosomal secDF operon is under control of the araB promoter. As a consequence, the strain JP352 synthesizes YajC, SecD and SecF from the chromosome and forms colonies on agar plates only when grown in the presence of arabinose. In culture, upon step-wise exchange of arabinose by glucose, the expression of SecDF-YajC decreases, and the cells grow slower.

After overnight growth at 37°C in LB media supplemented with 0.2% arabinose, cells were diluted (1:100 dilution) in LB media supplemented with 0.2% glucose. When the OD600nm reached 0.6, the cells were further diluted (1:50 dilution) into LB media supplemented with 0.2% glucose. After three hours, we harvested the cells and broke them by several passages through a French press cell. Unbroken cells and cell debris were removed by a centrifugation step (14,000 RPM, 1 hour, JLA20, 4°C) followed by an ultra-centrifugation step (45,000 RPM, 1.5 hour, Ti70 rotor, 4°C) to collect the membrane fraction. Next, a carbonate fractionation procedure was applied (Molloy et al., 2000) to further purify the membrane extracts and remove membrane-associated proteins. Approximately 3 mg membrane protein (determined by a Bradford assay) was dissolved in 1 ml ice-cold 100mM Na_2CO_3 and left on ice for 1 h, being vigorously shaken every 5 min. Membranes resulting from two samples, 'wild type' (i.e. JP352 cells grown in the presence of arabinose) and 'knock-out' (JP352 cells grown in the absence of arabinose) were analyzed by SDS-PAGE [Fig. 5-13].

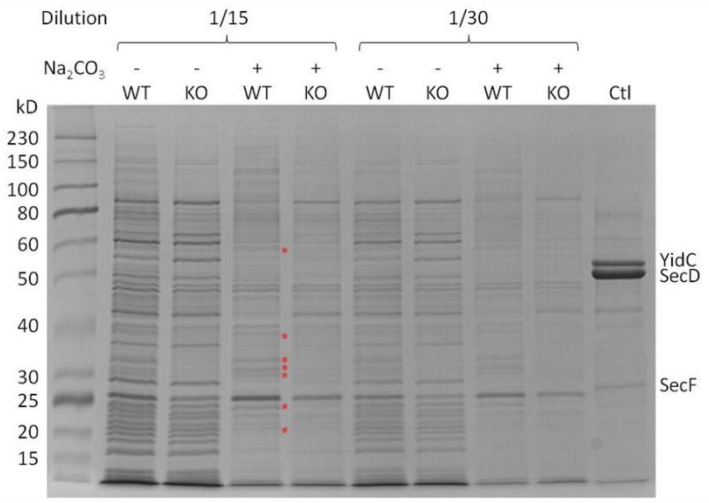

Figure 5-13. **Effect of the deletion of SecDF-YajC on the expression of membrane proteins in *E. coli*.** Membrane fractions of SecDF-YajC containing wild-type cells (WT) and knock-out cells (KO) were loaded onto a SDS-PAGE gel and Coomassie-stained. Samples were loaded with a 1/15 and 1/30 dilution. + and – indicate whether the membrane fraction was subjected to a carbonate fractionation. Red asterisks point to interesting proteins which are not found in the membrane of the KO cells. Purified SecDF-YajC was loaded as a control (ctl).

The gel was sent to the EDyP service at the CEA-Grenoble. The hits (protein bands which were only detected in the wild-type fraction) were excised from the gel, proteins were in-gel digested with trypsin, and the resulting peptides extracted and analyzed by LC-MS/MS. We obtained a list of membrane proteins which were affected by the deletion of SecDF-YajC. Interesting results are summarized in *table 1*. As a control, the first proteins that we checked were SecD and SecF. As expected, after depletion of SecDF, these proteins were either not detected in the "knockout" conditions or with a very high ratio between wild-type and knock-out conditions. As a second control, we checked for the presence of proteins needed for arabinose metabolism (proteins under the arabinose promoter). In fact, after switching from arabinose to glucose, the proteins involved in the arabinose metabolic pathway were not expressed in the knock-out cells. Subsequently, we identified several candidate membrane proteins for which the membrane protein integration was severely impaired when the SecDF-YajC complex was not expressed in the cell. These include FtsH, GlpT, LldP, NuoH and NuoL (Table 5-1). We cloned these substrate proteins into the pET21 vector under the control of a T7 promoter and tagged them with a myc-tag and a his-tag. The aim is to verify their dependence on the holotranslocon for membrane integration *in vitro* in a translation/translocation experiment using proteoliposomes containing SecYEG, YidC or holotranslocon. Further, the influence of the proton motif force on the integration of these proteins into the lipid bilayer could be tested experimentally. Unfortunately, such *in vitro* translation/translocation experiments turned out to be very difficult. In collaboration with Ian Collinson (chapter 3), we could show *in vitro* the integration of CyoA into HTL-containing proteoliposomes. Therefore, these experiments are doable. However, when we used FtsH or LldP for *in vitro* translation/translocation assays, the nascent (likely unfolded or partially folded) membrane proteins were sticking to the liposomes (negative control) and could not be removed by Proteinase K or by 5M urea. This resulted in a very high background such that the signal resulting from membrane protein integration into HTL-containing proteoliposomes could not be detected on top of this background. Optimization of the experimental conditions in order to get rid of the background signal is required.

Protein	Mass	SC WT/KO	Localisation		Function
			Periplasm	Cell inner Membrane	
Protein-export membrane protein secD	66638.67	WT only		X	Involved in protein export
Protein-export membrane protein SecF	35359.60	11.00		X	Involved in protein export
Arabinose-proton symporter *araE*	51890.07	WT only		X	Uptake of arabinose across the boundary membrane with the concomitant transport of protons into the cell (symport system)
L-arabinose-binding periplasmic protein *araF*	35566.25	WT only	X		Involved in the high-affinity L-arabinose membrane transport system. Binds with high affinity to arabinose, but can also bind D-galactose (approximately 2-fold reduction) and D-fucose (approximately 40-fold reduction).
L-arabinose transport system permease protein AraH	34524.39	WT only		X	Part of the binding-protein-dependent transport system for L-arabinose. Probably responsible for the translocation of the substrate across the membrane
FtsH	70759.39	WT only		X	ATP-dependent zinc metallopeptidase for both cytoplasmic and membrane proteins
Glycerol-3-phosphate transporter *glpT*	50612.61	WT only		X	Responsible for glycerol-3-phosphate uptake
L-lactate permease *lldP*	59369.53	WT only		X	Transports L-lactate across the membrane. Can also transport D-lactate and glycolate. Seems to be driven by a proton motive force
NADH-quinone oxidoreductase subunit L *nuoL*	66538.15	WT only		X	NDH-1 shuttles electrons from NADH, via FMN and iron-sulfur (Fe-S) centers, to quinones in the respiratory chain. The immediate electron acceptor for the enzyme in this species is believed to be ubiquinone. Couples the redox reaction to proton translocation (for every two electrons transferred, four hydrogen ions are translocated across the cytoplasmic membrane), and thus conserves the redox energy in a proton gradient
FtsH	70759.39	WT only		X	ATP-dependent zinc metallopeptidase for both cytoplasmic and membrane proteins
ATP synthase gamma chain	31653.26	2.50		X part of a complex	Produces ATP from ADP in the presence of a proton gradient across the membrane. The gamma chain is believed to be important in regulating ATPase activity and the flow of protons through the CF_0 complex
NADH-quinone oxidoreductase subunit H *nuoH*	36338.92	WT only		X	NDH-1 shuttles electrons from NADH, via FMN and iron-sulfur (Fe-S) centers, to quinones in the respiratory chain. The immediate electron acceptor for the enzyme in this species is believed to be ubiquinone. Couples the redox reaction to proton translocation (for every two electrons transferred, four hydrogen ions are translocated across the cytoplasmic membrane), and thus conserves the redox energy in a proton gradient

Table 5-1. **Membrane proteins affected by the deletion of SecDF-YajC.** Proteins affected by the switch from arabinose to glucose metabolism are shown in purple. Candidate holo-translocon substrates are indicated in red. The molecular weight of the identified protein is indicated in kDa. The expression ratio between wild-type and knock-out cells is indicated as well as the cellular localization. SecD and SecF data are given as a control.

5-6. Conclusion

Native mass spectrometry is a method which has been developed for soluble protein complexes. Adapting this technique to membrane protein complexes requires development of new instruments or technology such as laser activation of the micelles in the gas phase which is currently tested in the Robinson laboratory.

Similarly, crosslinking mass spectrometry (CLMS) is a relatively new technology which has been used mainly for soluble protein complexes to date. Development of new crosslinkers is required for the study of membrane protein complexes because the mostly hydrophobic transmembrane parts of the complexes cannot be crosslinked with lysine-reactive agents. One possibility would be to make use of non-natural amino acids which are photo-activatable like photo-leucine or photo-methionine. These modified amino acids could give information on the transmembrane interface which is an area of interaction in a membrane protein complex.

The application of these cutting-edge MS technologies to the holotranslocon complex has a great potential. Clearly, sample preparation and the MS techniques have to be further optimized in order to obtain structural insight into HTL architecture by nanoelectrospray MS or CLMS.

Chapter 6 : Discussion and conclusions

Résumé en français / French summary

La résolution de la structure de l'holotranslocon par cryo-microscopie électronique est une étape importante afin d'élargir notre connaissance du mécanisme de translocation co- et post-traductionnelle. Dans les faits, le complexe holotranslocon semble capable d'interagir avec des partenaires additionnels tels que des protéines cytosolique, périplasmique et membranaires conduisant ainsi à une augmentation de la complexité. De plus, la reconstruction par cryo-ME de HTL soulève un certain nombre de questions concernant la dynamique de l'holotranslocon et le réarrangement des sous-unités induit par l'attachement des partenaires de translocation. En effet, des résultats biochimiques et structuraux suggèrent une réorganisation des sous-unités au sein du HTL qui peuvent être diffèrent en fonction de la présence du ribosome ou de l'ATPase SecA. C'est pourquoi, une étude structurale et des analyses fonctionnelles plus approfondies du complexe HTL seul, en complexe avec un partenaire de translocation ou éventuellement de complexes translocon plus larges sont nécessaires afin de révéler le mécanisme de l'holotranslocon et sa fonction physiologique comparés au canal de translocation des protéines SecYEG. Pour terminer, même si les systèmes de translocation eucaryotes sont différents et apparaissent plus complexes, ce travail pourrait fournir un point de départ à des études futures sur les complexes de translocation eucaryotes sensiblement plus larges.

6-1. The holotranslocon structure

We solved the structure of the detergent-solubilized holotranslocon at 10.5 Å resolution by cryo-EM (Chapter 4). Based on this structure and on the available crystal structure of the individual subunits, we managed to build a quasi-atomic model which explains previous experimental results on the SecYEG protein-conducting channel and its accessory proteins. However, additional research is needed to further clarify the dynamics and functional interactions within the holo-complex.

For example the conformational change upon binding of the co- and post-translational translocation partner, the ribosome and SecA, respectively. As mentioned in chapter 1-2, Sachelaru et al. showed that the binding of YidC to the lateral gate of SecY is dynamic upon binding of 70S or a ribosome-nascent-chain complex (Sachelaru et al., 2013). Therefore, the HTL may adopt a different organization/conformation when bound to the ribosome. In chapter 5-3, we showed that it was possible to isolate a ribosome-HTL complex and that cryo-EM study was possible. By solving the structure of the ribosome-HTL complex at high resolution, we should be in a position to highlight any structural rearrangements occurring within the holotranslocon upon ribosome binding. In addition, crosslinking studies could help to further analyze subunit interactions within the HTL, like SecDF/SecYEG or SecDF/YidC. Comparison of these crosslinking profiles between HTL with or without bound ribosome can confirm dynamic interactions between subunits.

During post-translational translocation, SecA provides the energy for the translocation process (Rapoport, 2007). To perform its motor protein role, SecA has to bind to SecYEG (Matsumoto et al., 1997). Furthermore, the interaction of SecA with SecY has been shown to induce a conformational rearrangement of the lateral gate which is suggested to initiate the opening of the channel towards the lipid bilayer, allowing insertion of the signal sequence in the lateral gate (du Plessis et al., 2009; Tsukazaki et al., 2008; Zimmer et al., 2008). SecA binding and the concomitant conformational change of the lateral gate does not perturb the interaction of YidC with SecY as shown by crosslinking studies (Sachelaru et al., 2013). Moreover, several studies suggest that SecDF would be involved in the regulation of the SecA-SecYEG interaction (Duong & Wickner, 1997a, 1997b; Economou et al., 1995). Thus, the SecDF involvement could result in a different conformation of the SecA-SecYEG. These observations suggest that the holotranslocon adopts a different conformation during co- and post-translational translocation. Structure determination of the SecA-HTL complex and comparison with a ribosome-HTL structure could give new information regarding the specific mechanism of the co- and post-translational translocation involving the holotranslocon complex.

In this study, we analyzed the detergent-solubilized state of the HTL. It is well known that the membrane lipid bilayer has an effect on the structure/function of the membrane proteins (Tillman & Cascio, 2003). The lateral forces due to mechanical pressure caused by the packing of lipids and proteins have a significant effect on the folding and structure of membrane proteins (Marsh, 1996). Membrane proteins may adopt different conformations than the one observed in the detergent-solubilized state were less mechanical constraints are applied on the protein structure. For instance, the structure of the mechanosensitive channel MscL has been shown to be influenced by the membrane bilayer and specifically by the lateral pressure (Hamill & Martinac, 2001; Perozo et al., 2002; Spencer et al., 1999). The structure of SecYEG in complex with a ribosome has been solved by cryo-EM in detergent-solubilized state (Beckmann et al., 2001; Ménétret et al., 2007; Mitra et al., 2005) as well as in a native membrane-like environment (Frauenfeld et al., 2011). Unfortunately, the structures and their resolutions are too different to reveal important differences in the SecYEG conformation. However, it is likely that the HTL has a different conformation in a lipidic environment. In order to answer this question, as mentioned in chapter 5-4, we aim to solve the structure of the holotranslocon after reconstitution into a nanodisc (Bayburt et al., 2002) by cryo-EM. In a nanodisc, the organization of the HTL may reflect the assembly of this supercomplex within the bacterial membrane.

Another very important topic for future research is the functional relevance of the holotranslocon compared to SecYEG. As mentioned in the chapter 1, SecYEG is the most essential component of the translocation machinery (Akimaru et al., 1991; Brundage et al., 1990; D. B. Oliver & Beckwith, 1982). It can work independently or recruit accessory protein to form the HTL (Arkowitz & Wickner, 1994; Luirink et al., 2005). The exact conditions required to initiate the HTL complex assembly remain unknown. In chapter 3, we showed that HTL is capable of translocation and although HTL presents a lower efficiency than SecYEG for SecA-dependent translocation, the PMF seems to induce a higher stimulation of the translocation in HTL compared to SecYEG. Moreover, the copy number of subunits present in the bacterial membrane needs to be taken into account. YidC is present in a fivefold excess compared to SecYEG while SecDF exists in a ten-fold lower amount (Matsuyama et al., 1992; K. J. Pogliano & J. Beckwith, 1994; Schatz et al., 1991; Urbanus et al., 2002). Therefore, the HTL is likely to be used not for translocation of all substrates, but is likely to be recruited under certain conditions and/or for a certain class of substrates. In an attempt to identify HTL-specific substrates (chapter 5-5), we showed that the translocation of membrane proteins seems to be influenced by the absence of SecDF compared to ‘wild-type cells’. We have identified several multi-subunit membrane complexes (e.g. NuoL and NuoH (subunits of respiratory chain complex 1), or subunits of the F1F0 ATPase) which may in fact require the holotranslocon to support efficient translocation of periplasmic domains and

membrane protein folding as well as assembly. Even though this is a preliminary result, these identified putative substrates could help us to determine if HTL-substrates present common characteristics which are important for the recruitment of the accessory proteins forming the HTL.

6-2. Additional accessory proteins

The SecYEG protein conducting channel is the essential component of the translocation machinery (Brundage et al., 1990). The holotranslocon consists of SecYEG associated with an accessory domain composed of SecDF-YajC-YidC (Arkowitz & Wickner, 1994; Luirink et al., 2005). While this supercomplex consists of 7 membrane proteins it is the question whether this complex is stably associated with other membrane proteins. Several additional soluble or membrane-embedded proteins seem to interact structurally and/or functionally with part of the subunits forming the holotranslocon, and their impact on protein translocation needs to be addressed in the future.

6-2-1. PpiD

PpiD (Dartigalongue & Raina, 1998) is one of the putative members of a bigger translocation complex (Antonoaea et al., 2008). This 70 kDa periplasmic chaperone is anchored to the membrane by a single transmembrane helix located at the N-terminus and has been shown to interact with the SecYEG complex by crosslinking experiments (Sachelaru et al., 2013). Interestingly, PpiD shares the same interaction site at the lateral gate of SecY with YidC (Sachelaru et al., 2013). This suggests different requirements for these “chaperones” and therefore could point to a YidC- and a PpiD-dependent translocation pathway. PpiD is proposed to recognize specifically outer membrane protein characteristics of a peptide sequence (Bitto & McKay, 2003; Dartigalongue & Raina, 1998; Hennecke et al., 2005). In addition to its localization, PpiD has been shown to contact the preprotein on the periplasmic side of the membrane only in active translocation (Antonoaea et al., 2008). Furthermore, PpiD has been shown to accelerate the release of the translocated preprotein in the case of secretory protein. Taken together, these results suggest that PpiD associates with the SecYEG translocon and covers the periplasmic exit site, while promoting the proper folding of the nascent outer membrane proteins [Fig. 6-1].

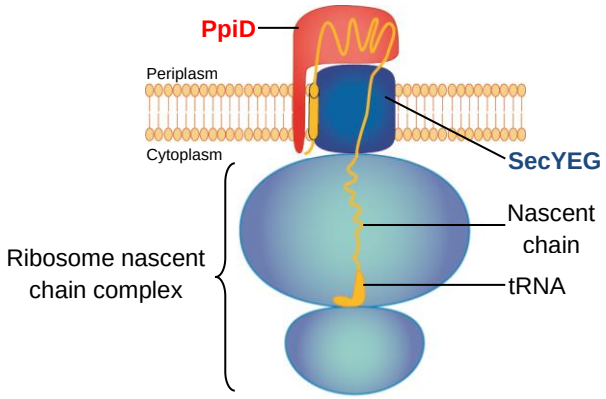

Figure 6-1. **Model of SecYEG-PpiD complex during co-translational translocation.** The ribosome is colored in light blue, the P-site tRNA and the nascent polypeptide chain in yellow, PpiD in red, SecYEG in blue, and the lipids in orange. (Adapted and modified from (Antonoaea et al., 2008)).

As SecDF is also suggested to play a role in the translocation by interacting with the preprotein at the periplasmic site of SecYEG (Matsuyama et al., 1993; Tsukazaki et al., 2011), it suggests a scanning process of the preprotein by SecDF, YidC and PpiD in order to determine which pathway the preprotein will use.

6-2-2. YidD

A second possible partner is YidD (Yu et al., 2011). The *yidD* gene encodes a 9.3 kDa cytoplasmic protein which is associated with the membrane via a putative amphipathic *alpha*-helix located at the N–terminus. Genetic studies indicate that *yidD* is located in the same gene cluster as YidC which is highly conserved. Moreover, *yidD* is a close neighbor of *yidC* (2 base pair spacing) and is suggested to contain an internal promoter for *yidC* (Burland et al., 1993; Yu et al., 2011). In the bacterium *Blochmannia pennsylvanicus*, the *yidC* gene is fused to the *yidD* gene indicating a linked function of the two proteins (Degnan et al., 2005). Concerning the possible role of YidD in translocation, even though no interactions between YidD and SecYEG or YidC have been shown so far, YidD has been shown to interact with the nascent chain on the cytoplasmic side of the membrane while YidC and SecYEG are contacting the preprotein [Fig. 6-2].

Taken together these results suggest that YidD could work as a cytosolic chaperone by mediating the folding of the cytosolic part of a preprotein (Yu et al., 2011).

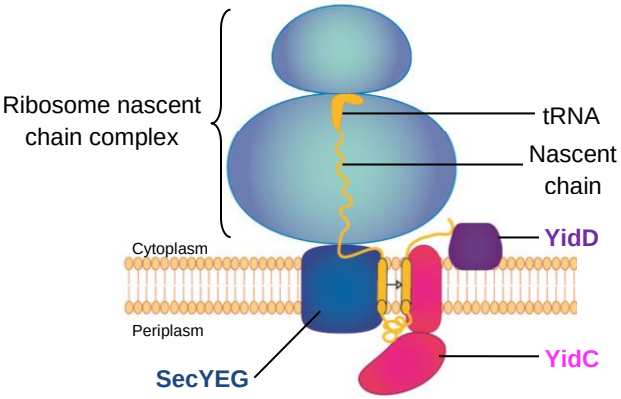

***Figure 6-2*. Model of the SecYEG-YidC-YidD complex during co-translational translocation.** The ribosome is colored in light blue, the P-site tRNA and the nascent polypeptide chain in yellow, YidC in magenta, YidD in purple, SecYEG in blue, and the lipids in orange. (Adapted and modified from (Yu et al., 2011)).

6-2-3. The FtsH/HlfK/HlfC complex

A further potential part of a bigger translocation complex is the membrane protein FtsH. FtsH forms a hexamer and a complex together with HlfK and HlfC. In a Sec-dependent translocation experiments, it has been shown that this complex was capable to interact with YidC (van Bloois et al., 2008). Furthermore, the interaction to YidC is mediated by the HlfK and HlfC proteins [Fig. 6-3] (van Bloois et al., 2008).

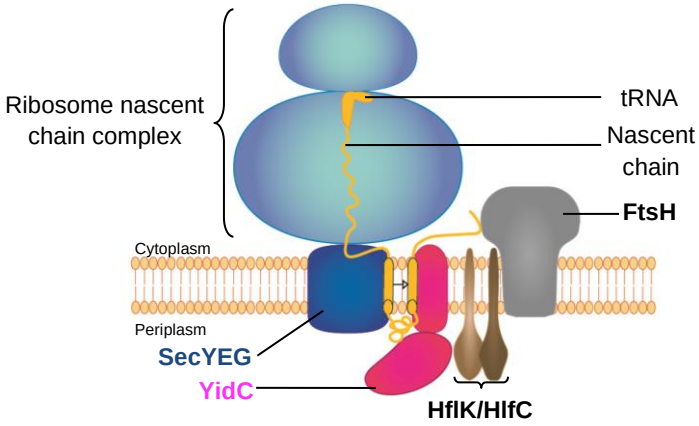

***Figure 6-3.* Model of the SecYEG-YidC-FtsH complex during co-translational translocation.** The ribosome is colored in light blue, the P-site tRNA and the nascent polypeptide chain in yellow, YidC in magenta, an hexamer of FtsH in grey, HflK/HflC complex in brown, SecYEG in blue, and the lipids in orange.

By crosslinking experiments it has also been shown that the nascent chain was interacting first with YidC and then with FtsH during co-translational translocation experiments [Fig. 6-3] suggesting a late function for FtsH in the translocation process which could be related to a quality control mechanism (van Bloois et al., 2008; van Stelten et al., 2009). Indeed, it is known that FtsH is an ATP-dependent endopeptidase and it has been shown to contribute to the quality control of inner membrane proteins (Ito & Akiyama, 2005). In addition to that, it is worth to note that homologues of YidC and FtsH in mitochondria, respectively Oxa1 and Yta10, Yta12 are implicated in a similar interaction (Rep et al., 1996). Furthermore, in this context, Oxa1 has been suggested to offer a protection to the newly

synthesized preprotein against the protease activity of Yme1p, a FtsH-like protease (Lemaire et al., 2000). Taken together, these results suggest a possible role for the YidC-FtsH complex in quality control. YidC can protect the preprotein from degradation by FtsH but could also direct misfolded membrane proteins to FtsH.

FtsH has another crucial role in early quality control of the translocation machinery. As mentioned in chapter 1-1-3, SecE is important to stabilize SecY (Matsuyama et al., 1990; Taura et al., 1993). In the context of different expression rates of SecY compared to SecE, the un-complexed SecY is directed to FtsH for degradation (Kihara et al., 1995).

6-3. Ribosome/SecA-dependent translocation

In Chapter 1, we pointed out that two targeting routes exist for a preprotein to be translocated in bacteria, either the SecA-dependent pathway or the SRP-pathway which direct the preprotein to the post-translational translocation or co-translational translocation, respectively (Valent et al., 1998). Whereas most of bacterial secretory proteins follow the post-translational pathway (H. G. Koch et al., 1999), bacterial membrane proteins are inserted co-translationally (Ulbrandt et al., 1997).

These pathways were thought to be distinct. However, it has been shown for some membrane proteins with large periplasmic domains which are targeted to the SecYEG complex by the SRP-pathway that SecA is necessary for their correct assembly in the membrane. One example is AcrB, a membrane protein with a large periplasmic domain. It is targeted to the translocon by the SRP-pathway (Qi & Bernstein, 1999). By depleting SecA in a temperature-sensitive mutant, it has been shown that the insertion of AcrB was completely blocked and that the preprotein was retained in the cytosol (Qi & Bernstein, 1999). Similarly, , the translocation of the large periplasmic domain of FtsQ has been shown to be SecA-dependent using *in vitro* translocation assays and SecYEG proteoliposomes (van der Laan et al., 2004).

Additional support for a ribosome/SecA interplay came from translocation experiments with a hybrid protein construct: The fusion construct ‘Momp2’ contained the signal anchor sequence of the mannitol permease (MtlA), an inner membrane protein which depends on the SRP-pathway for insertion in the membrane fused to the sequence of the precursor of the outer membrane protein A (pOmpA) which requires SecA/SecB for translocation across the inner membrane (Neumann-Haefelin et al., 2000). *In vitro* translocation experiment into inverted membrane vesicles (IMVs) showed that this hybrid construct was co-translationally targeted to SecY via the SRP-pathway, however, the preprotein was translocated only in presence of SecA (Neumann-Haefelin et al., 2000).

These results suggest that SecA and the ribosome work together in a sequential manner to translocate membrane proteins with a large periplasmic domain.

In an attempt to characterize the SRP/SecA dependent substrates, it has been shown that the SecA dependence could be abolished if the length of the periplasmic domain of SecA-dependent preprotein was shortened (Deitermann et al., 2005). YidC is also a multi-spanning membrane protein with a large periplasmic domain (chapter 1-2). By *in vitro* translocation experiments into inverted membrane vesicles, it has been shown that the correct assembly of YidC was strictly dependent on the presence of SecA only if the its periplasmic domain was longer than 30 amino acids (Deitermann et al., 2005). However, it has also been shown that in the case of a single-spanning membrane protein like Momp2, even a short version of the periplasmic domain (less than 30 amino acids) required SecA for translocation (Deitermann et al., 2005). Likewise, YidC constructs which contained only one transmembrane domain were shown to be SecA-dependent with no regards to the size of their periplasmic domains (Deitermann et al., 2005). Therefore, not only the length of the periplasmic domain but also the presence of a downstream transmembrane domain seems to be an important determinant for the recruitment of SecA as a part of the translocation machinery.

It has been proposed that the binding of SecA and the ribosome to the SecYEG complex was not competitive (Zito & Oliver, 2003) suggesting distinct binding site on the translocon for SecA and the ribosome. However, as revealed by the three-dimensional structures (chapter 1), SecA and the ribosome are sharing the same binding site on SecY, involving mainly the cytoplasmic loops C4 and C5 (Frauenfeld et al., 2011; Mitra et al., 2005; Zimmer et al., 2008). Mutational analysis revealed that these interactions were important for co- and post-translational translocation involving the ribosome or SecA, respectively (Cheng et al., 2005; van der Sluis, Nouwen, et al., 2006). These observations raise an important question: how are the ribosomes and SecA interacting with SecYEG during the ribosome/SecA-dependent translocation process? To address this crucial question, the impact of the presence of the ribosome on the SecA translocation was analyzed by *in vitro* translocation experiments using IMVs. It has been shown that the SecA-dependent translocation was occurring only after completion of the protein synthesis in the case of single-spanning membrane protein whereas for multi-spanning membrane protein the ribosome release was not a requirement (Deitermann et al., 2005).

Based on these results several hypotheses regarding the requirement of the ribosome/SecA-dependent translocation were put forward [Fig. 6-4].

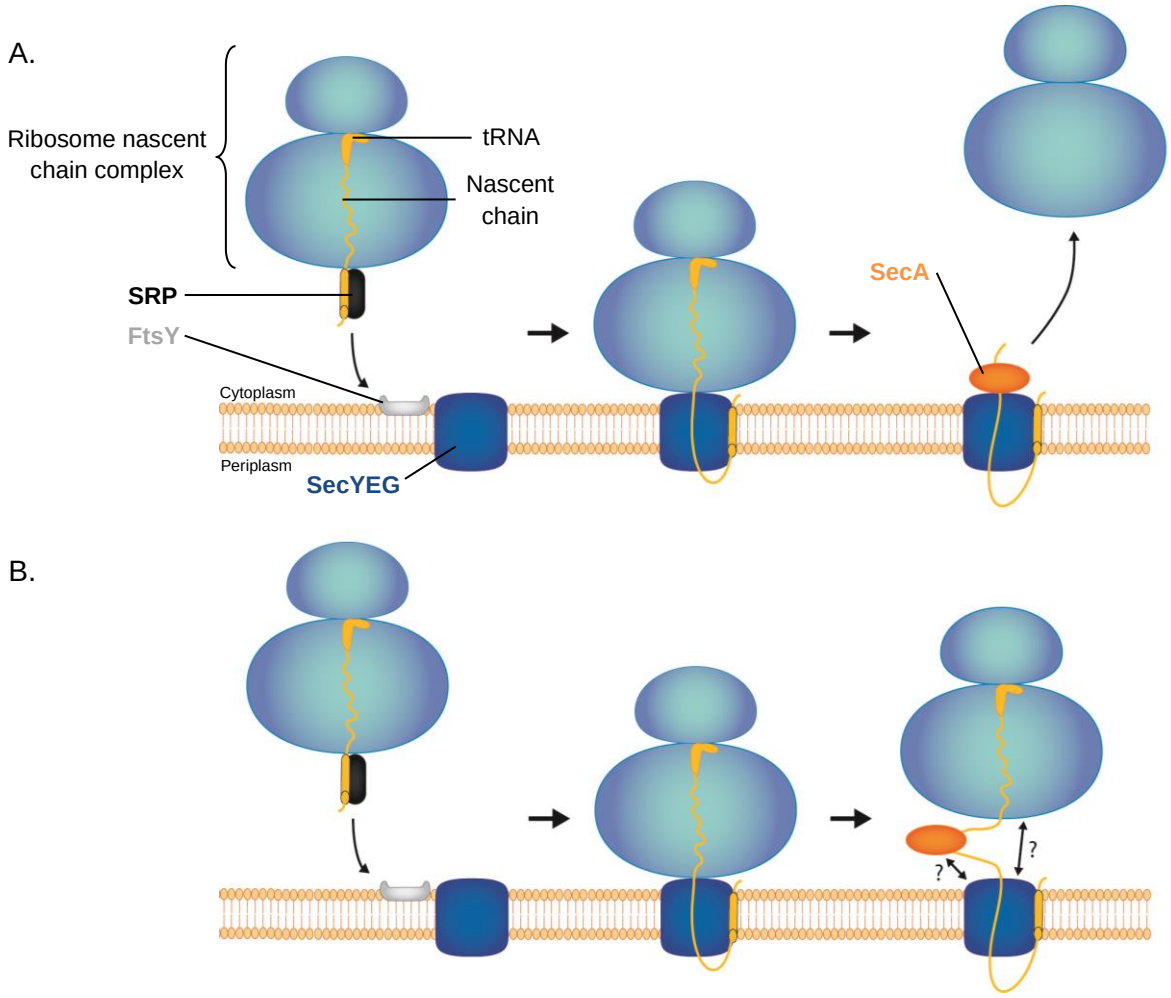

Figure 6-4. **Ribosome/SecA-dependent translocation model. A.** Translocation of a single-spanning membrane protein. **B.** Translocation of a multi-spanning membrane protein. The ribosome is colored in light blue, the P-site tRNA and the nascent polypeptide chain in yellow, SRP in black, FtsY in light grey, SecA in orange, SecYEG in blue, and the lipids in orange. Question marks highlight the unknown interaction mechanism between the ribosome, SecA and SecYEG during the ribosome/SecA interplay. (Adapted and modified from (Neumann-Haefelin et al., 2000)).

Insertion of SecA-dependent single spanning membrane proteins require SecA independently of their periplasmic domain size and SecA interacts with SecYEG only if the ribosome is released after termination of the protein synthesis [Fig. 6-4-A]. Multi-spanning membrane proteins depend on SecA for their translocation only if their periplasmic domain is larger than 30 amino acids (Andersson & von Heijne, 1993), and SecA contacts SecYEG while the ribosome is still translating the preprotein [Fig. 6-4-B].

Considering the observation that SecA interacts with SecYEG which is engaged in the co-translational translocation with the ribosome, this model suggests that the ribosome and SecA have to share the binding site. Even though the oligomeric state of active SecYEG is still under debate (Duong, 2003; Manting et al., 2000; Mitra et al., 2005; Yahr & Wickner,

2000), SecYEG oligomers could solve this problem by offering one binding site for SecA and one for the ribosome. In the context of the holotranslocon, SecA and the ribosome are expected to use the same binding site which suggests a succession of association and dissociation events, unless a new binding site for the ribosome or SecA would be offered by YidC or SecDF. A cryo-EM structure of HTL in complex with SecA and in complex with the ribosome may shed light on secondary binding sites offered by the holotranslocon.

6-4. Transport of folded proteins

The SecYEG translocon complex transports proteins in an unfolded state from the cytoplasm to the periplasm. However, some secreted proteins need to be folded in the cytoplasm prior to their transport in the periplasm. This is the case for proteins which require a cofactor prior to transport (Halbig et al., 1999), for example proteins which require metal ions to function (Tottey et al., 2008) and hetero-oligomeric complexes in which only one subunit contains an export signal sequence (Rodrigue et al., 1999; Sambasivarao et al., 2000). In reason of its limited opening of about 24 Å in diameter (Bonardi et al., 2011), the SecYEG channel can accommodate only an unfolded polypeptide chain which measures on average 12 Å in diameter. Therefore, folded proteins require another transport system to reach their correct destination. Nevertheless, the two translocation systems have been suggested to cooperate in some cases (see below).

The Tat pathway transports folded proteins (Berks et al., 2000). The PMF-dependent Tat transport system (Mould & Robinson, 1991; Yahr & Wickner, 2001) is not universally conserved in bacteria, and it is mainly composed of three membrane proteins TatA, TatB and TatC. It is capable of transporting folded proteins with a size of up to 70 Å in diameter (Berks et al., 2000). Giving the size of the channel which has to transport a 70 Å diameter protein the main difficulty is to maintain the impermeability of the membrane. This is achieved by recruiting the channel only when it is needed. Indeed, the formation of the translocation channel seems to be initiated by the interaction of the protein with the membrane (Mori & Cline, 2002).

Folded proteins are targeted to the Tat system via a specific signal sequence containing a conserved twin-arginine motif (Berks, 1996) and which is less hydrophobic than in the signal sequence in the Sec pathway (Cristobal et al., 1999). At the membrane, TatB and TatC form an integral membrane protein complex (Bolhuis et al., 2001; Tarry et al., 2009) which is responsible for the recognition and the binding of the protein at the membrane (Cline & Mori, 2001). Upon formation of the TatBC-substrate complex, TatA is recruited and generates a TatABC-substrate complex (Mori & Cline, 2002). Based on NMR structure, TatA is composed of two helices, one transmembrane helix and one amphipathic helix organize in

a L-shape with the amphipathic helix contacting the phospholipid head groups on the cytoplasmic side of the membrane (Hu et al., 2010; S. Koch et al., 2012). The active translocation mechanism is enigmatic but the most accepted hypothesis is that TatA is the main actor of the protein transport as it was the only TatABC component found to interact with a substrate in transport-stalled experiments [Fig. 6-5] (Panahandeh et al., 2008).

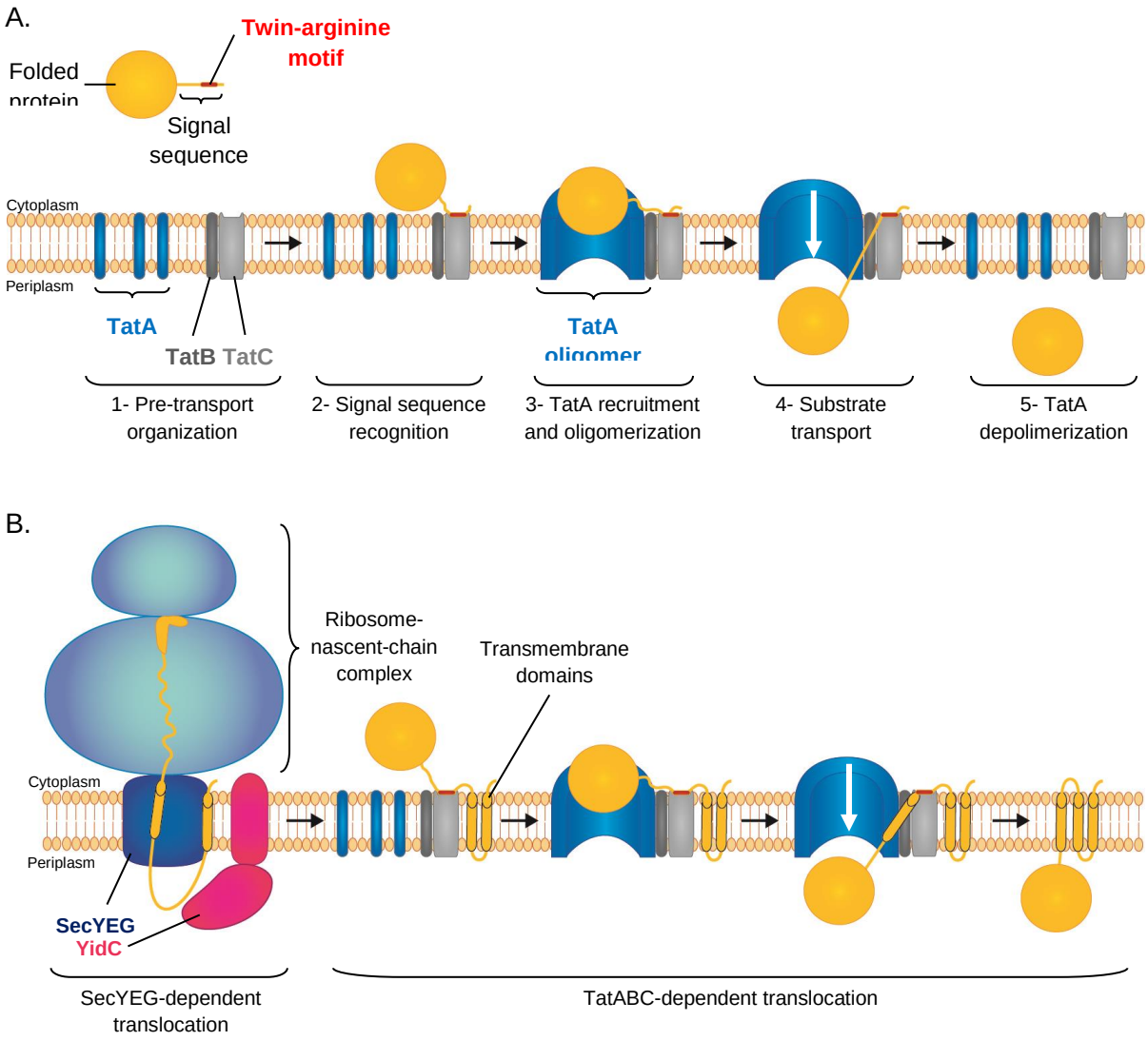

***Figure 6-5*. The Tat-translocation pathway. A.** Schematic model representing the TatABC-dependent translocation. **B.** Schematic model of the SecYEG-TatABC-dependent membrane protein translocation. The TatA subunits and oligomers are colored in blue, the TatB and TatC subunit in orange. A folded protein is represented as a grey sphere with its signal sequence represented as a grey line including the twin-arginine specific motif represented in red. The white arrow indicates the transport direction. The numbers reflect the different steps in the Tat-translocation pathway. (Adapted and modified from (Palmer & Berks, 2012)).

Recruitment of several TatA subunits by the TatBC complex is suggested be followed by polymerization of TatA and by formation of a channel-like structure as shown in a low-resolution EM structure (Gohlke et al., 2005). Different oligomerization states of TatA could offer a tight channel around the substrate and thus avoid leakage during the transport of protein (Gohlke et al., 2005; Leake et al., 2008). At the end of the transport, the TatABC complex may dissociate to maintain the membrane impermeability (Cline & McCaffery, 2007).

Interestingly, the Tat pathway is also capable to translocate a small subset of membrane proteins (Hatzixanthis et al., 2003). This is for example the case of the Rieske protein (Bachmann et al., 2006; De Buck et al., 2007). This protein belongs to the cytochrome bc_1 and b_6f complexes which play a role in the respiratory electron transport chain for example. Contrary to the small subset identified previously containing only C-terminal anchored membrane proteins (Hatzixanthis et al., 2003), in some Gram-positive bacteria the Rieske protein is connected to the membrane via three N-terminal transmembrane domains (Niebisch & Bott, 2001, 2003). Surprisingly, it has been shown that the Rieske protein was strictly depending on the SecYEG complex for the insertion of the first two transmembrane helices and that the translocation of the folded periplasmic domain as well as the third transmembrane helix which carries the twin-arginine motif was strictly dependent of the presence of the Tat translocase [Fig. 6-5-B] (Keller et al., 2012). This result implies a higher degree of complexity of the Tat pathway as well as the *E. coli* translocation pathways in general with possible cooperation between the different translocation systems for the correct insertion of a membrane protein.

High-resolution structures of the individual subunits as well as the different complexes formed during the Tat-dependent translocation will be required in order to reveal the exact mechanism of this transport system.

6-5. Translocation in eukaryotes

6-5-1. Co-translational translocation across the endoplasmic reticulum (ER) membrane via the SRP/Sec61 pathway

The protein conducting channel is universally conserved. The homologues of the bacterial SecYEG in eukaryotes are respectively the Sec61α, β and γ subunits. Like in bacteria the co-translational translocation pathway is initiated by the binding of the eukaryotic SRP to the signal sequence at the ribosomal exit tunnel (Walter & Blobel, 1980) forming a complex which is then targeted to the membrane via the SRP receptor. Unlike in bacteria, SRP is able to arrest the preprotein synthesis after binding to the signal sequence at the

ribosomal exit tunnel (Walter & Blobel, 1981). It has been shown that this translation arrest was crucial for the correct targeting of the protein and for the cell growth (Lakkaraju et al., 2008). At the membrane, the ribosome nascent chain complex is transferred to the Sec61 complex.

6-5-2. Post-translational translocation across the endoplasmic reticulum (ER) membrane via the Sec61-BiP pathway

The main difference in eukaryotes is displayed in the post-translational translocation mechanism. The SecA protein does not exist in eukaryotes, therefore they developed another mechanism to translocate the preprotein through the Sec61 complex. Contrary to bacteria where SecA plays the role of an active motor and acts on the cytoplasmic side of the membrane by "pushing" the preprotein through the channel, in eukaryotes, the BiP protein functions "passively" in the lumen of the endoplasmic reticulum (ER) by a ratcheting mechanism [Fig. 6-6] (Matlack et al., 1999).

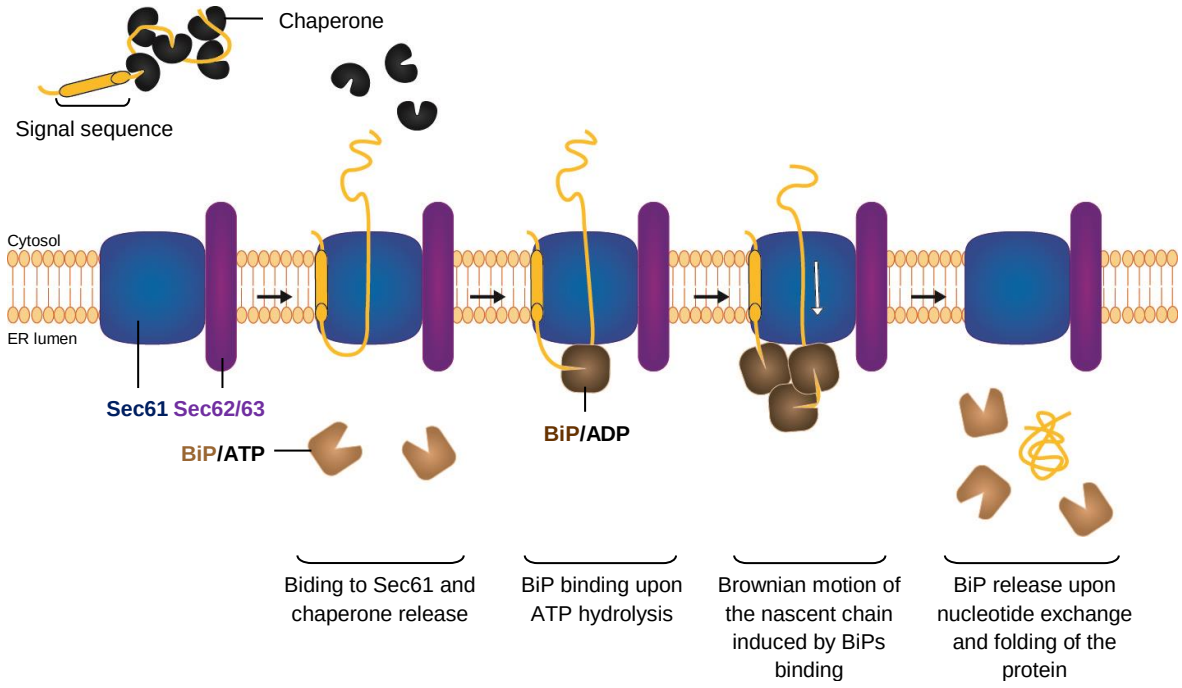

Figure 6-6. **The BiP-dependent post-translational translocation model.** Schematic representation of the different steps of the BiP-dependent translocation pathway. The Sec61 complex is represented in blue, the sec62/63 complex in purple, BiPs in complex with ATP in light brown, BiPs in complex with ADP in dark brown, cytosolic chaperones in black, the polypeptide chain in yellow and the membrane bilayer in orange (adapted and modified form (Park & Rapoport, 2012)).

Post-translational translocation starts after translation termination by the recognition and binding of the preprotein by Hsp70-like cytosolic chaperone (Plath & Rapoport, 2000). This chaperone-preprotein complex is then interacting with the Sec61 complex which is associated with an additional membrane protein complex, the Sec62/63 complex (Meyer et al., 2000). This Sec62/63 complex is not conserved and can contain additional nonessential components like Sec71p and Sec72p in the yeast complex (Deshaies et al., 1991). After binding of the preprotein to the Sec61-62/63 complex, the chaperones are dissociated from the preprotein and their rebinding is suggested to be prevented by Sec62 and Sec63 (Plath & Rapoport, 2000). At this step the preprotein can move in two directions by Brownian motion, either toward the cytosol or toward the ER lumen. The backward movement has been suggested to be prevented by the binding of BiP on the lumenal side of the ER (Matlack et al., 1999). Interaction between BiP and Sec63 in the ER lumen would induce ATP hydrolysis and a change of BiP conformation which will cause the trapping of the preprotein and therefore preventing the backwards movement (Matlack et al., 1999). After binding of several BiP molecules to translocate the entire preprotein, exchange of ATP for ADP in the BiP binding pocket would release the preprotein in the ER lumen (Matlack et al., 1999).

Surprisingly, this translocation mechanism based on Brownian motion is pretty similar to the “Brownian ratchet model” proposed for post-translational translocation by SecA and discussed in chapter 1-1-4 (Tomkiewicz et al., 2007). However, this model is under debate in bacteria especially because it is in contradiction with the step-wise translocation mechanism of SecA (Schiebel et al., 1991).

6-5-3. Eukaryotic accessory proteins

SecDFYajC and YidC are not conserved in eukaryotes. Like SecYEG in bacteria, the Sec61 complex can associate with accessory proteins to post-translationally modify proteins, assist in membrane protein folding and assembly of complexes. In addition, the necessity of preprotein modification in order to achieve the maturation exists in eukaryotes.

In addition to Sec62/63 (Meyer et al., 2000), Sec61 has been shown to interact with the oligosaccharyl-transferase (OST) complex which is responsible of co-translational N-linked glycosylation of the preprotein (Scheper et al., 2003; Shibatani et al., 2005). Other proteins associating with Sec61 were identified, like the TRAM protein (translocating-chain associating membrane protein) (Görlich et al., 1992), the TRAP complex (translocon-associated protein complex) (Ménétret et al., 2008; Shibatani et al., 2005) and RAMP4 (Pool, 2009). Even though their exact roles remain unclear, the TRAM protein and TRAP complex are suggested to be involved in efficient translocation of substrates (Fons et al., 2003; Snapp et al., 2004) and the RAMP4 is proposed to stabilize the preprotein and to regulate its N-

linked glycosylation (Schröder et al., 1999; Yamaguchi et al., 1999). Taken together, these accessory factors and their role in eukaryotic protein translocation are poorly characterized. This may be due to the absence of protocols for extraction of the intact complexes from the membrane or recombinant production of the factors.

Consequently, the three-dimensional information regarding these complexes are limited to the Sec61 complex. Cryo-electron microscopy structures exist of Sec61-ribosome complex (Beckmann et al., 2001; Ménétret et al., 2000). Even though one the cryo-EM structure suggested the presence of an additional protein, the resolution was too low to identify the partner associated with Sec61 (Ménétret et al., 2000). In summary, eukaryotic membrane protein integration, folding and co-translational translocation is a field of rich discovery.

6-6. Concluding remarks

The structural study of the holotranslocon and the observation that a lot of structural information is missing regarding the translocation pathway in prokaryotes and in eukaryotes reflects the difficulties of studying membrane proteins and in particular membrane protein complexes which are unstable. Large membrane proteins are often studied by electron microscopy as they often fail to crystallize However, to achieve high resolution structures, cryo-EM studies are still limited to proteins larger than 100 kDa. Smaller membrane proteins have traditionally been studied by electron crystallography (Breyton et al., 2002; Henderson et al., 1990; Kühlbrandt et al., 1994; Lotz et al., 2008). Larger membrane protein complexes may be more difficult to overexpress, to solubilize from the membrane and may show a higher degree of heterogeneity. Clearly, hybrid approaches are required to study membrane protein complexes. Biochemical and biophysical analyses needs to be combined with cryo-electron microscopy, X-ray crystallography of individual subunits/ domains and novel tools like crosslinking mass spectrometry in order to obtain a more complete picture of the structure and function of the machine studied. In the near future, the use of direct detectors and improved image processing software to sort for structural heterogeneity is expected to lead to higher-resolution cryo-EM structures, a better insight into the molecular organization of the complexes and therefore to a better understanding of the studied processes.

List of references

Akimaru, J., Matsuyama, S., Tokuda, H., & Mizushima, S. (1991). Reconstitution of a protein translocation system containing purified SecY, SecE, and SecA from *Escherichia coli*. *Proc. Natl. Acad. Sci. U. S. A.,* **88**, 6545-6549.

Alami, M., Dalal, K., Lelj-Garolla, B., Sligar, S. G., & Duong, F. (2007). Nanodiscs unravel the interaction between the SecYEG channel and its cytosolic partner SecA. *EMBO J.,* **26**, 1995-2004.

Alber, F., Dokudovskaya, S., Veenhoff, L. M., Zhang, W., Kipper, J., Devos, D., Suprapto, A., Karni-Schmidt, O., Williams, R., Chait, B. T., Rout, M. P., & Sali, A. (2007). Determining the architectures of macromolecular assemblies. *Nature,* **450**, 683-694.

Andersson, H., & von Heijne, G. (1993). Sec dependent and sec independent assembly of *E. coli* inner membrane proteins: the topological rules depend on chain length. *EMBO J.,* **12**, 683-691.

Angelini, S., Deitermann, S., & Koch, H. G. (2005). FtsY, the bacterial signal-recognition particle receptor, interacts functionally and physically with the SecYEG translocon. *EMBO Rep.,* **6**, 476-481.

Antonoaea, R., Furst, M., Nishiyama, K., & Müller, M. (2008). The periplasmic chaperone PpiD interacts with secretory proteins exiting from the SecYEG translocon. *Biochemistry,* **47**, 5649-5656.

Arkowitz, R. A., & Wickner, W. (1994). SecD and SecF are required for the proton electrochemical gradient stimulation of preprotein translocation. *EMBO J.,* **13**, 954-963.

Bachmann, J., Bauer, B., Zwicker, K., Ludwig, B., & Anderka, O. (2006). The Rieske protein from *Paracoccus denitrificans* is inserted into the cytoplasmic membrane by the twin-arginine translocase. *FEBS J.,* **273**, 4817-4830.

Back, J. W., de Jong, L., Muijsers, A. O., & de Koster, C. G. (2003). Chemical crosslinking and mass spectrometry for protein structural modeling. *J. Mol. Biol.,* **331**, 303-313.

Barrera, N. P., Di Bartolo, N., Booth, P. J., & Robinson, C. V. (2008). Micelles protect membrane complexes from solution to vacuum. *Science,* **321**, 243-246.

Bayburt, T. H., Grinkova, Y. V., & Sligar, S. G. (2002). Self-Assembly of Discoidal Phospholipid Bilayer Nanoparticles with Membrane Scaffold Proteins. *Nano Letters,* **2**, 853-856.

Beck, K., Eisner, G., Trescher, D., Dalbey, R. E., Brunner, J., & Müller, M. (2001). YidC, an assembly site for polytopic *Escherichia coli* membrane proteins located in immediate proximity to the SecYE translocon and lipids. *EMBO Rep.,* **2**, 709-714.

Beckmann, R., Spahn, C. M., Eswar, N., Helmers, J., Penczek, P. A., Sali, A., Frank, J., & Blobel, G. (2001). Architecture of the protein-conducting channel associated with the translating 80S ribosome. *Cell,* **107**, 361-372.

Berks, B. C. (1996). A common export pathway for proteins binding complex redox cofactors? *Mol. Microbiol.,* **22**, 393-404.

Berks, B. C., Sargent, F., & Palmer, T. (2000). The Tat protein export pathway. *Mol. Microbiol.,* **35**, 260-274.

Bieniossek, C., Nie, Y., Frey, D., Olieric, N., Schaffitzel, C., Collinson, I., Romier, C., Berger, P., Richmond, T. J., Steinmetz, M. O., & Berger, I. (2009). Automated unrestricted multigene recombineering for multiprotein complex production. *Nat. Methods,* **6**, 447-450.

Bitto, E., & McKay, D. B. (2003). The periplasmic molecular chaperone protein SurA binds a peptide motif that is characteristic of integral outer membrane proteins. *J. Biol. Chem.,* **278**, 49316-49322.

Bolhuis, A., Mathers, J. E., Thomas, J. D., Barrett, C. M., & Robinson, C. (2001). TatB and TatC form a functional and structural unit of the twin-arginine translocase from *Escherichia coli*. *J. Biol. Chem.,* **276**, 20213-20219.

Bonardi, F., Halza, E., Walko, M., Du Plessis, F., Nouwen, N., Feringa, B. L., & Driessen, A. J. (2011). Probing the SecYEG translocation pore size with preproteins conjugated with sizable rigid spherical molecules. *Proc. Natl. Acad. Sci. U. S. A.,* **108**, 7775-7780.

Breyton, C., Haase, W., Rapoport, T. A., Kühlbrandt, W., & Collinson, I. (2002). Three-dimensional structure of the bacterial protein-translocation complex SecYEG. *Nature,* **418**, 662-665.

Brundage, L., Hendrick, J. P., Schiebel, E., Driessen, A. J., & Wickner, W. (1990). The purified *E. coli* integral membrane protein SecY/E is sufficient for reconstitution of SecA-dependent precursor protein translocation. *Cell,* **62**, 649-657.

Burland, V., Plunkett, G., 3rd, Daniels, D. L., & Blattner, F. R. (1993). DNA sequence and analysis of 136 kilobases of the *Escherichia coli* genome: organizational symmetry around the origin of replication. *Genomics,* **16**, 551-561.

Cabelli, R. J., Dolan, K. M., Qian, L. P., & Oliver, D. B. (1991). Characterization of membrane-associated and soluble states of SecA protein from wild-type and SecA51(TS) mutant strains of *Escherichia coli*. *J. Biol. Chem.,* **266**, 24420-24427.

Chen, M., Xie, K., Yuan, J., Yi, L., Facey, S. J., Pradel, N., Wu, L. F., Kuhn, A., & Dalbey, R. E. (2005). Involvement of SecDF and YidC in the membrane insertion of M13 procoat mutants. *Biochemistry,* **44**, 10741-10749.

Cheng, Z., Jiang, Y., Mandon, E. C., & Gilmore, R. (2005). Identification of cytoplasmic residues of Sec61p involved in ribosome binding and cotranslational translocation. *J. Cell. Biol.,* **168**, 67-77.

Chou, Y. T., & Gierasch, L. M. (2005). The conformation of a signal peptide bound by *Escherichia coli* preprotein translocase SecA. *J. Biol. Chem.,* **280**, 32753-32760.

Cline, K., & McCaffery, M. (2007). Evidence for a dynamic and transient pathway through the TAT protein transport machinery. *EMBO J.,* **26**, 3039-3049.

Cline, K., & Mori, H. (2001). Thylakoid DeltapH-dependent precursor proteins bind to a cpTatC-Hcf106 complex before Tha4-dependent transport. *J. Cell. Biol.,* **154**, 719-729.

Cooper, D. B., Smith, V. F., Crane, J. M., Roth, H. C., Lilly, A. A., & Randall, L. L. (2008). SecA, the motor of the secretion machine, binds diverse partners on one interactive surface. *J. Mol. Biol.,* **382**, 74-87.

Cristobal, S., de Gier, J. W., Nielsen, H., & von Heijne, G. (1999). Competition between Sec- and TAT-dependent protein translocation in *Escherichia coli*. *EMBO J.,* **18**, 2982-2990.

Dartigalongue, C., & Raina, S. (1998). A new heat-shock gene, *ppiD*, encodes a peptidyl-prolyl isomerase required for folding of outer membrane proteins in *Escherichia coli*. *EMBO J.,* **17**, 3968-3980.

Das, S., & Oliver, D. B. (2011). Mapping of the SecA.SecY and SecA.SecG interfaces by site-directed *in vivo* photocrosslinking. *J. Biol. Chem.,* **286**, 12371-12380.

De Buck, E., Vranckx, L., Meyen, E., Maes, L., Vandersmissen, L., Anné, J., & Lammertyn, E. (2007). The twin-arginine translocation pathway is necessary for correct membrane insertion of the Rieske Fe/S protein in *Legionella pneumophila*. *FEBS Lett.,* **581**, 259-264.

Degnan, P. H., Lazarus, A. B., & Wernegreen, J. J. (2005). Genome sequence of *Blochmannia pennsylvanicus* indicates parallel evolutionary trends among bacterial mutualists of insects. *Genome Res.,* **15**, 1023-1033.

Deitermann, S., Sprie, G. S., & Koch, H. G. (2005). A dual function for SecA in the assembly of single spanning membrane proteins in *Escherichia coli*. *J. Biol. Chem.,* **280**, 39077-39085.

Denisov, I. G., Grinkova, Y. V., Lazarides, A. A., & Sligar, S. G. (2004). Directed self-assembly of monodisperse phospholipid bilayer Nanodiscs with controlled size. *J. Am. Chem. Soc.,* **126**, 3477-3487.

Deshaies, R. J., Sanders, S. L., Feldheim, D. A., & Schekman, R. (1991). Assembly of yeast Sec proteins involved in translocation into the endoplasmic reticulum into a membrane-bound multisubunit complex. *Nature,* **349**, 806-808.

Douville, K., Leonard, M., Brundage, L., Nishiyama, K., Tokuda, H., Mizushima, S., & Wickner, W. (1994). Band 1 subunit of *Escherichia coli* preportein translocase and integral membrane export factor P12 are the same protein. *J. Biol. Chem.,* **269**, 18705-18707.

du Plessis, D. J., Berrelkamp, G., Nouwen, N., & Driessen, A. J. (2009). The lateral gate of SecYEG opens during protein translocation. *J. Biol. Chem.,* **284**, 15805-15814.

Duong, F. (2003). Binding, activation and dissociation of the dimeric SecA ATPase at the dimeric SecYEG translocase. *EMBO J.,* **22**, 4375-4384.

Duong, F., & Wickner, W. (1997a). Distinct catalytic roles of the SecYE, SecG and SecDFyajC subunits of preprotein translocase holoenzyme. *EMBO J.,* **16**, 2756-2768.

Duong, F., & Wickner, W. (1997b). The SecDFyajC domain of preprotein translocase controls preprotein movement by regulating SecA membrane cycling. *EMBO J.,* **16**, 4871-4879.

Economou, A., Pogliano, J. A., Beckwith, J., Oliver, D. B., & Wickner, W. (1995). SecA membrane cycling at SecYEG is driven by distinct ATP binding and hydrolysis events and is regulated by SecD and SecF. *Cell,* **83**, 1171-1181.

Egea, P. F., & Stroud, R. M. (2010). Lateral opening of a translocon upon entry of protein suggests the mechanism of insertion into membranes. *Proc. Natl. Acad. Sci. U. S. A.,* **107**, 17182-17187.

Erlandson, K. J., Miller, S. B., Nam, Y., Osborne, A. R., Zimmer, J., & Rapoport, T. A. (2008). A role for the two-helix finger of the SecA ATPase in protein translocation. *Nature,* **455**, 984-987.

Faham, S., & Bowie, J. U. (2002). Bicelle crystallization: a new method for crystallizing membrane proteins yields a monomeric bacteriorhodopsin structure. *J. Mol. Biol.,* **316**, 1-6.

Fang, J., & Wei, Y. (2011). Expression, purification and characterization of the *Escherichia coli* integral membrane protein YajC. *Protein Pept. Lett.,* **18**, 601-608.

Fekkes, P., de Wit, J. G., van der Wolk, J. P., Kimsey, H. H., Kumamoto, C. A., & Driessen, A. J. (1998). Preprotein transfer to the *Escherichia coli* translocase requires the co-operative binding of SecB and the signal sequence to SecA. *Mol. Microbiol.,* **29**, 1179-1190.

Fekkes, P., van der Does, C., & Driessen, A. J. (1997). The molecular chaperone SecB is released from the carboxy-terminus of SecA during initiation of precursor protein translocation. *EMBO J.,* **16**, 6105-6113.

Fons, R. D., Bogert, B. A., & Hegde, R. S. (2003). Substrate-specific function of the translocon-associated protein complex during translocation across the ER membrane. *J. Cell. Biol.,* **160**, 529-539.

Frauenfeld, J., Gumbart, J., Sluis, E. O., Funes, S., Gartmann, M., Beatrix, B., Mielke, T., Berninghausen, O., Becker, T., Schulten, K., & Beckmann, R. (2011). Cryo-EM structure of the ribosome-SecYE complex in the membrane environment. *Nat. Struct. Mol. Biol.,* **18**, 614-621.

Gohlke, U., Pullan, L., McDevitt, C. A., Porcelli, I., de Leeuw, E., Palmer, T., Saibil, H. R., & Berks, B. C. (2005). The TatA component of the twin-arginine protein transport system forms channel complexes of variable diameter. *Proc. Natl. Acad. Sci. U. S. A.,* **102**, 10482-10486.

Gold, V. A., Robson, A., Bao, H., Romantsov, T., Duong, F., & Collinson, I. (2010). The action of cardiolipin on the bacterial translocon. *Proc. Natl. Acad. Sci. U. S. A.,* **107**, 10044-10049.

Görlich, D., Hartmann, E., Prehn, S., & Rapoport, T. A. (1992). A protein of the endoplasmic reticulum involved early in polypeptide translocation. *Nature,* **357**, 47-52.

Halbig, D., Wiegert, T., Blaudeck, N., Freudl, R., & Sprenger, G. A. (1999). The efficient export of NADP-containing glucose-fructose oxidoreductase to the periplasm of *Zymomonas mobilis* depends both on an intact twin-arginine motif in the signal peptide and on the generation of a structural export signal induced by cofactor binding. *Eur. J. Biochem.,* **263**, 543-551.

Hamill, O. P., & Martinac, B. (2001). Molecular basis of mechanotransduction in living cells. *Physiol. Rev.,* **81**, 685-740.

Hanada, K., Izawa, K., Nishijima, M., & Akamatsu, Y. (1993). Sphingolipid deficiency induces hypersensitivity of CD14, a glycosyl phosphatidylinositol-anchored protein, to phosphatidylinositol-specific phospholipase C. *J. Biol. Chem.,* **268**, 13820-13823.

Harris, C. R., & Silhavy, T. J. (1999). Mapping an interface of SecY (PrlA) and SecE (PrlG) by using synthetic phenotypes and *in vivo* crosslinking. *J. Bacteriol.,* **181**, 3438-3444.

Hartl, F. U., Lecker, S., Schiebel, E., Hendrick, J. P., & Wickner, W. (1990). The binding cascade of SecB to SecA to SecY/E mediates preprotein targeting to the *E. coli* plasma membrane. *Cell,* **63**, 269-279.

Hatzixanthis, K., Palmer, T., & Sargent, F. (2003). A subset of bacterial inner membrane proteins integrated by the twin-arginine translocase. *Mol. Microbiol.,* **49**, 1377-1390.

Henderson, R., Baldwin, J. M., Ceska, T. A., Zemlin, F., Beckmann, E., & Downing, K. H. (1990). Model for the structure of bacteriorhodopsin based on high-resolution electron cryo-microscopy. *J. Mol. Biol.,* **213**, 899-929.

Hennecke, G., Nolte, J., Volkmer-Engert, R., Schneider-Mergener, J., & Behrens, S. (2005). The periplasmic chaperone SurA exploits two features characteristic of integral outer membrane proteins for selective substrate recognition. *J. Biol. Chem.,* **280**, 23540-23548.

Hizlan, D., Robson, A., Whitehouse, S., Gold, V. A., Vonck, J., Mills, D., Kühlbrandt, W., & Collinson, I. (2012). Structure of the SecY complex unlocked by a preprotein mimic. *Cell. Rep.,* **1**, 21-28.

Hu, Y., Zhao, E., Li, H., Xia, B., & Jin, C. (2010). Solution NMR structure of the TatA component of the twin-arginine protein transport system from gram-positive bacterium *Bacillus subtilis*. *J. Am. Chem. Soc.,* **132**, 15942-15944.

Hunt, J. F., Weinkauf, S., Henry, L., Fak, J. J., McNicholas, P., Oliver, D. B., & Deisenhofer, J. (2002). Nucleotide control of interdomain interactions in the conformational reaction cycle of SecA. *Science,* **297**, 2018-2026.

Ito, K., & Akiyama, Y. (2005). Cellular functions, mechanism of action, and regulation of FtsH protease. *Annu. Rev. Microbiol.,* **59**, 211-231.

Jia, L., Dienhart, M., Schramp, M., McCauley, M., Hell, K., & Stuart, R. A. (2003). Yeast Oxa1 interacts with mitochondrial ribosomes: the importance of the C-terminal region of Oxa1. *EMBO J.,* **22**, 6438-6447.

Jiang, F., Chen, M., Yi, L., de Gier, J. W., Kuhn, A., & Dalbey, R. E. (2003). Defining the regions of *Escherichia coli* YidC that contribute to activity. *J. Biol. Chem.,* **278**, 48965-48972.

Kastner, B., Fischer, N., Golas, M. M., Sander, B., Dube, P., Boehringer, D., Hartmuth, K., Deckert, J., Hauer, F., Wolf, E., Uchtenhagen, H., Urlaub, H., Herzog, F., Peters, J. M., Poerschke, D., Lührmann, R., & Stark, H. (2008). GraFix: sample preparation for single-particle electron cryomicroscopy. *Nat. Methods.,* **5**, 53-55.

Keller, R., de Keyzer, J., Driessen, A. J., & Palmer, T. (2012). Co-operation between different targeting pathways during integration of a membrane protein. *J. Cell. Biol.,* **199**, 303-315.

Kihara, A., Akiyama, Y., & Ito, K. (1995). FtsH is required for proteolytic elimination of uncomplexed forms of SecY, an essential protein translocase subunit. *Proc. Natl. Acad. Sci. U. S. A.,* **92**, 4532-4536.

Kimsey, H. H., Dagarag, M. D., & Kumamoto, C. A. (1995). Diverse effects of mutation on the activity of the *Escherichia coli* export chaperone SecB. *J. Biol. Chem.,* **270**, 22831-22835.

Klenner, C., & Kuhn, A. (2012). Dynamic disulfide scanning of the membrane-inserting Pf3 coat protein reveals multiple YidC substrate contacts. *J. Biol. Chem.,* **287**, 3769-3776.

Koch, H. G., Hengelage, T., Neumann-Haefelin, C., MacFarlane, J., Hoffschulte, H. K., Schimz, K. L., Mechler, B., & Müller, M. (1999). *In vitro* studies with purified components reveal signal recognition particle (SRP) and SecA/SecB as constituents of two independent protein-targeting pathways of *Escherichia coli*. *Mol. Biol. Cell.,* **10**, 2163-2173.

Koch, S., Fritsch, M. J., Buchanan, G., & Palmer, T. (2012). *Escherichia coli* TatA and TatB proteins have N-out, C-in topology in intact cells. *J. Biol. Chem.,* **287**, 14420-14431.

Kohler, R., Boehringer, D., Greber, B., Bingel-Erlenmeyer, R., Collinson, I., Schaffitzel, C., & Ban, N. (2009). YidC and Oxa1 form dimeric insertion pores on the translating ribosome. *Mol. Cell.,* **34**, 344-353.

Kühlbrandt, W., Wang, D. N., & Fujiyoshi, Y. (1994). Atomic model of plant light-harvesting complex by electron crystallography. *Nature,* **367**, 614-621.

Kuhn, A., Stuart, R., Henry, R., & Dalbey, R. E. (2003). The Alb3/Oxa1/YidC protein family: membrane-localized chaperones facilitating membrane protein insertion? *Trends Cell. Biol.,* **13**, 510-516.

Kuhn, P., Weiche, B., Sturm, L., Sommer, E., Drepper, F., Warscheid, B., Sourjik, V., & Koch, H. G. (2011). The bacterial SRP receptor, SecA and the ribosome use overlapping binding sites on the SecY translocon. *Traffic,* **12**, 563-578.

Lakkaraju, A. K., Mary, C., Scherrer, A., Johnson, A. E., & Strub, K. (2008). SRP keeps polypeptides translocation-competent by slowing translation to match limiting ER-targeting sites. *Cell,* **133**, 440-451.

Lasker, K., Förster, F., Bohn, S., Walzthoeni, T., Villa, E., Unverdorben, P., Beck, F., Aebersold, R., Sali, A., & Baumeister, W. (2012). Molecular architecture of the 26S proteasome holocomplex determined by an integrative approach. *Proc. Natl. Acad. Sci. U. S. A.,* **109**, 1380-1387.

Leake, M. C., Greene, N. P., Godun, R. M., Granjon, T., Buchanan, G., Chen, S., Berry, R. M., Palmer, T., & Berks, B. C. (2008). Variable stoichiometry of the TatA component of the twin-arginine protein transport system observed by *in vivo* single-molecule imaging. *Proc. Natl. Acad. Sci. U. S. A.,* **105**, 15376-15381.

Lemaire, C., Hamel, P., Velours, J., & Dujardin, G. (2000). Absence of the mitochondrial AAA protease Yme1p restores F0-ATPase subunit accumulation in an *oxa1* deletion mutant of *Saccharomyces cerevisiae*. *J. Biol. Chem.,* **275**, 23471-23475.

Lill, R., Dowhan, W., & Wickner, W. (1990). The ATPase activity of SecA is regulated by acidic phospholipids, SecY, and the leader and mature domains of precursor proteins. *Cell,* **60**, 271-280.

Lotz, M., Haase, W., Kühlbrandt, W., & Collinson, I. (2008). Projection structure of yidC: a conserved mediator of membrane protein assembly. *J. Mol. Biol.,* **375**, 901-907.

Luirink, J., von Heijne, G., Houben, E., & de Gier, J. W. (2005). Biogenesis of inner membrane proteins in *Escherichia coli*. *Annu. Rev. Microbiol.,* **59**, 329-355.

Lund, S., Orlowski, S., de Foresta, B., Champeil, P., le Maire, M., & Møller, J. V. (1989). Detergent structure and associated lipid as determinants in the stabilization of solubilized Ca2+-ATPase from sarcoplasmic reticulum. *J. Biol. Chem.,* **264**, 4907-4915.

Manting, E. H., van Der Does, C., Remigy, H., Engel, A., & Driessen, A. J. (2000). SecYEG assembles into a tetramer to form the active protein translocation channel. *EMBO J.,* **19**, 852-861.

Marsh, D. (1996). Lateral pressure in membranes. *Biochim. Biophys. Acta,* **1286**, 183-223.

Martoglio, B., Hofmann, M. W., Brunner, J., & Dobberstein, B. (1995). The protein-conducting channel in the membrane of the endoplasmic reticulum is open laterally toward the lipid bilayer. *Cell,* **81**, 207-214.

Matlack, K. E., Misselwitz, B., Plath, K., & Rapoport, T. A. (1999). BiP acts as a molecular ratchet during posttranslational transport of prepro-alpha factor across the ER membrane. *Cell,* **97**, 553-564.

Matsumoto, G., Mori, H., & Ito, K. (1998). Roles of SecG in ATP- and SecA-dependent protein translocation. *Proc. Natl. Acad. Sci. U. S. A.,* **95**, 13567-13572.

Matsumoto, G., Yoshihisa, T., & Ito, K. (1997). SecY and SecA interact to allow SecA insertion and protein translocation across the *Escherichia coli* plasma membrane. *EMBO J.,* **16**, 6384-6393.

Matsuyama, S., Akimaru, J., & Mizushima, S. (1990). SecE-dependent overproduction of SecY in *Escherichia coli*. Evidence for interaction between two components of the secretory machinery. *FEBS Lett.,* **269**, 96-100.

Matsuyama, S., Fujita, Y., & Mizushima, S. (1993). SecD is involved in the release of translocated secretory proteins from the cytoplasmic membrane of *Escherichia coli*. *EMBO J.,* **12**, 265-270.

Matsuyama, S., Fujita, Y., Sagara, K., & Mizushima, S. (1992). Overproduction, purification and characterization of SecD and SecF, integral membrane components of the protein translocation machinery of *Escherichia coli*. *Biochim. Biophys. Acta,* **1122**, 77-84.

Ménétret, J. F., Hegde, R. S., Aguiar, M., Gygi, S. P., Park, E., Rapoport, T. A., & Akey, C. W. (2008). Single copies of Sec61 and TRAP associate with a nontranslating mammalian ribosome. *Structure,* **16**, 1126-1137.

Ménétret, J. F., Neuhof, A., Morgan, D. G., Plath, K., Radermacher, M., Rapoport, T. A., & Akey, C. W. (2000). The structure of ribosome-channel complexes engaged in protein translocation. *Mol. Cell.,* **6**, 1219-1232.

Ménétret, J. F., Schaletzky, J., Clemons, W. M., Jr., Osborne, A. R., Skånland, S. S., Denison, C., Gygi, S. P., Kirkpatrick, D. S., Park, E., Ludtke, S. J., Rapoport, T. A., & Akey, C. W. (2007). Ribosome binding of a single copy of the SecY complex: implications for protein translocation. *Mol. Cell.,* **28**, 1083-1092.

Meyer, H. A., Grau, H., Kraft, R., Kostka, S., Prehn, S., Kalies, K. U., & Hartmann, E. (2000). Mammalian Sec61 is associated with Sec62 and Sec63. *J. Biol. Chem.,* **275**, 14550-14557.

Miroux, B., & Walker, J. E. (1996). Over-production of proteins in *Escherichia coli*: mutant hosts that allow synthesis of some membrane proteins and globular proteins at high levels. *J. Mol. Biol.,* **260**, 289-298.

Mitra, K., Schaffitzel, C., Shaikh, T., Tama, F., Jenni, S., Brooks, C. L., 3rd, Ban, N., & Frank, J. (2005). Structure of the *E. coli* protein-conducting channel bound to a translating ribosome. *Nature,* **438**, 318-324.

Molloy, M. P., Herbert, B. R., Slade, M. B., Rabilloud, T., Nouwens, A. S., Williams, K. L., & Gooley, A. A. (2000). Proteomic analysis of the *Escherichia coli* outer membrane. *Eur. J. Biochem.,* **267**, 2871-2881.

Mori, H., & Cline, K. (2002). A twin arginine signal peptide and the pH gradient trigger reversible assembly of the thylakoid [Delta]pH/Tat translocase. *J. Cell. Biol.,* **157**, 205-210.

Mori, H., & Ito, K. (2006). Different modes of SecY-SecA interactions revealed by site-directed *in vivo* photo-crosslinking. *Proc. Natl. Acad. Sci. U. S. A.,* **103**, 16159-16164.

Mould, R. M., & Robinson, C. (1991). A proton gradient is required for the transport of two lumenal oxygen-evolving proteins across the thylakoid membrane. *J. Biol. Chem.,* **266**, 12189-12193.

Murphy, C. K., & Beckwith, J. (1994). Residues essential for the function of SecE, a membrane component of the *Escherichia coli* secretion apparatus, are located in a conserved cytoplasmic region. *Proc. Natl. Acad. Sci. U. S. A.,* **91**, 2557-2561.

Nagamori, S., Nishiyama, K., & Tokuda, H. (2002). Membrane topology inversion of SecG detected by labeling with a membrane-impermeable sulfhydryl reagent that causes a close association of SecG with SecA. *J. Biochem.,* **132**, 629-634.

Neumann-Haefelin, C., Schäfer, U., Müller, M., & Koch, H. G. (2000). SRP-dependent co-translational targeting and SecA-dependent translocation analyzed as individual steps in the export of a bacterial protein. *EMBO J.,* **19**, 6419-6426.

Niebisch, A., & Bott, M. (2001). Molecular analysis of the cytochrome bc1-aa3 branch of the Corynebacterium glutamicum respiratory chain containing an unusual diheme cytochrome c1. *Arch. Microbiol.,* **175**, 282-294.

Niebisch, A., & Bott, M. (2003). Purification of a cytochrome bc-aa3 supercomplex with quinol oxidase activity from *Corynebacterium glutamicum*. Identification of a fourth subunity of cytochrome aa3 oxidase and mutational analysis of diheme cytochrome c1. *J. Biol. Chem.,* **278**, 4339-4346.

Nishiyama, K., Hanada, M., & Tokuda, H. (1994). Disruption of the gene encoding p12 (SecG) reveals the direct involvement and important function of SecG in the protein translocation of *Escherichia coli* at low temperature. *EMBO J.,* **13**, 3272-3277.

Nishiyama, K., Mizushima, S., & Tokuda, H. (1993). A novel membrane protein involved in protein translocation across the cytoplasmic membrane of *Escherichia coli*. *EMBO J.,* **12**, 3409-3415.

Nishiyama, K., Suzuki, T., & Tokuda, H. (1996). Inversion of the membrane topology of SecG coupled with SecA-dependent preprotein translocation. *Cell,* **85**, 71-81.

Nouwen, N., & Driessen, A. J. (2002). SecDFyajC forms a heterotetrameric complex with YidC. *Mol. Microbiol.,* **44**, 1397-1405.

Nouwen, N., Piwowarek, M., Berrelkamp, G., & Driessen, A. J. (2005). The large first periplasmic loop of SecD and SecF plays an important role in SecDF functioning. *J. Bacteriol.,* **187**, 5857-5860.

Oliver, D. B., & Beckwith, J. (1982). Regulation of a membrane component required for protein secretion in *Escherichia coli*. *Cell,* **30**, 311-319.

Oliver, D. C., & Paetzel, M. (2008). Crystal structure of the major periplasmic domain of the bacterial membrane protein assembly facilitator YidC. *J. Biol. Chem.,* **283**, 5208-5216.

Osborne, A. R., Clemons, W. M., Jr., & Rapoport, T. A. (2004). A large conformational change of the translocation ATPase SecA. *Proc. Natl. Acad. Sci. U. S. A.,* **101**, 10937-10942.

Osborne, A. R., & Rapoport, T. A. (2007). Protein translocation is mediated by oligomers of the SecY complex with one SecY copy forming the channel. *Cell,* **129**, 97-110.

Palmer, T., & Berks, B. C. (2012). The twin-arginine translocation (Tat) protein export pathway. *Nat. Rev. Microbiol.,* **10**, 483-496.

Panahandeh, S., Maurer, C., Moser, M., DeLisa, M. P., & Müller, M. (2008). Following the path of a twin-arginine precursor along the TatABC translocase of *Escherichia coli*. *J. Biol. Chem.,* **283**, 33267-33275.

Papanikolau, Y., Papadovasilaki, M., Ravelli, R. B., McCarthy, A. A., Cusack, S., Economou, A., & Petratos, K. (2007). Structure of dimeric SecA, the *Escherichia coli* preprotein translocase motor. *J. Mol. Biol.,* **366**, 1545-1557.

Park, E., & Rapoport, T. A. (2012). Mechanisms of Sec61/SecY-mediated protein translocation across membranes. *Annu. Rev. Biophys.,* **41**, 21-40.

Perozo, E., Cortes, D. M., Sompornpisut, P., Kloda, A., & Martinac, B. (2002). Open channel structure of MscL and the gating mechanism of mechanosensitive channels. *Nature,* **418**, 942-948.

Plath, K., Mothes, W., Wilkinson, B. M., Stirling, C. J., & Rapoport, T. A. (1998). Signal sequence recognition in posttranslational protein transport across the yeast ER membrane. *Cell,* **94**, 795-807.

Plath, K., & Rapoport, T. A. (2000). Spontaneous release of cytosolic proteins from posttranslational substrates before their transport into the endoplasmic reticulum. *J. Cell. Biol.,* **151**, 167-178.

Pogliano, J. A., & Beckwith, J. (1994). SecD and SecF facilitate protein export in *Escherichia coli*. *EMBO J.,* **13**, 554-561.

Pogliano, K. J., & Beckwith, J. (1994). Genetic and molecular characterization of the *Escherichia coli* secD operon and its products. *J. Bacteriol.,* **176**, 804-814.

Pool, M. R. (2009). A trans-membrane segment inside the ribosome exit tunnel triggers RAMP4 recruitment to the Sec61p translocase. *J. Cell. Biol.,* **185**, 889-902.

Qi, H. Y., & Bernstein, H. D. (1999). SecA is required for the insertion of inner membrane proteins targeted by the *Escherichia coli* signal recognition particle. *J. Biol. Chem.,* **274**, 8993-8997.

Randall, L. L., & Hardy, S. J. (2000). The promiscuous and specific sides of SecB. *Nat. Struct. Biol.,* **7**, 1077-1079.

Randall, L. L., Hardy, S. J., Topping, T. B., Smith, V. F., Bruce, J. E., & Smith, R. D. (1998). The interaction between the chaperone SecB and its ligands: evidence for multiple subsites for binding. *Protein Sci.,* **7**, 2384-2390.

Rapoport, T. A. (2007). Protein translocation across the eukaryotic endoplasmic reticulum and bacterial plasma membranes. *Nature,* **450**, 663-669.

Ravaud, S., Stjepanovic, G., Wild, K., & Sinning, I. (2008). The crystal structure of the periplasmic domain of the *Escherichia coli* membrane protein insertase YidC contains a substrate binding cleft. *J. Biol. Chem.,* **283**, 9350-9358.

Rep, M., Nooy, J., Guélin, E., & Grivell, L. A. (1996). Three genes for mitochondrial proteins suppress null-mutations in both Afg3 and Rca1 when over-expressed. *Curr. Genet.,* **30**, 206-211.

Rodrigue, A., Chanal, A., Beck, K., Müller, M., & Wu, L. F. (1999). Co-translocation of a periplasmic enzyme complex by a hitchhiker mechanism through the bacterial tat pathway. *J. Biol. Chem.,* **274**, 13223-13228.

Sachelaru, I., Petriman, N. A., Kudva, R., Kuhn, P., Welte, T., Knapp, B., Drepper, F., Warscheid, B., & Koch, H. G. (2013). YidC occupies the lateral gate of the SecYEG translocon and is sequentially displaced by a nascent membrane protein. *J. Biol. Chem.,* **288**, 16295-16307.

Sambasivarao, D., Turner, R. J., Simala-Grant, J. L., Shaw, G., Hu, J., & Weiner, J. H. (2000). Multiple roles for the twin arginine leader sequence of dimethyl sulfoxide reductase of *Escherichia coli*. *J. Biol. Chem.,* **275**, 22526-22531.

Saparov, S. M., Erlandson, K., Cannon, K., Schaletzky, J., Schulman, S., Rapoport, T. A., & Pohl, P. (2007). Determining the conductance of the SecY protein translocation channel for small molecules. *Mol. Cell.,* **26**, 501-509.

Schatz, P. J., Bieker, K. L., Ottemann, K. M., Silhavy, T. J., & Beckwith, J. (1991). One of three transmembrane stretches is sufficient for the functioning of the SecE protein, a membrane component of the *E. coli* secretion machinery. *EMBO J.,* **10**, 1749-1757.

Scheper, W., Thaminy, S., Kais, S., Stagljar, I., & Römisch, K. (2003). Coordination of N-glycosylation and protein translocation across the endoplasmic reticulum membrane by Sss1 protein. *J. Biol. Chem.,* **278**, 37998-38003.

Schiebel, E., Driessen, A. J., Hartl, F. U., & Wickner, W. (1991). Delta mu H+ and ATP function at different steps of the catalytic cycle of preprotein translocase. *Cell,* **64**, 927-939.

Schröder, K., Martoglio, B., Hofmann, M., Hölscher, C., Hartmann, E., Prehn, S., Rapoport, T. A., & Dobberstein, B. (1999). Control of glycosylation of MHC class II-associated invariant chain by translocon-associated RAMP4. *EMBO J.,* **18**, 4804-4815.

Sharon, M., Ilag, L. L., & Robinson, C. V. (2007). Evidence for micellar structure in the gas phase. *J. Am. Chem. Soc.,* **129**, 8740-8746.

Shibatani, T., David, L. L., McCormack, A. L., Frueh, K., & Skach, W. R. (2005). Proteomic analysis of mammalian oligosaccharyltransferase reveals multiple subcomplexes that contain Sec61, TRAP, and two potential new subunits. *Biochemistry,* **44**, 5982-5992.

Snapp, E. L., Reinhart, G. A., Bogert, B. A., Lippincott-Schwartz, J., & Hegde, R. S. (2004). The organization of engaged and quiescent translocons in the endoplasmic reticulum of mammalian cells. *J. Cell. Biol.,* **164**, 997-1007.

Spencer, R. H., Chang, G., & Rees, D. C. (1999). 'Feeling the pressure': structural insights into a gated mechanosensitive channel. *Curr. Opin. Struct. Biol.,* **9**, 448-454.

Sugai, R., Takemae, K., Tokuda, H., & Nishiyama, K. (2007). Topology inversion of SecG is essential for cytosolic SecA-dependent stimulation of protein translocation. *J. Biol. Chem.,* **282**, 29540-29548.

Tam, P. C., Maillard, A. P., Chan, K. K., & Duong, F. (2005). Investigating the SecY plug movement at the SecYEG translocation channel. *EMBO J.,* **24**, 3380-3388.

Tarry, M. J., Schäfer, E., Chen, S., Buchanan, G., Greene, N. P., Lea, S. M., Palmer, T., Saibil, H. R., & Berks, B. C. (2009). Structural analysis of substrate binding by the TatBC component of the twin-arginine protein transport system. *Proc. Natl. Acad. Sci. U. S. A.,* **106**, 13284-13289.

Taura, T., Baba, T., Akiyama, Y., & Ito, K. (1993). Determinants of the quantity of the stable SecY complex in the *Escherichia coli* cell. *J. Bacteriol.,* **175**, 7771-7775.

Tillman, T. S., & Cascio, M. (2003). Effects of membrane lipids on ion channel structure and function. *Cell. Biochem. Biophys.,* **38**, 161-190.

Tomkiewicz, D., Nouwen, N., & Driessen, A. J. (2007). Pushing, pulling and trapping--modes of motor protein supported protein translocation. *FEBS Lett.,* **581**, 2820-2828.

Törnroth-Horsefield, S., Gourdon, P., Horsefield, R., Brive, L., Yamamoto, N., Mori, H., Snijder, A., & Neutze, R. (2007). Crystal structure of AcrB in complex with a single transmembrane subunit reveals another twist. *Structure,* **15**, 1663-1673.

Tottey, S., Waldron, K. J., Firbank, S. J., Reale, B., Bessant, C., Sato, K., Cheek, T. R., Gray, J., Banfield, M. J., Dennison, C., & Robinson, N. J. (2008). Protein-folding location can regulate manganese-binding versus copper- or zinc-binding. *Nature,* **455**, 1138-1142.

Tsukazaki, T., Mori, H., Echizen, Y., Ishitani, R., Fukai, S., Tanaka, T., Perederina, A., Vassylyev, D. G., Kohno, T., Maturana, A. D., Ito, K., & Nureki, O. (2011). Structure and function of a membrane component SecDF that enhances protein export. *Nature,* **474**, 235-238.

Tsukazaki, T., Mori, H., Fukai, S., Ishitani, R., Mori, T., Dohmae, N., Perederina, A., Sugita, Y., Vassylyev, D. G., Ito, K., & Nureki, O. (2008). Conformational transition of Sec machinery inferred from bacterial SecYE structures. *Nature,* **455**, 988-991.

Ulbrandt, N. D., Newitt, J. A., & Bernstein, H. D. (1997). The *E. coli* signal recognition particle is required for the insertion of a subset of inner membrane proteins. *Cell,* **88**, 187-196.

Urbanus, M. L., Fröderberg, L., Drew, D., Björk, P., de Gier, J. W., Brunner, J., Oudega, B., & Luirink, J. (2002). Targeting, insertion, and localization of *Escherichia coli* YidC. *J. Biol. Chem.,* **277**, 12718-12723.

Urbanus, M. L., Scotti, P. A., Fröderberg, L., Saaf, A., de Gier, J. W., Brunner, J., Samuelson, J. C., Dalbey, R. E., Oudega, B., & Luirink, J. (2001). Sec-dependent membrane protein insertion: sequential interaction of nascent FtsQ with SecY and YidC. *EMBO Rep.,* **2**, 524-529.

Valent, Q. A., Scotti, P. A., High, S., de Gier, J. W., von Heijne, G., Lentzen, G., Wintermeyer, W., Oudega, B., & Luirink, J. (1998). The *Escherichia coli* SRP and SecB targeting pathways converge at the translocon. *EMBO J.,* **17**, 2504-2512.

van Bloois, E., Dekker, H. L., Fröderberg, L., Houben, E. N., Urbanus, M. L., de Koster, C. G., de Gier, J. W., & Luirink, J. (2008). Detection of crosslinks between FtsH, YidC, HflK/C suggests a linked role for these proteins in quality control upon insertion of bacterial inner membrane proteins. *FEBS Lett.,* **582**, 1419-1424.

Van den Berg, B., Clemons, W. M., Jr., Collinson, I., Modis, Y., Hartmann, E., Harrison, S. C., & Rapoport, T. A. (2004). X-ray structure of a protein-conducting channel. *Nature,* **427**, 36-44.

van den Heuvel, R. H., & Heck, A. J. (2004). Native protein mass spectrometry: from intact oligomers to functional machineries. *Curr. Opin. Chem. Biol.,* **8**, 519-526.

van der Laan, M., Nouwen, N., & Driessen, A. J. (2004). SecYEG proteoliposomes catalyze the Deltaphi-dependent membrane insertion of FtsQ. *J. Biol. Chem.,* **279**, 1659-1664.

van der Sluis, E. O., Nouwen, N., Koch, J., de Keyzer, J., van der Does, C., Tampé, R., & Driessen, A. J. (2006). Identification of two interaction sites in SecY that are important for the functional interaction with SecA. *J. Mol. Biol.,* **361**, 839-849.

van der Sluis, E. O., van der Vries, E., Berrelkamp, G., Nouwen, N., & Driessen, A. J. (2006). Topologically fixed SecG is fully functional. *J. Bacteriol.,* **188**, 1188-1190.

van Stelten, J., Silva, F., Belin, D., & Silhavy, T. J. (2009). Effects of antibiotics and a proto-oncogene homolog on destruction of protein translocator SecY. *Science,* **325**, 753-756.

Wagner, S., Pop, O. I., Haan, G. J., Baars, L., Koningstein, G., Klepsch, M. M., Genevaux, P., Luirink, J., & de Gier, J. W. (2008). Biogenesis of MalF and the MalFGK(2) maltose transport complex in *Escherichia coli* requires YidC. *J. Biol. Chem.,* **283**, 17881-17890.

Walter, P., & Blobel, G. (1980). Purification of a membrane-associated protein complex required for protein translocation across the endoplasmic reticulum. *Proc. Natl. Acad. Sci. U. S. A.,* **77**, 7112-7116.

Walter, P., & Blobel, G. (1981). Translocation of proteins across the endoplasmic reticulum III. Signal recognition protein (SRP) causes signal sequence-dependent and site-specific arrest of chain elongation that is released by microsomal membranes. *J. Cell. Biol.,* **91**, 557-561.

Whitehouse, S., Gold, V. A., Robson, A., Allen, W. J., Sessions, R. B., & Collinson, I. (2012). Mobility of the SecA 2-helix-finger is not essential for polypeptide translocation via the SecYEG complex. *J. Cell. Biol.,* **199**, 919-929.

Woodbury, R. L., Topping, T. B., Diamond, D. L., Suciu, D., Kumamoto, C. A., Hardy, S. J., & Randall, L. L. (2000). Complexes between protein export chaperone SecB and SecA. Evidence for separate sites on SecA providing binding energy and regulatory interactions. *J. Biol. Chem.,* **275**, 24191-24198.

Xie, K., Kiefer, D., Nagler, G., Dalbey, R. E., & Kuhn, A. (2006). Different regions of the nonconserved large periplasmic domain of *Escherichia coli* YidC are involved in the SecF interaction and membrane insertase activity. *Biochemistry,* **45**, 13401-13408.

Xu, Z., Knafels, J. D., & Yoshino, K. (2000). Crystal structure of the bacterial protein export chaperone secB. *Nat. Struct. Biol.,* **7**, 1172-1177.

Yahr, T. L., & Wickner, W. T. (2000). Evaluating the oligomeric state of SecYEG in preprotein translocase. *EMBO J.,* **19**, 4393-4401.

Yahr, T. L., & Wickner, W. T. (2001). Functional reconstitution of bacterial Tat translocation *in vitro*. *EMBO J.,* **20**, 2472-2479.

Yamaguchi, A., Hori, O., Stern, D. M., Hartmann, E., Ogawa, S., & Tohyama, M. (1999). Stress-associated endoplasmic reticulum protein 1 (SERP1)/Ribosome-associated membrane protein 4 (RAMP4) stabilizes membrane proteins during stress and facilitates subsequent glycosylation. *J. Cell. Biol.,* **147**, 1195-1204.

Yu, Z., Lavèn, M., Klepsch, M., de Gier, J. W., Bitter, W., van Ulsen, P., & Luirink, J. (2011). Role for *Escherichia coli* YidD in membrane protein insertion. *J. Bacteriol.,* **193**, 5242-5251.

Zhang, B., & Miller, T. F., 3rd. (2010). Hydrophobically stabilized open state for the lateral gate of the Sec translocon. *Proc. Natl. Acad. Sci. U. S. A.,* **107**, 5399-5404.

Zhou, M., Morgner, N., Barrera, N. P., Politis, A., Isaacson, S. C., Matak-Vinković, D., Murata, T., Bernal, R. A., Stock, D., & Robinson, C. V. (2011). Mass spectrometry of intact V-type ATPases reveals bound lipids and the effects of nucleotide binding. *Science,* **334**, 380-385.

Zimmer, J., Nam, Y., & Rapoport, T. A. (2008). Structure of a complex of the ATPase SecA and the protein-translocation channel. *Nature,* **455**, 936-943.

Zimmer, J., & Rapoport, T. A. (2009). Conformational flexibility and peptide interaction of the translocation ATPase SecA. *J. Mol. Biol.,* **394**, 606-612.

Zito, C. R., & Oliver, D. (2003). Two-stage binding of SecA to the bacterial translocon regulates ribosome-translocon interaction. *J. Biol. Chem.,* **278**, 40640-40646.